DOCTOR OF PHILOSOPHY

Synthetic models to study the role of aromatic residues in radical dependent enzymes

García Caballero., Alfonso

Award date:
2005

Awarding institution:
University of Wales, Bangor

Synthetic Models to Study the Role of Aromatic Residues in Radical Dependent Enzymes

by

Alfonso García Caballero

Chemistry Department

University of Wales, Bangor

• PRIFYSGOL CYMRU •
UNIVERSITY OF WALES
BANGOR

1884

A Thesis submitted for the degree of

Doctor of Philosophy

of the University of Wales, Bangor

Acknowledgments

Firstly, I would like to thank Dr. Anna K. Croft, my PhD supervisor, who had the patience to help and advise me throughout the Project.

Thanks to my research committee, Professor Mark S. Baird and Dr Michael Beckett.

I am also grateful to Dr. Kalaji, who provided his expertise and guided me through the electrochemistry experiments. Extensive thanks to the whole of the electrochemistry group, Tânia Anjos, Duarte Tito, Eric Lascombe, Ben Jones and Chris Gwenin for their immeasurable help. Thanks to Professor Bruce Gilbert for his professional help with the ESR studies and Adrian Whitwood for running the spectra. Thanks to Dr. I. R. Butler for his expert advice with anthracenes.

I would like to thank the EPSRC for financial support and the University of Wales.

For their technical assistance I am indebted to the staff of the Chemistry Department and in particular to Gwynfor Davies, Glyn Connolly, Mike Lewis, Steven Jones, John Charles and Denis Williams. Many thanks to all my colleagues, in particular Dr Juma Al-Dulayymi, Gani, Mark and Mohan.

For the unforgettable experiences, I would like to thank to the 'Chemistry Football Club'. A special thanks to all my friends in Bangor for making it clear that life does go on outside chemistry, particularly to Jokin Ayestaran, Baldomero Molina, Enrique Gallardo, Andrés Moreno, Julia Gómez, Gorka, Cristina, Ester and Itxaso.

Por todo el apoyo y cariño recibido a lo largo de los años, me gustaría dedicar esta Tesis a mis padres, Alfonso y Josefina, a mi hermana Carmen, a mi cuñado Miguel y a mis sobrinos Miguel y Marcos. Una dedicatoria muy especial para Tânia, que siempre ha estado a mi lado durante estos años.

Summary

A mixture of techniques, both experimental and theoretical, have been used to elucidate the effect of proximal aromatic residues on free-radical reactions.

Synthetic model compounds, such as anthracene adducts, and acyclic models with both no aromatic groups and with substituted aromatic groups remote from the putative radical site, have been prepared.

The relative rates of reaction towards *tri*-butyl tin hydride of synthetic models containing differently substituted aromatic groups follow a linear Hammett relationship with a positive value of the reaction constant and demonstrate that electron withdrawing groups increase the reactivity of the substrate by stabilising the δ^- transition state during bromine abstraction. Theoretical calculations of the radical stabilisation energies of anthracene derivatives at the RMP2/6-31G(d)//B3-LYP/6-31G(d) level of theory show that stabilisation of the radical intermediate is negligible for this particular system. Analysis of the hyperfine structure of the ESR spectrum of anthracene models shows that the radical formed by bromine abstraction interacts with the α-protons and the β-protons, but it does not interact significantly with the aromatic moiety.

The electrochemical reduction by cyclic voltammetry of the carbon-bromine bond of the synthetic models is primarily governed by the kinetics of the electron transfer step and takes place through a concerted mechanism. Hammett plots indicate that electron donating groups at the aromatic ring destabilise the intermediate, whereas electron withdrawing groups have a stabilising effect of the δ^- transition state, consistent with the results of the relative rate studies.

Paracyclophane derivatives are excellent models to study aromatic-radical interactions due to their constrained geometry. Intramolecular cyclisation promoted by samarium iodide, the McMurry coupling and ring closing metathesis afford different products other than the cyclised paracyclophane as the major components. The acyloin condensation gives low yield of paracyclophane and is difficult to reproduce. Instead, the cycloaddition of quaternary ammonium hydroxides initiated by the Hoffmann elimination constitutes a reliable method to prepare [8]-paracyclophanes and is the most likely route for a successful synthesis of [9]-paracyclophanes.

Abstract

A mixture of techniques, both experimental and theoretical, has been used to elucidate the effect of proximal aromatic residues on free-radical reactions.

Synthetic model compounds have been prepared with no aromatic groups and substituted aromatic groups remote from the putative radical site, so that the influence of the aromatic electronic density in the stability of the radical can be investigated. Anthracene and acyclic models, bearing a bromine atom that can be reduced to form a radical intermediate, have been synthesised following a general three-step sequence. Preparation of anthracene models consists of a Diels Alder reaction on the appropriate 2,6-substituted anthracene with ethyl acrylate, followed by reduction of the resulting ester derivative and then conversion of the corresponding alcohol into the final bromide derivatives. 2,6-Substituted anthracene precursors, suitable for Diels Alder reaction, have been obtained by reduction of the quinone moiety of the appropriate 2,6-substituted anthraquinone. Acyclic derivatives have been synthesised first by construction of the skeleton structure using a Grignard reaction. Substitution at the aromatic ring has been accomplished by direct nitration of the benzene ring. Reduction of the nitro derivative followed by Sandmeyer reaction afforded the amino- and bromo-substituted aromatic derivatives.

Examination of the relative rates of reaction towards *tri*-butyl tin hydride of anthracene and acyclic models containing differently substituted aromatic groups follow a Hammett linear relationship and demonstrates that electron withdrawing groups increase the reactivity of the substrate, suggesting that a lower electron density at the aromatic ring stabilises the δ^- transition state during bromine abstraction. Theoretical calculations of the RSEs of anthracene derivatives at the RMP2/6-31G(d)/B3-LYP/6-31G(d) level of theory show that stabilisation of the radical intermediate is negligible for this particular system, providing further evidence for the δ^- transition state stabilisation. Analysis of the hyperfine structure

of the ESR spectrum of anthracene derivatives demonstrates that the radical formed by bromine abstraction interacts with the α-protons and the β-protons. The absence of observed interaction between the radical and the aromatic moiety provides supplementary evidence for δ^- transition state stabilisation during bromine abstraction.

The electrochemical reduction of the carbon-bromine bond of the anthracene and acyclic models using cyclic voltammetry is primarily governed by the kinetics of the electron transfer step and consists of concerted mechanism without the formation of a radical anion as intermediate, but direct formation of the radical. Hammett plots indicate that electron donating groups destabilise the intermediate, whereas electron withdrawing groups have a stabilising effect. The positive value of the reaction constant corroborates that the electroreduction of the carbon-bromine bond in anthracene and acyclic models passes through a δ^- transition state. However, the sensitivity of the potential towards electronic density at the aromatic ring is substantially smaller than in the bromine abstraction by hydride illustrating the bigger influence of the thermodynamical stability of the radical compared to the electronic effect.

The synthesis of paracyclophane models has been investigated as they are expected to provide an excellent model to study aromatic-radical interactions due to their constrained geometry. The high deficit in entropy and strain that has to be overcome to bring together two alkyl chains in a *para*-substituted benzene to form a medium ring of nine members makes intramolecular cyclisation procedures difficult to successfully carry out in most cases. Intramolecular cyclisation promoted by samarium iodide, the McMurry coupling and RCM afford different products other than the cyclised paracyclophane as the major components. The acyloin condensation gives a very low, almost negligible, yield of paracyclophane, and is difficult to reproduce. Instead, the cycloaddition of quaternary ammonium hydroxides initiated by the Hoffmann elimination provides a reliable method to prepare [8]-paracyclophanes, which could be further derivatised into [9]-paracyclophane derivatives.

Table of contents

Introduction

Proteins are linear polymers formed as macromolecules with typical molecular weights ranging from about 6000 to more than 600000 Da. Of the twenty common *L*-amino acids that are used to form proteins, phenylalanine **1**, tryptophan **2**, and tyrosine **3** are aromatic (Figure i.1).[1] Proteins play a vital role in biology and thus in life with their importance arising from the fact that the subset that constitutes enzymes has evolved by the life process to be extremely specific catalysts. Each enzyme is a catalyst for only one biological reaction or, sometimes, one class of reaction. Typical enzymes work by having a catalytic site that binds specifically to a single (or multiple) reactant and activates it. Each enzyme has a unique three dimensional structure that usually includes a pocket or cleft presenting an array of functional groups to the reactant molecule.[2] An enzyme-catalysed reaction is always initiated by the formation of an enzyme-substrate complex (ES), from which catalysis takes place. As the reaction proceeds, the enzyme conforms to the transition-state structure, leading to the tightest interactions (increased binding energy) with the transition-state structure. This increased binding, known as transition-state stabilisation, results in rate enhancement.[3]

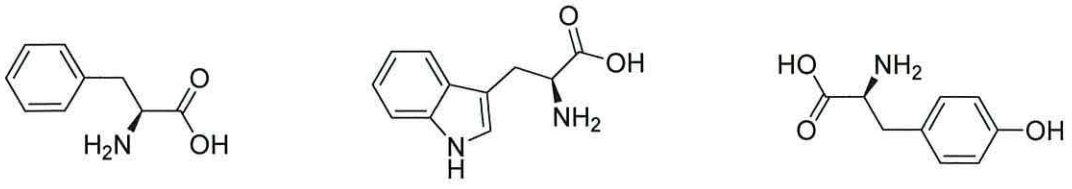

Figure i.1. Aromatic residues present in the active site of enzymes.

Enzymes can demonstrate almost complete stereochemical specificity: in other words, they can distinguish between optical or even geometrical isomers. They are stereospecific catalysts because they are asymmetric structures formed uniquely of chiral amino acid centres. The great specificity of enzymes is explained principally

by their structures, about which information has been afforded in the last few decades by X-ray diffraction crystallography. In recent years, increasing availability of high resolution X-ray structures of enzymes that carry out difficult chemical transformations has led to novel mechanistic insights into the reactions of these bio-catalysts, allowing the chemistry of enzymes to be elucidated in detail. Although much work has been devoted to the subject, many questions still remain unsolved. In particular, the role specific residues within the active sites of these enzymes remain unclear. However, it is known that amino acid chains in the active site contribute to the formation of the ES complex mostly *via* non-covalent interactions, including electrostatic interactions, ion-dipole interactions, dipole-dipole interactions, hydrogen bonding, charge transfer, hydrophobic interactions and van der Waals interactions.[3]

Of particular interest are those enzymes that act *via* radical mechanisms, including enzymes such as ribonucleotide reductase, methylmalonyl-CoA or glutamate mutase.[4-12] These enzymes are of interest because they can catalyse highly unusual chemistry that is difficult to reproduce under laboratory conditions.

Radicals have become increasingly significant intermediates for chemists in the last 100 years since their discovery. However, it has only been in the last 20 or 30 years when the importance of radicals has started to be really appreciated in both chemistry and biology due to the large number of processes in which they participate.[4] This is, in part, due to the ability of radicals to carry out processes that would be normally inaccessible using heterolytic reactions. Because of the utility of free radical reactions, enzymes too use this chemistry. In these cases, the reactivity must be contained in order to preserve the radicals generated in the active site and allow desired reactions to occur.

The advantages of using radicals as intermediates in enzymatic transformations are their high reactivity and special properties. Nowadays, it is generally accepted that the cleavage of all inactivated C-H bonds occurs *via* radical intermediates.[4,13] The rates of radical reactions are much faster than the corresponding ionic processes, and

the limiting step is not always the interconversion of the radicals, but either their formation from a neutral precursor or their decomposition to a neutral product. In enzymes that utilise free radicals, the presence of aromatic residues in the active sites of these enzymes has been related to the maintenance of those long-lived radicals.[4,14,15]

Radicals can be easily quenched by reaction with both oxidizing and reducing agents. Since radicals are highly reactive towards dioxygen, they are found especially in enzymes from anaerobic (oxygen free) micro-organisms. Two classes of dioxygen-independent enzymatic reactions are recognised as proceeding through radical based mechanisms: S-adenosylmethionine-sulfur-dependent enzymes (SAM) and adenosylcobalamin-dependent enzymes (AdoCbl), whose main characteristic is that, for both, reactions are initiated by the 5'-deoxyadenosyl **5**.[16] Cobalamins **4**, which are derivatives of vitamin B_{12}, are complex organometallic cofactors with a central cobalt coordinated equatorially to four pyrrolic nitrogens with 5'-deoxyadenosine bound (Figure i.2).[17]

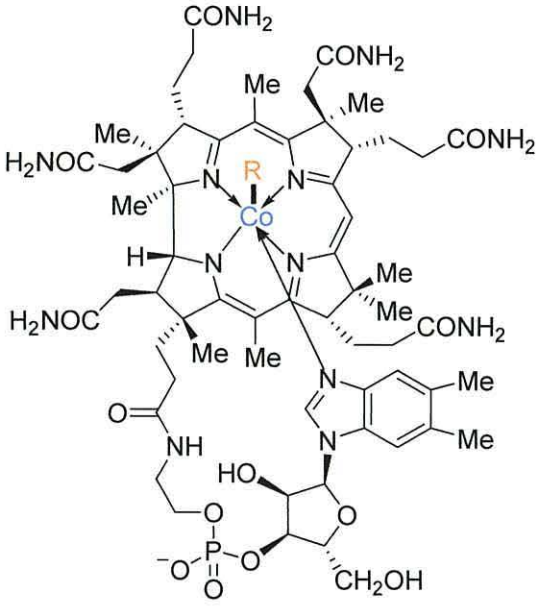

4

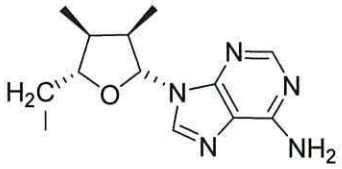

R (5'-deoxyadenosyl)

5

Figure i.2. General diagram for cobalamins.

Catalysis in coenzyme B_{12}-dependent reactions proceeds with the homolytic cleavage of the organometallic bond of the cofactor to yield a 5'-desoxyadenosyl radical. This radical then abstracts a hydrogen atom from the protein-bound substrate to initiate the rearrangement reaction. However, the cofactor does not appear to have a directly participating role during the radical rearrangement reaction.[16] Instead, the role of the B_{12} cofactor is to function as a free radical reservoir responsible for the controlled generation of a substrate radical at the initiation of the reaction cycle.

Nonetheless, certain free radicals generated at active sites of certain enzymes are stable and protected such that they persist for hours or longer. This ability to protect a radical seems to be a general property of enzymes that function by radical mechanisms. A perfect example of how this can be accomplished structurally is the manner in which methylmalonyl CoA binds its substrate, with the methylmalonyl group projected deeply within the structure, where the Co-C-5' bond is buried.[16]

Methylmalonyl Coenzyme A mutase is a coenzyme-B_{12} dependent enzyme of great importance because it is involved in neurological damage in humans, being the only coenzyme B_{12}-dependent enzyme that is present in both microbial and animal kingdoms.[18] Adenosyl radicals are involved in the reversible enzyme-catalysed conversion of methylmalonyl CoA to succinyl CoA, a reaction important in fatty acid metabolism (Figure i.3).[19] One of the remarkable features of this reaction is that methylmalonyl CoA mutase effects catalysis using radical intermediates under aerobic conditions.[17]

Figure i.3. Reaction catalysed by methylmalonyl-Co A mutase.

The crystal structure of methylmalonyl-CoA mutase (2 Å resolution) from *Propionibacterium shermanii* shows, firstly with coenzyme B_{12} and secondly with the partial substrate desulpho-CoA (lacking the succinyl group and the sulphur atom

of the substrate), that the cobalt atom is coordinated through a long bond to a histidine from the protein.[20] The histidine-cobalt distance is very long 2.5 Å compared with 1.95-2.2 Å in free cobalamins, leading to the suggestion that the enzyme positions the histidine in order to weaken the metal-carbon bond of the cofactor and favour the formation of the initial radical species.[20]

Tyr89 is a wholly conserved residue in methylmalonyl CoA mutases that has previously been found to influence catalysis involved in substrate binding.[20] The role of Tyr89 has been investigated by using site directed mutagenesis studies by replacement of this residue with phenylalanine. The mutant Tyr89Phe was characterised by X-ray diffraction, determination of its steady-state parameters, measurement of kinetic deuterium isotope effects and the measurement of rate of tritium release.[19] From this work, it seems that the loss of a single interaction involving the hydroxyl group of Tyr89 affects both the stability of radical intermediates and decreases the rate of interconversion of the substrate and product-derived radicals, showing that Tyr89 plays a key role in the stabilisation of the free radical intermediates.[19]

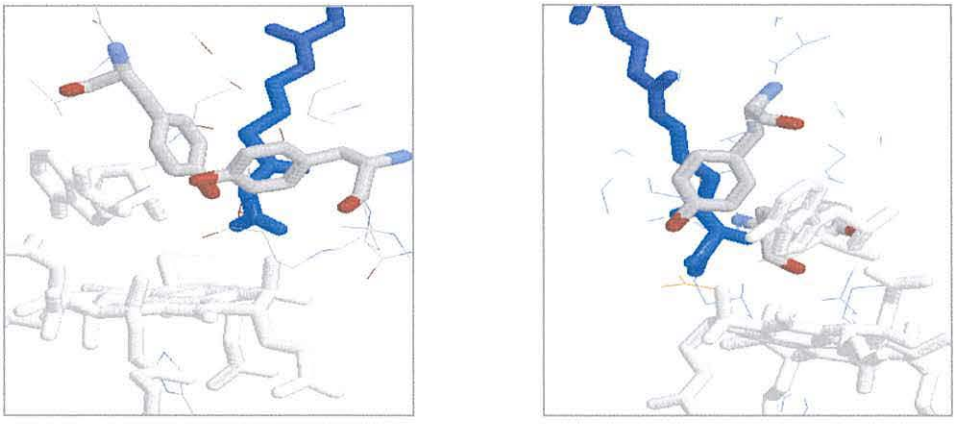

Figure i.4. Methylmalonyl CoA mutase (Tyr243, 3.4 Å and Tyr89, 4.5 Å).

The crystal structure of methylmalonyl CoA mutase (Figure i.4) also reveals that only a few polar active site amino acids, in particular His244, Arg207, and Tyr89, are in direct contact with the substrate. Moreover, His244 is in hydrogen bonding distance with the carbonyl group of the CoA moiety of the substrate (Figure i.5).

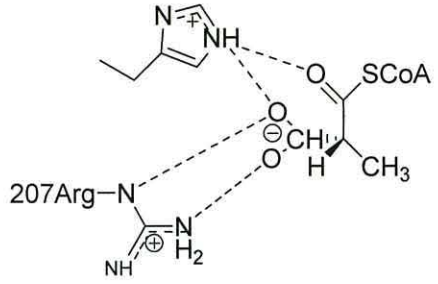

Figure i.5. Interactions between the substrate and residues in the active site of Methylmalonyl CoA mutase.[6]

Mutagenesis of this His244 to alanine, glutamine or asparginine results in a small lowering of the catalytic efficiency, and the loss of one of the two kinetic pKa's.[17]

It also shows the two tyrosine residues, Tyr243 and Tyr89, flanking the site of radical formation in the substrate, are at a distance of only 3.4 Å in the case of Tyr243 and 4.5 Å for Tyr89.[6] The location of these aromatic residues suggests a possible role for them in catalysis either by radical stabilisation, or by direct participation, or both. Although the mechanism by which the initially formed substrate radical isomerises to the product radical during the rearrangement is unknown, *ab initio* molecular orbital theoretical calculations predict that partial proton transfer can contribute significantly to the lowering of the barrier for the rearrangement reaction (Figure i.6).[6]

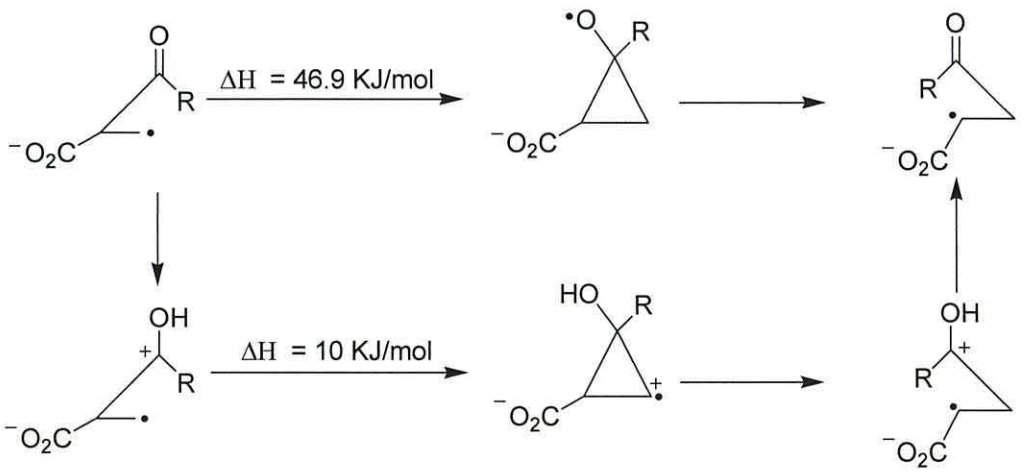

Figure i.6. Postulated mechanism for the rearrangement of the substrate radical in Methylmalonyl Coenzyme A mutase, R = CoA.[6]

Ribonucleotide reductase (RNR) was the first protein-based radical to be discovered. Ribonucleotide reductases are important because they provide the building blocks for DNA replication in all living cells.[16] All ribonucleotide reductases use radical chemistry for ribonucleotide reduction.[21] They carry out the conversion of nucleotides to deoxynucleotides in all organisms, providing the monomeric precursors required for DNA biosynthesis. This is achieved by the enzyme facilitating the difficult conversion of the hydroxyl group at the 2-position of the ribose sugar to a hydrogen atom, generating 2'-deoxyribose (Figure i.7), in what constitutes the rate-determining step.[15,22,23]

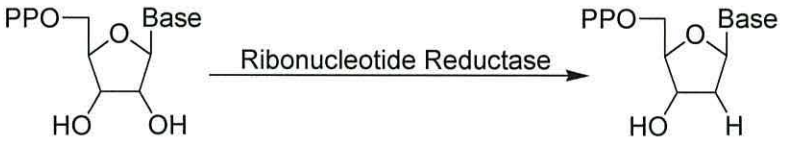

Figure i.7. Conversion of ribonucleotides to the corresponding deoxy-ribonucleotides through the action of RNR.

Ribonucleotide reductases can be grouped into three major classes based on both the mechanisms they use for radical generation and their structural differences.[24] The small β-chain of class I contains an oxygen-linked diferric centre and, in its active form, a stable tyrosyl free radical.[23] Class II RNR's have a simple structure and contain no stable radical. In these enzymes adenosylcobalamin is used to generate a transient radical during catalysis. The α-polypeptide of class III contains a stable oxygen-sensitive glycyl radical. One remarkable difference among the three classes is the reactivity of their free radicals towards oxygen: For class I, oxygen is a component of the system that generates the tyrosyl radical, so aerobic conditions are essential. For class III, the glycyl radical is rapidly destroyed by oxygen with cleavage of the polypeptide chain at the location of the radical, so strictly anaerobic conditions are required. Class II is insensitive to oxygen so works in both aerobic and anaerobic conditions.[21]

In the history of ribonucleotide reductases, the biggest surprise came when an organic free radical, identified as tyrosyl 122, was discovered as forming part of the polypeptide structure of one of the subunits of the *Escherichia coli* enzyme and that

it is required for activity. The radical is a strong oxidant and so extremely stable that it could survive the two weeks it took to purify the enzyme.[21] RNR class I contains two different subunits or proteins, R1 and R2, with the radical located in protein R2, the smaller one. The subunit R2 gives an electron spin resonance signal that arises from a tyrosine phenoxyl radical.[25]

The tyrosyl radical is buried in the protein matrix close to both a dinuclear iron centre and a cluster of three hydrophobic residues, Phe208, Phe212, and Ile234. These three residues are also known to be conserved throughout the R2 family (Figure i.8). To examine the requirement for such residues, mutants of R2 proteins F208Y, F212Y, F212W, and I234N were constructed.[5] In the case of F208Y, the yield of tyrosyl radical Y122 was substantially lower than in the wild type case due to a competing reaction resulting in hydroxylation of Y208. This result implies that the phenylalanine at position 208 may direct the hydrogen abstraction reaction.

The most prominent result of the site directed mutagenesis is that all mutant proteins show impaired radical half-life. In three of the four mutants, the half-lives are several orders of magnitude shorter than that of the wild type radical. The authors suggested therefore that the major role of the hydrophobic pocket is to stabilise the tyrosyl radical.[5] This hypothesis has been corroborated by comparative studies of the environment of other naturally occurring tyrosyl radicals.[5]

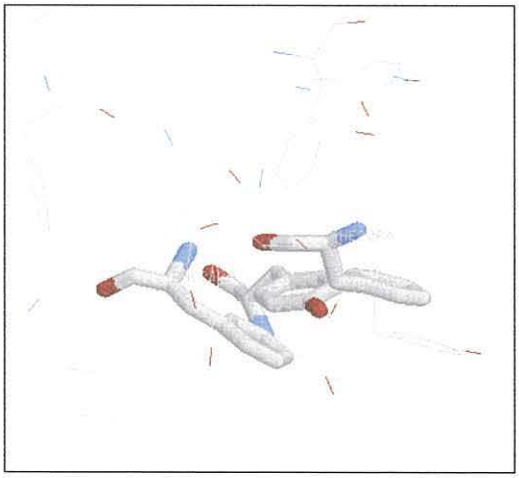

Figure i.8. The active site of ribonucleotide reductase, R2 shows Tyr122 between Phe208 and Phe212.

In class III, anaerobic ribonucleotide reductase (ARR), hydrogen abstraction from Gly681 results in a radical located on the protein main chain. The Gly681 radical appears to serve the same function in ARR as the tyrosyl radical in ribonucleotide reductases from aerobic bacteria and eukaryotes. It functions as a protected radical centre that projects radical chemistry into the active site, perhaps through reaction with intervening cysteine residues, culminating in the formation of a thiyl radical at the active site. Hydrogen abstraction from the substrate is probably analogous to the reactions of other ribonucleotide reductases.[16]

Glutamate mutase (Glm) is a coenzyme-B_{12} dependent enzyme that catalyses the conversion of L-glutamate to L-β-methyl aspartate (Figure i.9).[16]

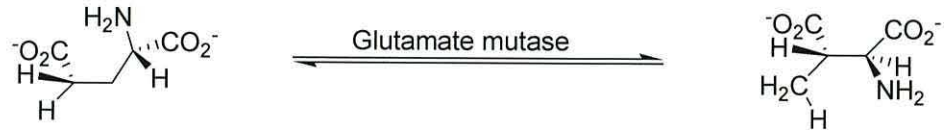

Figure i.9. Reaction catalysed by glutamate mutase.

The glutamate mutase crystal structure from *Clostridium cochlearium* shows that the protein is heterotetrameric, with features that show close similarity to the structure of methylmalonyl CoA mutase.[20] Each of the two independent B_{12} cofactor molecules are associated with a substrate-binding site, which is occupied in the crystal structure by the substrate analogue (2*S*, 3S)-tartrate. The tight binding of the tartrate ion conforms to the requirements of tight control of the reactive intermediates and suggests how the enzyme might use the substrate-binding energy to initiate cleavage of the cobalt-carbon bond.[11] The dimethylbenzimidazole base (DMB) is deeply buried in a hydrophobic pocket (residues Leu8, Ile23, Pro27, Leu29, Val90, Gly91, and Tyr117). The bond lengths between the cobalt atom and nitrogen of His16 are of 2.27 Å and 2.30 Å for the two independent subunits of Glutamate Cyanocobalamin (Glm-CN). The tartrate molecule is tightly bound to the active site through a complex hydrogen-bonding network involving residues Gly1171, Tyr1177, Arg1100, Tyr1181, Arg1149, Arg1066, Arg1149 and Thr1094.[11] The structure notably shows

the aromatic ring of Phe216 directly above the putative radical site in the substrate (Figure i.10), at a distance of only 3.5 Å.

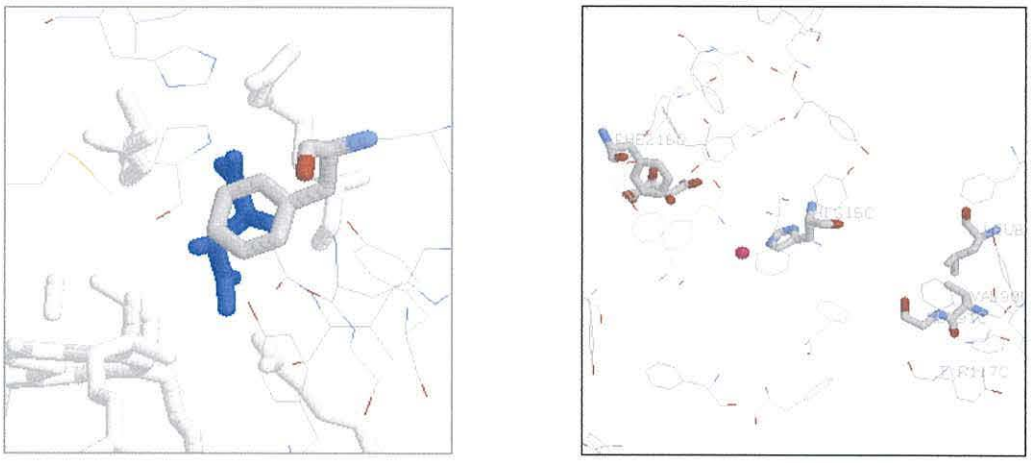

Figure i.10. Glutamate mutase with Phe216 3.5 Å from tartrate (left) and in the context of the enzyme active site (right).

Methionine synthase from *Escherichia coli* is a B_{12}-dependent enzyme that utilises a methylcobalamin prosthetic group. In the catalytic cycle, the methyl group from methyltetrahydrofolate is transferred to homocysteine *via* the enzyme-bound cofactor methylcobalamin, generating methionine and cob(I)-alamin, which is then re-methylated by a methyl group from methyltetrahydrofolate.[8] To carry out this reaction, the enzyme must alternately stabilise the six-coordinate methylcobalamin and four-coordinate cob(I)alamin oxidation states. Methionine synthase, however, occasionally undergoes side reactions that produce the inactive cob(II)alamin form of the enzyme. One such reaction is photolytic homolysis of the methylcobalamin C-Co bond.[8]

The crystal structure of the cobalamin-binding region of methionine synthase suggests how the protein might protect the methylcobalamin cofactor in the inactive enzyme. In particular, the upper face (methyl) of the cobalamin cofactor is in contact with several hydrophobic residues provided by a helical domain, and these residues could slow photolysis by caging the methyl radical and favouring recombination of the CH_3/cob(II)alamin radical pair. To study this suggestion, mutations to alanine at three positions in the cap domain; Phe708, Phe714 and Leu715, have been examined.

Calculations based on the wild type structure predicted that two of these three mutations, Phe708Ala and Leu715Ala, would increase solvent accessibility to the methylcobalamin cofactor, and in fact these mutations result in dramatic increases in the rate of photolysis. The third mutation, Phe714Ala, is not predicted to increase the accessibility of the cofactor but has still a modest effect on the photolysis rate of the enzyme. In addition, protein residues in the cap domain prevent solvent accessibility to the methyl group of the cofactor and appear to slow the rate of methyl radical escape from the protein cage.[20] These results confirm that the helical domain covers the cofactor in the inactive methylcobalamin enzyme and that residues from this domain can protect the enzyme against photolysis. These residues form a cage that provides a relatively un-reactive environment that could slow escape of the methyl radical and favour radical recombination. In particular, Phe708 and Leu715 are located above and to the side of the methyl group in the structure of bound methylcobalamin in the active site and within van der Waals contact of the upper face of the cobalamin cofactor, and these residues limit solvent access to the upper face (Figure i.11). In fact, Phe708 and Leu715 are conserved in the known sequences of methionine synthase. Other residues in the cap domain may contribute to this shielding effect by enforcing a degree of conformational rigidity on those residues that make direct contact with the cofactor.[8]

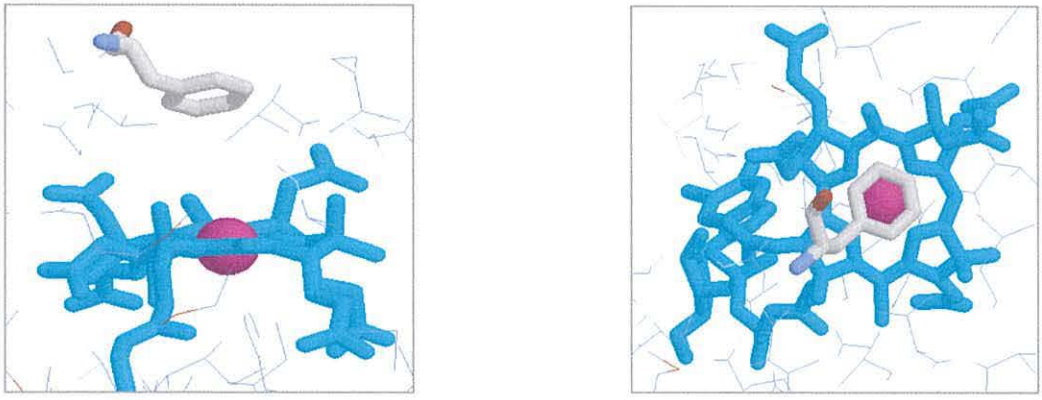

Figure i.11. Methionine synthase (F708 above methyl of cobalamin).

Pyruvate formate lyase (PFL) from *Escherichia coli* plays a central role in anaerobic glucose fermentation, catalysing the reversible conversion of pyruvate and coenzyme

A (CoA) to acetylCoA (AcCoA) and formate (Figure i.12). The PFL mechanism involves an unusual and reversible radical cleavage of the C1-C2 bond of pyruvate using the Gly734 radical and two cysteine residues, Cys418, Cys419.[14]

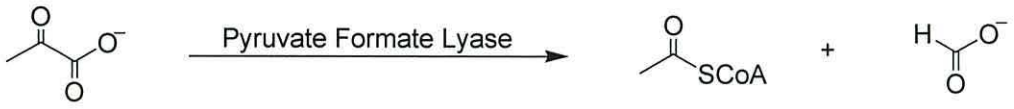

Figure i.12. Reaction catalysed by pyruvate formate lyase.

The X-ray crystallographic structures of PFL in its non-radical form, its complex with the substrate analogue oxamate, and the C418A/C419A double mutant have recently been determined.[9] The enzyme consists of a dimer of 759 residues whose architecture, a 10-stranded beta/alpha barrel assembled in an anti-parallel manner from two parallel five stranded beta-sheets, resembles that of the aerobic ribonucleotide reductase. Gly734 and Cys419 are in close proximity (Cα-Sγ = 3.7 Å). Oxamate fits into a compact pocket where C2 is juxtaposed with Cys418Sγ at 3.3 Å, which in turn is close to Cys419Sγ at 3.7 Å.[9]

Knappe[9] proposed a homolytic radical mechanism for PFL that involves Cys418 and Cys419 both as thiyl radicals, with distinct chemical functions. The structure reveals how the active site aligns the scissile bond of pyruvate for radical attack, prevents non-radical side reactions of the pyruvate, and confines radical migration. The structure shows CoA in a *syn* conformation awaiting pyruvate cleavage. By changing to an *anti*-conformation, without affecting the adenine binding mode of CoA, the thiol of CoA could pick up the acetyl group resulting from pyruvate cleavage.[26]

The stability of the glycyl radical has been attributed to the captodative effect.[16] The residues Cys418 and Cys419 are believed to facilitate the process of relaying the radical centre from Gly734 to the active site. The nature of this process can be deduced by the steric relationships among Ala418, Ala419 and Gly734 in the structure of doubly mutated C418A/C419A-PFL. The amino acids residues are aligned with just the right spacing to allow cysteinyl residues at positions 418 and

419 to mediate hydrogen transfer between Gly734 and ultimately Cys418 at the active site. The spacing allows hydrogen abstraction by the Gly734 radical from Cys419 to form the Cys419-thiyl radical, and hydrogen abstraction from Cys418 in turn would relay the radical centre from the Cys419-thiyl radical centre to Cys418 in the pyruvate binding site.[16]

Several residues near the active-site cysteines can also be ascribed roles in the catalytic mechanism: Arg176 and Arg435 are positioned near Cys419 and may bind pyruvate/formate, and Trp333 partially buries Cys418 being positioned directly over it (Figure i.13). Both cysteine residues are accessible to each other owing to their *cis* relationship at the tip of the finger.[10] Crystallisation of PFL with the substrate analogue oxamate reveals a phenylalanine Phe432 located underneath a putative formyl radical intermediate.[9]

Figure i.13. Pyruvate formate lyase. Trp333 sits 3.6 Å above Cys418 (left) and Phe432 3.4 Å from the substrate analogue oxamate (right).

The active site of methyl-CoM reductase, the enzyme responsible for the formation of methane under strictly anaerobic conditions, possesses many phenylalanine residues. In particular, Phe361 is only 3.8 Å from the α-carbon of a backbone thioglycine residue that is believed to be involved in the mechanism as a radical transfer agent (Figure i.14).[12]

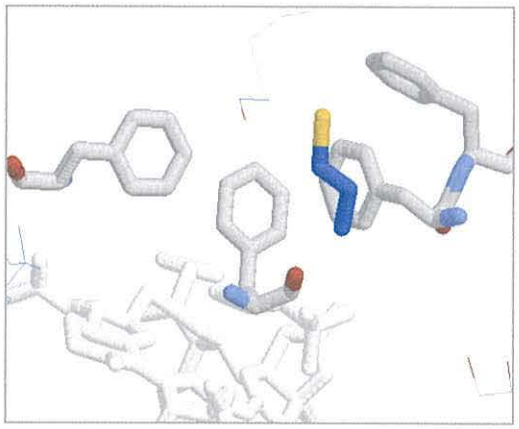

Figure i.14. Methyl-CoM reductase (Phe361, 3.8 Å from α-C).

From all of the above examples, high resolution X-ray crystal structures of radical dependent enzymes indicate that aromatic residues are common about 3.4-4.5 Å from putative radical sites. This fact, combined with site directed mutagenesis studies in many of these enzymes, suggests that these residues could play a key role in the maintenance of long-lived, stable radicals, essential in the functioning mechanism of such enzymes.[5-8] There is nonetheless a lack of understanding of the mechanism by which these radicals are stabilised and the exact role of the aromatic residues within the active site. Therefore, it is necessary to explore whether the aromatic residues are stabilising the radicals by electronic interaction or on the contrary, that these residues are simply providing a pocket capable of preserving the radical intermediate, or whether there is no effect and these residues are just there by coincidence. In this regard, studying radical stabilisation through chemical methods can shed light in the way these important biological systems work and help to understand and control radical behaviour. The use of small, appropriate model systems can assist in investigating the interactions between radicals and aromatics. Chapter One of this thesis will describe the synthesis of some such model systems with Chapters Two and Three discussing investigations into their chemistry.

From the chemical point of view, almost all radicals can be defined as 'free radicals', as they exist independently from other species. Therefore, a free radical can be defined as a species that contains one or more unpaired electrons. Such is their reactivity that, free radicals, when generated in the correct environment, can effect

chemistries that are not accessible by heterolytic mechanisms, as it has already been highlighted in the case of enzymatic reactions. Radicals are, for example, effective neighbouring groups for inducing nucleophilic substitution reactions, and are capable of abstracting hydrogen from inactivated carbon-hydrogen bonds.[4,27,28]

Typical reactions of radicals are dimerisation, disproportionation, addition to an unsaturated system, oxidation and reduction. Radical reactions have a marked susceptibility to polar effects in both the reactants and reagents. Many chemical transformations involving radicals are chain reactions, which consist of an initiation, propagation and a termination step.[29] Radical combination is the bonding of two radicals to give a covalent molecule. It is a termination step since it destroys radicals. As has previously been stated, radical abstraction involves the attack on a halogen atom as in, for example, the reaction of *tri*-butyl tin radicals with an alkyl halide (Figure i.15). These reactions can be considered as displacement reactions, which will be favoured if the bond being formed is stronger than the bond being broken.

Figure i.15. An example of radical abstraction.

An example of radical addition to multiple bonds is the anti-Markovnikov addition of hydrobromic acid to alkenes (Figure i.16). The addition of halogen acids to alkenes is a process that generally involves a carbocation intermediate. The resulting carbocation is formed on the carbon of the alkene that is best able to stabilise the cationic centre. However, the addition of hydrobromic acid to alkenes in the presence of peroxides converts the alkene into an alkyl bromide through a radical reaction. The overall addition of hydrobromic acid to the double bond is anti-Markovnikov, with the bromine being bonded to the alkene carbon that would form the most stable radical intermediate.

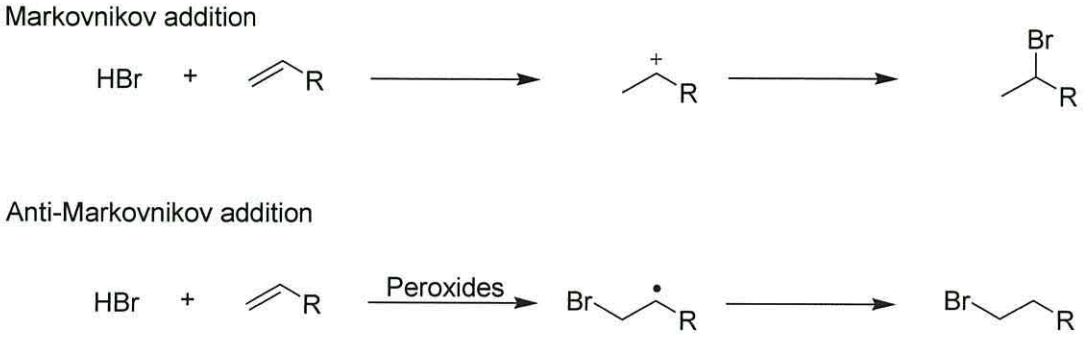

Figure i.16. Markovnikov (top) and anti-Markovnikov (bottom) HBr addition to a double bond.

Fragmentation is the microscopic reverse of radical addition. Fragmentations will be favoured when the newly formed bond has high bond energy. Rearrangements include intramolecular versions of atom abstraction, addition reactions leading to cyclisation and fragmentations. Disproportionation is an atom transfer between two radicals leading to two spin paired molecules.

Radicals are typically generated through homolytic fission of a covalent bond, so that each fragment keeps one electron. The main types of reactions leading to the production of radicals are summarised below.[30]

Compounds considered as possessing weak bonds are those with bond dissociation energies (BDE) less than 160 $kJmol^{-1}$ (eg. AIBN, Figure i.27). These compounds undergo homolysis at a convenient rate at temperatures below 150 °C. Examples of these types of compounds are acyl peroxides and azocompounds (Figure i.17). All such compounds have in common that they undergo homolytic cleavage to give stabilised radicals, often accompanied by the formation of small, stable, spin-paired molecules such as nitrogen. Homolysis is normally preferred in the gas phase. In solution, it tends to be unaffected by the nature of the solvent, indicating that there is little energy of interaction between the radical and the medium.[31]

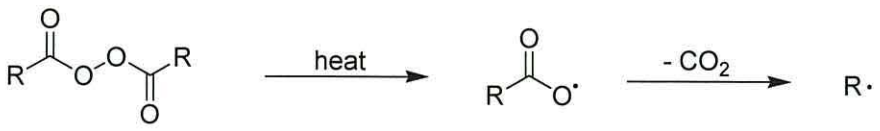

Figure i.17. Thermal cleavage of a peroxide.

Thermolysis is usually promoted by an initiator. A good initiator is azoisobutyronitrile (AIBN) (Figure i.18), since the C-N bond is very easily broken due its small dissociation energy.

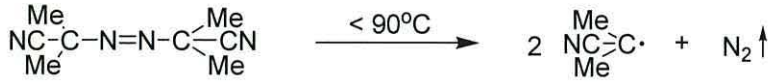

Figure i.18. AIBN as an initiator for radical reactions.

A more useful method to generate radicals is by photolysis of the α-bond of the carbonyl of a ketone (Figure i.19). In this case, the energy for bond dissociation can be supplied by either a quantum of radiation or by bombardment with an electron beam. Such methods of radical generation allow the lifetime of the radical to be easily monitored by ESR spectroscopy.

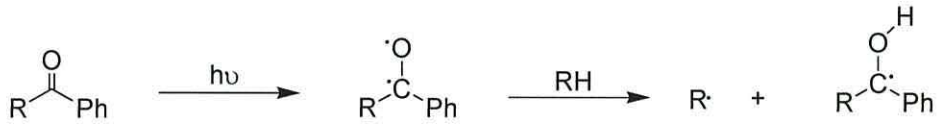

Figure i.19. Photolysis of a ketone.

The efficiency of ketone photolysis is very low in solution. However, it increases considerably when the carbonyl-alkyl bond is weakened, as is observed in the case of di-*t*-butyl ketone.[32] Generally, if the reaction products are unstable, and is better to generate the radical at room temperature or below, then photolysis is the preferred method, provided that the substrate absorbs light of an appropriate wavelength. Examples of the sort of compounds susceptible to photolytic cleavage include bromine (Figure i.20) and diaryl peroxides. The energy of light in the 300-600 nm range is 48-96 kcal mol^{-1} and is of the order of magnitude as some covalent bond energies.

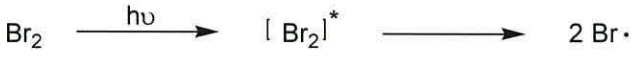

Figure i.20. Photochemical cleavage of bromine.

The donation or removal of one electron from a spin-paired molecule, through a process of either reduction or oxidation, will lead to the formation of a radical. Examples of this class of process are the reduction of hydrogen peroxide and the oxidation of carboxylate anions (Figure i.21).

Figure i.21. Electron oxidation of carboxylate anions.

The use of electrochemical methods provides a means for the generation of a radical species without the need for a chemical reagent. In particular, the use of cyclic voltammetry is especially useful in determining the electrochemical potential at which radical formation occurs.[33] A good precursor for the generation of a radical electrochemically is the carbon-halogen bond, whose electrolytic fission is known to be an irreversible process.[34]

Cyclic voltammetry (CV) is one of the most widely used techniques for the study of electroactive species and it is often the first experiment performed in an electroanalytical study.[35] This method enables a wide potential range to be scanned rapidly, uses a variable time scale and has a good sensitivity. All these factors, combined with ease of measurement, have resulted in extensive use of CV in the fields of organic and inorganic chemistry, electrochemistry and biochemistry.[36] The power of cyclic voltammetry results from its ability to rapidly provide considerable information on the thermodynamics of redox processes, on the kinetics of heterogeneous electron-transfer reaction, and on coupled chemical reactions or adsorption processes.[37]

In cyclic voltammetry the electrode potential is cycled, between the limits E_1 and E_2 and the cell current is recorded as a function of the applied potential (Figure i.22).[38]

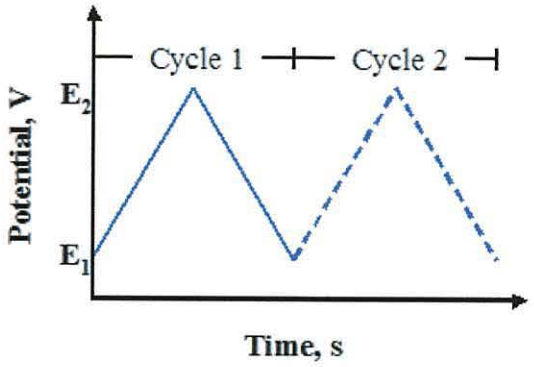

Figure i.22. Triangular waveform of a linear potential scan.

The repetitive triangular potential excitation signal for CV causes the potential of the working electrode to sweep back and forth between two designated values known as the switching potentials. Since the potential varies linearly with time, the horizontal axis can also be regard as a time axis.[36] The resulting plot of current (vertical axis) *versus* potential (horizontal axis) is termed a cyclic voltammogram. Current peaks are recorded that are due to oxidative and reductive electrochemical reactions.[38]

In cyclic voltammetry a waveform generator is used to produce the excitation signal, a potentiostat to apply this signal to an electrochemical cell, a current-to-voltage converter to measure the resulting current, and an XY recorder to display the voltammogram.[36] The potentiostat applies the desired potential between the working electrode (WE) and the reference electrode (RE). The working electrode is the electrode at which the reaction of interest occurs and is composed of a chemically inert material, such as platinum.[39] The reference electrode, e.g. a saturated calomel electrode (SCE), provides a stable and reproducible potential against which the potential of the WE is compared.[38] A third electrode, known as either the counter or secondary electrode (CE), is used to complete the electrical circuit and to transport the current required to sustain the electrolysis at the working electrode.[38]

To perform voltammetric measurements, three-electrode cells such as the one shown in Figure i.23 are commonly used.

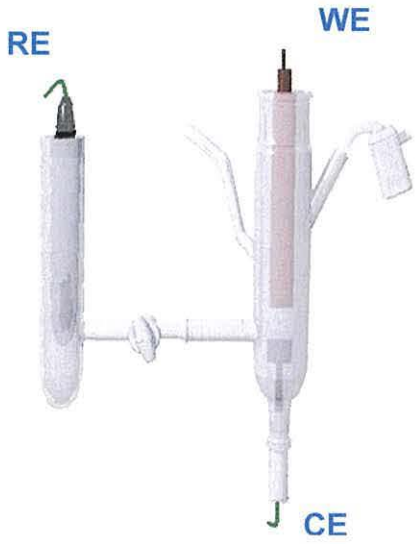

Figure i.23. Schematic diagram of an electrochemical cell. RE (reference electrode), WE (working electrode) and CE (counter electrode).

The three-electrode glass cell is filled with an analyte solution and the potential is cycled between the working electrode and the counter electrode. The potential is measured against the reference electrode.

Chapter Three will examine the electroreduction of the model systems in detail. This reduction can be achieved by applying a current using cyclic voltammetry as illustrated in Figure i.24.

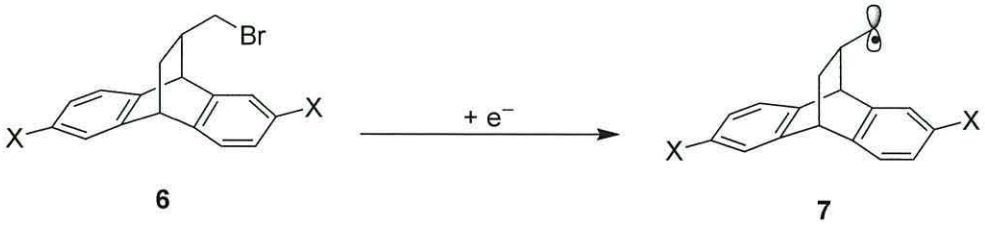

Figure i.24. Electrochemical generation of anthracene radicals.

Atom abstraction is one of the most versatile processes in order to generate a radical at a specific position. It requires the attack of a radical at the σ-bond of an atom such as a halogen, undergoing abstraction to form a new, more stable, product radical. *Tri*-butyl tin hydride is usually a good reagent to induce the attack at a halogen bond

because it is a very good hydrogen donor. Hydrogen transfer from organotin hydrides to radicals is indeed a very fast process ($k = 10^4$-10^6 $M^{-1}sec^{-1}$). Such is their reactivity that they react readily with oxygen in the air.[40] This atom abstraction process is known to take place by a S_H2 or bimolecular homolytic substitution through a partially negatively polarised transition state (Figure i.25).[41,42]

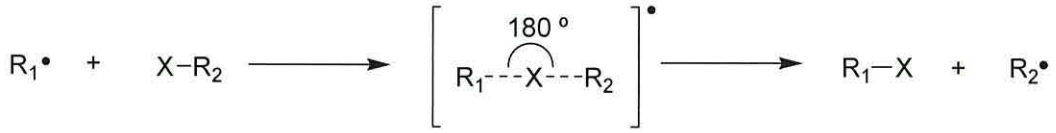

Figure i.25. Bimolecular homolytic substitution.

The homolytic fission of the carbon-halogen bond depends in the strength of the bond to be broken. This has been calculated as C-F (485 $kJmol^{-1}$), C-Cl (326 $kJmol^{-1}$), C-Br (280 $kJmol^{-1}$), C-I (213 $kJmol^{-1}$), C-H (414 $kJmol^{-1}$).[34] Although iodine-carbon is the easiest bond to be broken, as it requires the least amount of energy for cleavage, the bromine-carbon bond is usually utilised to generated radicals, as bromo derivatives are easily synthesised in the laboratory.

Usually the rate constant of radical reactions are calculated by product analysis of competing reactions.[43] Therefore, the relative reactivity of compounds bearing a carbon-bromine bond towards *tri*-butyl tin hydride can be determined. Consider two compounds, AH and BH. The rate of consumption of each from the starting mixture can be written as in Equation i.1 and Equation i.2.

$$\frac{-d[AH]}{dt} = K_{AH}[Br\cdot][AH]$$

Equation i.1. Rate of consumption for AH.

$$\frac{-d[BH]}{dt} = K_{BH}[Br\cdot][BH]$$

Equation i.2. Rate of consumption for BH.

Equation i.1 and Equation i.2 can be combined into Equation i.3.

$$\frac{d[AH]}{d[BH]} = \frac{K_{AH}[AH]}{K_{BH}[BH]}$$

Equation i.3. Relative rate of reaction.

Finally, Equation i.4 can be integrated over the limits of the initial (i) and final (f) concentrations of AH and BH to obtain the equation used in this thesis to calculate all relative rates.[42]

$$\frac{K_{AH}}{K_{BH}} = \frac{\ln\left([AH]_i / [AH]_f\right)}{\ln\left([BH]_i / [BH]_f\right)}$$

Equation i.4. Equation to calculate the relative rates of reaction.

Chapter Two discusses the relative reactivities of anthracene and acyclic derivatives towards *tri*-butyl tin hydride. The bromo derivative **6** shown below can be treated with *tri*-butyl tin hydride or *di*-tributyl tin (Figure i.26) to afford the corresponding radical **7**. Other halo derivatives can also be treated in a similar fashion.

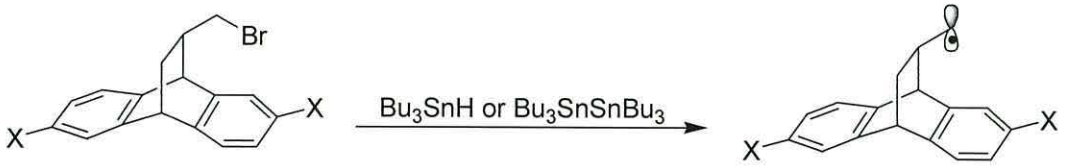

6 **7**

Figure i.26. Generation of radicals *via* chemical treatment.

Reactivity depends upon which radical is studied and with what substrates that radical is presented. When a free radical reacts with a non-radical, a new radical results, and a chain reaction can be initiated. The resultant radical may add to another neutral molecule. In this case, the adduct must still have an unpaired

electron. The radical may be a reducing agent; therefore donating a single electron either to a non-radical or to a recipient molecule that has an unpaired electron. It also may be an oxidising agent; hence accepting a single electron from a non-radical. The non-radical must have an unpaired electron left behind. It could also abstract a hydrogen atom from a C-H bond. As the hydrogen atom would only have one electron, an unpaired electron must be left on the carbon. In this way, a chain reaction generates a steady-state concentration of free radicals.

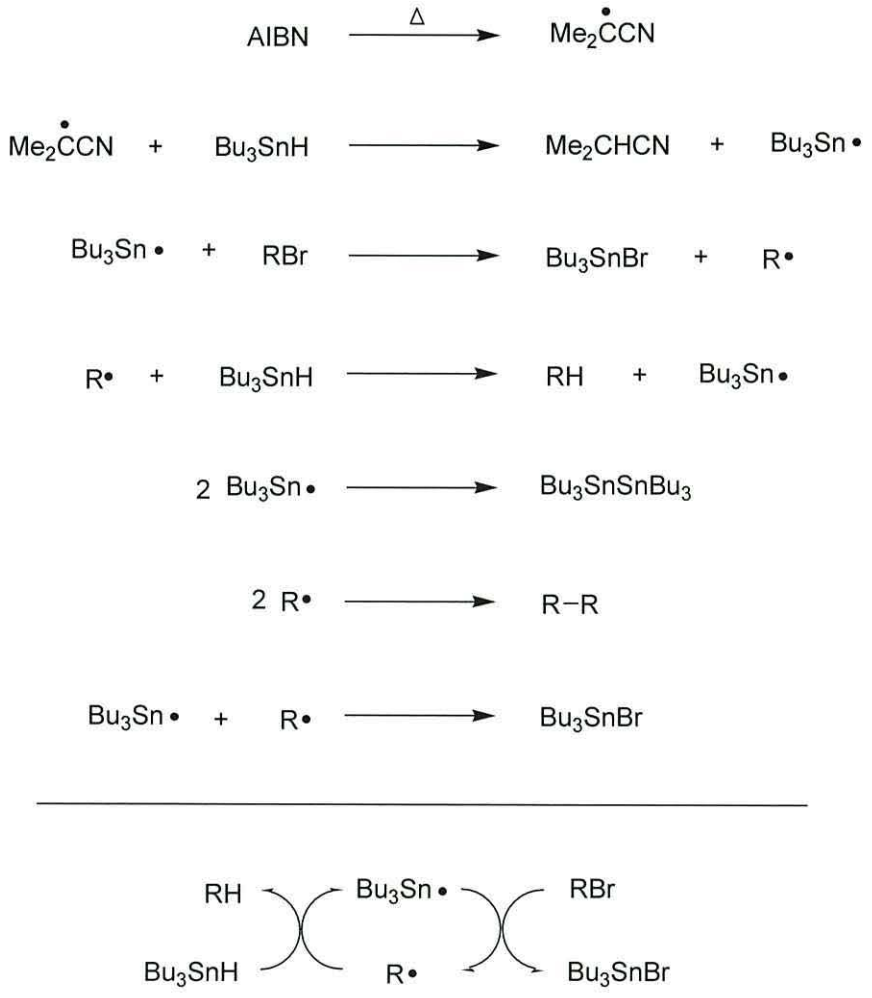

Figure i.27. Example of a chain reaction initiated by AIBN.

A typical example of a chain reaction is the reduction of alkyl bromides by *tri*-butyl tin hydride, which can be induced on heating with the initiator AIBN (Figure i.27). Initiation consists of thermal dissociation of AIBN to isobutyronitrile radicals that

can then abstract hydrogen from the weak tin-hydrogen bond to give the key *tri*-butyl tin radicals. Reaction of *tri*-butyl tin radicals with the alkyl bromide to give alkyl radicals is favoured by the relatively high tin-bromine bond energy. The second propagation step is favoured by the relatively weak tin-hydrogen bond being broken, coupled with the relatively strong carbon-hydrogen bond formed.[32]

Radicals are usually directly detected by one major technique: electron spin resonance (ESR), also called electron paramagnetic resonance (EPR). This technique is used to detect the presence and concentration of radicals at very low limits, down to 10^{-8} mol dm^{-3}. The principles behind this technique are similar to those of NMR, except that detection of changes in the electronic spin, rather than nuclear spin, are measured upon application of an external magnetic field. As a result, only those species with unpaired spin, which are paramagnetic, can give rise to an ESR spectrum. Consequently, the unpaired electron under the magnetic field will undergo transitions between spin states if energy of the correct frequency is applied. The difference in energy of these spin states is given by Equation i.5, where g is a dimensionless proportionality constant, B is the magnetic induction and μ_B is the Bohr magneton, equal to $eh/4\pi m_e$, where e and m_e are the charge and mass of the electron, respectively, and h is the Planck's constant.[44]

$$\Delta E = h\mu = g\mu_B B = g\frac{eh}{4\pi m_e}B$$

Equation i.5. Difference in energy between spin states in a given electron transition.

ESR spectrometers operate with less powerful magnets than NMR instruments. In order to improve the intensity of the absorption signal, the spectrum is recorded as the first derivative instead of the direct absorption curve in which a conventional NMR spectrum is presented, i.e. a singlet in NMR would appear as two singlets in ESR, one with positive sign and another with negative sign (Figure i.28).

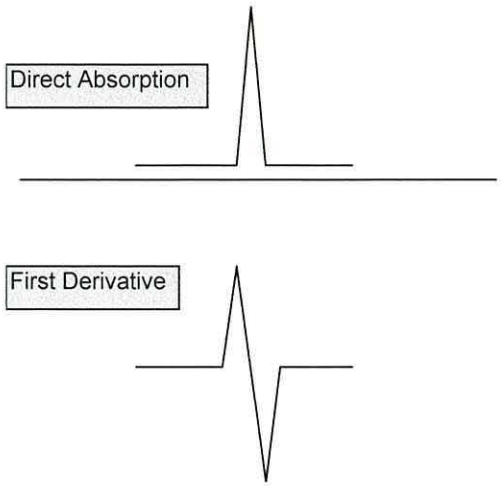

Figure i.28. The difference in appearance of NMR spectra *vs.* ESR spectra.

ESR spectra are characterised by three parameters, *g*-factors, hyperfine splitting constants and the line widths. The *g*-factor is similar to the chemical shift in NMR. Its value depends on the orientation of the radical with respect to the applied magnetic induction. These anisotropic effects are averaged for small radicals in solution where rapid tumbling occurs. In fact, the differences between *g*-factors in different molecules are very small and become only especially relevant when the radicals are embedded in single crystals.

The hyperfine splitting (A) is the most useful characteristic of ESR spectra for elucidating the structure and the shape of the radical under study. This splitting arises from the interaction between the unpaired electron and the neighbouring nuclei. The separation between two peaks is known as the hyperfine coupling constant, measured in Gauss (G). The splitting depends on the nuclear spin quantum number, I, in such a way that the interaction of an unpaired electron with a nucleus spin, I, gives (2I + 1) lines. Therefore, analysis of the hyperfine structure can lead to assignments of the radical structure, and in particular the neighbouring atoms.[45]

ESR spectroscopy is especially valuable, not only because it can measure radicals *in situ* but also because it can provide information about the structure of the molecule by analysis of the hyperfine structure. It is also a versatile technique in the sense that virtually every method available in order to generate a radical can be fitted within

experimental procedures. However, sometimes a high enough concentration of radicals is difficult to obtain. In these cases, the higher the working frequency, the higher the sensitivity. Weak interactions are often difficult to obtain. In such case, an ESR technique called electron nuclear double resonance (ENDOR) can be used in order to improve the sensitivity.[44] ENDOR technique needs nonetheless a higher concentration of radicals. The ESR spectra of radicals generated from anthracene derivatives are discussed in Chapter Two, whose hyperfine structure would give us important information about the radical geometry and interactions.

Free radicals are generally regarded as metastable species due to their high energy and kinetic reactivity. It is this high-energy that makes observation and characterisation difficult. The high reactivity arises from the unpaired electron, which is looking to pair with a second electron to produce a filled outer shell. Thus the driving force for radical reactions is the formation of a covalent bond.

A system is said to be thermodynamically stable if the corresponding standard free enthalpy change is largely positive. The thermodynamic stability of radicals can be described in terms of how easily bonds are broken homolytically to form the corresponding radical. The energy necessary to break a bond homolytically is the bond dissociation energy (BDE), whose magnitude depends on the thermodynamic stability of the product radicals. The more stable the radicals, the lower the BDE. The stability of the radicals resulting from the cleavage of a molecule can be therefore compared by looking at the relative value of BDE for individual bonds within that molecule. The strongest bonds are formed when orbitals of similar energy overlap. Some average BDE's have been calculated by different authors, and from these values it is possible to predict which bonds more easily break within a molecule.[43,46,47]

Whereas the thermodynamic stability of radicals is related to electronic effects, the lifetime is principally determined by steric factors. The larger the substituents around a radical centre, the more stable the radical will be and the greater its lifetime. Radical lifetimes range from about $t_{1/2} = 0.2 \times 10^{-3}$ s to around 20 hours or longer.[42]

Generally, when a radical possesses a half-life greater than 10^{-3} s, it is regarded as a persistent or stable radical. Leroy classified the radicals according to their relative stability towards the methyl radical: a radical is transient if its lifetime is comparable to that of methyl radical, it is persistent if its lifetime is significantly greater than that of methyl and it is kinetically stable if it can be handled and stored without special precautions.[48]

Figure i.29. Relative stability of alkyl radicals.

As with carbocations, the stability order of free radicals is tertiary > secondary > primary > methyl (Figure i.29). There are two possible structures for simple alkyl radicals. They might have sp^2-bonding, in which case the structure would be planar, with the odd electron in a *p*-orbital. Alternatively, the bonding might be sp^3, which would make the structure pyramidal and place the odd electron in a sp^3-orbital. ESR spectra of simple alkyl radicals indicate that these radicals have planar structures. This also explains the known loss of optical activity when a free radical is generated at an asymmetric carbon. Nevertheless, pyramidal structures are not impossible as evidence from studies on bridgehead compounds show. Sometimes, the energy difference between planar and pyramidal structure is not great: when the carbon is connected to atoms of high electronegativity (e.g. CF_3), the pyramidal shape is preferred.[31]

Where there are resonance possibilities, the stability of free radicals increases due to the interaction of the *p*-orbital with either a π-bond or lone pair (Figure i.30). The consequent electron delocalisation leads to a lower BDE. Benzylic and allylic radicals are more stable than simple alkyl radicals due to resonance by conjugation. Planarity helps electron delocalisation and therefore makes the radical more stable by conjugation. In general, the more resonance hybrids that can be drawn for a radical, the greater the stability.[31]

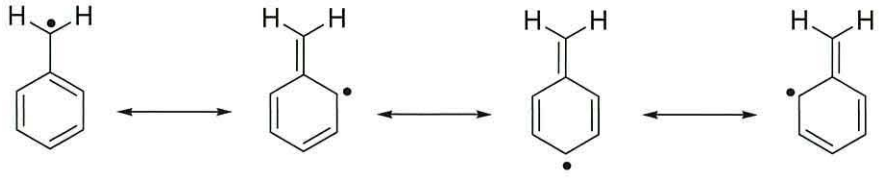

Figure i.30. Resonance structures for benzyl radical.

In addition to conjugation, a phenomenon known as hyperconjugation can add to the stability of radicals. Hyperconjugation describes the interaction of the *p*-orbital of the radical with a pair of bonding electrons in a neighbouring σ-bond. Electrons in the filled (C_{sp3}-H_{1s}) σ-bond can be donated to the semi-occupied *p*-orbital of the radical (Figure i.31). The resulting delocalisation has a stabilising effect.

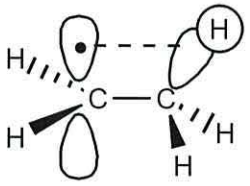

Figure i.31. Example of hyperconjugation in the ethyl radical.

Radicals can also be highly stabilised when both electron-donating and withdrawing groups are in the α-position with respect to the radical, as explained by the captodative effect.[49] When both types of substituents are present, there is a synergistic effect between them. As a result, the radical stabilisation is greater than the sum of the stability inferred by the two separate substituents. This is termed captodative stabilisation and has been reported in numerous articles.[49-52] For instance, the enhanced stability of the glycyl radical in Pyruvate Formate Lyase (PFL) has been attributed in part to the summation of the effects of resonance electron withdrawal by the glycyl-carbonyl group and the electron donation by the adjacent amide nitrogen through its lone electron pair.[16]

Not all the ways in which radicals can be stabilised are well understood, however, particularly those factors that seem to arise in biological systems. Therefore, it is important to discern which factors may play a role. A good way to explore such

hypothesis is by testing them in models. It is accepted that radicals are usually stabilised by through bond interactions. Evidence from biological systems seems to indicate that interactions through space can have an effect on the stability of reactive intermediates. Such interactions may also be relevant for radical systems.

Cations bind to the π-face of an aromatic structure through an unexpectedly strong, non-covalent force termed the cation-π interaction. The reasons for these interactions have been the subject of numerous studies and they are thought be one of the driving forces in molecular recognition processes.[53-55] Chronologically, it was already in 1981 when Kebarle and co-workers[56] demonstrated that the interaction between a molecule of benzene and K^+ was comparable in strength to the interaction between K^+ and a single water molecule.[56] Numerous studies concerning the interaction between metal cations and aromatic systems have been reported since then. For instance, Gokel[57] demonstrated the first ever evidence for the cation-π interaction between the phenolic side chain and a K^+ cation, whose relative distance to one another was found to be of only 3.26 Å.

From the electrostatic point of view, the dominating component of a cationic-π interaction is the attraction of the charge towards the quadrupole created by the electron cloud of the aromatic ring. It has been suggested that the cation creates an electric field, which polarises the π-electron cloud of the aromatic system inducing a dipole moment in the ring, which in turn interacts with the polarising charge *via* its electrostatic potential. Furthermore, it has recently been proposed that cation interactions are formed when the distance is less than 3.7 Å and the angle of approach does not exceed 45 °.[53]

The interaction between ammonium ions and aromatic systems has also been studied using *ab initio* calculations.[58] These studies suggested that positively charged side chains make enthalpically favourable interactions with the π-electron cloud of aromatic side chains within van der Waals contact distances.

Cation-π interactions have been identified in biological systems. Cation-π interactions can occur between the cationic side chains of either lysine or arginine and the aromatic side chains of phenylalanine **1**, tyrosine **3** or tryptophan **2**.[59] Burley and Petsko[54] examined the frequency and geometry of interactions between the side chains of phenylalanine **1**, tyrosine **3** and tryptophan **2**, and the amino groups of lysine, arginine, asparagine, glutamine and histidine by looking at protein crystal structures. They found that beyond 6 Å, the observed frequency of amino-aromatic contacts is nearly constant, suggesting that amino groups prefer van der Waals contact with aromatic groups. They concluded that amino and aromatic groups in proteins are preferentially separated by between 3.4-6.0 Å, hence defining the amino aromatic interaction as 3.4-6.0 Å. The most common cation-π interaction is between neighbouring residues in the amino acid sequence, with 7.3 % of the interactions occurring between adjacent residues.[59] Over 70 % of all arginine side chains are near an aromatic and 26 % of all tryptophans are reported as being involved in at least one energetically significant cation-π interaction.[59] However, on average one amino group participates in only one amino aromatic contact, and the preferred interaction geometry places the amino group adjacent to the face of the aromatic ring.[54] It is currently generally accepted that, although they are not crucial for the stability of the proteins, cation-π interactions could influence their folding.[60-62] Other studies have established a role for cation-π interactions in biological recognition, especially in the binding of acetylcholine.[63,64] The active site of acetylcholinoesterase is composed of two moieties, the estearic and the anionic subsites.[65,66] The most remarkable feature of the structure is the presence of a deep narrow gorge in the active site, which contains fourteen aromatic residues that are within van der Waals distance, at about 3.5 Å from the quaternary ammonium moiety of choline.[63]

In a related fashion, enzymes also show the stabilisation of cationic intermediates by aromatic systems. Pentalene synthase is an enzyme responsible for the cyclisation of farnesyl diphosphate into the tricyclic hydrocarbon pentalene, a tricyclic sesquiterpene that is important because it is the hydrocarbon precursor of the pentalenolactone family of antibiotics.[67] This enzyme could well provide an example of how aromatic residues may be involved in the stabilisation of cationic

intermediates. From its three dimensional structure, at 2.6 Å resolution, it can be observed that the active site cavity is predominantly hydrophobic in nature and contains aromatic residues, Phe76, Phe57, Phe77, and Trp308, and other aliphatic residues. The upper region of the active site cavity, in contrast, is more hydrophilic in nature and includes the polar or charged side chains of His309, Asn219, Arg44, Arg157, Arg175, Lys226, and Arg230. The mechanism of action of Pentalene synthase is known to proceed *via* the formation of several stabilised carbocationic intermediates. According to Lesburg,[67] Phe77 and Asn219 are optimally located to stabilise highly reactive carbocation intermediates through favourable quadrupole-charge and dipole-charge interactions (Figure i.32).

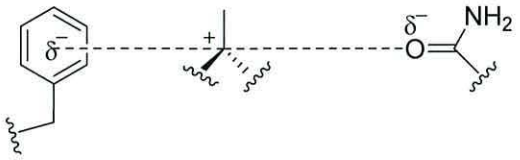

Figure i.32. Proposed mechanism of stabilisation of carbocationic intermediates in Pentalene Synthase.[67]

To examine cationic-π interactions, synthetic models have also been utilised. Paracyclophane derivatives, and in particular those of [9]-paracyclophane have been used as model compounds to study aromatic stabilisation of cationic reaction intermediates.[68] The fate of carbonium ions has been examined when generated at different distances from, and over several positions in, the face of a benzene ring.[69-71] The solvolysis of some paracyclophane tosylates has been studied by Cram[69] and the reported rates for each reaction centre are marked in Figure i.33. The rate of the reaction increases considerably when the carbonium ion intermediate is formed over the face of the benzene ring, especially at the 4-position, suggesting that the π-electron cloud is involved in the process.

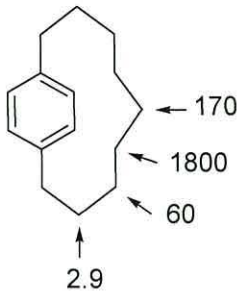

Figure i.33. Rate of solvolysis for paracyclophane tosylates.[69]

Paracyclophane derivatives **8** are appropriate models to study cationic-π interactions as they possess rigid geometry, which allows individual factors in their conformation to be studied in detail. As it can be appreciated from Figure i.34, the carbon number five of the paracyclophane structure is located right above the aromatic electron cloud ring at a distance of between 3.5-4.5 Å.

Figure i.34. Three dimensional structure of [9]-Paracyclophane.

There is evidence that radicals, as well as cations, could be stabilised by aromatic systems. Previous work carried out by Russell,[72,73] in which he studied the photochlorination of 2,3 –dimethylbutane (DMB), showed that the distribution of products resulting from the radical-based reaction of DMB was dependent upon the solvent used. Whereas aromatic solvents dramatically alter the ratio of the products of the photochemical chlorination of DMB, aliphatic solvents did not have any effect, even using solvents with a wide range of polarity. When monochlorination of DMB was performed using an aliphatic solvent, chlorine atoms reacted at the tertiary C-H centre around four times as readily as at the primary C-H centre. When benzene

was used as the solvent, the substitution selectivity increased to a factor of around sixty. He postulated that this effect could be due to the association of the chlorine atom with the π-electrons of the aromatic system. This association was hypothesised to produce a complexed chlorine atom that has a lower reactivity and hence a greater selectivity than a free chlorine atom. This is supported by the fact that the solvent effect for photochlorination is small for aromatics containing an electron-withdrawing substituent and large for aromatics with electron releasing substituents. This observation suggested the solvent effect of a given aromatic solvent would thus increase with the stability of the chloro-aromatic complex formed. In addition, the solvent effect was found to be dependent on the concentration of aromatic solvent but not on the concentration of DMB, additionally indicating the role of the solvent in this reaction.[72,73] Further studies using laser flash photolytic techniques have confirmed the role of the solvent in the photochlorination of DMB and the formation of a π-complex.[74,75]

Synthetic model compounds, such as [9]-paracyclophane derivatives **8** (Figure i.35) would make excellent models to probe the effect of aromatic residues in the stabilisation of reactive intermediates.

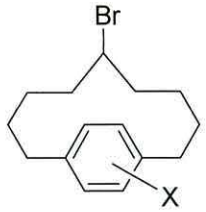

8

Figure i.35. Paracyclophane models, where X = EDG or EWG.

Paracyclophanes are ideally structured to shed light on the biological importance of aromatic-radical interactions since the distance between aromatic residues and radical intermediates in the models is constrained to a similar distance to that found in the enzyme active sites of interest. They also have enough rigidity to hold the central carbon of the aliphatic ring above the aromatic ring within a distance of 2.4-3.5 Å (Table i.1), making them excellent model compounds to study *p*-interactions

(*e.g.* cation-π interactions). These derivatives additionally provide a means for systematic variation of substituents at the benzene ring, which allows electronic effects to be studied. The construction of models is particularly useful as it is extremely difficult to carry out these studies in biological systems. The synthesis and properties of a number of [9]-paracyclophanes carrying different functional groups have been previously described in the literature, indicating these models should be easily accessible synthetic targets.[68,71]

Table i.1. Transannular distances between some carbons in 5-keto-[9]-paracyclophane.

Carbons	Distance (Å)
C_2-C_{13}	2.4
C_3- C_{13}	2.8
C_4- C_{13}	3.2
C_4- C_{12}	2.7
C_5- C_{13}	3.0

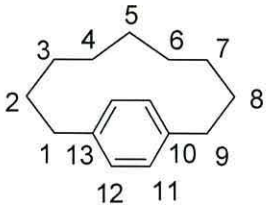

Figure i.36. Numbering of [9]-paracyclophane.

A series of homologous paracyclophanes have already been prepared by Cram and co-workers.[76-78] The acyloin ring closure however fails when the bridge formed consists of less than eight carbon atoms. In theory, [7]-paracyclophane would contain about the same strain energy as does cyclopropane, and it should therefore be thermodynamically stable enough to isolate. In practice, however, when the product is rather thermodynamically unstable, the ring contraction needs a clean process with a large driving force.[79] [9]-Paracyclophane thus is the smallest cycle of its kind that has been prepared. The acyloin ring closure that leads to it is reported in the

literature to afford a 25 % yield.[76,80] Chapter Four discusses the attempts to synthesise paracyclophane molecules for use as model compounds to explore free radical π-interactions.

Alternative models suitable to study radical stability may be anthracene adduct derivatives of general structure **2**, as the system possesses enough rigidity to hold a radical above the aromatic ring. Such models are designed to constrain the radical in a similar conformation and spatial orientation as the putative radical sites identified in the X-ray structures of enzymes with relation to the aromatic moiety. In fact, a tetrameric unit of the type of anthracene adduct **6** shown in Figure i.37 has previously been used as a host model to study the interaction of the aromatic moiety with quaternary ammonium compounds.[81] From these studies, it was found that there exists a cation-π interaction between the ammonium ion and the aromatic rings of anthracene with a dissociation constant of K_d = 50 μM, a value comparable to those of the biological recognition sites, indicating the suitability of such models in the investigation of aromatic interactions.

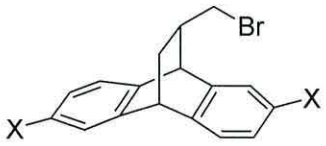

6

Figure i.37. Anthracene models, where X = EWG or EDG.

The stability of the radicals formed by radical abstraction of the bromine moiety can be compared with respect to less rigid systems such as acyclic derivatives **9**, which allow mobility of the alkyl chain, and with a system that does not possess the aromatic moiety **10**, both shown in Figure i.38. These studies could give a deeper insight as to what influence the aromatic moiety has in the formation and subsequent reactivity of the radical.

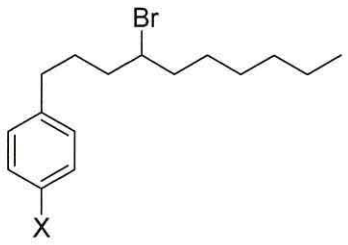

9

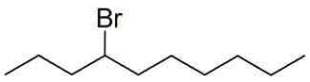

10

Figure i.38. Acyclic models **9** and **10**.

Systematic variation of the substituent in all of the models allows the study of the different electronic density of the aromatic ring upon the stability of the radical. If the electronic density at the aromatic ring has an effect, then the stability of the radical will vary by changing the type of substituent. In principle, as happens with carbocations, a free radical is deficient in electrons, hence would be predicted as being stabilised by a higher electron density. Chapter One describes the preparation of anthracene and acyclic models, appropriate to examine such effects.

Chapter 1

Synthesis of anthracene and acyclic models

As has been outlined in the general introduction, two different types of model compounds have been selected in order to study the influence of the aromatic moiety in the reactions of radicals.

Anthracene compounds **6** of the type shown in Figure 1.1 have a suitable geometric structure to study the interaction between the aromatic ring and a radical intermediate. The model allows for the radical to be formed above the aromatic ring whilst maintaining a relatively restricted geometry. The presence of a given substituent at both of the aromatic rings allows the interaction to be studied in terms of the variation in electronic density of the ring.

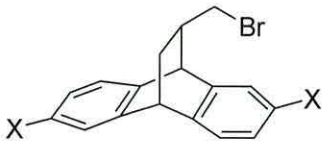

X = EWG or EDG.

6

Figure 1.1. Anthracene models **6** with either electron donating (EDG) or electron withdrawing (EWG) substituents.

Chemical modelling of structurally different types of compounds will allow a comparison with the reactivity of the anthracene model **6** towards halide abstraction to be made. The acyclic compounds **9** of the type shown in Figure 1.2 have been chosen because they provide a model that possesses the same characteristics as the anthracene models, *i.e.* an alkyl chain of ten carbons with bromine attached at the 4-position, which is required to generate a radical, and an aromatic ring at the end of the alkyl chain, essential to study whether or not this moiety influences the stability

of the radical. The main difference with respect to the anthracene models is the fact that these systems are much less restricted by geometry, allowing the radical to vary in distance from the aromatic ring. The alkyl chain also possesses more conformational freedom, resulting in a gain of entropy in the system, relative to the anthracene models **6**.

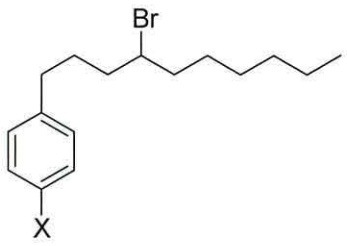

9

Figure 1.2. Acyclic models **9** with an aromatic ring varying in electronic density.

Acyclic compound **10** has also been chosen because it does not posses the aromatic ring, but maintains the bromo group necessary to generate the radical and a 10-carbon chain. This model acts as a control model system to which the reactivity of the other two models can be compared.

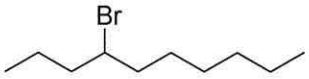

10

Figure 1.3. Acyclic model **10** without the aromatic ring.

Paracyclophane models will be addressed separately in Chapter Four.

Results

The synthesis of 2,6-substituted anthracene derivatives **6** is challenging since there are no anthracene derivatives functionalised at the 2,6-position commercially available. In addition, anthracenes and anthraquinones are often difficult to handle and in many cases very insoluble materials in common organic solvents. The results section of this Chapter is divided in six main parts in such a way that the compounds have been grouped according to their structural characteristics.

Reaction of benzoquinone **11** with isoprene **12** at room temperature, in an autoclave under pressure, and subsequent oxidation by atmospheric oxygen in an ethanolic solution containing 5 % potassium hydroxide, afforded the 2,6- and 2,7-dimethylanthraquinones **13** and **14**, as outlined in Scheme 1.1.

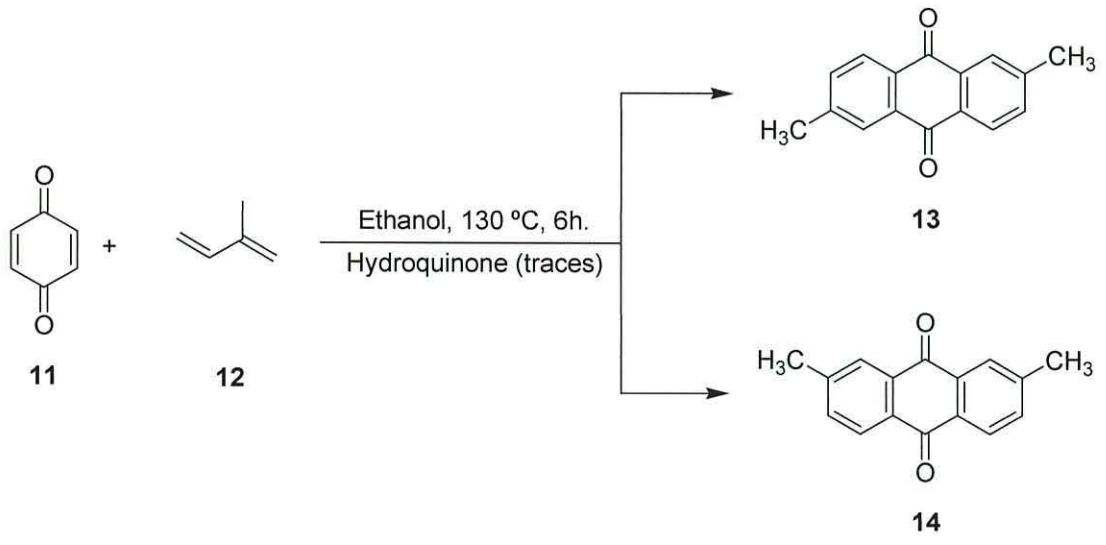

Scheme 1.1. Synthesis of 2,6- and 2,7-dimethylanthraquinone **13** and **14**.

Attempted separation of the two reaction products, anthraquinones **13** and **14**, by fractional crystallisation using ethanolic solution, was unsuccessful. Nevertheless, a few milligrams of each of the two isomers could be isolated by fractional crystallisation. The mixture of both isomers was characterised by ^{1}H NMR spectral analysis. The expected pattern for the aromatic protons was identified in the

spectrum, and they appear as two distinctive doublets, δ 8.24 and δ 7.58, and one singlet at δ 8.09. The methyl groups appear as a singlet at δ 2.54. Additionally, the ^{13}C NMR spectrum showed the carbonyl group at δ 183.0. The molecular ion, at m/*z* 236, was also found by GCMS analysis.

Hydroxyanthraquinone **16** was made from diaminoanthraquinone **15** by a typical Sandmeyer reaction in sulphuric acid using sodium nitrite (Scheme 1.2).

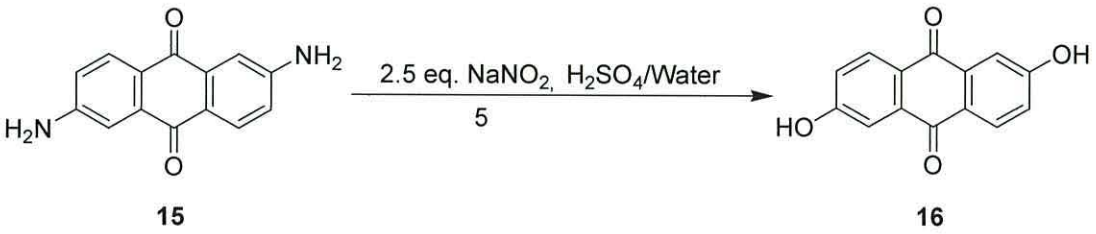

15 **16**

Scheme 1.2. Synthesis of 2,6-dihydroxyanthraquinone **16**.

Hydroxyanthraquinone **16** was very insoluble in general organic solvents. The ^{1}H NMR spectrum was made in DMSO-d_6, and confirmed the presence of the phenolic groups at δ 10.5, integrating as two hydrogens.

2,6-Dibromoanthraquinone **17** was obtained by a Sandmeyer reaction using *tert*-butyl nitrite and copper (II) bromide in anhydrous conditions (Scheme 1.3).

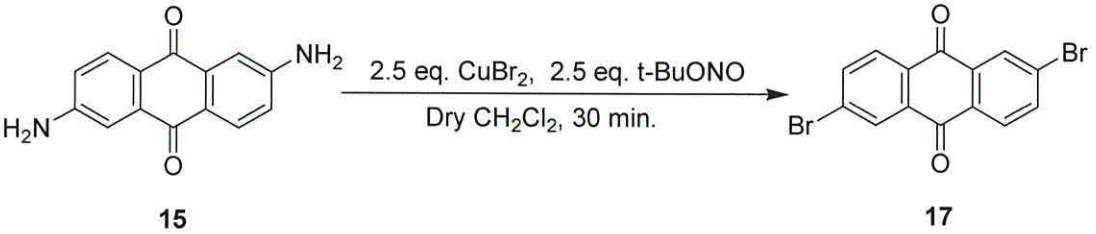

15 **17**

Scheme 1.3. Synthesis of 2,6-dibromoanthraquinone **17**.

Aqueous work-up yielded a brownish solid, which was recrystallised from hot toluene to afford the bromide product derivative **17** as a yellow powder. This was characterised by spectroscopic methods. The ^{1}H NMR spectrum showed the

expected pattern for a 2,6-disubstituted anthraquinone with three signals at δ 8.37 (2H), δ 8.10 (2H) and δ 7.88 (2H). Further analysis by mass spectrometry confirmed the presence of the molecular ions at m/*z* 364, 366 and 368, in ratio 1:2:1, confirming the presence of two bromine atoms in the molecule.

2,6-Diaminoanthraquinone **15**, the only 2,6-disubstituted derivative commercially available, was reduced to its anthracene analogue. Two methods were used with different results. Reduction of amino derivative **15** using hydriodic acid as the reducing agent in acetic acid medium was unsuccessful (Scheme 1.4).

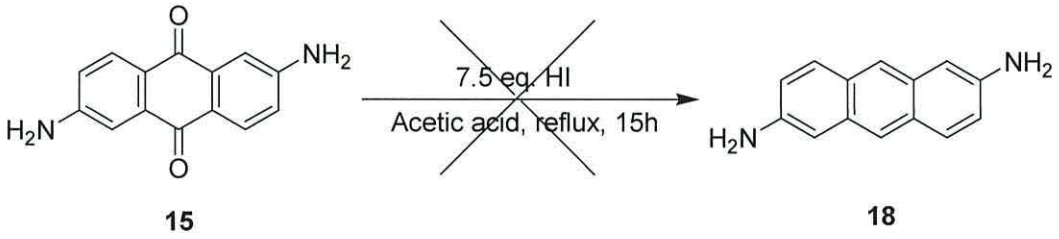

15 **18**

Scheme 1.4. Attempted reduction of 2,6-diaminoanthraquinone **15** by hydriodic acid.

Work-up produced an orange solid, which was unable to be characterised by NMR spectral analysis or GCMS for different reasons. While the ^{1}H NMR spectrum showed the formation of what is thought to be a mixture of partially reduced material, the GCMS did not show any identifiable peaks, indicating a non-volatile substance.

The reduction of 2,6-diaminoanthraquinone **15** was carried out in a 10 % sodium hydroxide aqueous solution using zinc dust as the reducing agent, as outlined in Scheme 1.5.

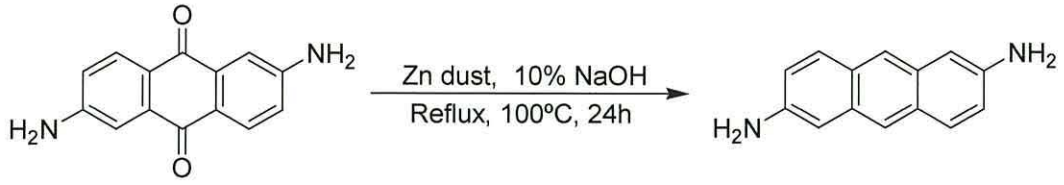

15 **18**

Scheme 1.5. Synthesis of 2,6-diamino anthracene **18**.

The reduction was completed after 24 hours. It was monitored by the change of colour in the solution. The colour changes from deep red, then purple, different shades of yellow and finally green. When the reaction was stopped after eight hours, a yellow colour was apparent and negligible product was recovered. A green colour was indicative that the reaction was fully completed after 24 hours. The reaction was worked up by hot filtration and the resulting zinc residue was extracted by continuous extraction using a soxhlet unit and acetone as the solvent of choice. The resulting acetone solution was green fluorescent, which was a sign that indicated the presence of a highly conjugated system, such as the anthracene moiety. The product, anthracene derivative **18**, was characterised by ^{1}H NMR spectral analysis. The aromatic protons followed the pattern for a 2,6-disubstituted anthracene, as they appeared as two doublets at δ 7.63 (2H) and 6.92 (2H), and two singlets at δ 7.82 (2H) and 6.79 (2H), with the shifts similar in value to those found in the literature for related compounds.[82]

The 2,6-dimethylanthraquinone derivative **13** was also reduced using the same procedure as for 2,6-diaminoanthraquinone **15**, as illustrated in Scheme 1.6.

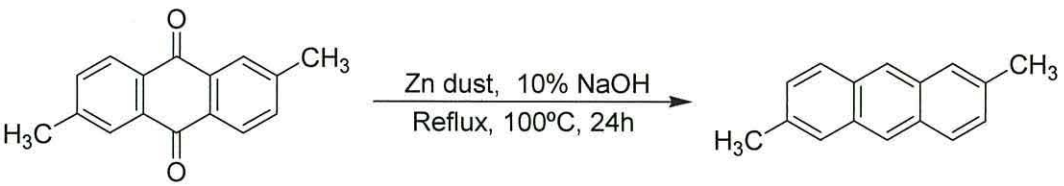

13 **19**

Scheme 1.6. Synthesis of 2,6-dimethylanthracene **19** by reduction of 2,6-dimethylanthraquinone **13**.

After hot filtration, the product was extracted from the solid residue by repetitive extraction using hot toluene as the solvent of choice. The product, anthracene derivative **19** was, as for 2,6-diaminoanthracene **18**, green fluorescent and was characterised by ^{1}H NMR spectral analysis. The presence of two doublets δ 8.19 (2H, *J* 7.9) and 7.59 (2H, *J* 7.9), and two singlets, δ 7.27 (2H) and 8.09 (2H), was evidence of the 2,6-disubstituted anthracene moiety. Furthermore, its melting point, 230-231 °C, was consistent with the literature value of 224-225 °C.[83]

Dimethylanthraquinone **13** was reduced by an alternative method, using zinc and ammonia in the presence of pyridine and copper sulfate as outlined in Scheme 1.7.

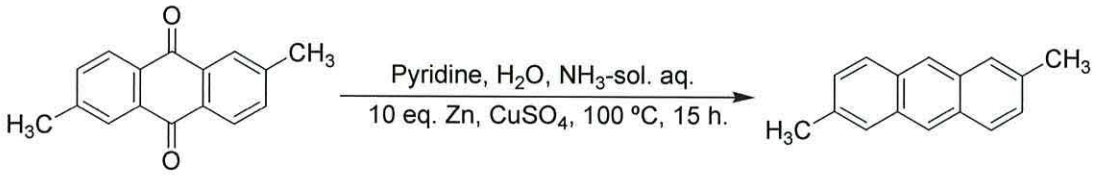

13 **19**

Scheme 1.7. Reduction of 2,6-dimethylanthraquinone **13** with zinc and ammonia.

The product **19**, obtained in a 29 % yield, was extracted from the reaction mixture with toluene, in which it was green fluorescent as a positive sign of the formation of anthracene derivative. Analysis of anthracene **19** confirmed its structure. The molecular ion was found by GCMS, at m/*z* 206. In addition, the ^{1}H NMR spectrum showed the aromatic protons as two doublets, δ 8.19 (2H) and 7.59 (2H), and two singlets 8.09 (2H) and 7.27 (2H), which are characteristic of a 2,6-disubstituted anthracene. Furthermore, the absence of a carbonyl peak in the ^{13}C NMR spectrum demonstrated complete reduction of the quinone moiety.

Another anthraquinone, 2,6-dibromoanthraquinone **19**, was also reduced to its corresponding anthracene derivative **20**. Different methodologies were used with mixed results. Reduction of bromo derivative **19** direct to the corresponding anthracene derivative **20** was attempted using zinc in an aqueous ammonia solution as described in Scheme 1.8.

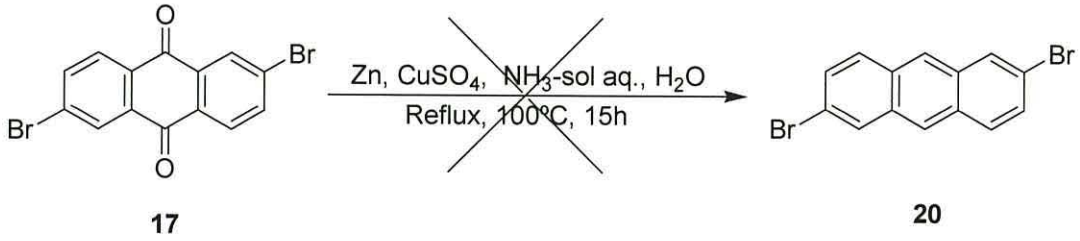

17 20

Scheme 1.8. Reduction of 2,6-dibromoanthraquinone **17** by zinc powder in ammonia solution.

Work-up, followed by extraction of the zinc residue with hot toluene, gave a green fluorescent yellow powder, which indicated the presence of a highly conjugated system. Analysis of this solid by GCMS showed a mixture of four components, which were identified as 9,10-dihydroanthracene **21** in 10.2 % yield, anthracene **24** in 55.4 % yield, 10H-anthracen-9-one **22** in 31.5% yield, and 2-bromoanthracene **23** in 2.9 % yield (Figure 1.4). This mixture could not be separated by column chromatography.

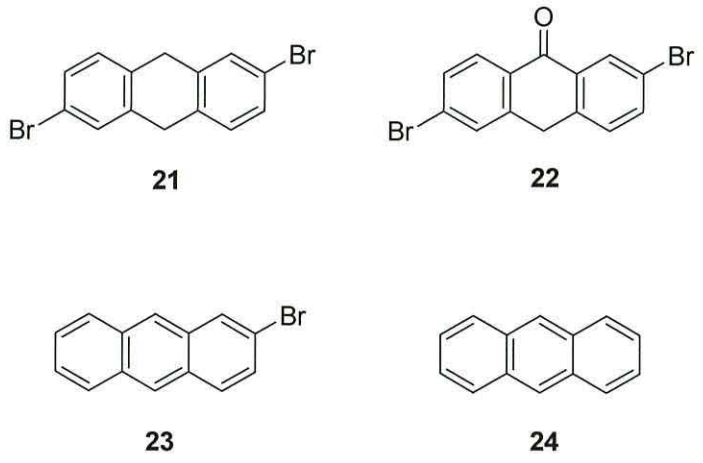

21 22 23 24

Figure 1.4. Products derived from the reduction of dibromoanthraquinone **17** by GCMS analysis.

Three other approaches were made towards the synthesis of 2,6-dibromoanthracene **20**. Reduction of the dibromo derivative **17** was also examined using the same procedure as for 2,6-diaminoanthraquinone **13**. This required the use of zinc dust in an aqueous sodium hydroxide solution as outlined in Scheme 1.9 to achieve proper reduction.

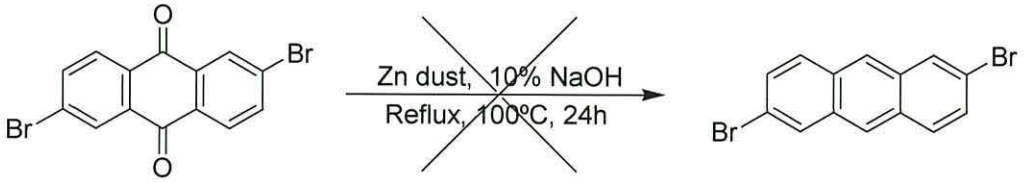

17 20

Scheme 1.9. Reduction of 2,6-dibromoanthraquinone **17** by zinc dust in sodium hydroxide solution.

Work-up by hot filtration left a solid zinc residue that was extracted with hot toluene to afford a fluorescent yellow powder, which was identified as anthracene **24** by GCMS analysis, instead of the expected 2,6-dibromoanthracene **20**.

Another failed attempt at the synthesis of bromo derivative **17** was also made using aluminium amalgam as the reducing agent (Scheme 1.10).

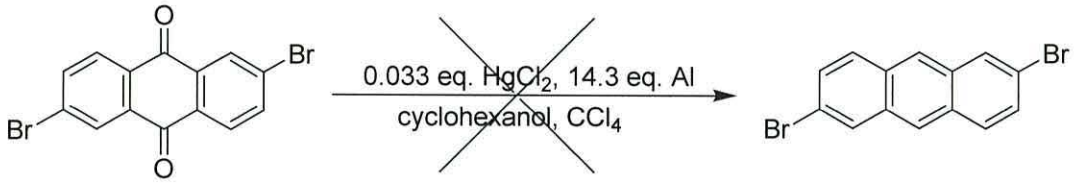

17 20

Scheme 1.10. Attempted reduction of 2,6-dibromo anthraquinone **17** by aluminium amalgam.

Work-up of the reaction yielded a yellow solid hardly soluble in any general organic solvent. This was identified by GCMS as 10H-anthracen-9-one.

The successful reduction was carried out in a well-defined two-step reaction. Partial reduction to dialcohol derivative **25** was first achieved in methanol using sodium borohydride as the reducing agent, as outlined in Scheme 1.11.

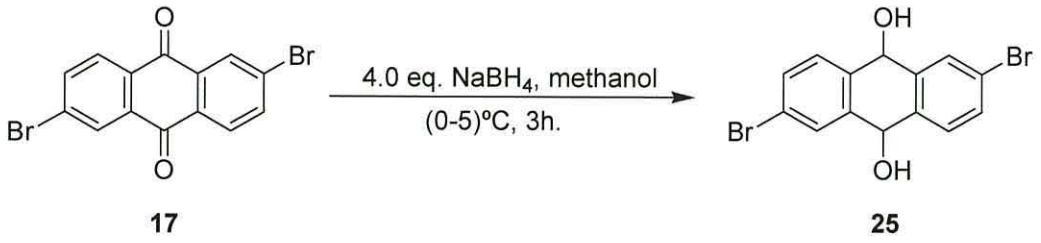

17 **25**

Scheme 1.11. Synthesis of 2,6-dibromo-9,10-dihydroanthracene-9,10-diol **25**.

Aqueous work-up followed by simple filtration gave a white precipitate, which after analysis confirmed the formation of derivative **25**. The appearance of two doublets at δ 5.70 and δ 5.50 suggested the presence of the *cis* and *trans* isomers. However, a peak that appeared at δ 206.2 also indicating partial reduction of the quinone functionality. The formation of derivative **25** was further confirmed by identification of its molecular ion, at m/*z* 370, by GCMS analysis.

Derivative **25** was immediately used for a second reduction as it spontaneously oxidises to the quinone starting material. This second step was achieved by dissolving the recovered derivative **25** in glacial acetic acid and subsequently reacting it with excess tin chloride dihydrate (Scheme 1.12).

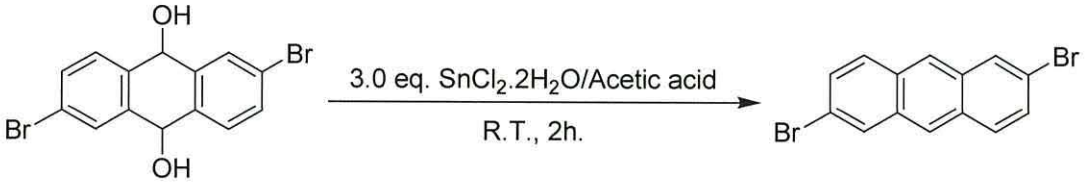

25 **20**

Scheme 1.12. Synthesis of 2,6-dibromoanthracene **20** from the corresponding hydroquinone **25**.

The formation of a yellow precipitate during the course of the reaction indicated the successful dehydration of derivative **25**. This yellow precipitate product, anthracene derivative **20**, was isolated by simple filtration, washed thoroughly with water, and air-dried in order to eliminate any trace of the remaining acetic acid. The product, anthracene derivative **20**, was isolated as a bright yellow powder. It was highly insoluble in common organic solvents, except those containing aromatic moieties

such as toluene. When it was dissolved in toluene, it appeared blue fluorescent under UV light. Its structure was confirmed by ^{1}H NMR spectral analysis, which showed two singlets, δ 8.32 and 8.18, and two doublets, δ 7.89 and 7.54, which are characteristic of a 2,6-disubstituted anthracene. Further analysis by GCMS showed the molecular ions at m/*z* 338, 336 and 334, in a 1:2:1 ratio, denoting the presence of two bromine atoms in the molecule.

Results for the reduction of dibromoanthraquinone **17** have been summarised in Table 1.1 and Figure 1.4.

Table 1.1. Products derived from the reduction of dibromoanthraquinone **17**.

	Zn/NaOH	$HgCl_2$/Al	Zn, NH_3 $CuSO_4$	$NaBH_4$ $SnCl_2$/AcOH
Anthracene **(24)**	100 %	--------	55.4 %	--------
10H-anthracen-9-one **(22)**	--------	100 %	31.5 %	--------
9,10-dihydroanthracene **(21)**	--------	--------	10.2 %	--------
2-bromoanthracene **(23)**	--------	--------	2.9 %	--------
2,6-bromoanthracene **(20)**	--------	--------	--------	100 %

Reduction of hydroxy derivative **16** was carried out unsuccessfully by employing the same procedure described in the preparation of 2,6-diaminoanthracene **18** using zinc dust in aqueous sodium hydroxide solution, as outlined in Scheme 1.13.

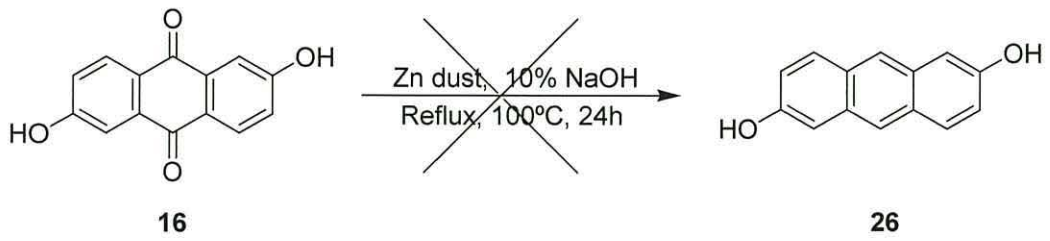

16 **26**

Scheme 1.13. Attempted reduction of 2,6-dihydroxyanthraquinone **16** by zinc dust.

Work-up gave a green solid, but no signals relating to the product could be identified by either NMR or GCMS in their respective spectra.

Another approach to the reduction of 2,6-dihydroxyanthraquinone **16** was made using aluminium amalgam as the reducing agent as outlined in Scheme 1.14.

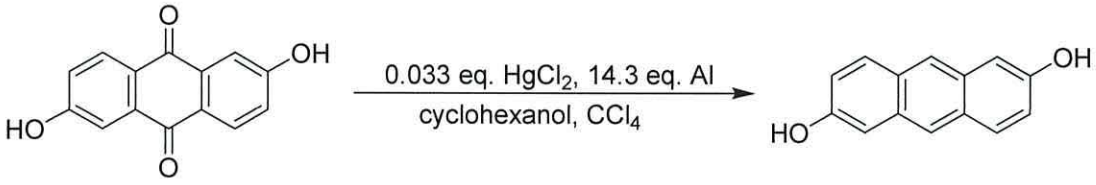

16 **26**

Scheme 1.14. Reduction of 2,6-dihydroxyanthraquinone **16** with aluminium amalgam.

Aqueous work-up, followed by extraction with dichloromethane, afforded 2,6-dihydroxyanthracene **26** in very low 11.7 % yield. ^{1}H NMR spectral analysis of the few milligrams obtained confirmed the successful synthesis. The aromatic protons followed the expected pattern for a substituted anthracene molecule showing peaks at δ 8.32 (2H), 8.18 (2H), 7.89 (2H) and 7.54 (2H). Moreover, the melting point, 293-295 °C, was consistent with the literature value of 294-297 °C.[84]

Several procedures and reagents were used in order to derivatise 2,6-diaminoanthracene **18** to the corresponding bromo derivative **20** using typical Sandmeyer conversions. Firstly, 2,6-diaminoanthracene **18** was converted to the sulfate salt **27** by diazotisation with nitrosylsulfuric acid in sulphuric acid as outlined in Scheme 1.15.

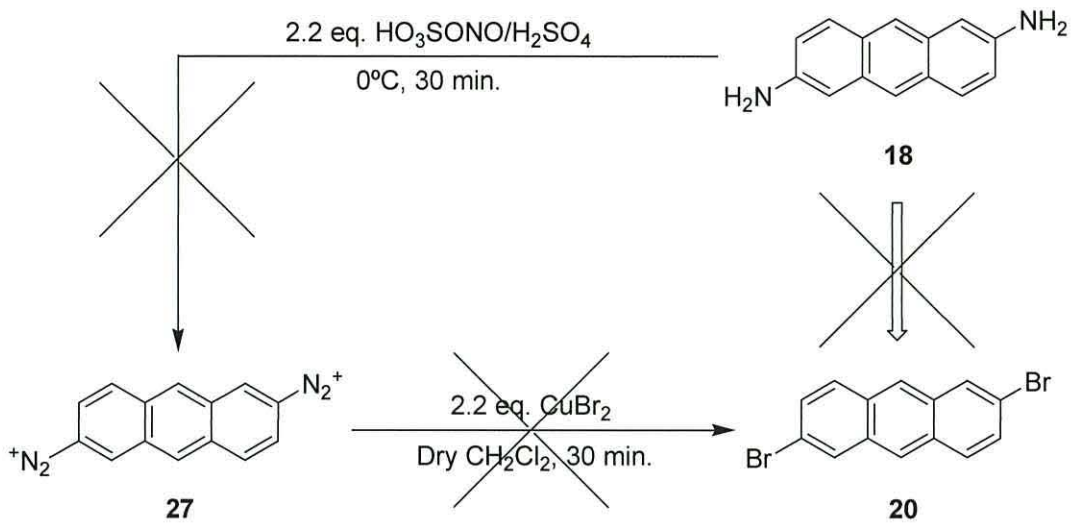

Scheme 1.15. Conversion of diaminoanthracene **18** to bromoanthracene **20** by isolation of its diazonium salt intermediate **27**.

The sulfate salt **27** was stabilised by conversion to its borate salt in an aqueous solution containing tetrafluoroborate. The resulting reddish-black solid thus obtained was unsuccessfully analysed by GCMS and NMR, due to insolubility in common solvents. However, it was used as recovered for a second reaction using copper (II) bromide in anhydrous dichloromethane for conversion to the bromo derivative **20** (Scheme 1.15). Aqueous work-up, followed by extraction with dichloromethane yielded a solid that was unable to be identified either by NMR spectral analysis or GCMS.

Another Sandmeyer reaction was applied to diaminoanthracene **18**, using sodium nitrite as the diazotising agent and copper (II) bromide *in situ* under anhydrous conditions as outlined in Scheme 1.16.

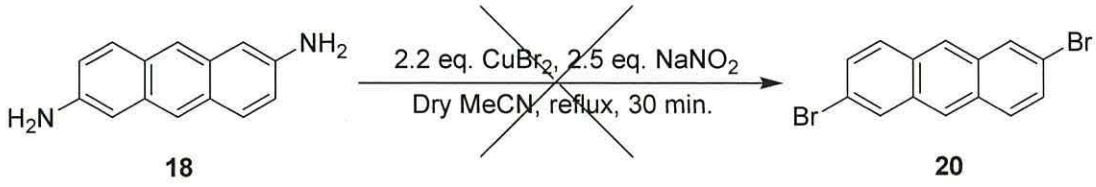

Scheme 1.16. Sandmeyer reaction on diaminoanthracene **18**.

However, no product could be identified after the work-up of the reaction. Spectroscopic methods such as either ^{1}H NMR or GCMS failed to reveal any relevant peaks.

When the same Sandmeyer-type reaction (Scheme 1.17) was carried out in wet conditions, similar results were found and peaks corresponding to the bromide derivative **20** could not be identified.

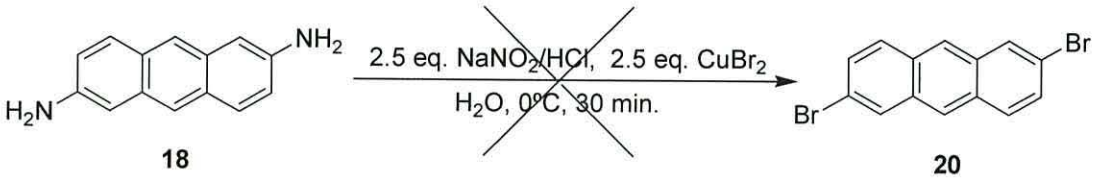

Scheme 1.17. Sandmeyer reaction of diaminoanthracene **18** using sodium nitrite.

The Sandmeyer reaction of diaminoanthracene **18** with a different diazotising agent, *tert*-butyl nitrite, and copper (II) bromide in anhydrous conditions, was then attempted according to a general literature procedure as illustrated in Scheme 1.18.[85]

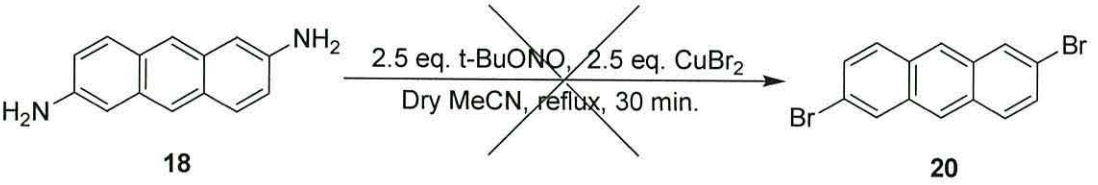

Scheme 1.18. Sandmeyer reaction on anthracene **18** using anhydrous conditions.

After acid/aqueous work-up, no reaction product could be identified either by GCMS or ^{1}H NMR spectral analysis.

The 2,6-disubstituted anthracene derivatives that were able to be synthesised were subjected to Diels-Alder reactions using ethyl acrylate as the dienophile and aluminium chloride as the Lewis acid catalyst, under anhydrous conditions. Initially, anthracene **24** was treated as depicted in Scheme 1.19.

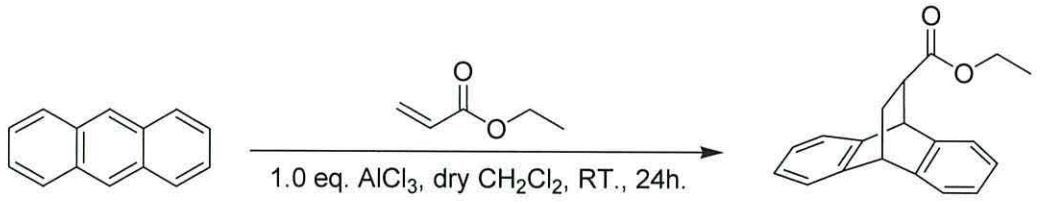

24 **28**

Scheme 1.19. Diels-Alder reaction with anthracene **24**.

The product, derivative **28**, was isolated by column chromatography following aqueous work-up. Molecular ions were found by high resolution mass spectrometry at m/*z* 301.1191, corresponding to $M+Na^+$, and 579.2485, corresponding to $2M+Na^+$. GCMS showed a molecular ion at m/*z* 278, which is consistent with the calculated value. The ^1H NMR spectrum confirmed the formation of the bridge at the middle ring of the anthracene due to the characteristic signals of the two protons at δ 4.74 and 4.39.

Anthracene derivative **19** was also subjected to a Diels-Alder reaction as outlined in Scheme 1.20.

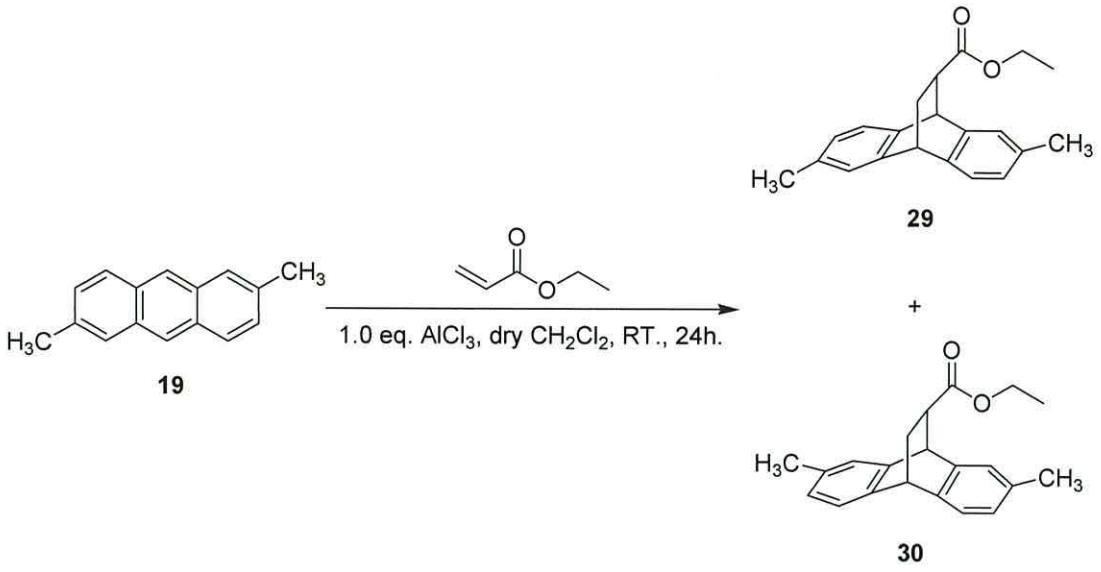

Scheme 1.20. Diels-Alder reaction on anthracene derivative **19**.

The product, a mixture of dimethyl derivatives **29** and **30**, was also purified by column chromatography and fully characterised. The mixture was recrystallised in a solution of dichloromethane and petrol to obtain crystals. These crystals afforded the X-ray structure as a mixture of two regioisomers, 2,6-dimethyl derivative **29** and 2,7-dimethyl derivative **30**, as can be seen in Figure 1.5.

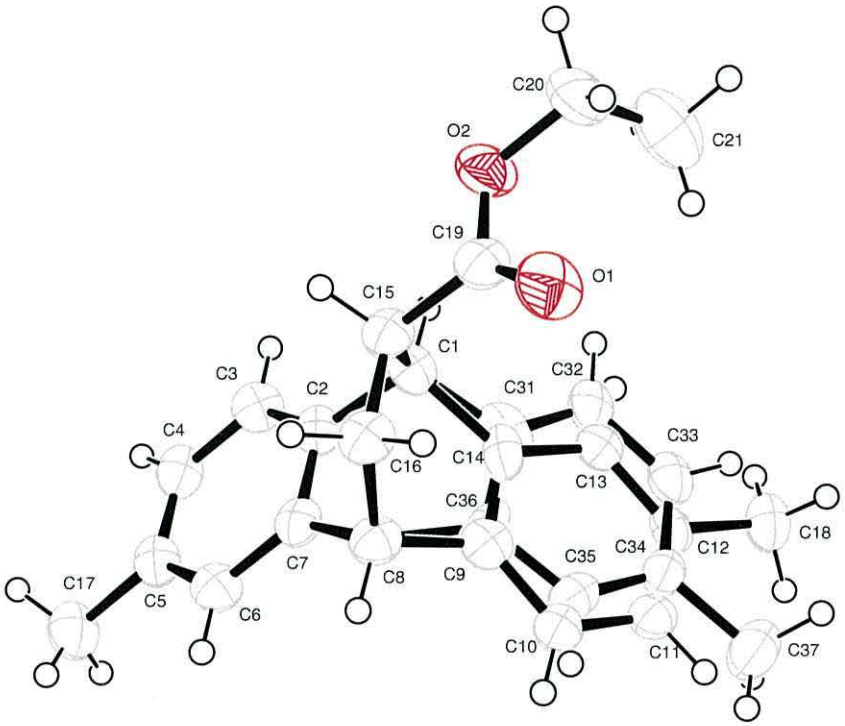

Figure 1.5. Single crystal structure of 2,6- and 2,7-dimethylderivatives **29** and **30**, respectively.

Finally, dibromoanthracene derivative **20** was reacted in a Diels-Alder fashion, as illustrated in Scheme 1.21.

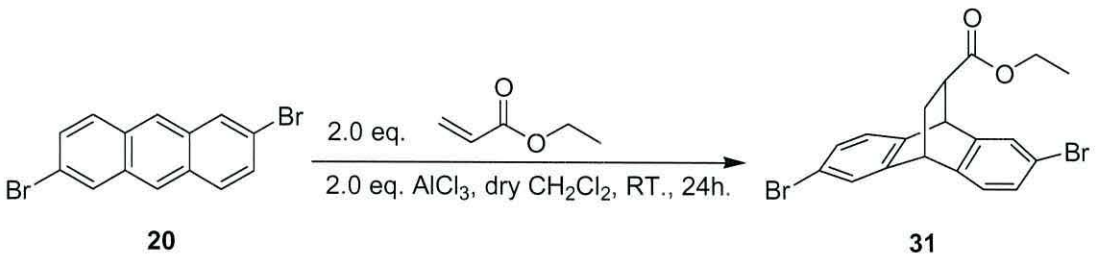

20 **31**

Scheme 1.21. Diels-Alder reaction with dibromoanthracene **20**.

In this case, the yield of the reaction was improved when two equivalents of the reagents, ethyl acrylate as the dienophile and aluminium chloride as the Lewis acid catalyst, were added. The product was eluted with a mixture of petrol and ether to afford the bromo derivative **31** as a yellow-reddish solid in 53.8 % yield. The IR

spectrum identified the carbonyl group at 1731 cm^{-1}. The two protons corresponding to the anthracene bridge were identified in the ^1H NMR spectrum at δ 4.24 and δ 5.30. In addition the molecular ion was found by GCMS at m/*z* 436. Furthermore, when the reaction was carried out with 1.2 equivalents of reagents negligible product could be recovered.

The nitro derivative **32** was obtained by reaction of anthracene derivative **28** with trifluoroacetic anhydride and ammonium nitrate in chloroform at room temperature using a modified literature procedure as outlined in Scheme 1.23.[86,87]

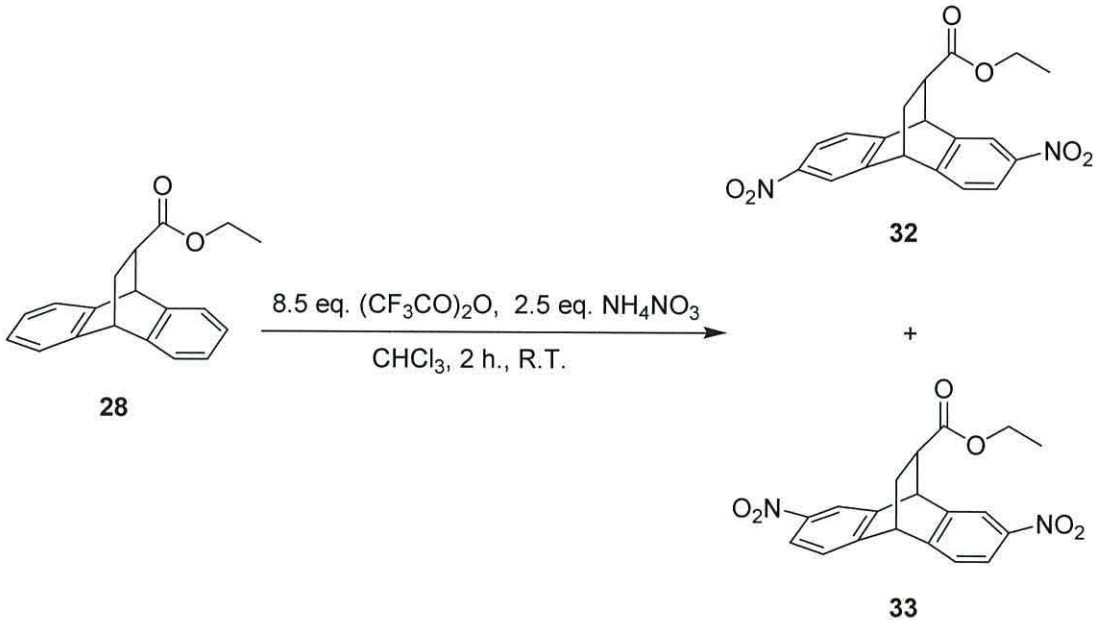

Scheme 1.22. Nitration of anthracene derivative **28**.

After aqueous work-up, the product was identified as a mixture of the 2,6- and 2,7-dinitro substituted product, **32** and **33** (Scheme 1.22), with a combined yield of 90.9 %. This oil was absorbed onto silica and purified by column chromatography eluting with a mixture of petrol and ether to afford the 2,6-dinitro derivative **32** as a thick yellow oil, which under high vacuum became a yellow solid. Characterisation of the solid product confirmed the *di*-substitution at the anthracene moiety. High-resolution mass spectrometry gave the molecular ions at m/*z* 391.0855, corresponding to $M+Na^+$ and m/*z* 759.1900, corresponding to $2M+Na^+$.

Furthermore, the GCMS spectrum showed the molecular ion minus the bridge at m/*z* 268, in addition to a peak at m/*z* 223 corresponding to the loss of one nitro group. The ^{1}H NMR spectrum showed the correct integration for the aromatic protons, which appeared in four different chemical environments at δ 8.21, δ 8.17, δ 8.08 and δ 7.49. This splitting pattern contrasts with the parent compound **28** that showed only two different chemical environments integrating for four protons.

The 2,7-anthracene derivative **33**, was eluted with a mixture of petrol and ether. Analysis of the ^{1}H NMR spectrum confirmed the same general structural pattern as for the 2,6-derivative **32**, as it showed similar peaks. The main difference between both isomers was their distinctive melting point, 110-111 °C for the 2,7-derivative **33** and mp 65-66 °C for the 2,6-derivative **32**. The dipole moment, characterised by their R_f values from thin layer chromatography analysis, was also different with $R_f = 0.55$ for the 2,6-derivative **32** and $R_f = 0.45$ for the 2,7-derivative **33**.

When the same reaction was carried out in the presence of less equivalents of reagent (Scheme 1.23), as per the literature procedure applied to similar anthracenes,[87] different results were found.

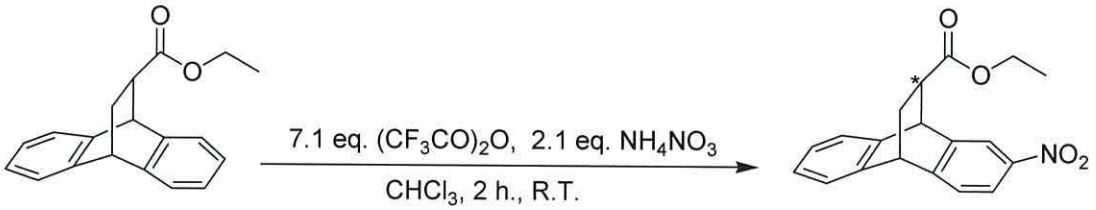

28 **34**

Scheme 1.23. Nitration of anthracene derivative **28**.

The reaction, in this case, yielded a mixture of *di*-substituted products **32** and **33**, plus the *mono*-derivative **34**. The *mono*-substituted derivative **34** was identified spectroscopically to be the 2-substituted anthracene derivative **34**. The ^{1}H NMR spectrum showed the correct integration for the aromatic protons at δ 8.02, 7.89, 7.29, 7.5, 7.20 and 7.05. High resolution mass spectroscopy found the molecular ions at m/*z* 346.1063, corresponding to M+Na$^+$, m/*z* 362.0803, corresponding to

$M+K^+$, and m/z 699.2211, corresponding to $2M + Na^+$. GCMS could only find the ion corresponding to the loss of a bridge group at 223 plus a signal corresponding to the loss of a nitro group at m/z 194. The stereochemistry of anthracene derivative **34** could not be determined by spectral analysis.

The dinitration of the anthracene derivative **28** had been also attempted unsuccesfully by reaction with a mixture of potassium nitrate and sulphuric acid as shown in Scheme 1.24.

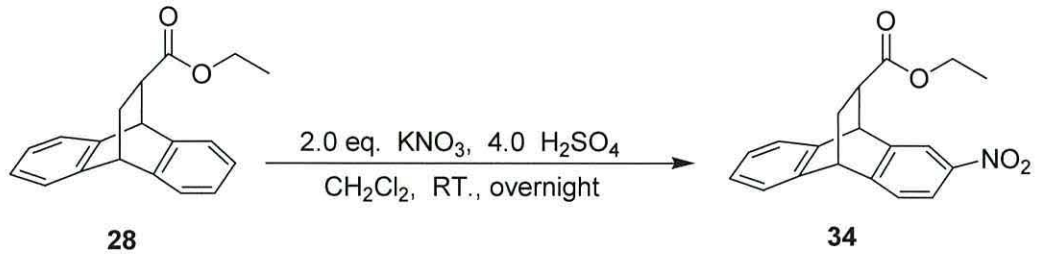

Scheme 1.24. Reaction of anthracene derivative **28** with potassium nitrate and sulphuric acid.

Isolation of the product by column chromatography afforded only the *mono*-derivative **34**, as was confirmed by comparison of the spectroscopic data with that of the derivative previously obtained (see above).

The Diels-Alder reaction of diaminoanthracene **18** was attempted by several methods. The first approach was using the same standard methodology that has been described in the examples above, *i.e.* reaction promoted by a Lewis acid catalyst as illustrated in Scheme 1.25.

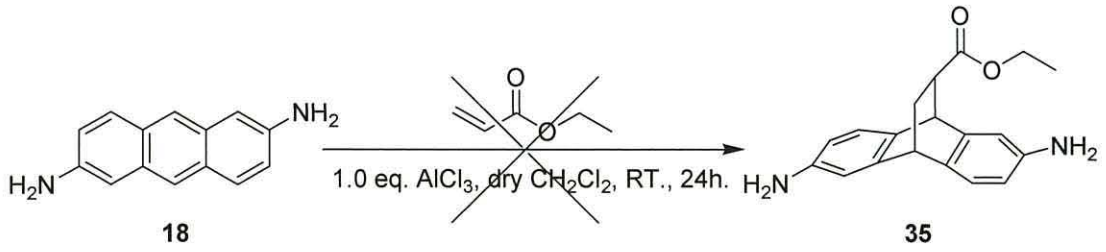

Scheme 1.25. Attempted Diels-Alder reaction of anthracene **18**, catalytically promoted by aluminium chloride.

Another attempt at the Diels-Alder reaction between diaminoanthracene **18** and ethyl acrylate was made in benzene solution at reflux as illustrated below in Scheme 1.26.

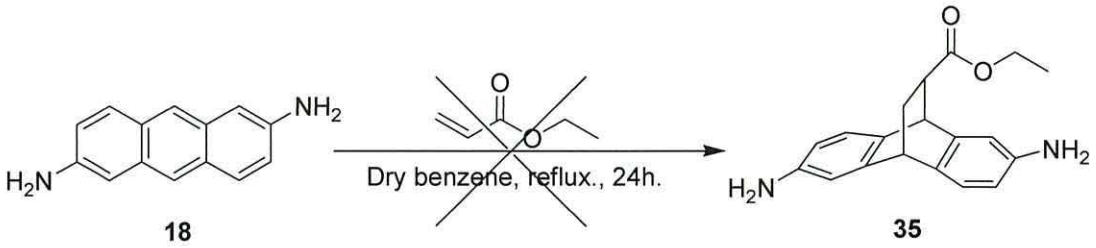

18 **35**

Scheme 1.26. Diels-Alder reaction with diaminoanthracene **18** in anhydrous benzene.

Analysis of the crude product showed a complicated mixture of products. The ^{1}H NMR spectrum showed the peaks corresponding to the hydrogens at the anthracene bridge at δ 4.21 and δ 3.92 in very low concentration in comparison with the rest of the spectrum. Purification of the product mixture was unsuccessful and no side products could be identified.

The Diels-Alder reaction of diaminoanthracene **18** was also conducted at 150 °C inside an autoclave as outlined in Scheme 1.27. After aqueous work-up, only starting material could be recovered.

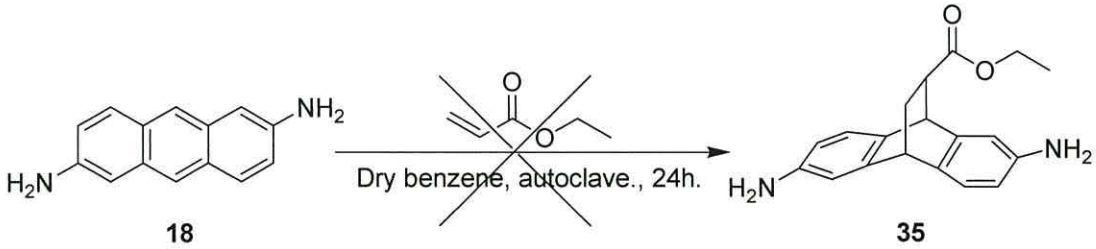

18 **35**

Scheme 1.27. Diels-Alder on anthracene **18** in dry benzene in an autoclave.

Reduction of ester derivative **28** to alcohol analogue **36** was made in the presence of excess lithium aluminium hydride (Scheme 1.28), which is a powerful reducing agent appropriate for the synthesis of similar compounds.

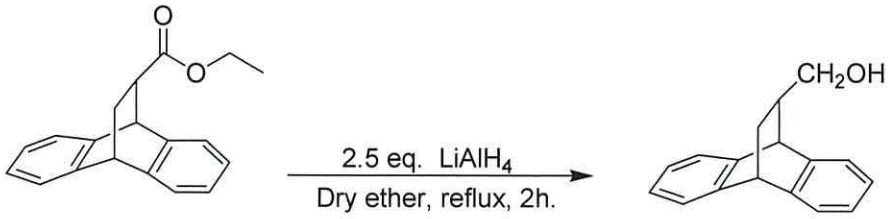

28 36

Scheme 1.28. Reduction of ester derivative **28**.

The reaction was completed after two hours, with the alcohol derivative **36** being the sole product of the reaction. The alcohol derivative **36** was easily isolated by column chromatography, as it is a more polar molecule than its parent compound, ester derivative **28**. Identification of the product was made using spectroscopic methods and by comparison of some features with its parent compound **28**. For instance, the disappearance of the ester group was apparent in both the ^{1}H NMR and the IR spectra, as well as the ^{13}C NMR spectrum. The peak of the carbonyl group had disappeared in the IR with the appearance at the same time of a strong band at 3193 cm^{-1} corresponding to the hydroxyl group. The ^{1}H NMR spectrum showed a singlet accounting for the hydroxyl group at δ 1.55, whereas the peaks corresponding to the ethyl ester were no longer present. The ^{13}C NMR spectrum confirmed the loss of the ester corresponding to the carbonyl group, and a peak of the carbon attached to the hydroxyl group appeared at δ 66.1.

Ester derivative **29** was also reduced according to the same methodology employed above, using lithium aluminium hydride as the reducing agent (Scheme 1.29).

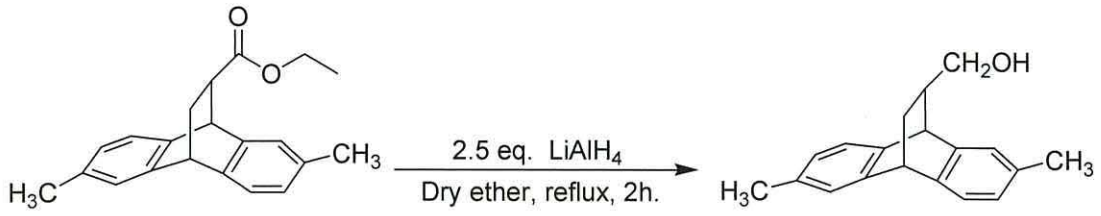

29 37

Scheme 1.29. Reduction of ester derivative **29** to alcohol derivative **37**.

Aqueous work-up, followed by column chromatography, afforded alcohol derivative **37**, and this was corroborated by spectroscopic methods. IR spectroscopy showed the hydroxyl group as a broad band at 3355 cm^{-1}. ^{1}H NMR spectral analysis gave the correct signals with the right integration, particularly confirming the alcohol group as a singlet at δ 1.78. The alcohol was also apparent in the ^{13}C NMR spectrum as a peak at δ 66.2. In addition, the molecular ions were found by high resolution mass spectrometry at m/*z* 287.1435, corresponding to $M+Na^{+}$, 551.2836, corresponding to $2M+Na^{+}$ and 303.1142, corresponding to $M + K^{+}$.

Ester derivative **31** was also reduced to its alcohol analogue **38** (Scheme 1.30).

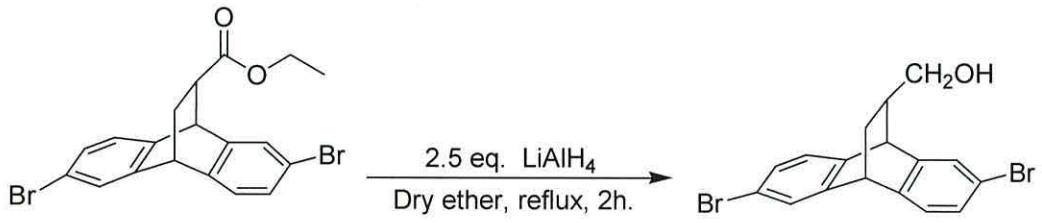

31 **38**

Scheme 1.30. Reduction of ester derivative **31**.

The product **38** was isolated by column chromatography as a yellow solid in 95.2 % yield. Identification of the alcohol group and disappearance of the carbonyl group were characteristic features in order to achieve positive identification of the product. The hydroxyl group was identified by IR spectroscopy as a broad band at 3381 cm^{-1}, and no peak of the carbonyl group was found. Moreover, the ^{13}C NMR spectrum also showed the carbon attached to the hydroxyl group at δ 65.5.

The conversion of anthracene alcohol derivatives **36** into their corresponding bromide analogues of general structure **6** was generally made using carbon tetrabromide and triphenylphosphine. Initially, the conversion of alcohol derivative **36** was achieved by the method outlined in Scheme 1.31.

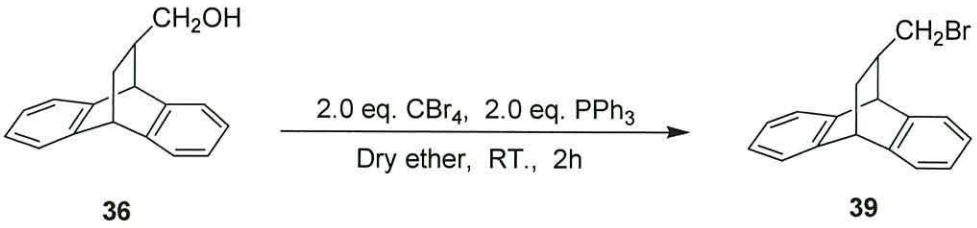

36 **39**

Scheme 1.31. Conversion of alcohol derivative **36** into bromide analogue **39**.

The reaction was complete after two hours. Work-up involved removal of reaction by-products, such as triphenylphosphine oxide and the excess of other reagents used. This purification was achieved firstly by filtration of the phosphine oxide residue and secondly by column chromatography. The product, bromide derivative **39**, was eluted with a mixture of petrol and ether and was confirmed as being the correct material by spectroscopic methods. The ^{1}H NMR spectrum confirmed the disappearance of the alcohol peak at δ 1.55. Analysis by GCMS identified the molecular ions at m/*z* 300 and 298 with a 1:1 ratio, which indicated the presence of the two bromine isotopes, plus another peak corresponding to the loss of hydrobromic acid at m/*z* 219. The bromide **39** was recrystallised by slow evaporation and X-ray analysis afforded the structure illustrated in Figure 1.6.

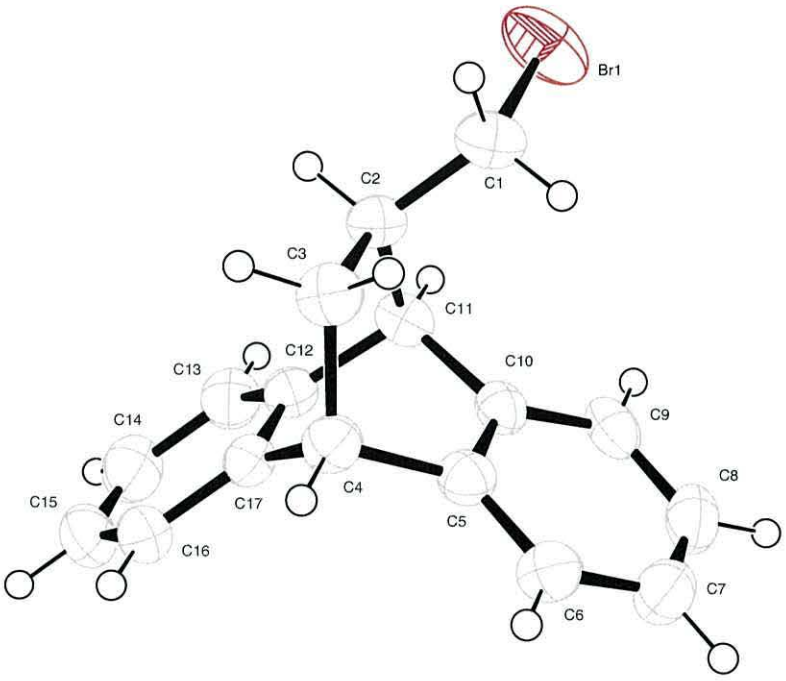

Figure 1.6. Single crystal structure of bromide derivative **39**.

The dimethylderivative **37** was also converted to its corresponding bromide analogue **40** using the same methodology as described in Scheme 1.32.

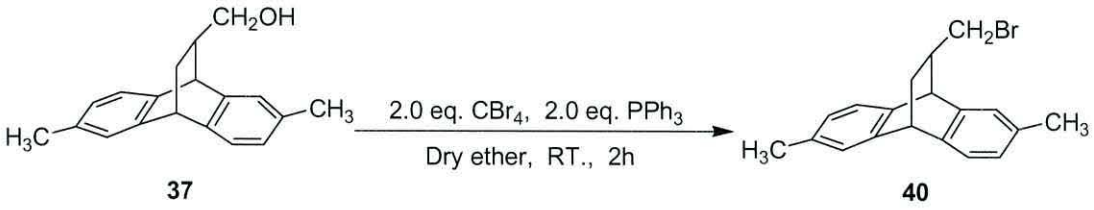

37 **40**

Scheme 1.32. Synthesis of anthracene derivative **40**.

The work-up of the reaction mixture was essentially the same as described in the previous reaction to afford the unsubstituted derivative **39**. The product, bromide derivative **40**, was isolated by column chromatography by eluting with a mixture of petrol and ether. GCMS analysis showed two isomer peaks with slightly different retention times of Rt = 21.35 and 21.43 min., but near identical chromatograms. The

molecular ion was not found, but instead the peaks corresponding to the breakdown of the molecule as a result of the loss of hydrobromic acid were identified at m/*z* 247.

The synthesis of the bromo nitro derivative **41** was approached by different methodology. Anthracene derivative **36** was dinitrated by a mixture of ammonium nitrate and trifluoroacetic anhydride at room temperature as outlined in Scheme 1.33.

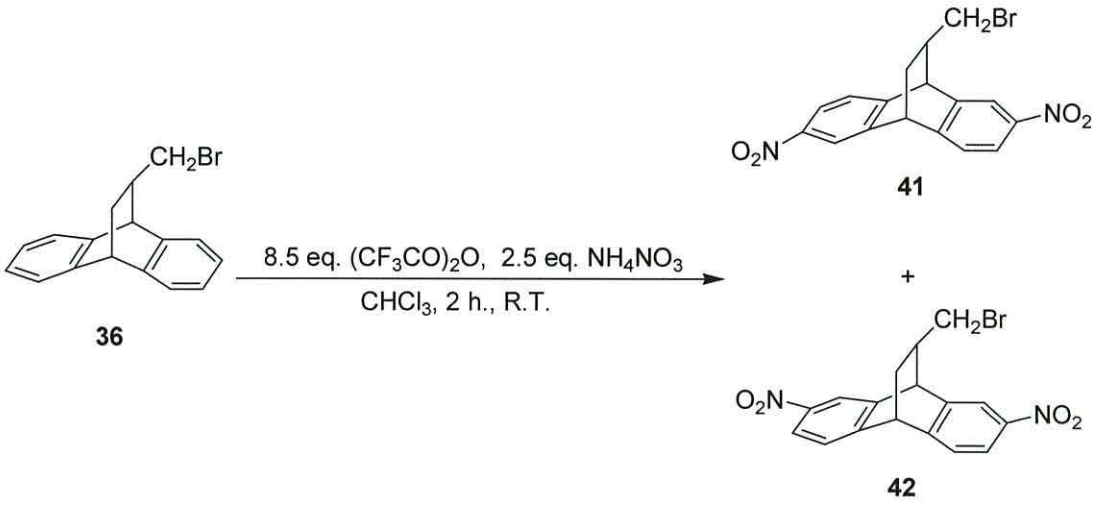

Scheme 1.33. Dinitration of anthracene derivative **36**.

Work-up of the reaction mixture afforded two isomers, nitroderivative **41** and nitroderivative **42** in a combined 92.3 % yield. They were separated by column chromatography and they exhibited similar spectroscopic patterns. The product ratio was found as 1.3:1 (**42**:**41**), which is a consistent result with the nitration of similar anthracene adducts.[87]

The ^{1}H NMR spectrum of **42** showed the aromatic protons as two doublets at δ 8.15 and δ 8.12, two doublets of doublets at δ 8.01 and δ 7.97 and two overlapping doublets that appeared as a triplet at δ 7.39, which confirmed appropriate substitution by the nitro group at the aromatic rings. Additionally, the molecular ions were found by GCMS at m/*z* 300 and 298 with a 1:1 ratio, which indicated the presence of the two isotopes of bromine. The 2,7-nitro derivative **42** was further characterised by X-ray analysis to afford the crystal structure shown in Figure 1.7.

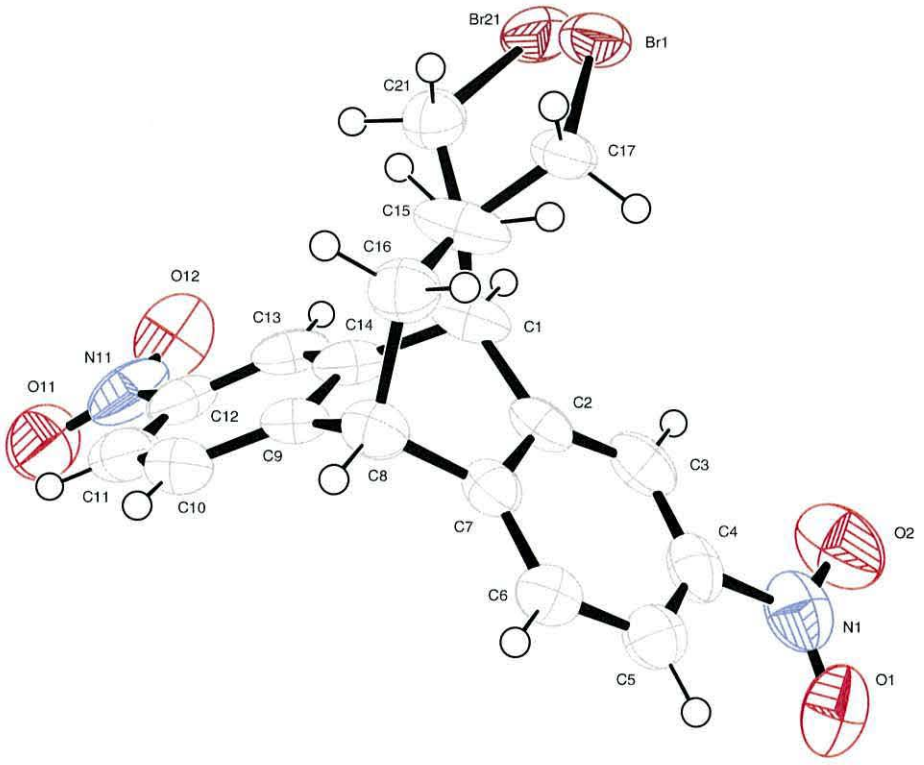

Figure 1.7. Single crystal structure of the nitro derivative **42**.

In order to synthesise acyclic model compounds it was necessary to start from a suitable starting material. To that end, bromide **43** was reacted with heptanal in a Grignard fashion reaction to yield alcohol **44** as outlined in Scheme 1.34.

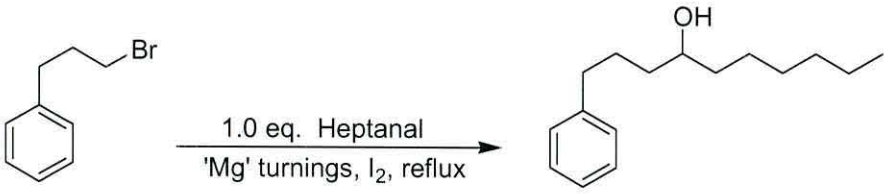

43 **44**

Scheme 1.34. Synthesis of 1-phenyldecan-4-ol **44**.

Alcohol **44** was isolated by column chromatography and fully characterised using spectroscopic methods. The infrared spectrum shows a broad band at 3351 cm^{-1},

which indicates the presence of an hydroxyl group corresponding to the four-position in the alkyl chain. The ^{1}H NMR spectrum also shows the hydroxyl group as a singlet at δ 1.52, which was corroborated in the ^{13}C NMR spectrum at δ 71.5. In addition, the molecular ion was not found in its GCMS spectrum, but the ion of the corresponding molecule derived from the loss of water at m/*z* 216 was. Alcohol **44** was not the sole product of the reaction, as two other by-products, benzene derivative **45** and benzene derivative **46**, were separated by column chromatography and analysed to confirm their structure (Scheme 1.35).

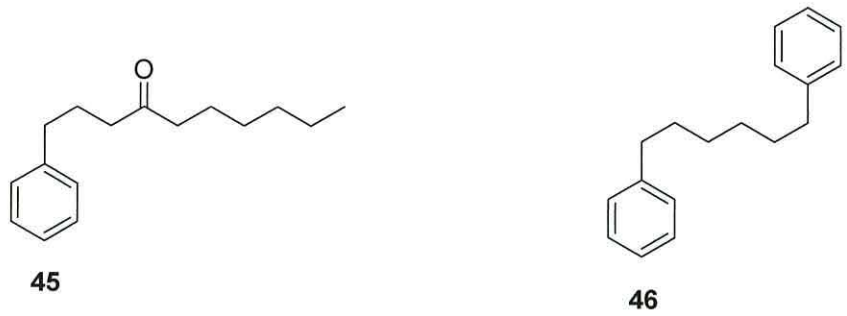

45 **46**

Scheme 1.35. By-products derived from the synthesis of 1-phenyldecan-4-ol **44**.

Diaromatic derivative **46** was confirmed by its ^{1}H NMR spectrum, as the alkyl chain protons appear in three distinctive environments, δ 2.74, 1.76, and 1.52, due to the symmetry of the system. This symmetry is also apparent in the ^{13}C NMR spectrum, where only three carbon signals, δ 36.1, 31.6 and 29.2, account for an alkyl chain of six members. The molecular ion, m/*z* 238, was also found in the mass spectrum.
Benzene derivative **45** was also analysed and its structure confirmed. The infrared spectrum shows the presence of the carbonyl group at 1714 cm^{-1}, which is corroborated by the ^{13}C NMR spectrum as a peak at δ 210.8. In addition, the GCMS shows the molecular ion at m/*z* 232.

Further conversion of alcohol **44** into its bromide derivative **47** was carried out using triphenylphosphine and carbon tetrabromide in dry ethereal solution at room temperature as stated in Scheme 1.36.

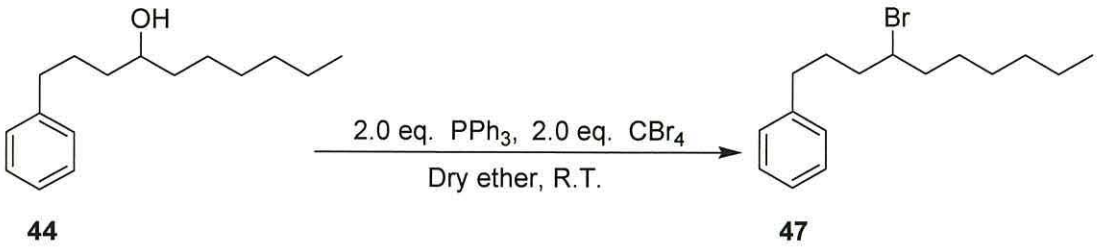

Scheme 1.36. Synthesis of 1-(4-bromodecyl) benzene **47**.

The reaction reached full conversion after one hour. Triphenylphosphine oxide was filtered out and the product was isolated by column chromatography. The resulting liquid was further purified from traces of excess bromoform and carbon tetrabromide by distillation to afford the bromide derivative **47** as a colourless liquid, bp 125-127 °C at 0.3 mmHg. The structure was easily recognised by spectral analysis and by comparison with the starting material. Disappearance of the alcohol group was apparent from the infrared spectrum where the broad band at 3351 cm^{-1} was no longer present. The molecular ions were found by GCMS analysis at m/*z* 296 and m/*z* 298 with a ratio of 1:1, indicating the two isotopes of bromine.

The benzene ring of derivative **47** was substituted to produce the nitro derivative **48** as described in Scheme 1.37.

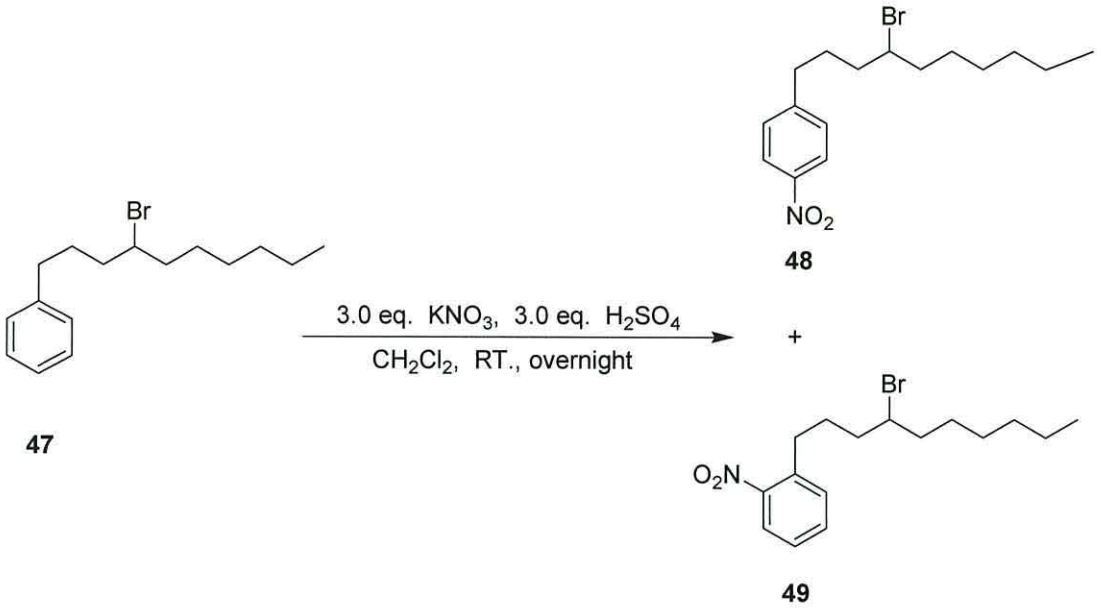

Scheme 1.37. Synthesis of 1-(4-bromodecyl)-4-nitrobenzene **48**.

The reaction yielded the two expected isomers, *ortho*-derivative **49** and *para*-derivative **48**, in 40:60 ratio, in a combined yield of 78.3 %. Both of the two nitro derivative isomers, **48** (R_f = 0.32) and **49** (R_f = 0.41), were isolated by column chromatography using a petrol spirit and ether mixture (94:4).

Both of the structures of isomers **48** and **49** were confirmed by spectroscopic methods. ^{1}H NMR spectral analysis provided a very good method of elucidating which isomer corresponded to which fraction by examination of the chemical shifts and couplings of the aromatic protons. The ortho derivative **49** showed three resonances at δ 7.65, δ 7.28, and δ 7.11, whereas the *para*-derivative **48**, due to its clearly more symmetrical structure, only showed two distinctive environments. These were well defined at δ 8.16 and δ 7.36.

The same reaction described above was carried out using one equivalent of nitrating agent with a 15 % yield and using two equivalents of reagent giving a 35 % yield.

The *para*-nitro derivative **48** was reduced to its amino analogue by reacting it with two equivalents of hydrazine monohydrate in the presence of 20 % catalytic amount of synthetic graphite as outlined in Scheme 1.38.

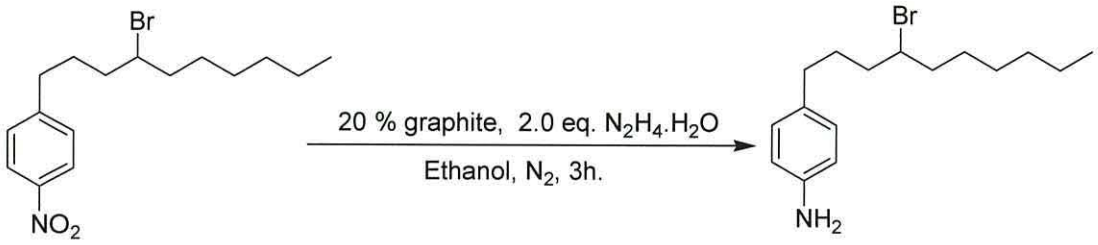

48 **50**

Scheme 1.38. Reduction of *para*-nitroderivative **48**.

Evaporation of the solvent left an oil that was purified by column chromatography by eluting with 50:50 (petroleum spirit/ether) to afford the amino derivative **50** as a pure yellow oil in 72 % yield. This was spectroscopically characterised. ^{1}H NMR spectral analysis showed the typical pattern of an X,Y-*para*-substituted benzene ring with a doublet at δ 7.00 and another doublet δ 6.66, whereas the protons corresponding to the amino group appeared at δ 3.56 as a broad singlet. Further analysis by high resolution mass spectrometry confirmed the molecular ions at m/*z* 312.1332 and m/*z* 314.1318, corresponding to M+H$^+$. GCMS only showed the ion corresponding to the loss of the hydrobromic acid molecule at m/*z* 231.

Substituted *para*-bromo derivative **51** obtained by Sandmeyer reaction of amino derivative **50** with *tert*-butyl nitrite and copper (II) bromide in anhydrous conditions (Scheme 1.39).

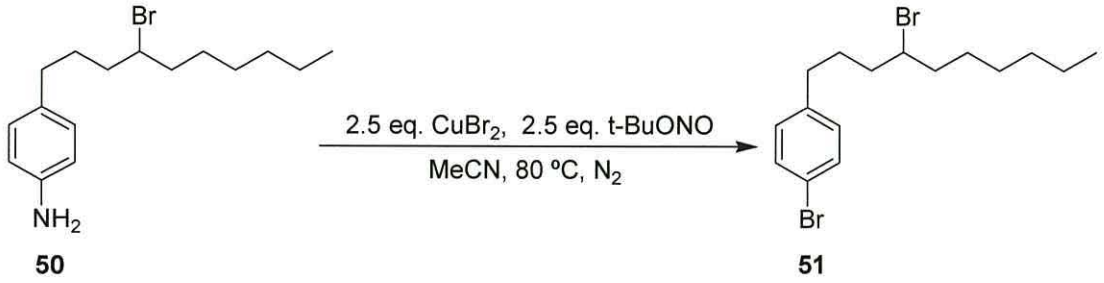

50 **51**

Scheme 1.39. Conversion of amino derivative **50** into bromo derivative **51**.

Bromo derivative **51** was purified by column chromatography eluting with pure petroleum spirit, and its structure was confirmed by spectroscopic methods. ^{1}H NMR spectral analysis indicated the X,Y-para substitution as it showed two distinctive doublets at δ 7.52 and δ 7.01. Further analysis by GCMS identified the correct molecular ion at m/*z* 376.

Another acyclic derivative **10**, lacking the aromatic moiety but containing an alkyl chain of 10-members and the bromine functionality, was synthesised according to Scheme 1.40.

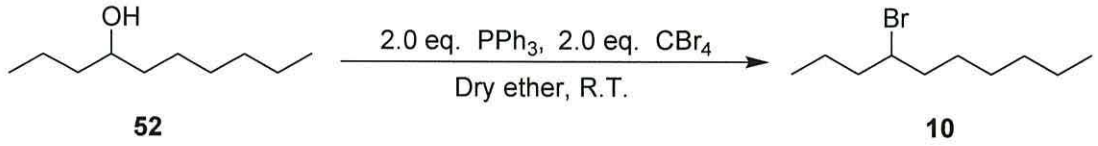

52 **10**

Scheme 1.40. Conversion of alcohol **52** into bromide **10**.

Work-up of the reaction mixture involved filtration of the ethereal solution, in order to remove triphenylphosphine oxide residue, and evaporation of the solvent. The product, bromide derivative **10**, was isolated in a very good 96 % yield by column chromatography using pure petroleum spirit as the eluant and subsequent distillation of the product at 52-54 °C and 0.4 mmHg to eliminate any remaining trace of bromoform. Derivative **10** was fully characterised using spectroscopic techniques. The total conversion of the alcohol group was indicated by the disappearance of the hydroxyl band in the infrared spectrum with respect to its parent compound **52**. NMR spectral analysis showed the hydrogen on the carbon of the bromide at δ 4.06

in the ^{1}H NMR spectrum and at δ 58.57 in the ^{13}C NMR spectrum. The molecular ion could not be found by GCMS due to the loss of a molecule of hydrobromic acid, which gave rise to a peak at m/*z* 141.

Discussion

Since the ultimate goal of this work is to study the interaction of a remote aromatic moiety with a radical generated within the molecule, the synthesis of symmetric anthracene models was focused on, which seems an entirely appropriate approach to model the interaction and facilitates the synthesis.

The fact that anthracene undergoes Diels-Alder reactions in the middle ring prompted the use of this reaction as the general strategy in the synthesis of anthracene derivatives as is outlined in Scheme 1.41.[88]

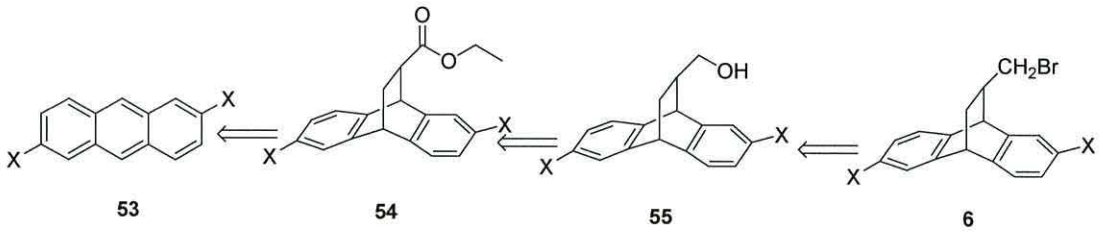

Scheme 1.41. General strategy for the synthesis of anthracene models of general structure **6**.

This synthetic strategy was initially applied to the anthracene compound **24** according to Scheme 1.42, and then was extended to other substituted anthracenes **18-20**.[88] The Diels-Alder reaction of anthracene **24** was accomplished using ethyl acrylate to afford ester derivative **28**.

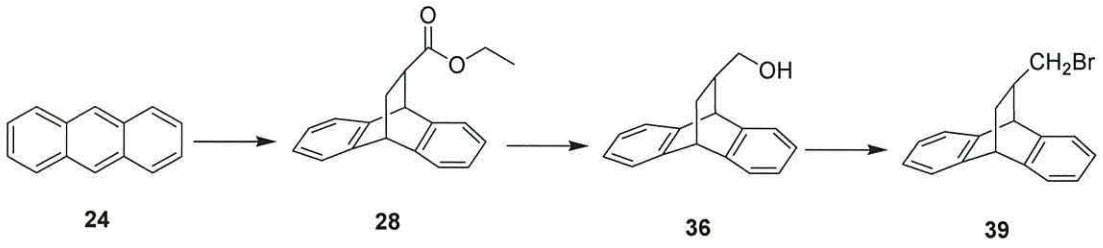

Scheme 1.42. Synthesis of bromide derivative **39**.

The Diels-Alder reaction is a pericyclic type of reaction and, as such, it has a cyclic transition state in which all bond forming and bond breaking takes place in concert without the formation of an intermediate (Scheme 1.43). More specifically, the Diels-Alder is a [4 + 2] cycloaddition that is favoured by the mobilisation of six electrons in order to replace two π bonds by two new stronger σ bonds, which provides the driving force for the reaction to take place. The presence of electron withdrawing substituents in the dienophile additionally accelerates the reaction.[89]

Scheme 1.43. General mechanism for the Diels-Alder reaction.

The ability of anthracene to undergo Diels-Alder cycloaddition is explained in terms of its structure.[90] Anthracene is an aromatic conjugated system with four resonance forms, in which there is a high contribution to the diene character of the middle ring, whilst the aromaticity of the two flanking rings is left intact (Scheme 1.44).

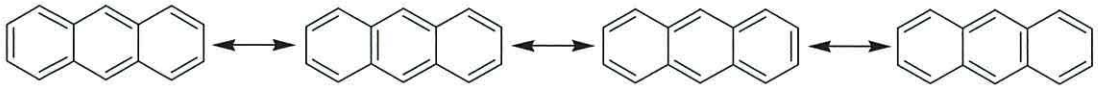

Scheme 1.44. Resonance forms of anthracene 17.

Anthracene **24** is a cyclic diene and the Diels-Alder reaction of cyclic dienes is governed by three principles: the '*cis* principle', whereby the *cis* or *trans* stereochemistry of the diene and dienophile is retained in the product; the 'endo addition rule', whereby the substituent is predominantly in the *endo*-position in the product; and 'steric approach control' whereby the diene and dienophile approach each other from their less hindered sides.[91,92] In particular, the Diels-Alder reaction mechanism of anthracene with dienophiles involves exclusive *cis*-addition of the dienophile to anthracene where the *cis* or *trans* stereochemistry of the dienophile is retained in the product. The retention of the stereochemistry has led to postulation that reaction proceeds through a concerted mechanism, where the new σ bonds are

formed simultaneously either by direct addition or *via* an intermediate complex as explained below.[93]

The presence of a Lewis acid catalyst permits the reaction to be carried out in milder conditions at room temperature. It is well documented that the use of a Lewis acid catalyst can accelerate the Diels-Alder reaction by the formation of an intermediate complex.[91,93] As the amount of catalyst increases, the reaction time decreases and the yields of adducts increase. This is because aluminium chloride forms a strong 1:1 complex with methyl acrylate (Scheme 1.45), where the aluminium chloride complexes with the carbonyl oxygen.[91,94]

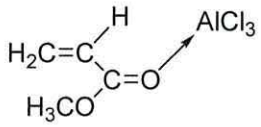

Scheme 1.45. Complex formed between aluminium chloride and ester dienophiles.

When addition of ethyl acrylate over aluminium chloride in solution was carried out, the development of a strong orange colour was observed, which indicated the formation of a complex.

Reduction of the ester derivative **28** was carried out using lithium aluminium hydride. Conversion of the resulting alcohol derivative **36** afforded the final and required product, bromide derivative **39**. This was the final product of this series as it achieved the bromide functionality suitably in the correct position relative to the aromatic moiety.

The only commercially available substrate, 2,6-diaminoanthraquinone **15**, was used as the starting material for the synthesis of the anthracene derivatives with other substituents **18-20**. Different pathways could be taken at this point.

The first pathway that will be discussed is the obvious reduction of 2,6-diaminoanthraquinone **15** to its anthracene analogue **18**. More than one method

is available for the reduction of substituted anthraquinones to their corresponding anthracene analogues. The first consideration to take into account is that a general method that can be applied to the conversion of every anthraquinone does not yet exist. There is no general method available in literature to afford the reduction of polyarene quinones directly to the parent hydrocarbons. Instead, the reduction of anthraquinones is highly dependent on the type of substituent that is attached to the aromatic moiety. Two methods were initially employed for the reduction of 2,6-diaminoanthraquinone **15** as illustrated in Scheme 1.46.

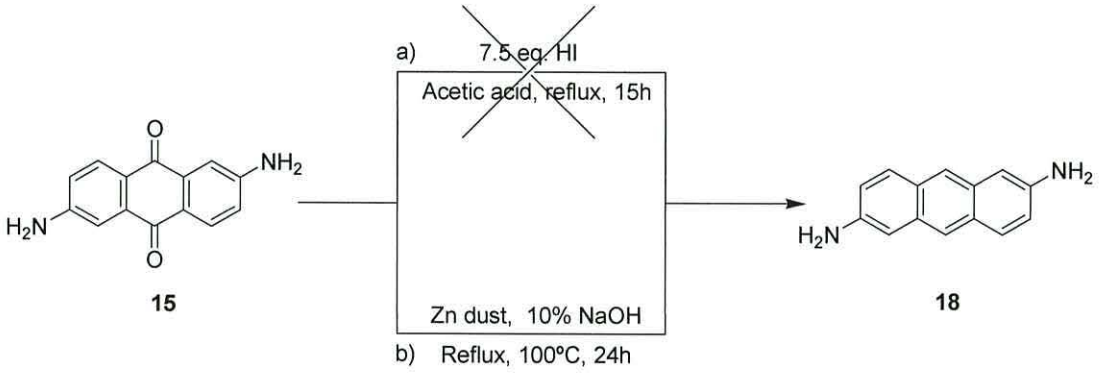

Scheme 1.46. Reduction of 2,6-diaminoanthraquinone **15**.

Treatment with hydriodic acid (Scheme 1.46 (a)) was chosen based on previous successes for the preparation of similar compounds.[95] The reaction was carried out in acetic acid because it provides a medium capable of dehydrating any possible alcohol intermediate. The mechanism of this reaction is believed to go through successive protonation and hydride transfer from HI with formation of one molar equivalent of I_2 and dehydration at each stage involving phenolic intermediates (Scheme 1.47). However, this method sometimes requires extreme conditions and it can lead to complex mixtures of phenols and *poly*-hydrogenated products.

Treatment with zinc dust (Scheme 1.46 (b)) proved to be the best possible method for the reduction of 2,6-diaminoanthraquinone. It involved the use of zinc as the reducing agent in a sodium hydroxide solution (10 %). The yield was not very high, 31 %, but this reaction had the advantage that it could be done on a large scale.

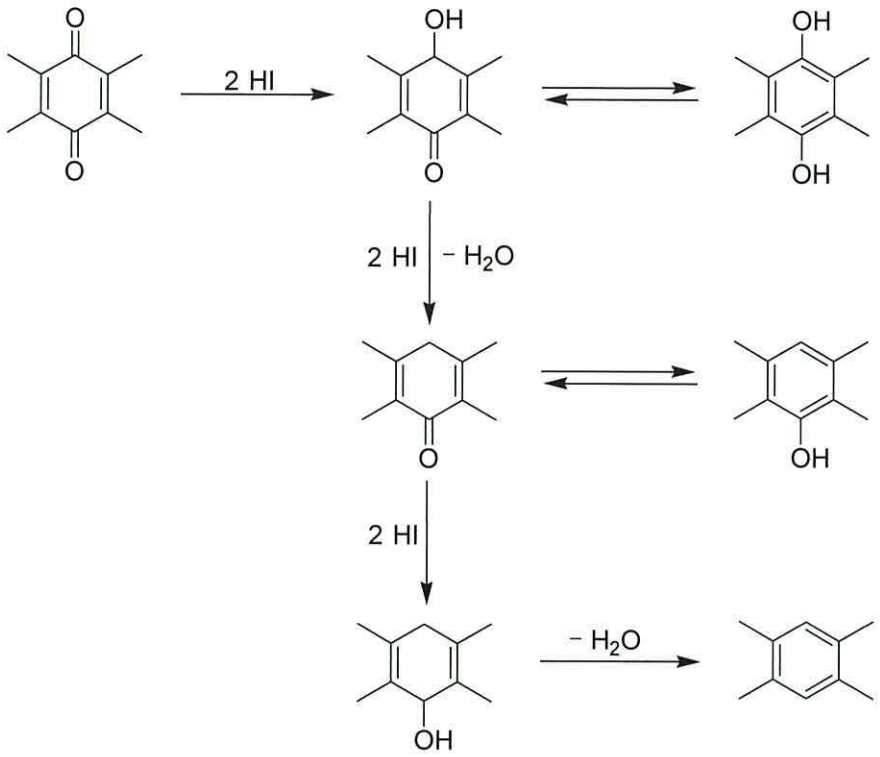

Scheme 1.47. Mechanism of the reduction of quinones by HI in acetic acid.[95]

Having already obtained 2,6-diaminoanthracene **18**, the next step towards the final synthesis of bridge anthracene derivatives of general structure **6** was to perform the Diels-Alder reaction. At this stage, two routes could be taken as illustrated in Scheme 1.48.

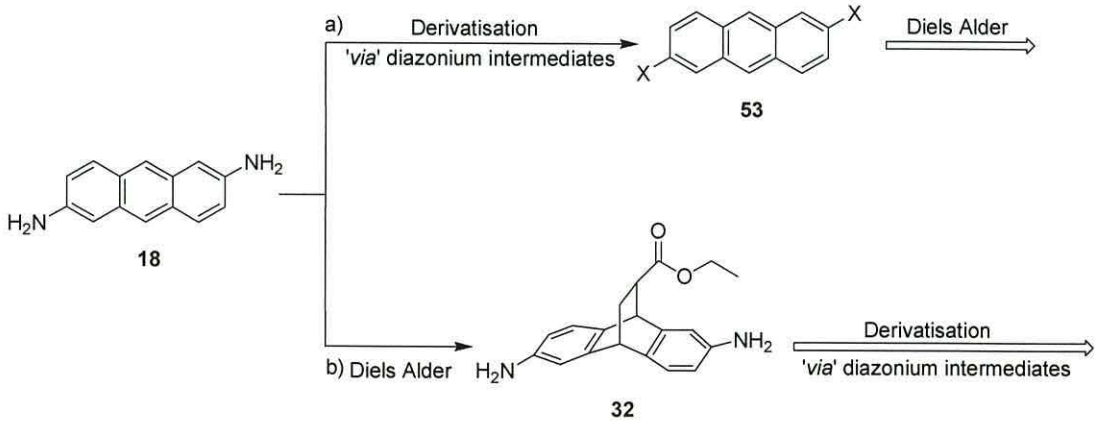

Scheme 1.48. Derivatisation routes for 2,6-diaminoanthracene **18**.

Aromatic amines are classic and versatile precursors in order to synthesise a variety of functional groups such as halogens, phenols or nitriles.[85,96-99] Diazonium salts derived from aromatic amines are also more stable than those from their aliphatic counterparts. This is because the cation being formed can be stabilised by resonance with π system of the aromatic moiety (Scheme 1.49). The use of diazonium intermediates was thus considered as a facile approach towards the synthesis of functional groups such as bromo.

Scheme 1.49. Diazonium cation stabilised by resonance.

The main difference between both routes, a) and b), in Scheme 1.48 was at what stage in the synthesis the derivatisation would take place. In principle, route b) would be a better approach because it would avoid derivatisation until a later stage, minimising the number of overall steps, whilst maximising the yield of substituted anthracenes.

The easiest group to obtain through diazonium intermediates is usually the bromide. For this reason this functionality was chosen in order to test which of the routes in Scheme 1.48, a) or b), was best suited to the derivatisation process. Route a) involves the direct derivatisation of 2,6-diaminoanthracene **18** into its bromide analogue **20**. This could be achieved by two pathways, route a.1.) and route a.2.) (Scheme 1.50). The synthesis of aryl halides from arylamines by the conventional Sandmeyer procedure involves initial diazotisation of the arylamine followed by addition of the diazonium salt to either a cuprous or a cupric halide.[85] Isolation of a stable diazonium salt (see route a.1.) was first attempted using nitrosylsulfuric acid as the diazotising agent, and the resulting sulfate salt was stabilised by anion displacement with tetrafluoroboric acid, thus converting it into its borate salt.[100] Analysis of this salt, collected as a dark red blackish precipitate, proved unsuccessful due to solubility problems in common organic solvents. The borate diazonium salt was therefore used as obtained. Further reaction of this salt with copper (II) bromide

under anhydrous conditions did not yield the expected bromide derivative **20**. This could be due to the fact that the intermediate diazonium salt **27** had not been generated in the previous step.

In situ Sandmeyer reactions (route a.2.) were carried out by three alternate procedures. Firstly, using copper (II) bromide and sodium nitrite in anhydrous conditions, secondly, diazotising with sodium nitrite in aqueous solution followed by copper (II) bromide addition and thirdly, diazotising with *tert*-butyl nitrite and *in situ* reaction with copper (II) bromide in anhydrous conditions (Scheme 1.50).

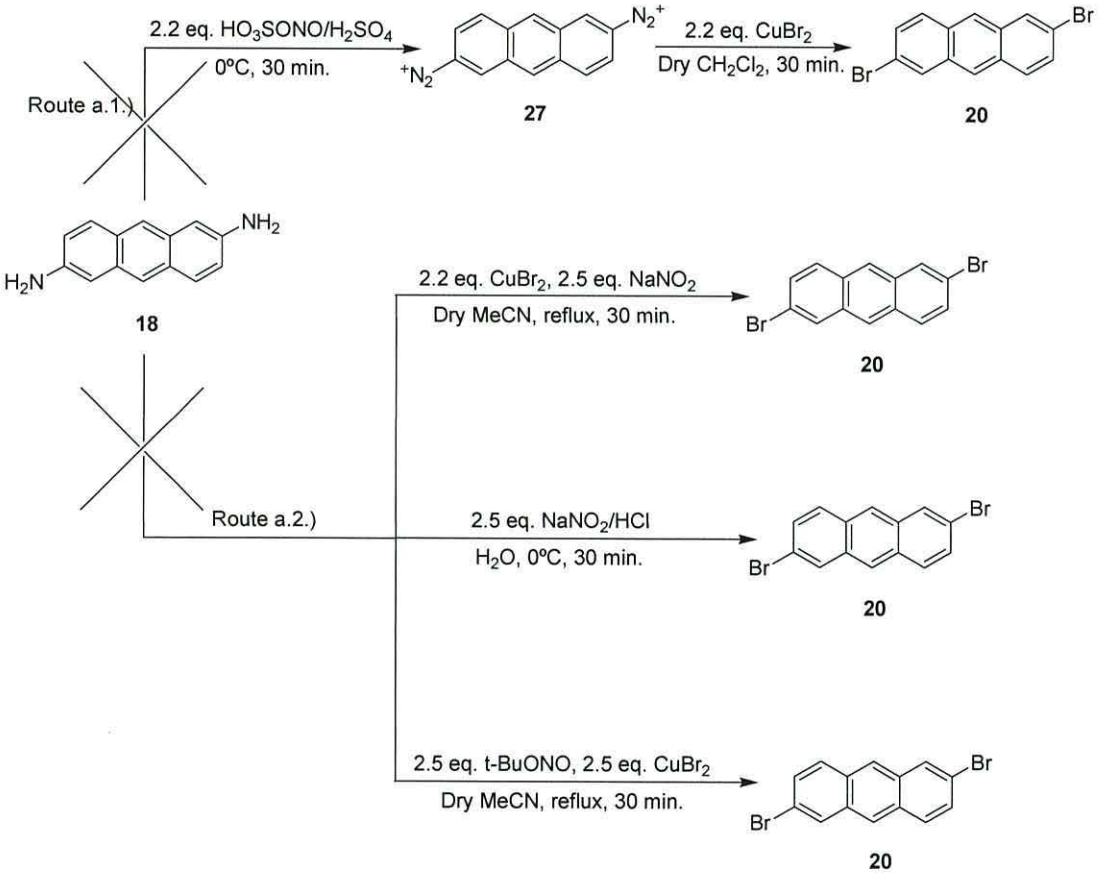

Scheme 1.50. Sandmeyer reactions towards the synthesis of anthracene derivative **20**.

None of the three procedures afforded a positive result. This outcome, combined with the fact that it had not been possible to isolate the diazonium salt **27** by route a.1.) indicated that the formation of the diazonium salt **27** could be the step that was

failing, especially as it was highly unlikely that the Sandmeyer reaction was failing in all cases. Furthermore, the use of *tert*-butyl nitrite has been reported one of the best methods for various reasons. Firstly, it generates the diazonium salt *in situ*, hence not allowing it to decompose, secondly, it is conducted in anhydrous conditions, thus avoiding competing side reactions; and thirdly it results in the rapid and quantitative evolution of nitrogen and in the formation of aryl halides, cupric oxide and *tert*-butyl alcohol (Scheme 1.51).[85,96]

Scheme 1.51. Reaction of *tert*-butyl nitrite with arylamines.

In order to explain the lack of conversion of anthracene derivative **18** to anthracene derivative **20** it is important to look at the nature of the anthracene moiety. It is known that the anthraquinone state of an anthracene molecule is thermodynamically favoured over its anthracene analogue and that oxidation at the middle ring of anthracene occurs with ease. This suggests that the reagents used for the diazotising step might be oxidising the middle ring instead, therefore hampering the formation of the diazonium intermediate. This suggests that the 9,10-position needs to be blocked in order to successfully carry out the conversion of the amino group at the 2,6-position into other functional groups.

Route b) in Scheme 1.48 proceeds through a Diels-Alder reaction on diaminoanthracene **18** in order to obtain anthracene adduct **32** prior to its later derivatisation at the 2,6-position (Scheme 1.52). The synthesis of anthracene adduct **32** was considered as a better alternative towards the synthesis of multiple different anthracene adducts. The reason for this is that the number of steps would be minimised considerably if the functionalisation at the 2,6-position would be left for a later stage.

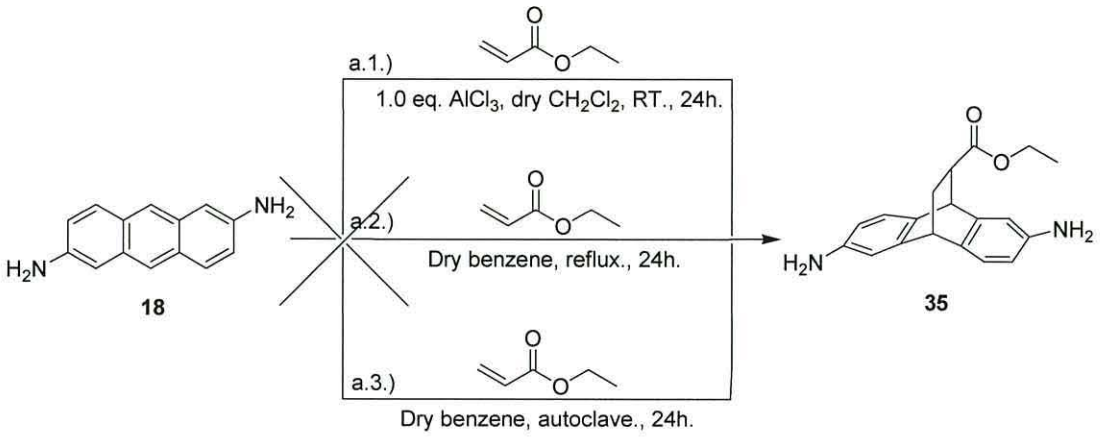

Scheme 1.52. Diels-Alder approaches carried out on anthracene derivative **18**.

Three different approaches were attempted as depicted above, but none of them afforded positive results for different reasons. The Diels-Alder promoted by aluminium chloride as a Lewis acid catalyst (Scheme 1.52 b.1.) failed to produce significant yield of product. This was attributed to the nature of the lone pair of electrons that the amino group possesses, which could form a complex with the Lewis acid catalyst, inhibiting the catalysis of the reaction.

In view of the failure to produce anthracene adduct **32** by Lewis acid catalysed Diels-Alder reaction, thermal promotion of the reaction was attempted firstly, by heating the reaction under reflux in dry benzene (Scheme 1.52 b.2.) and secondly by heating the reaction under pressure in an autoclave (Scheme 1.52 b.3.). None of the thermally induced Diels-Alder reactions afforded any product. The starting material was recovered in both cases. This result could be explained by the fact that the retro Diels-Alder reaction might be the faster process in this case, as the retro Diels-Alder reaction is known to generally be favoured at higher temperatures. The increased rate of the back reaction will additionally be more likely when the anthracene moiety is more stabilised by resonance, as is the case when it possesses a very strong donating group such as it is the amino group.

In light of the failure to obtain other functional groups from 2,6-diaminoanthracene **18** through the use of diazonium intermediates, either directly

or after Diels-Alder derivatisation, it was decided to convert the 2,6-diaminoanthraquinone **15** to appropriately substituted derivatives and then follow the proposed pathway indicated in Scheme 1.43. The 2,6-Diaminoanthraquinone **15** could be readily converted into two other substituted analogues, the bromide **17** and the phenol **17**, by means of Sandmeyer conversions as outlined in Scheme 1.53.

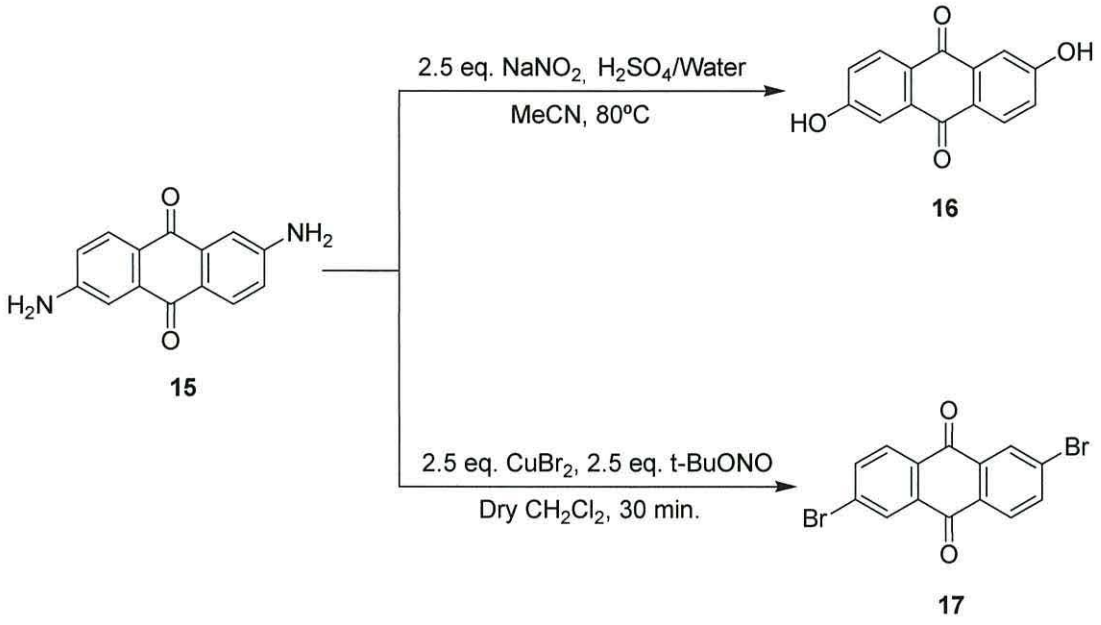

Scheme 1.53. Synthesis of functional groups from diaminoanthraquinone **9**.

Whereas the diamino derivative **15** was diazotised in aqueous solution by sodium nitrite and converted to its phenol analogue **16**,[97,101] the bromide derivative **17** was obtained by reaction of the *in situ* formed diazonium intermediate with copper (II) bromide under anhydrous conditions. The use of anhydrous conditions eliminated, to a certain extent, competing reactions, such as the unwanted formation of the corresponding phenol derivative **16**. The successful formation of derivative **17** highlights the fact that it is possible to convert the arylamine of an anthraquinone to its corresponding bromide derivative but not the arylamine of the anthracene moiety. The readiness of the middle ring of anthracene to be attacked by nucleophiles, interfering with Sandmeyer reaction and also to its propensity to be easily oxidised, seems consistent with this result.

The next step in the sequence would be the reduction of anthraquinone derivatives **16** and **17** to their corresponding anthracene counterparts **26** and **20** respectively. Reduction of anthraquinone **16** was approached by two distinctive methods (Scheme 1.54). The standard reduction using zinc in aqueous sodium hydroxide solution failed. On the other hand, reduction by mercury amalgam afforded the hydroxyanthracene **26**, as could be identified from the resulting ^{1}H NMR spectrum. The yield of the reaction was negligible and therefore this route to the hydroxy anthracene derivative **26** was abandoned.

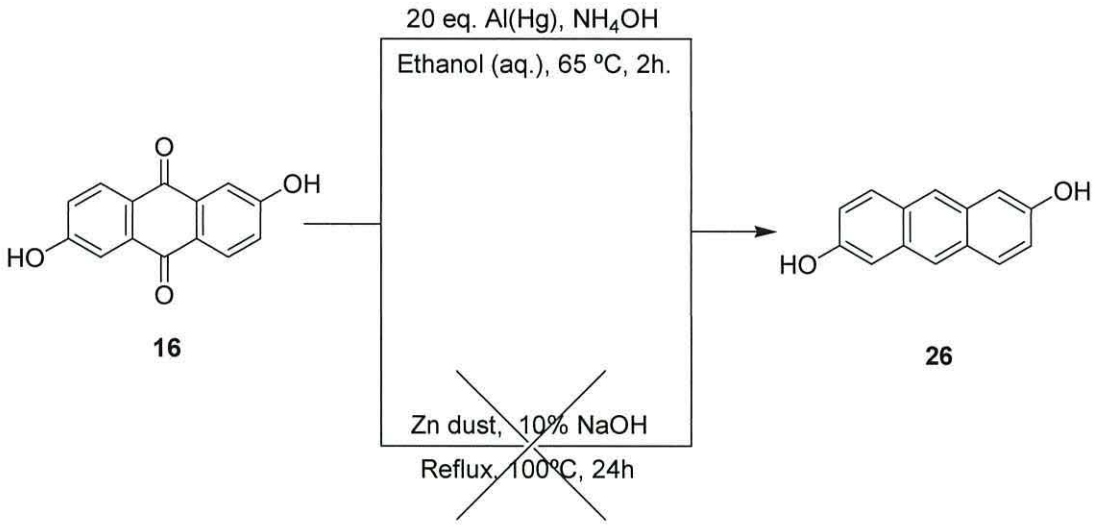

Scheme 1.54. Reduction approaches to the synthesis of hydroxyanthracene **26**.

Reduction of anthraquinone **17** was also approached by using a range of different methodologies as illustrated in Scheme 1.55.

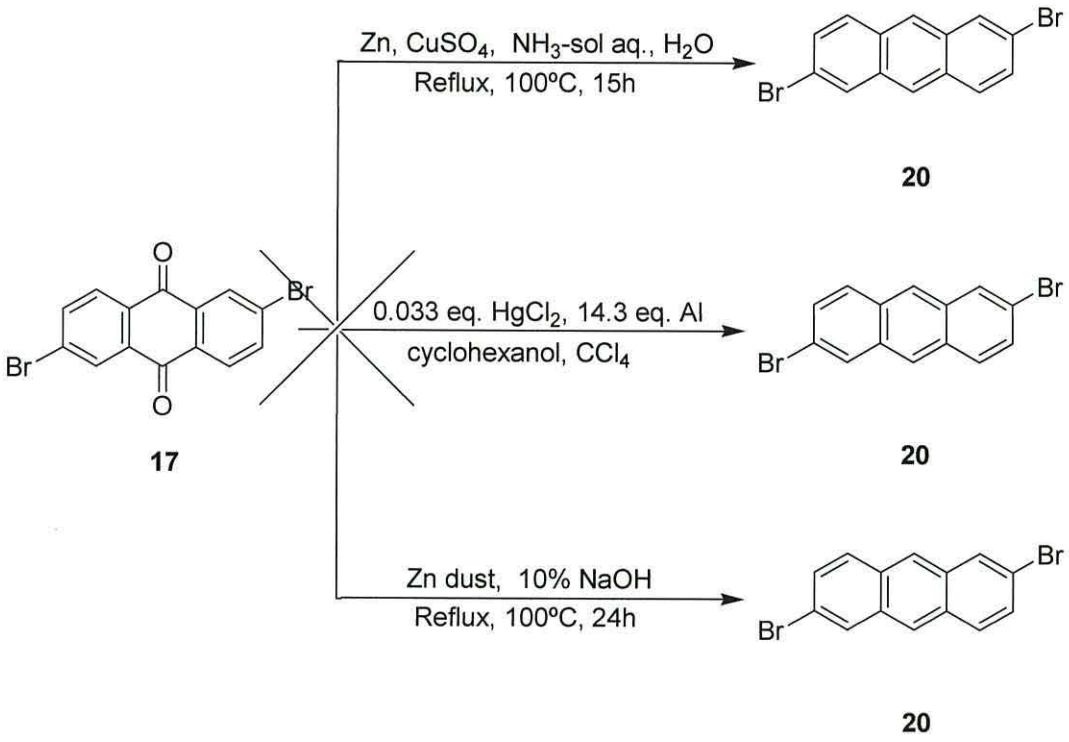

Scheme 1.55. Attempted reductions of dibromoanthraquinone **17**.

None of the three methods shown in Scheme 1.55 afforded the desired reduction product **20**. Reduction by zinc dust and sodium hydroxide yielded solely anthracene **24**. Reduction by mercury amalgam yielded solely anthracene derivative **22**. Reduction by zinc and ammonia in the presence of copper sulfate yielded a mixture of four components, anthracene **24** (55 %), anthracene **22** (32 %), dihydroanthracene **21** (10 %) and bromoanthracene **23** (3 %). The failure of the three methods described above suggested that the reagents used were reducing not only the quinone functionality but they were also reacting with the bromine atoms.

The successful reduction occurred when a two-step method was employed, as illustrated in Scheme 1.56.

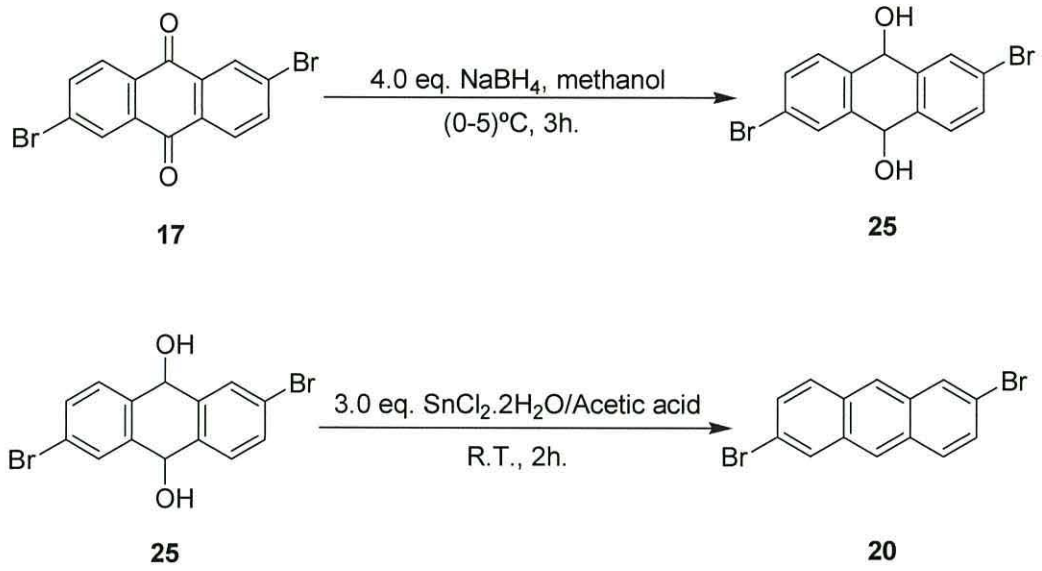

Scheme 1.56. Succesful reduction of dibromoanthraquinone **17**.

Sodium borohydride has been used previously for the reduction of anthrones to anthracenes.[102,103] This is a more effective reagent than lithium aluminium hydride in reducing anthraquinone derivatives.[104] It has also been used in the reduction of anthraquinones to anthracenes in a three-step reaction involving the use of lithium metal.[105] Tin chloride is also known to reduce diols in the presence of an acid.[106] Therefore, it was decided to combine both reagents, sodium borohydride and tin chloride, in a novel and more direct two-step reduction of dibromoanthraquinone **17** into anthracene derivative **20**. Sodium borohydride, could partially reduce the quinone functionality to its alcohol analogue **25**, which was reduced by tin chloride in acetic acid to afford the dibromoanthracene **20**, as a very insoluble material in common organic solvents.

Dibromoanthracene **20** was derivatised to anthracene derivative **38** as outlined in Scheme 1.57. The Diels-Alder reaction of anthracene derivative **20** with ethyl acrylate, catalysed by aluminium chloride, did not produce any significant yield of product **25** when one equivalent of both reagents was used. The Diels-Alder reaction afforded a reasonable yield of 54 % when two equivalents of both reagents were used. The need to use aluminium chloride and ethyl acrylate in excess could be attributed to their possible complexation of the bromo group. Ester derivative **25**

was further reduced to its corresponding alcohol derivative **38**. However, not enough of alcohol derivative **38** could be obtained for conversion to the corresponding bromo derivative **56**.

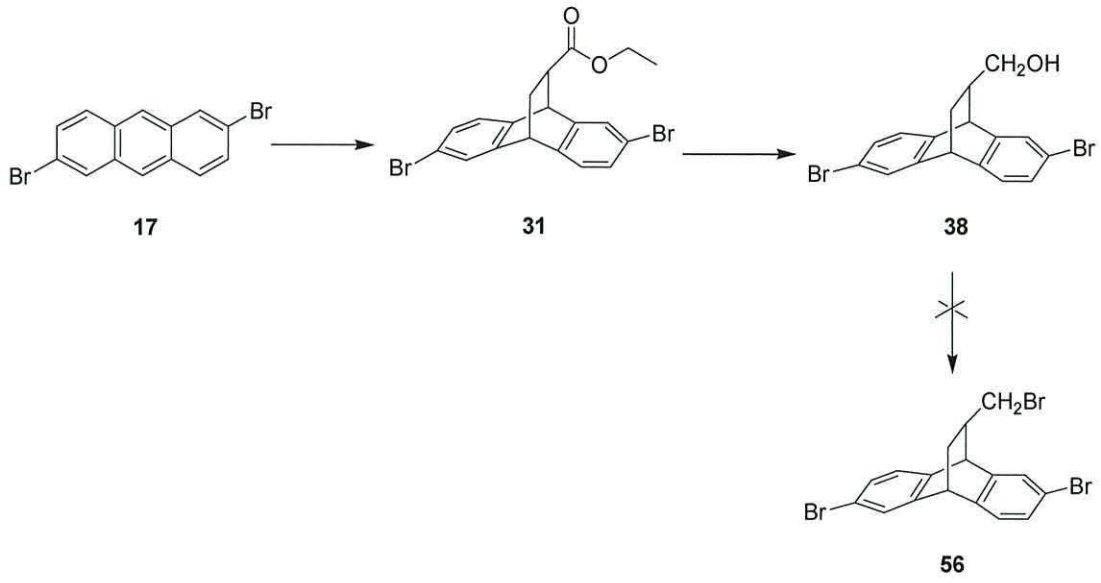

Scheme 1.57. Derivatisation of anthracene **17**.

The methyl group is a moderately electron donating substituent (σ_p = -0.17).[107] The synthesis of dimethyl derivative **40** followed a different strategy in the first stage since the methyl substitution at the 2,6-position is not commercially available and is not possible to be synthesised from the corresponding amino derivative **18**. The synthetic route towards the dimethyl derivative **40** has been outlined in Scheme 1.58.

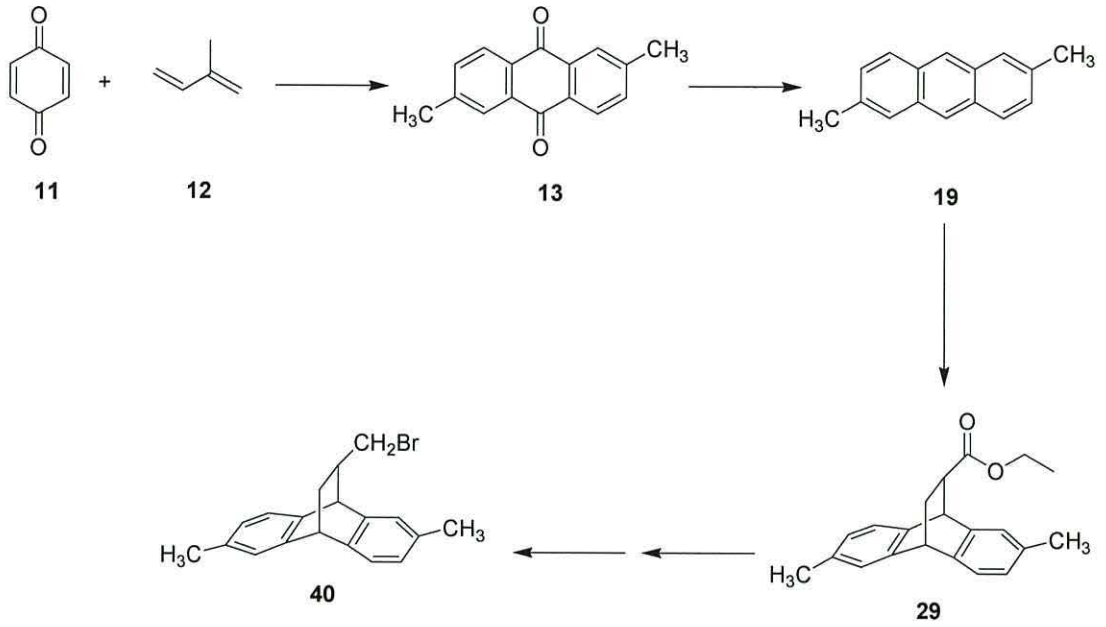

Scheme 1.58. Strategy for the synthesis of dimethyl derivative **40**.

The carbon skeleton was at first constructed by reaction of quinone **11** with isoprene **12** in 78 % yield. This gave two isomers, 2,6- and 2,7-dimethylanthraquinones, **13** and **14**, which could not be separated by fractional crystallisation and were therefore used as a mixture for later reactions. This would not be a problem in later kinetic studies as both of the two isomers display very similar spectroscopic features due to their symmetry. In fact, their ^{1}H NMR spectra appear identical, showing two doublets at δ 8.20 and δ 7.58 and one singlet at δ 8.09 for the aromatic protons and one singlet at δ 2.54 corresponding to the methyl group. Since there was no difference for either derivative in the chemical shift of the remote substituents, this suggests that they would have the same effect on the remote radical. From here on, the synthesis follows the same pathway that has already been described for other derivatives and shown in Scheme 1.41. Reduction of dimethylanthraquinone **7** into dimethylanthracene **19** was carried out using zinc as the reducing agent. Thereafter, the Diels-Alder reaction, followed by the reduction of the ester group and conversion of the resulting alcohol afforded bromide derivative **40**. This synthesis affords the bromide derivative **40** with a moderately electron donating substituent. It could also be further oxidised to its acid analogue, which would give entry to a different variety of substituents that are beyond the scope of this thesis.

A completely different route to access the nitro derivatives was developed by the use of nitration procedures. It is known that nitration of a bridged anthracene with one equivalent of nitrating agent occurs at the 2-position.[87] When a second equivalent is used, the nitration takes place at the 6-position and the 7-position, giving an equimolar mixture of two isomers as, for example, happens in the dinitration of 9,10-dihydromethanoanthracene **57** (Figure 1.8).[86]

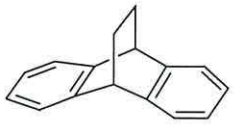

57

Figure 1.8. Dihydromethanoanthracene **57**.

Taking these precedents into consideration, a trial reaction was run on ester derivative **28** in order to identify which nitrating reagent was more effective and which were the best experimental conditions. This trial has been summarised in Scheme 1.59.

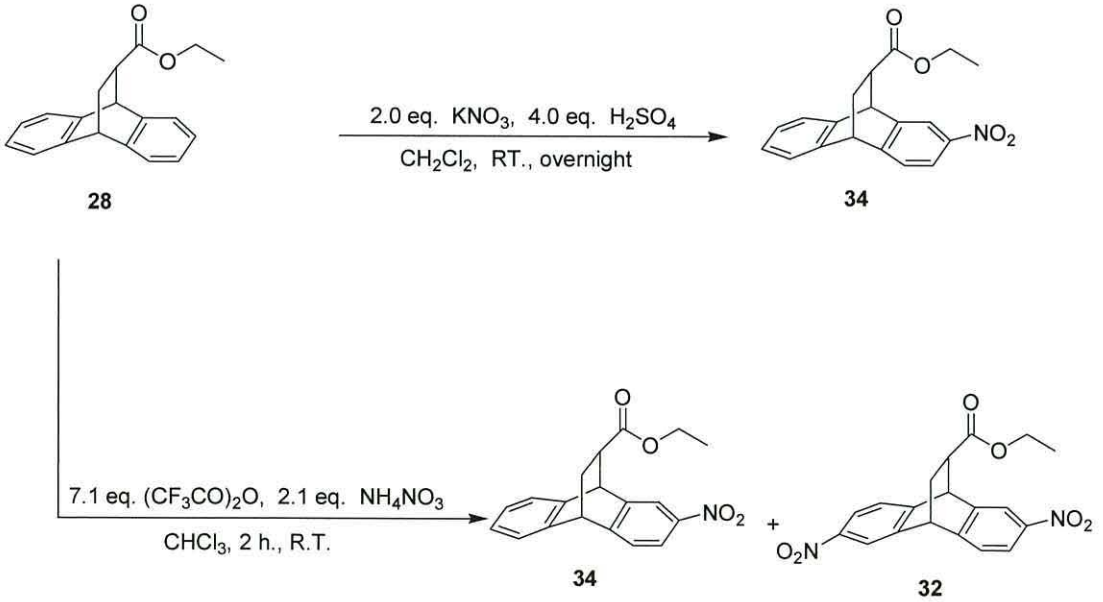

Scheme 1.59. Nitration procedures used for bridged anthracene **28**.

The nitration of aromatic compounds is an example of the general reaction electrophilic aromatic substitution, for which the mechanism involves the attack of an electrophilic reagent, such as the nitronium ion, onto the aromatic ring. Two different nitrating agents were surveyed. The first method involved the use of two equivalents of potassium nitrate. This nitrating agent afforded as the only product of the reaction the *mono*-derivative **34**. In this case, the nitronium ion is generated by an acid-base equilibrium between the potassium nitrate and sulphuric acid. The resulting nitronium ion attacks the aromatic ring and is stabilised by resonance.

When ammonium nitrate and trifluoroacetic anhydride were used in similar quantities (i.e. two equivalents of nitrating agent), a mixture of *mono*-derivative **34** and disubstituted derivative **32** were obtained, suggesting that the later reagent was more effective in the nitration of the aromatic moiety than potassium nitrate. The reaction was optimised by using 2.5 equivalents of nitrating agent as is illustrated in Scheme 1.60.

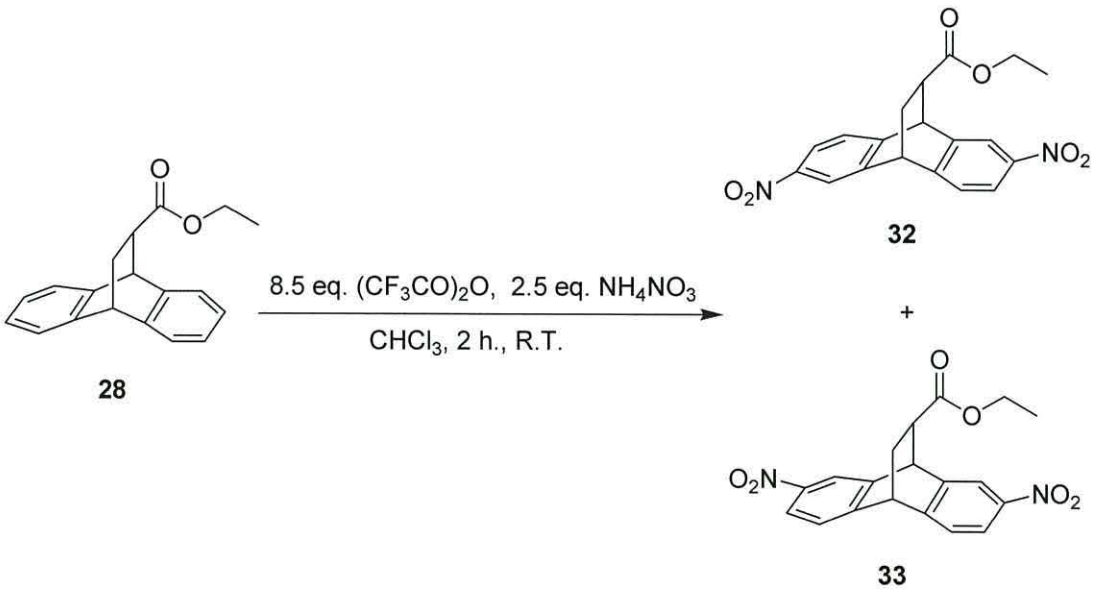

Scheme 1.60. Optimised method for the dinitration of bridged anthracenes **32** and **33**.

The reaction yielded an equimolar mixture of the expected 2,6-derivative **32** and 2,7-derivative **33**, which were able to be separated by column chromatography in a 1:1 ratio despite their very similar dipole moment.

This nitration procedure was extended to the synthesis of bromide derivatives **41** and **42**, for which the starting material **39** was already available in the laboratory from previous synthesis. The reaction is illustrated in Scheme 1.61.

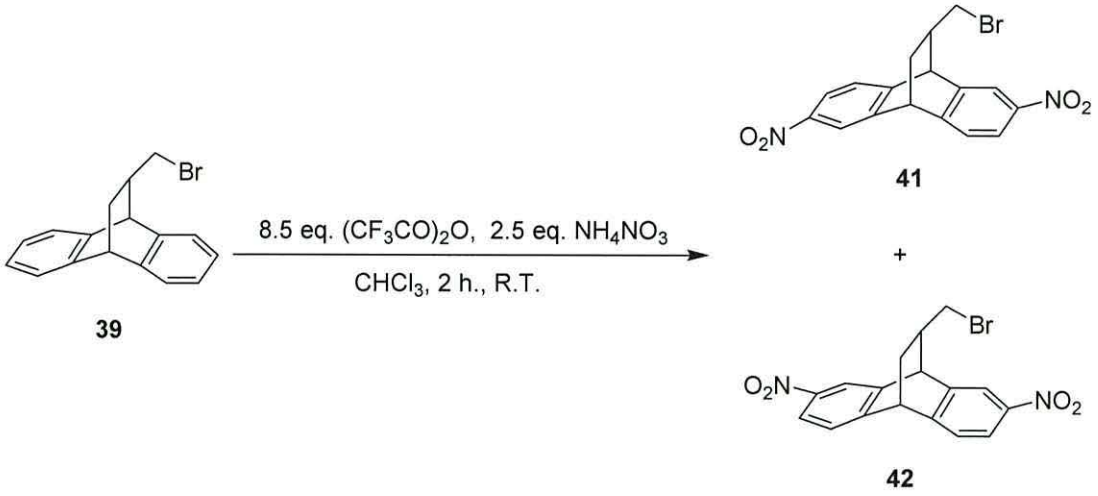

Scheme 1.61. Dinitration of bromide derivative **39**.

In this case, the reaction again yielded a mixture of two isomers, 2,6-derivative **41** and 2,7-derivative **42**, which were separated by column chromatography. The structure of the 2,7-derivative **42** was confirmed by X-ray diffraction (Figure 1.7).

The synthesis of the nitro derivative **41** provides a breakthrough in the production of anthracene derivatives as it provides a very strong electron withdrawing substituent and, at the same time, a versatile precursor for the synthesis of other substituents.

Acyclic models were synthesised according to Scheme 1.62.

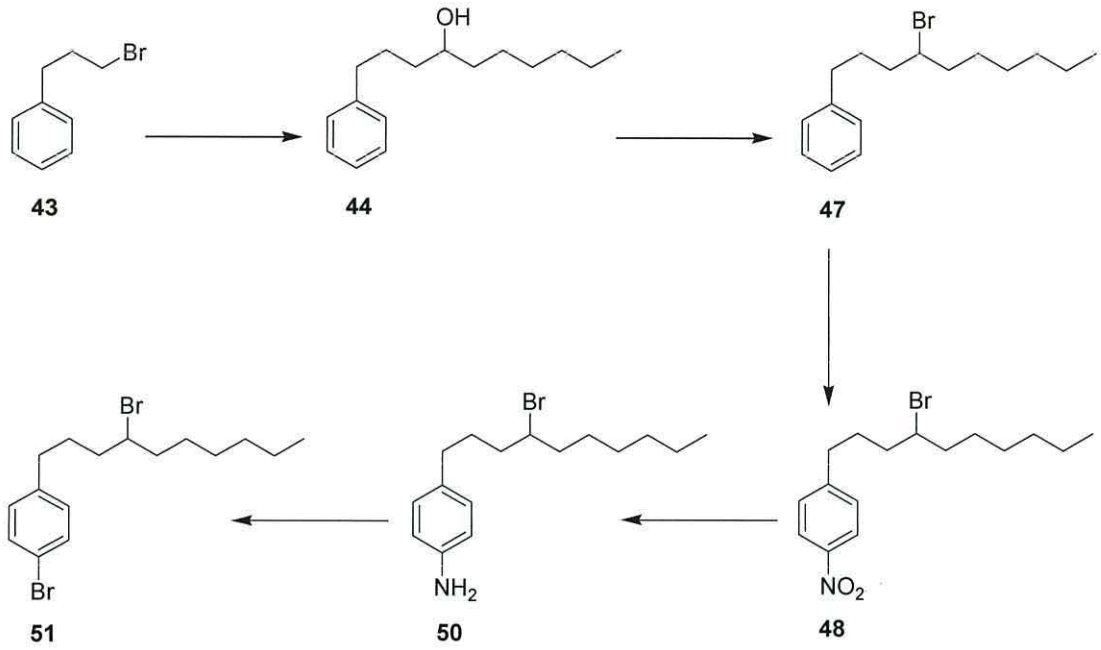

Scheme 1.62. Strategy for the synthesis of acyclic models **9**.

The first consideration in the synthesis of acyclic models of general structure **9** was how to design the carbon skeleton. This was achieved by starting from the appropriate commercially available starting materials using a Grignard reaction.[108] The Grignard reaction is in fact one of the most useful methods in order to generate secondary alcohols. The reaction of benzyl bromide **43** with heptaldehyde in a Grignard fashion reaction produced the desired alkyl chain of 10-members, acyclic derivative **44**, giving at the same time the essential substitution at the 4-position. The Grignard reaction proceeds through a nucleophilic addition pathway to the carbonyl group. This reaction did also produce two other residual by-products, as has been previously outlined in Scheme 1.35. The presence of radical intermediates during the Grignard reaction has been reported in the past,[109] which could explain the formation of side-product **46**, by dimerisation of radical **58** (Scheme 1.63).

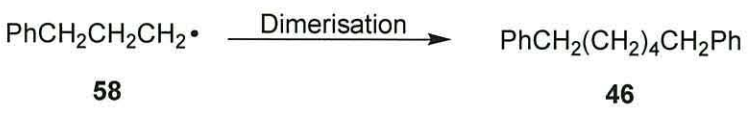

Scheme 1.63. Proposed radical dimerisation during the Grignard reaction.

The alcohol derivative **44** was easily converted to the bromide derivative **47** in an almost quantitative reaction, which proceeds through an ionic mechanism with concomitant precipitation of triphenylphosphine oxide.[110]

The next important step in the sequence was to produce the appropriate substitution at the *para*-position of the benzene ring. Ideally this substitution should give a substituent that could be further derivatised in order to afford a range of electronic distribution on the aromatic ring in the final model compounds. In this way, the generation of the nitro derivative **48** provides a good precursor for further functionalisation. This was synthesised by nucleophilic aromatic substitution using the milder nitrate salts instead of the more traditional acid approach. Potassium nitrate was chosen because it was found in literature examples to be an effective nitrating agent.[111] The reason for that is that storage and handling of concentrated nitric acid may represent difficulties, due to the strong oxidising nature of the acid. The acid, however, can be generated *in situ* from a cheap nitrate by freeing the acid with concentrated sulphuric acid. The use of nitric acid inorganic salts have the advantage that they are, in general, very stable chemicals and from them the generated nitric acid is relatively cheap, environmentally friendly and safe to handle.[112]

The aromatic electrophilic substitution yielded the two expected isomers, the *para*-derivative **48** and the *ortho*-derivative **49** in a 60:40 ratio. The formation of the *para*-derivative **48** as the major product can be explained by the higher accessibility of the *para*-centre towards the nitrating species, NO_2^+, rather than the *ortho*-position, which is hindered by the presence of the alkyl chain.

Isolation of the two isomers was not possible by distillation due to the fact that the more volatile *ortho*-isomer **49** decomposed at high temperatures. This left only a small residue with pure *para*-derivative **48**, this being the less volatile of the two. Therefore, each of the isomers was isolated by using column chromatography. This was a difficult task considering the fact that the dipole moment was very similar for

both of the isomers, giving rise to a very similar R_f value for each by thin layer chromatography.

The literature documents a wide range of available methods to reduce nitroaromatic substituents. Traditional methods such as the reduction of nitroaromatics with palladium were not considered due to the expense of the transition metal.[113] Other approaches involved the rapid, reasonably fast, clean and high yielding reduction at room temperature by employing hydrazine monohydrate in the presence of low cost graphite.[114-116] The reduction of the nitro *para*-derivative **48** by graphite and hydrazine monohydrate afforded amino analogue **50** in a high 76 % yield after purification by column chromatography. This yield is comparable to other reductions of nitroaromatics by hydrazine, ranging from 72-95 %.[114] This reaction is effective because the carbon serves as an adsorbent and electrical conductor to enable the reaction. By serving as an adsorbent and collecting hydrazine on the carbon surface, it is possible to execute a four electron reduction using a two electron reducing agent such as hydrazine.[117]

The synthesis of the amino derivative **50** was important because it achieved two objectives. Firstly, the amino functional group was obtained, which is a powerful electron donating group. This contrasts with the powerful electron withdrawing character of the nitro group. Secondly, the synthesis of a functionality such as the amino group is a versatile precursor for further derivatisation. In fact, it is well known that amino aromatics are the best precursors for the synthesis of other groups through Sandmeyer reactions.[85,97-99,113,118]

Amino derivative **50** was thus converted to its bromo analogue **51** by a Sandmeyer reaction using anhydrous conditions. Here again, literature describes a wide range of methodology using Sandmeyer reactions.[85,96,100] One alternative was to form a stable diazonium salt, which could be isolated and reacted ultimately with a copper salt in order to generate the corresponding derivative.[97] In the case of the bromide derivative **51**, an alternative straightforward deamination in a single step reaction was carried out.[85] This was possible by generating the diazonium intermediate using

tert-butyl nitrite and then reacting that diazonium intermediate *in situ* with copper (II) bromide salt.

In summary, **10**, **39-41**, **47**, **48**, **50** and **51**, have been synthesised as model compounds to study radical formation at remote centres. The identification of the role of these aromatic groups by using these models is described in Chapters Two and Three of this Thesis.

Chapter 2

Competitive, ESR and Computational Studies

Examining the rates of reaction of model systems (Figure 2.1) containing differently substituted aromatic groups can help illustrate the influence of the aromatic moiety on that reaction. By locating a remote radical forming site on the model systems prepared in the previous chapter, the active site of radical-mediated enzyme systems can be mimicked. Anthracene models have already been used to probe the mechanisms of binding through cation-π interactions of the ammonium group of the neurotransmitter acetylcholine to acetyl choline esterase.[81]

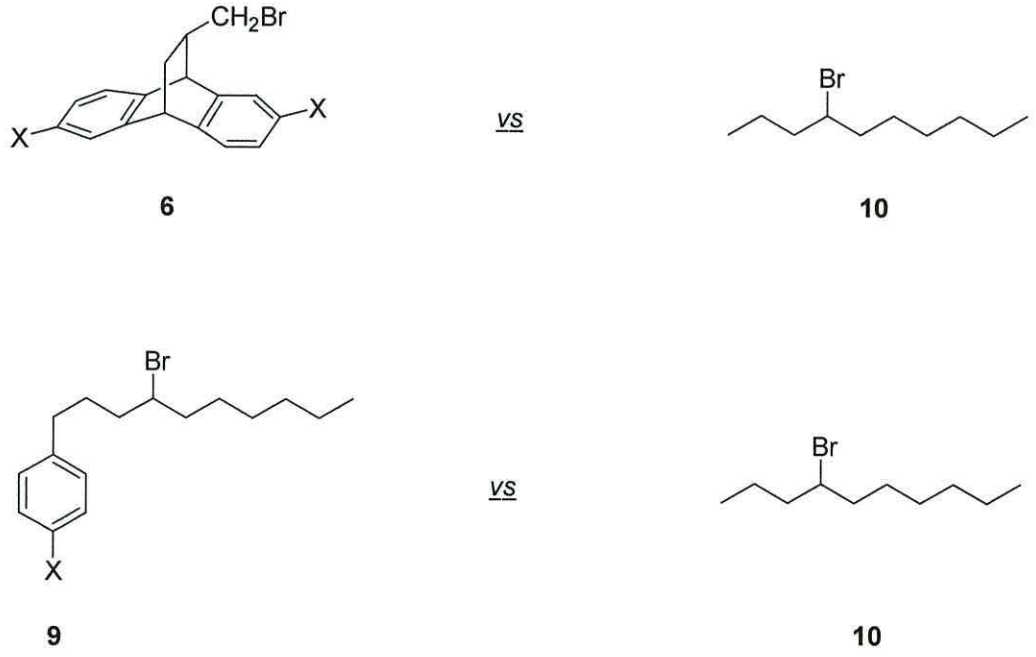

Figure 2.1. Competitive reaction between either anthracene models **6** or acyclic models **9** with acyclic model **10**.

Results

Model derivatives (Figure 2.1) were reacted with a *tri*-butyl tin hydride and the results presented in Appendix F can be manipulated to calculate the relative ratio of each substrate with respect to the derivative **10** (Appendix G). These results have been summarised in Table 2.1.

Table 2.1. Rates of reaction of derivatives **39**, **40**, **41** and **47**, relative to the derivative **10**.

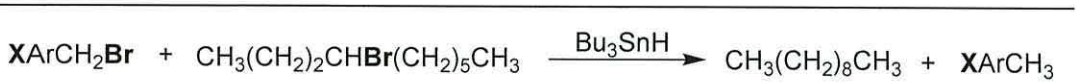

Compound	Ar	X	k_{rel} (Bu_3SnH)	RSD (%)
39	Anthracene adduct	-H	1.4 ± 0.1	3.99
40	Anthracene adduct	$-CH_3$	1.1 ± 0.1	3.67
41	Anthracene adduct	$-NO_2$	8.0 ± 0.3	3.99
47[†]	Acyclic derivative	-H	1.2 ± 0.1	4.89
10[‡]	-----	-----	1	-----

[†] Data obtained *via* GCMS.
[‡] Assigned as unity as the reference and included only for comparative purposes.

The energies (Appendix H) and structures (Appendix I) of anthracene derivatives of general type **59** (Figure 2.2) have been calculated using the high level computational methods B3LYP/6-31G*//B3LYP/6-31G* and RMP2/6-31G*//B3LYP/6-31G*.

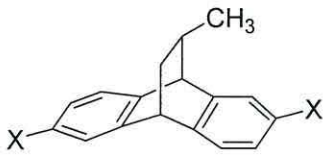

59

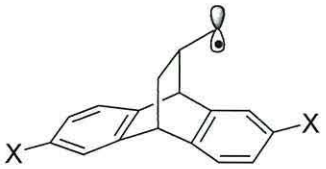

60

Figure 2.2. Models used to calculate RSEs.

Radical stabilisation energies (RSEs) for anthracene derivatives of general structure **60** have been calculated according to the general isodesmic reaction shown in Equation 2.1 and Equation 2.2. This is a well established method to obtain RSEs, which has been used with satisfactory reliability for radicals in the past.[119,120] The success of the method resides in the use of an isodesmic reaction that is, by definition, a reaction in which all the bonds are conserved in number and nature.[121]

$$CH_3X + CH_4 \longrightarrow \bullet CH_3 + CH_3X$$

Equation 2.1.

$$RSE\ (\bullet CH_2X) = BDE\ (CH_4) - BDE\ (CH_3X)$$

Equation 2.2.

The results corresponding to the relative radical stabilisation energies have been summarised in Table 2.2.

Table 2.2. Relative RSEs for anthracene radicals **60a, 60b, 60c** and **60d**.

		RSE relative to X = H (kJ mol^{-1})	
X	Radical	B3LYP/6-31G*	RMP2/6-31G*
-H	**60a**	0.00	0.00
$-CH_3$	**60b**	0.16	0.16
$-NO_2$	**60c**	-0.41	-0.32
-Br	**60d**	-0.40	-0.38

In order to obtain the ESR spectrum of anthracene derivative **39**, the radical intermediate **60a** was generated *in situ* by reaction of bromide derivative **39** with *di*-butyltin in toluene as the solvent of choice (Scheme 2.1). This solvent was chosen because it gives the better solubility of anthracene derivative **39**, despite the fact that aromatic solvents such as benzene or toluene should not be used as the ultimate goal is to detect any interaction between the aromatic ring and the radical intermediate. It was also not possible to choose a polar solvent either. Within these restrictions, the only solvent that afforded a minimum solubility was toluene.

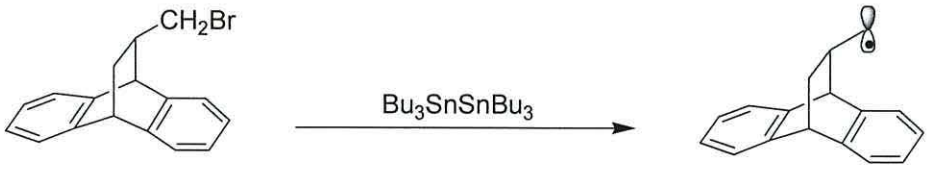

39 **60a**

Scheme 2.1. Reaction between *di*-butyltin and anthracene **39** in toluene.

The ESR spectrum for radical **60a** (Figure 2.3) was recorded in the Department of Chemistry at the University of York.

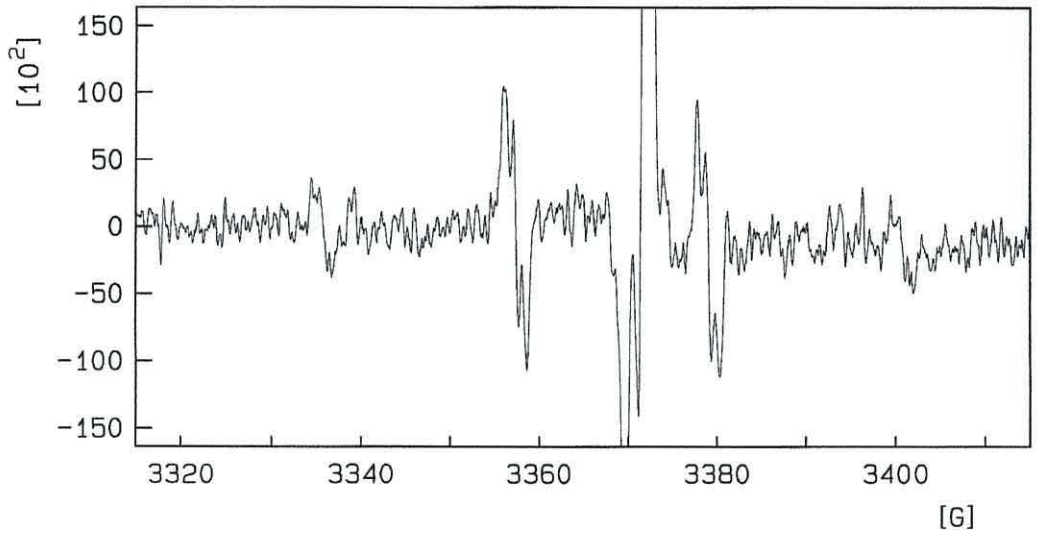

Figure 2.3. ESR spectrum of anthracene derivative **60a**.

Discussion

Anthracene derivatives of general structure **6** and acyclic derivatives of general type **9** provide good models in order to study the interactions of aromatics with free radicals. This is because of their distinctive geometric characteristics. A radical intermediate of general structure **60** can be formed readily by abstraction of the bromo functionality in the presence of tin hydride. This radical is remotely located in relation to the aromatic ring. In the case of anthracene derivatives, the distance between the aromatic moiety and the radical being formed is relatively constrained and similar to that found in the active site of radical dependent enzymes. In the case of acyclic derivatives, the bromo functionality is located further away from the aromatic moiety and the long aliphatic chain allows free rotation in order to find the best conformation. These two models provide therefore contrasting geometries, which can be used in order to examine the relative contributions of entropy and aromatic interactions.

The relative reactivities of anthracene derivatives **39**, **40** and **41** have been determined by reacting them with Bu_3SnH. The mechanism by which an organotin hydride reacts with an alkyl halide is well know and has already been outlined in the Introduction of the thesis.[40,122] The relative ease with which an organotin radical abstracts a halogen can be determined by placing a halide in competition with another for an insufficient amount of hydride. The rate of reaction will depend on the strength of the carbon-halogen bond and the stability of the resulting carbon free radicals, as the prime factors.[40] Since the reaction is of compounds with the same halogen, in this case bromine, the main factor contributing to the relative rate of reaction is the stability of the radical intermediate.

Either GCMS or NMR spectroscopy were used to measure the necessary parameters to calculate the relative rates of reaction, as each conveys advantages in the measurement of different classes of molecules. GCMS chromatograms, corresponding to the solutions containing the analytes, were recorded before and after addition of *tri*-butyl tin hydride. It was possible to distinguish all of the

analytes because they offered distinctive retention times. The relative rates were calculated as the relative rate of disappearance of the peaks corresponding to each of the analytes. The peaks were measured as the area of each analyte divided by the area of the internal reference in order to normalise the results.

GCMS analysis has one main disadvantage. Some of the analytes were more likely to be detected than others. This property has been attributed to the fact that some of the analytes, as in the case of the nitro-substituted derivatives, were less thermally stable, and hence unreliable results were obtained by this method. This is consistent with synthetic results shown in Chapter One, where nitro derivatives **48** and **49** were unable to be separated by fractional distillation due to their thermal instability. The only analyte for which the rate of reaction could reliably be calculated was acyclic derivative **47**. It reacted 1.24 times faster than acyclic derivative **10**. Although a correlation between the aromatic substituents and the relative reactivity could not be established, it appears as if the aromatic moiety, which is the only difference between the two analytes, was influencing the reactivity. This influence is reflected in a faster rate of reaction of the acyclic derivative **47** over the simple derivative **10** of 1.24 times. The reactivity of the bromo functionality was further confirmed by identification in the GCMS spectra of the peak corresponding to *tri*-butyl tin bromide at R_t = 16.04 min. and identification of the resulting product of bromine abstraction by hydrogen at R_t = 14.59 min.

NMR spectroscopy was also used to measure relative rates of reaction. The analytical principle is basically the same as for the GCMS method. The NMR spectra of the solutions containing the analytes were recorded before and after addition of *tri*-butyl tin hydride. In this case, in order to calculate the rate of disappearance, assignment of the relevant peaks corresponding to the protons of the carbons attached to the bromine functionality was crucial. The peaks corresponding to the protons attached to the bromo functionality were integrated between a given shift range and divided by the integrated protons corresponding to the internal reference in order to normalised the results.

Acyclic derivatives of general structure **9** were unable to be analysed by the NMR method because the relevant peaks corresponding to the protons attached to the bromine functionality appear at exactly the same shift as the reference material **10** (Scheme 2.2).

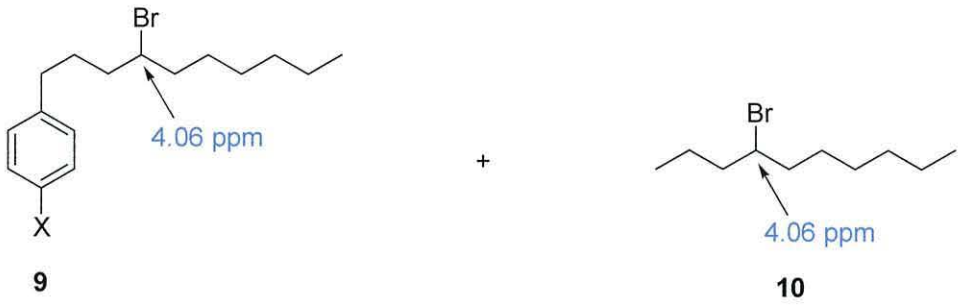

9 **10**

Scheme 2.2. NMR shifts of the protons of the acyclic derivatives **9** in comparison with derivative **10**.

Anthracene derivatives of general structure **6** could successfully be analysed by the NMR method because the protons attached to the C-Br functionality appear at distinct shifts from the acyclic derivative **10** (Scheme 2.3).

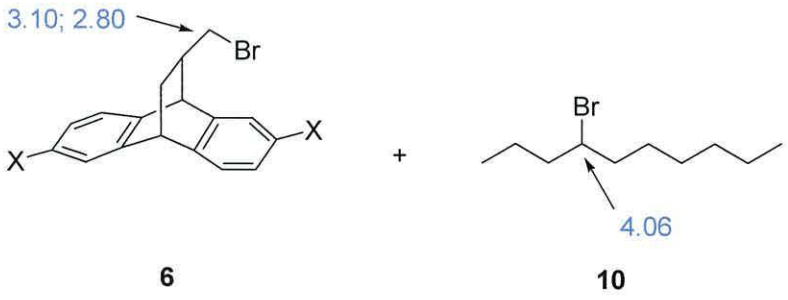

6 **10**

Scheme 2.3. NMR shifts of the protons of the anthracene derivatives **6** in comparison with derivative **10**.

The use of NMR spectroscopy, a non-destructive analytical technique, seems to be a reliable methodology in order to obtain the relative rates of reaction of anthracene derivatives towards Bu_3SnH. Consistent results were obtained when fresh Bu_3SnH was used. The reliability of the GCMS method should be treated more carefully, since only one consistent result could be obtained. In addition some compound could be lost due to different affinities of the analytes with the chromatographic column plus thermal decomposition.

Evidence for an electronic effect exerted by different aromatic substituents on the relative rates of reaction of anthracene derivatives can be obtained from the Hammett relationship. This can be written as in Equation 2.3, where ρ is known as the reaction constant.[123]

$$\log\left(K_X / K_H\right) = \rho\sigma$$

Equation 2.3. Hammett equation.

In order to define the substituent effect, hydrogen is normally adopted as the 'zero' substituent leaving the rest of the possible substituents as electronically donating or withdrawing groups with respect to it. The reason for this choice is that hydrogen has no unshared π-electrons. Groups can therefore be categorised according to the value of a substituent constant, σ, which is characteristic for each of them. Electron withdrawing groups are characterised by positive values of σ and electron donating groups by negative values.[123]

The Hammett equation is a linear free energy relationship (LFER).[31] Substituents located at the *para*-position to the site of interest are best suited for the study of electronic effects. The reason is that changes in the reaction rate brought about by *para*- or *meta*-substituents are virtually only changes of ΔH, since substitution does not greatly affect entropy changes measured by ΔS. However, the *ortho*-substituents give rise to additional steric effects.

The Hammett equation was applied to the relative rates of reaction obtained from the competitive studies. Plotting $\log\left(K_X / K_H\right)$ *vs.* σ should give a straight line if the Hammett relationship is to be satisfied. These results are shown in Table 2.3 and Figure 2.4.

Table 2.3. Relative rates of reaction of anthracene derivatives **39**, **40** and **41** towards Bu_3SnH.

X =	Compound	K_X/K_H	log (K_X/K_H)	σ_p
$-CH_3$	**39**	0.806	-0.094	-0.17
-H	**40**	1.000	0.000	0.00
$-NO_2$	**41**	5.741	0.759	0.78

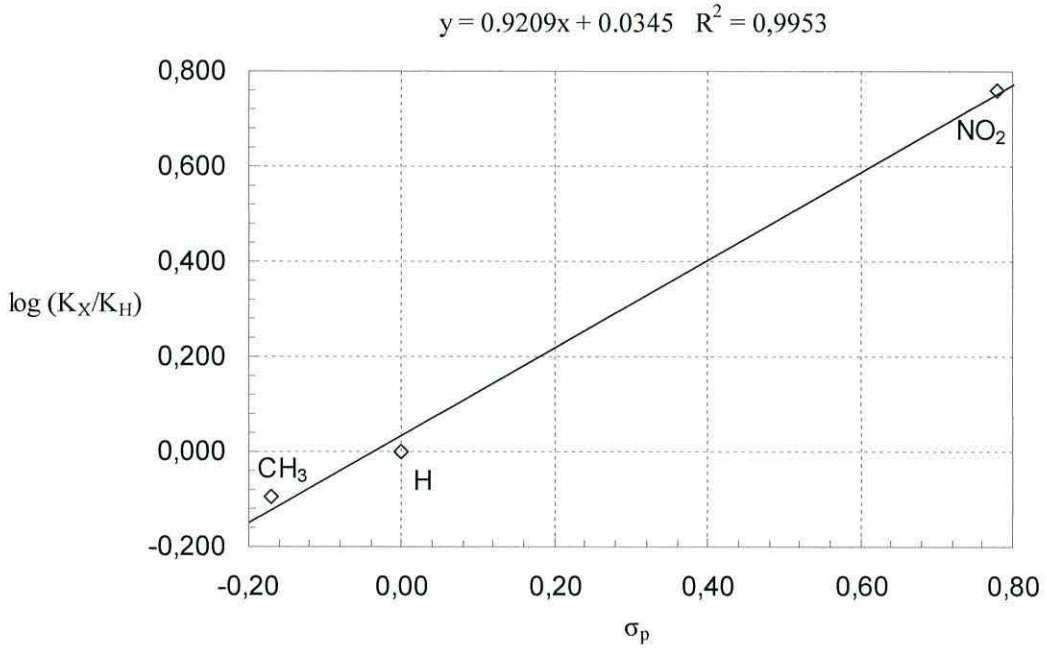

Figure 2.4. Plot of the relative rates of bromine abstraction from anthracene derivatives **39**, **40** and **41** against σ_p.[107] $\rho = 0{,}92$, indicating a negatively charged transition state or intermediate.

As it can be appreciated from Figure 2.4, the bromine abstraction by *tri*-butyl tin hydride at anthracene derivatives follows a Hammett relationship, giving a straight line with an excellent correlation coefficient, $R^2 = 0.9953$, and a positive ρ value of 0.92, indicating a negatively transition state, which is in accordance with the mechanism for halogen abstraction by Bu_3SnH. This shows that the stability of the intermediate is affected by electronic density at the aromatic ring, being stabilised by electron withdrawing substituents. Furthermore, the Hammett equation can be used in order to predict the influence of other functional groups.

The slope of the Hammett plot, known as the reaction constant, ρ, is a measure of the sensitivity of a reaction to the effects of electronic perturbation.[123] The magnitude and sign of the reaction constant can give valuable information about the reaction. The bigger the slope is, the bigger the electronic effect of a substituent on the reaction is. Since it is logarithmic scale, a change in ρ of 0.92 indicates approximately an 8-fold change in rate for each increase in σ. The value of 0.92 is higher than previous values already reported for similar reactions. For instance, the reaction constant for benzyl halogens with Bu_3SnH is 0.40,[124] whereas the highest value for a halogen abstraction reaction was reported by Ingold[125] ($\rho = 0.64$) when he measured the abstraction of benzyl chlorides by $Et_3SiSiEt_3$. If it is considered that previous values were measured for halogens directly attached to the benzene moiety, the reaction constant of 0.92 acquires special significance as the interaction of the aromatic density is stronger through space in the case of anthracene derivatives **6**. This may explain to a certain degree why some aromatic residues have the tendency to be located in the vicinity during radical formation within the active site of radical-dependent enzymes.

From the relative rate data in Table 2.1 and the Hammett plot, it appears that each of the anthracene derivatives **39, 40** and **41** react faster than the acyclic derivative **10**, a fact that, in principle, could be attributed to the presence of the aromatic moiety. A variation in the substituent effect would provide support for this premise. The presence of a moderately strong electron-donating group such as methyl means derivative **40** reacts slower than the corresponding hydrogen group substituted derivative **39** by a ratio of 1:1.24. In contrast, anthracene derivative **41**, possessing the strong electron withdrawing nitro group, reacts faster than the anthracene hydrogen substituted derivative **39** by a factor of 5.74 to 1.

The greater reactivity of anthracene models of general structure **6** over acyclic derivative **10** towards *tri*-butyl tin hydride could, theoretically, be attributed to an intermolecular rather than intramolecular effect of the aromatic ring upon radical formation. However, if such was the case, the same effect would be expected for both the anthracene and the acyclic model. Therefore, it is possible to affirm that the

greater reactivity of anthracene models of general structure **6** over acyclic derivative **10** is due to an intramolecular effect, and the same principle can be applied to acyclic model of general type **9**.

These results suggest firstly that the reactivity of anthracene derivatives is affected by the electronic density at the aromatic ring. Electron donating groups increase the electronic density lowering the reactivity, whereas electron-withdrawing groups decrease the electronic density increasing the reactivity. This implies that electron-withdrawing groups may have a stabilising effect on the intermediate formed during the halogen abstraction by lowering the electron density at the aromatic ring. According to the mechanism for halogen abstraction by tin hydride, there could be two possible rationales (Figure 2.5). Firstly, the radical being formed is being directly stabilised by lower electron density. Secondly, the δ^- transition state leading towards the radical intermediate is being stabilised by an electrostatic interaction, supported by a positive value of the reaction constant of 0.92. To test this hypothesis, the stability of the radical should be known.

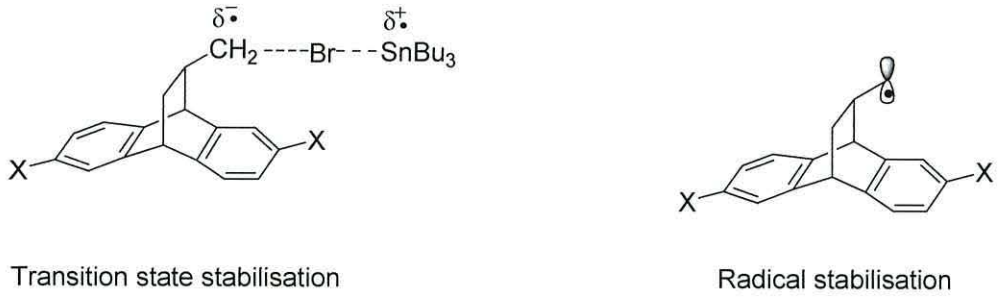

Figure 2.5. Mechanisms for the electronic effect in the halogen abstraction by Bu_3SnH.

Theoretical calculations allow examination of the relationship between the stability of a radical and its rate of formation by comparison of calculated RSEs with experimentally determined relative rates of reaction. Therefore, to probe the electronic effects on the formation of radicals in anthracene derivatives **59a**, **59b**, **59c** and **59d**, their RSEs were calculated (Table 2.2).

The use of B3LYP/6-31G* and RMP2/6-31G* have been demonstrated to be reliable methods in order to calculate RSEs, although B3LYP/6-31G* performs slightly less well than RMP2/6-31G*.[126] Table 2.2, where positive values indicate stabilisation and the negative values indicate destabilisation, shows that the values corresponding to the RSEs of anthracene derivatives **60a**, **60b**, **60c** and **60d** are all within $\pm$ 1 kJ mol^{-1} implying that stabilisation in negligible for this particular system.

Another important parameter to bear in mind is the geometry of the anthracene models of general structure **6**, particularly the distances between the centre of radical formation and the aromatic moiety, which have been summarised in Table 2.4 and Table 2.5. As in can be appreciated in Table 2.4 and Table 2.5, the difference between the average calculated distance of the radical site and the aromatic ring of anthracene derivatives of general structure **59** is slightly smaller than the distance between the radical and carbon and the aromatic ring in derivatives of general type **60**. This is consistent with the calculated RSEs that show no electronic effect exerted by the substituent in the stabilisation of the radical. A tendency towards proximity of the radical centre with the aromatic moiety was not expected as the anthracene adduct is a restrictive system. However, it is important to note that the average distance between the radical formation site and the aromatic moiety is about 4.1 Å. This distance confirms the anthracene system as an appropriate model to study radical-aromatic interactions, as it resembles the distance between aromatic residues and the radical formation site in radical-dependent enzymes, as outlined in the Introduction of this thesis.

Table 2.4. Calculated distances for anthracene derivatives **59a**, **59b**, **59c** and **59d** derived from computationally obtained structures.

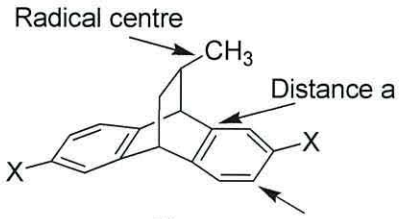

59 Distance b

X =	Compound	a (Å)	b (Å)	Average (Å)
-H	**59a**	3,095	5,178	4,137
$-CH_3$	**59d**	3,098	5,187	4,143
-Br	**59c**	3,102	5,199	4,151
$-NO_2$	**59b**	3,094	5,167	4,131

Table 2.5. Calculated distances for anthracene radical derivatives **60a**, **60b**, **60c** and **60d** derived from computationally obtained structures.

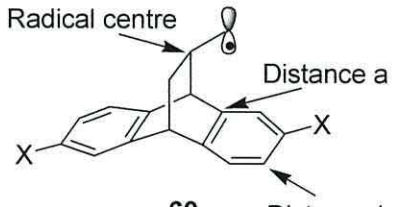

60 Distance b

X =	Compound	a (Å)	b (Å)	Average (Å)
-H	**60a**	3,082	5,166	4,124
$-CH_3$	**60d**	3,085	5,175	4,130
-Br	**60c**	3,087	5,183	4,135
$-NO_2$	**60b**	3,083	5,156	4,120

It seems more likely that the δ^- transition state is stabilised rather than the radical intermediate. This assumption is supported by two distinct data. Firstly, relative RSEs indicate that the radical intermediate is unaffected by placing different substituents at the aromatic ring. Secondly, if the radical intermediate were to be stabilised, it would have been expected to be stabilised by electron donating substituents rather than the observed effect of stabilisation by electron withdrawing substituents. This is because a radical is an electron deficient species, and as in the case of carbocations, would have been expected to be stabilised by an electron rich group, such as the aromatic ring. Electron rich substituents on this ring would further increase the electron donating power. Since it is very unlikely that this remote stabilisation is occurring through bond, as the substituents are extremely remote from the reactive centre, it is logical to believe that it is occurring through space. In fact, anchimeric assisted radical reactions exerted by groups located at the β and δ positions have been reported recently.[127,128] One way to confirm this would be to see if there were a direct interaction between the aromatic ring and the radical.

As it has been outlined in the Introduction, one of the best methods to study a radical directly is by using electron spin resonance, because it can give important information about the structure of the radical and also because it could reveal interactions between the aromatic moiety and the radical. The use of ESR in a small model such as the anthracene derivative **39** could show aromatic interactions that would otherwise be impossible to detect in the case of enzymes. The ESR spectrum of anthracene derivative **39** was thus recorded in order to see if there was interaction observable in the hyperfine structure between the radical and the aromatic moiety. The hyperfine structure shows a doublet of a triplet centred at g = 2.0013, a value that is smaller than the *g*-factor for the free electron (2.0023). The triplet is consistent with the coupling between the radical and the two methylene protons in the α-carbon with a calculated coupling constant of 13.5 G. The doublet is due to the coupling of the radical with the β-hydrogen showing a coupling constant of 1.3 G. However, no interaction between the radical and the aromatic ring is observed. If such an interaction would have been measurable, further splitting due to the four aromatic protons would have been detected.

The lack of observed interaction between the radical and the aromatic protons can be attributed partially to low solubility of the anthracene derivative **39** in toluene, resulting in a very low concentration of radicals in solution. This could explain why no further splitting due to the aromatic protons was observed, since the spectrum obtained contain a great deal of noise that may occlude the splitting of interest. This is reflected in the very low signal to noise ratio in the spectrum (Figure 2.3). The usual technique to improve the signal to noise ratio is ENDOR. However, this technique could not be applied as it normally requires very high sample concentration, which was hampered by the low solubility of anthracene derivative **39**. This result does not exclude the possibility that interaction between the radical and the aromatic moiety exists, but confirms that, if it does exist, it is small and a higher concentration of radicals is needed for such a remote interaction to be detected.

These results have bigger implications. It appears that the stabilisation of the intermediate is slightly greater when the radical is constrained by geometry to a distance of about 4.1 Å, as in the case of the anthracene derivatives, rather than in the case of acyclic derivatives, where the aliphatic chain allows free rotation to find the best conformation. The effect of restraining geometry can be quantified as 1.2 times bigger for the anthracene derivatives with respect to the acyclic derivatives if the reactivities of their corresponding hydrogen substituted derivatives **39** and **47** are compared. Most importantly, it is possible to establish a correlation between the propensity of aromatic residues in the vicinity of the active site of radical dependent enzymes and the possibility that these residues are stabilising the radical intermediates formed.

Chapter 3

Electrochemistry Studies

In the previous Chapter it was shown that the relative rates of reduction could be influenced remotely by an aromatic substituent. To further explore this effect, cyclic voltammetry can be used to provide additional information concerning the influence of the aromatic substituent on the potential of reduction of the carbon-bromine bond and the mechanism of reduction of the carbon-bromine bond. Therefore, the synthetic models (Figure 3.1) obtained in Chapter One were studied by cyclic voltammetry.

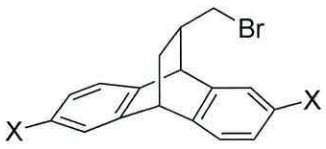

6

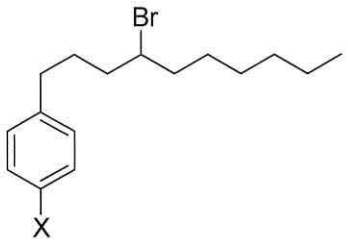

9

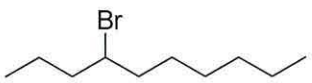

10

Figure 3.1. Models to be studied by electrochemical means.

Results

Cyclic voltammetry was used in order to calculate the potential at which the bromide moieties of compounds **6**, **9**, and **10** are reduced homolytically to afford radical intermediates. A platinum wire electrode was used, which, in contrast to the mercury electrode or other reactive electrodes, is believed to be sufficiently inert in chemical reactions where radical intermediates are formed during the reduction process.[129,130]

The cyclic voltammograms obtained for acyclic model bromo derivatives **10, 47, 48, 50,** and **51,** and for anthracene model bromo derivatives **39, 40** and **41** are shown in the following figures.

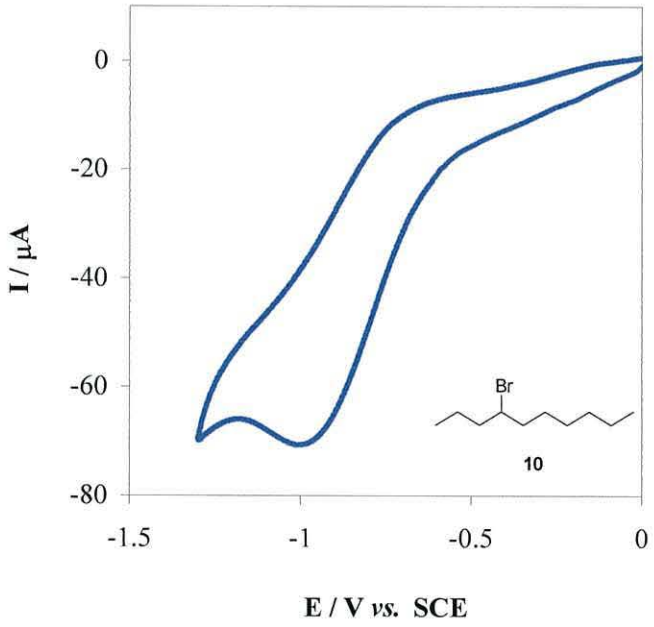

Figure 3.2. Voltammogram of bromo derivative **10** in DCM at 0.2 $V.s^{-1}$, recorded between 0 to -1.3 V. Irreversible reduction peak at -0.99 V.

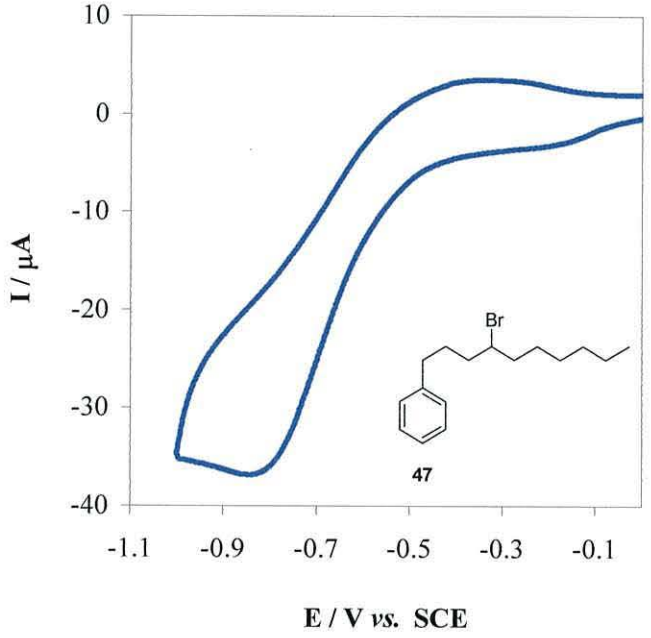

Figure 3.3. Voltammogram of bromo derivative **47** in DCM at 0.2 $V.s^{-1}$, recorded between 0 to -1.0 V. Irreversible reduction peak at -0.84 V.

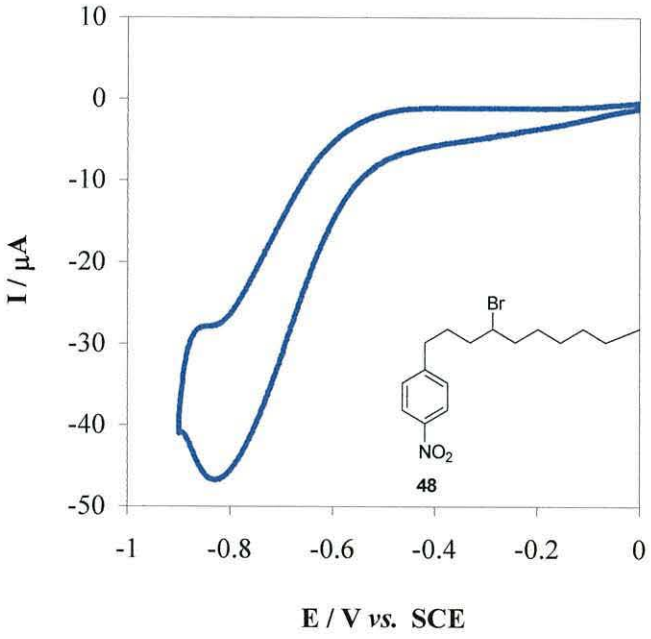

Figure 3.4. Voltammogram of bromo derivative **48** in DCM at 0.2 $V.s^{-1}$, recorded between 0 to -0.9 V. Irreversible reduction peak at -0.82 V.

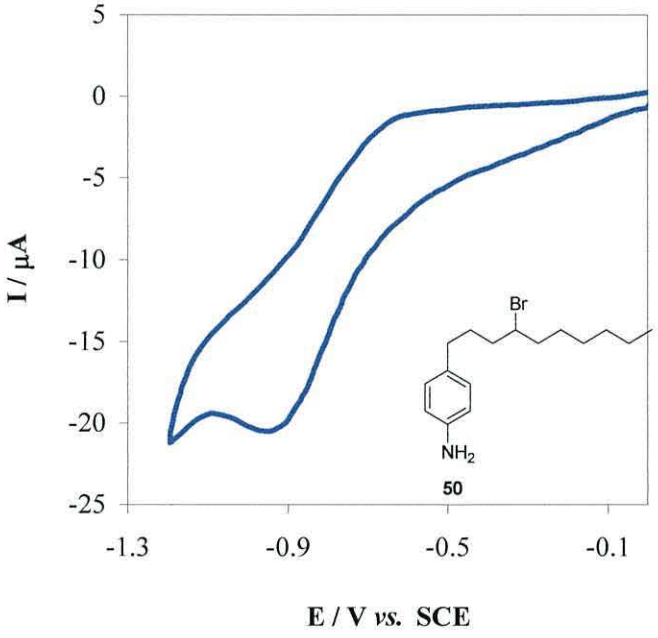

Figure 3.5. Voltammogram of bromo derivative **50** in DCM at 0.2 $V.s^{-1}$, recorded between 0 to -1.25 V. Irreversible reduction peak at -0.91 V.

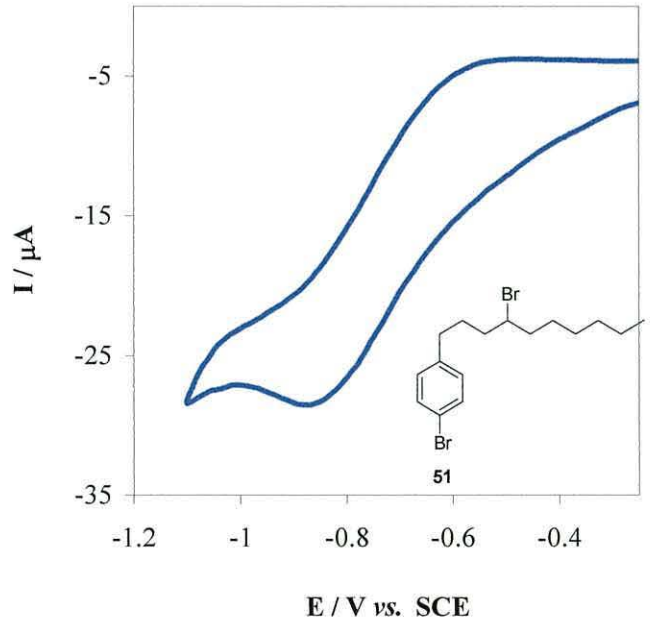

Figure 3.6. Voltammogram of bromo derivative **51** in DCM at 0.2 $V.s^{-1}$, recorded between -0.25 to -1.2 V. Irreversible reduction peak at -0.85 V.

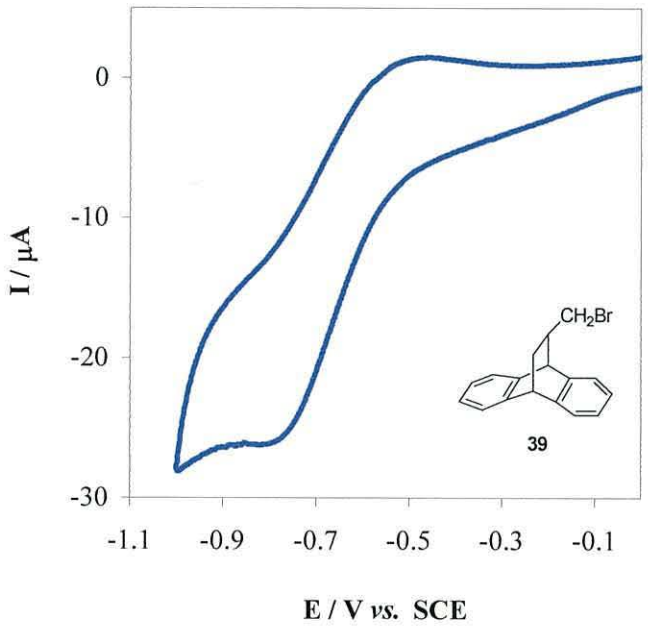

Figure 3.7. Voltammogram of bromo derivative **39** in DCM at 0.2 $V.s^{-1}$, recorded between 0 to -1.0 V. Irreversible reduction peak at -0.79 V.

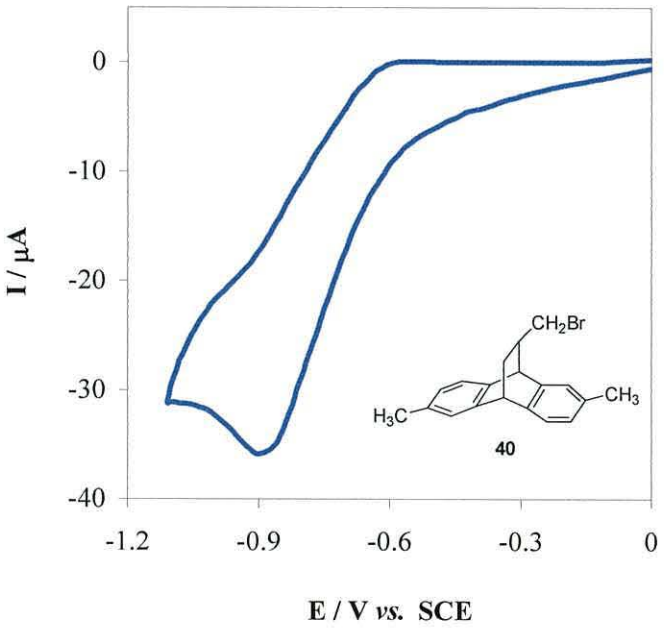

Figure 3.8. Voltammogram of bromo derivative **40** in DCM at 0.2 $V.s^{-1}$, recorded between 0 to -1.1 V. Irreversible reduction peak at -0.89 V.

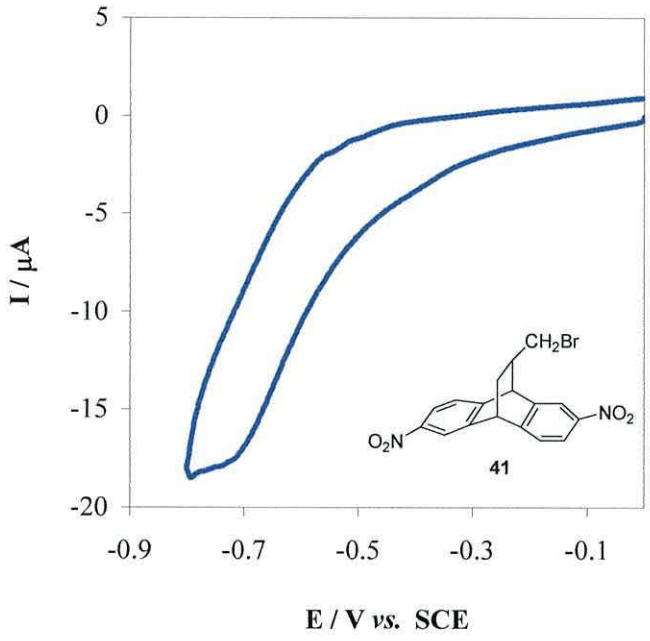

Figure 3.9. Voltammogram of bromo derivative **41** in DCM at 0.2 $V.s^{-1}$, recorded between 0 to -0.8 V. Irreversible reduction peak at -0.72 V.

Discussion

The cathodic reduction of halogenated organic compounds and consequent cleavage of the carbon-halogen bond is now a very well documented field in organic electrochemistry.[35,131,132] The electrolytic fission of the carbon-halogen bond is an irreversible process.[34]

When inert electrodes are used in the voltammetric study of halogenated compounds, two main behaviours have been distinguished according to the nature of the carbon atom. When the functional carbon is directly attached to an aromatic ring, the anion radical formed upon injection of one electron appears as an intermediate in most cases, even though it may cleave very rapidly into the corresponding aryl radical and the halide ion (Scheme 3.1) [133]

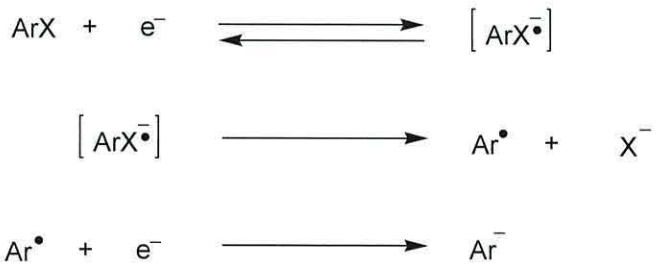

Scheme 3.1. Stepwise mechanism for the electrochemical reduction of the carbon-halogen bond in aromatic compounds.

In the case of an aliphatic carbon, there is extensive evidence that the radical anion does not actually exist as an intermediate. The reductive cleavage of these molecules is expected to proceed along a dissociative electron transfer pathway in the sense that electron transfer and breaking of the carbon-halogen bond are concerted processes. A radical and an anion will then be produced in a single step (Scheme 3.2).[132,134,135]

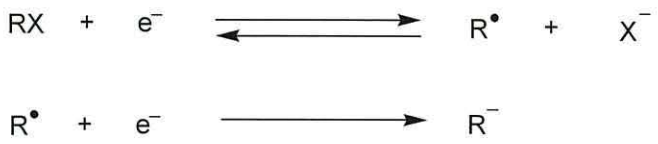

Scheme 3.2. Concerted mechanism for the electrochemical reduction of the carbon-halogen bond in aliphatic compounds.

Figure 3.10 shows the two situations mentioned above where, in one case, the radical anion, $R^{\bullet -}$, is an intermediate whereas, in the other, the energy of the radical anion is so high that the concerted pathway is energetically more advantageous.[132]

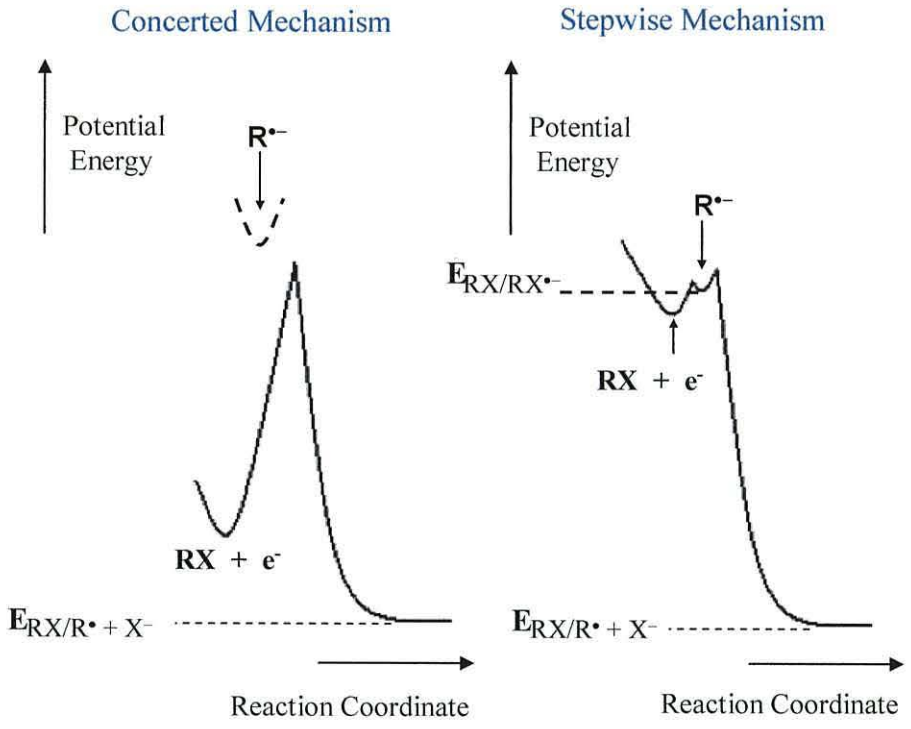

Figure 3.10. Potential energy diagram showing the concerted and stepwise mechanisms.[130]

The free radical formed upon one-electron reductive cleavage of the C-X bond can be further reduced to a carbanion as shown in the following scheme.[136]

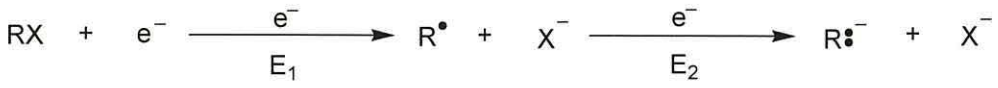

Scheme 3.3. Reduction of a halogenated compound to a carbanion.

The potential, E_2, at which the radical (R•) is reduced is generally positive or at least equal to the potential at which the reductive cleavage occurs, E_1, hence normally a single two electron wave is observed in the cyclic voltammogram, with the radical formation as the rate determining step.[136,137] If the radical is not reduced at E_1, it then has to be reduced at a more negative potential, giving rise to a second peak.[133]

Analysing the cyclic voltammograms shown in the results section, a single irreversible cathodic wave is seen for all the compounds studied. This observation is consistent with the conclusions of earlier workers that reductive cleavage of carbon-halogen bond of cyclic alkyl and secondary alkyl bromides is generally a one-step irreversible, two-electron process due to the ease of reduction of the formed radical.[129,133,137,138]

The main characteristics of the direct electrochemical reduction of these compounds, as derived from cyclic voltammetry, are summarised in Tables 4.1 and 4.2.

Table 3.1. Summarised cyclic voltammetry data for anthracene derivatives **39**, **40** and **41**.

Anthracene derivatives	E_p (V) *vs.* SCE	$E_{p/2}$ (V) *vs.* SCE	Transfer coefficient (α)
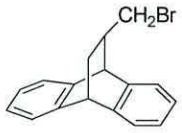 **39**	-0.79	-0.65	0.33
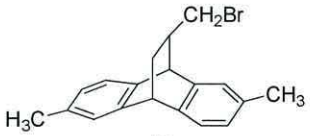 **40**	-0.89	-0.73	0.29
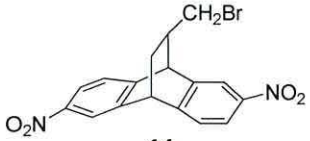 **41**	-0.72	-0.67	0.31

Table 3.2. Summarised cyclic voltammetry data for acyclic derivatives **10**, **47**, **48**, **50** and **51**.

Acyclic derivatives	E_p (V) *vs.* SCE	$E_{p/2}$ (V) *vs.* SCE	Transfer coefficient (α)
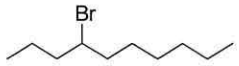 **10**	-0.99	-0.80	0.25
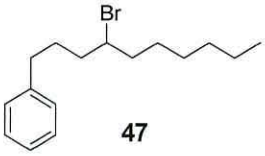 **47**	-0.84	-0.67	0.27
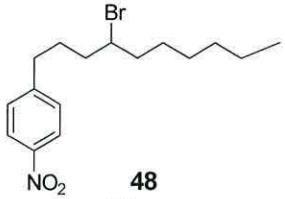 **48**	-0.82	-0.66	0.29
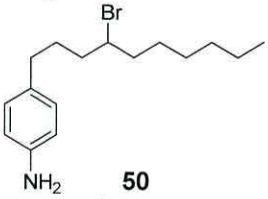 **50**	-0.92	-0.75	0.27
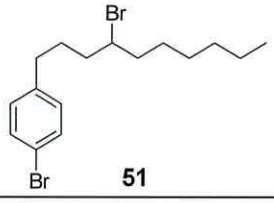 **51**	-0.85	-0.70	0.31

As previously stated, the single irreversible peak seen for all the compounds studied indicates that the reductive cleavage of carbon-halogen bond is a one-step irreversible, two-electron process due to the ease of reduction of the obtained radicals. Also, the large broadness of the reduction peak suggests that the rate determining step is the radical formation.[130,132,139]

In order to discern if the electron transfer reaction is taking place through a stepwise or a concerted mechanism, the value of the transfer coefficient, α, can be utilised. Due to its slow rate, the concerted electron transfer process has a very small value of α, often much smaller than 0.5 and typically around 0.3, whereas the stepwise

mechanism is characterised by α values about 0.5 or greater.[134,140] The value of α can be determined from the cyclic voltammetry peak widths, assuming that the Butler-Volmer kinetics apply (Equation 3.1).[130,133,141,142]

$$\alpha = \frac{1.85RT}{F} \times \frac{1}{(E_{p/2} - E_p)}$$

Equation 3.1. General equation to calculate the transfer coefficient (α).

Where,

α - Transfer coefficient

T - Temperature (293 K)

F - Faraday constant (96485.309 C mol^{-1})

R - Rydberg constant (8.314 J K^{-1} mol^{-1})

$E_{p/2}$ - E_p – Peak width

The calculated transfer coefficients for all analytes are shown in Table 3.2 and Table 3.1. The values of α were small for all the substrates, being between 0.25 and 0.33. This is consistent with similar observations that have been reported by Saveant *et al.*[133] on the electrochemical reduction of simple aliphatic halides. The fact that the transfer coefficients were smaller than 0.5 falls in line with the concept that the reduction pathway does not involve the anion radical as an intermediate. It can then be concluded that the reductive cleavage for the studied derivatives follows a concerted mechanism.

Considering the mechanism of the reduction of a carbon-halogen bond, the relative ease with which the halogen is abstracted will depend on the strength of the carbon-halogen bond and the stability of the resulting carbon free radicals as the prime factors. Since the carbon-halogen bond is of the same nature in all the compounds studied (C-Br), a correlation can be established between the ease of reduction and the stability of the radical intermediate as the fundamental factor affecting it.[40] Furthermore, it is possible to directly make a relationship between the potential measured and the substituent at the aromatic ring. This is because the reaction

conditions were all kept identical for all of the substrates. In particular, the substrate concentrations were normalised at 10 mM, which is the usual concentration for these type of experiments.

From Table 3.2 it is possible to see a significant difference between the reduction potentials (0.15 V) of the acyclic derivative **10** (non-aromatic moiety) and the acyclic derivative **47** (-H substituted aromatic), suggesting that the aromatic moiety might be having an influence in the stabilisation of the intermediate of the reduction. Furthermore, the reduction of the acyclic derivative **48**, containing a strong electron-withdrawing group ($-NO_2$), occurs 0.02 V before the reduction of acyclic derivative **47** (-H). This is in contrast with acyclic derivative **50** containing a strong electron-donating group ($-NH_2$), whose reduction occurs at 0.10 V after the reduction of acyclic derivative **47** (-H). These results seem to indicate that the presence of the substituent on the aromatic ring has an influence on the stability of the reaction intermediate and therefore on the electrochemical reduction of the carbon-bromine bond.

When the reduction was carried out on the more geometrically restricted anthracene models, the substituent effect appeared to be bigger, which is likely due to the proximity between the aromatic moiety and the radical intermediate. In these models, whose results are summarised in Table 3.1, the difference in the reduction potential between anthracene derivative **41** ($-NO_2$) and anthracene derivative **39** (-H) is 0.07 V, which is slightly greater than the same difference for the case of the acyclic derivatives. The difference in the reduction potential between anthracene derivative **40** ($-CH_3$) and anthracene derivative **39** (-H) is significant (0.10 V), which is considerable bearing in mind that $-CH_3$ is only a moderate electron-donating group.

A comparison between the different models can also be established. The most negative reduction potential, or least stabilised model, corresponds to the acyclic derivative **10**, which contains no aromatic moiety. However, between the acyclic and the anthracene models, the latter appears to reduce at a less negative potential

indicating that it provides a better model for the stabilisation of the reaction intermediate. The increased stabilisation could be explained in terms of the more restrictive geometry of the anthracene system compared to the acyclic model. This geometry allows the anthracene system to hold the radical above the aromatic ring, hence providing a stronger interaction between either the radical, or transition state leading to the radical, and the aromatic ring. Furthermore, this distance, which has been calculated by computational studies in Chapter Two to be in the order of 4.1 Å is especially relevant as it bears a resemblance with the distance between the active site of radical-mediated enzymes and aromatic residues (Introduction).

Further mechanistic implications can be deduced by applying the Hammett equation shown in Equation 3.2.

$$\ln k = \rho\sigma$$

Equation 3.2. General Hammett relationship.

The rate constant can be related to the potential using Equation 3.3.[143] This is an example of a linear free energy relationship where a kinetic parameter, the logarithm of the rate constant, varies linearly with a thermodynamic parameter, the potential.

$$\alpha = \frac{RT}{F}\left|\frac{d\ln k}{dE}\right| = \frac{d\Delta G}{dE}$$

Equation 3.3. Relationship between the rate constant, *k*, and the potential, E.

Equation 3.3 can be rearranged into Equation 3.4.

$$\frac{\alpha F}{RT}dE = d\ln k$$

Equation 3.4. Proportionality between the potential and the rate constant.

Then, combining Equation 3.2 and Equation 3.3, Equation 3.5 can be obtained.

$$E = \rho\sigma$$

Equation 3.5. Hammett equation applied to electrochemistry parameters.

Applying the above Equation 3.5, it is possible to plot the potential *versus* the substituent constant.

Hammett plots have been produced for acyclic (Figure 3.12) and anthracene (Figure 3.11) derivatives. The observation that the ease of reduction of anthracene derivatives is increased by electron-withdrawing groups is supported by the Hammett plot of the potential of reduction against the substituent parameters. The plot gives a relatively good correlation coefficient ($R^2 = 0.8056$), with a positive ρ value of 0.15 indicating a negatively polarised transition state or intermediate. These data support the assumption that the electroreduction of anthracene derivatives is primarily governed by the stability of the radical intermediate and not by polarity in the transition state, therefore being in agreement with a radical mechanism.

Similar conclusions can be drawn for acyclic derivatives. In this case, the plot gives a slightly better correlation coefficient ($R^2 = 0.8965$), with a positive ρ value of 0.06, indicating a negatively polarised transition state or intermediate. In the case of acyclic derivatives, polar effects are even smaller than for anthracene derivatives, which can be attributed to geometry factors, with the anthracene model being a more constrained system. If an intermolecular effect was responsible for the change of the potential of reduction during carbon-bromine reduction, then it would be expected that changing a substituent in the anthracene models **6** should have a effect twice in magnitude to changing a substituent in the acyclic models, because there is twice the concentration of aromatic rings in the anthracene solution. However, this is not the case, and changing the substituent in the anthracene model **6** contributes considerably more than twice the effect of changing a substituent in the acyclic model **9**, as can be appreciated from the reaction constants of 0.15 and 0.06, respectively. This implies that changing a substituent at the aromatic ring influences the potential of reduction with a component due to thorough-space interaction.

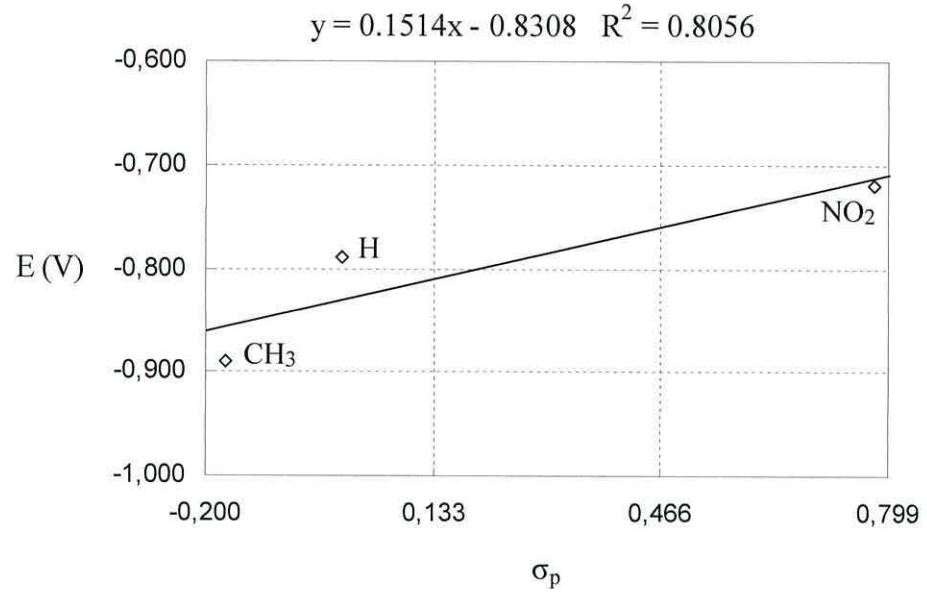

Figure 3.11. Plot of the potential of anthracene derivatives **39**, **40** and **41** against σ_p.[107] $\rho = 0.15$, indicating a negatively charged transition state or intermediate.

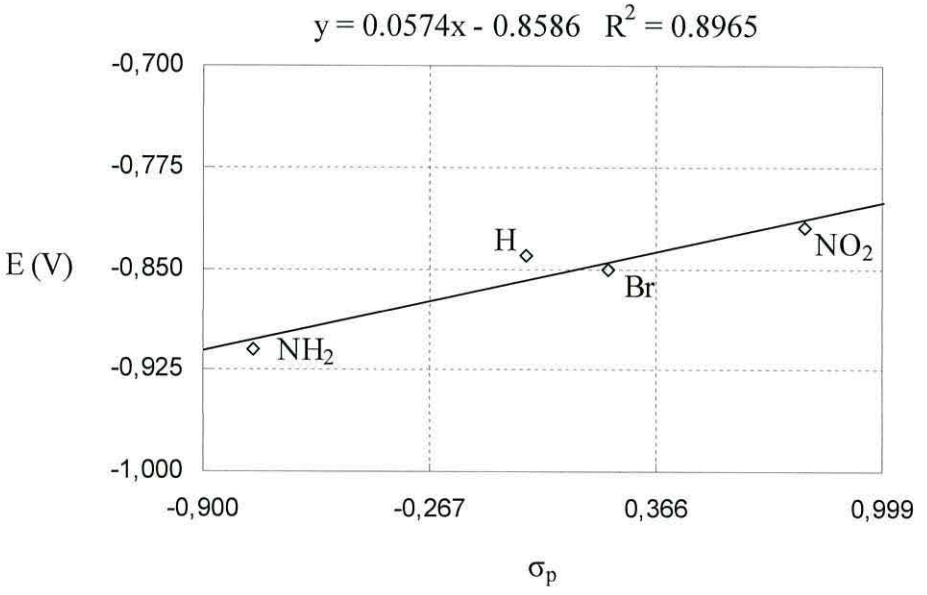

Figure 3.12. Plot of the potential of acyclic derivatives **10**, **47**, **48**, **50** and **51** against σ_p.[107] $\rho = 0.06$, indicating a negatively charged transition state or intermediate.

The information derived from the Hammett plots of the electroreduction of acyclic and anthracene derivatives contrasts with the results obtained in Chapter Two concerning the relative rate of reaction towards Bu_3SnH. In both cases, bromine abstraction passes through a negatively transition state or intermediate. However, as it was shown in Chapter Two, polar effects due to change of the substituent from electron-donating to electron-withdrawing have a greater influence. In the case of bromine abstraction by Bu_3SnH, the effect on the relative reactivity is six times bigger than that seen in the electroreduction of the carbon-bromine bond, suggesting that the intermediate is less polarised in the latter.

Other radical-assisted reactions have been reported through anchimeric assistance, mostly by remote stabilisation of the radical intermediate by substituents in the β and δ-positions.[127,128] Particularly, the hydrogen transfer to bromine with *N*-bromo succinimide (NBS) in remotely substituted amides from the putative reaction site was found to be assisted anchimerically, although no aromatic π-system was involved.[127] In the case of anthracene and acyclic models the influence of the aromatic π-system in the stabilisation provides the first example of remote stabilisation through space by an aromatic π-system, although there have been reports in the literature of cation-π interactions as it was explained in the Introduction.[56,57,62] This effect has further implications as it could be directly linked to the case of enzymatic reactions *via* radical mechanism, where aromatic residues have been observed at similar distances from active site (Introduction).

As discussed above, the broadness and shape of the observed reduction peaks indicates that the reduction is governed by the kinetics of an electron transfer step. In addition, the transfer coefficient (symmetry factor) of the rate controlling electron transfer step is distinctly lower than 0.5. This provides evidence that the electrochemical reductive cleavage of the investigated derivatives follows a concerted mechanism *i.e.*, one not involving the formation of a radical anion as intermediate, but the radical. Furthermore, the connection between the potential of reduction of the carbon-halogen bond and the stabilisation of the δ^- transition state has been established. The aromatic moiety seems to have an influence in the

stabilisation of the δ^- transition state. This has been corroborated by the difference in reduction when the substituent is changed from an electron-donating to an electron-withdrawing group. In addition, it has been possible to demonstrate that anthracene adducts provide better stabilisation than acyclic derivatives.

Trends obtained from the electrochemical results are consistent with those from relative rate studies. It was discussed in Chapter Two that the reactivity of the anthracene derivative **41** ($-NO_2$) is higher than the reactivity of anthracene derivative **39** (-H), and the latter higher than that of anthracene derivative **40** ($-CH_3$). This supports the rationalisation that electron-donating groups destabilise the intermediate, whereas electron-withdrawing groups have a stabilising effect. It has therefore been shown that the electronic density at the aromatic ring affects the stability of the δ^- transition state for reactions passing through a δ^- transition state, especially in anthracene models, where both the radical and the aromatic moiety are close in space to each other due to a fairly restrictive geometry. It has also been shown that the effect of the electronic density is very small in both acyclic and anthracene models, providing evidence that the electroreduction of such derivatives is governed by the stability of the radical intermediate and less by polarity in the transition state.

Chapter 4

The Paracyclophane Model

It has been shown in previous chapters that anthracene derivatives give us a reasonable model to study the influence of the aromatic moiety upon the formation of a radical intermediate. However, the geometries in anthracene derivatives are not ideal. Paracyclophanes **8** of the type shown in Figure 4.1 are rigid systems ideally set up to examine the influence of an aromatic ring on a remote centre.[68] Anthracenes are easily accessible synthetically, but, based on Cram's work,[69] paracyclophanes are expected to show a greater effect of the proximal aromatic on reactive intermediates, as already discussed in the Introduction.

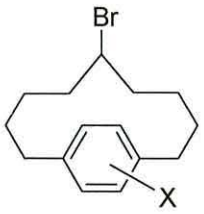

8

Figure 4.1. Paracyclophane models **8**.

This chapter will deal with the investigation of the different approaches used towards the synthesis of paracyclophanes of the general structure **8** shown in Figure 4.1.

Results

The synthesis of paracyclophane derivatives can be made following a procedure already developed by Cram and co-workers during the sixties and seventies *via* acyloin condensation, which first requires the preparation of the suitable precursor.[76] This synthesis was achieved starting out from cheap and simple materials. Friedel-Crafts reaction between benzene **61** and glutaric anhydride, in the presence of a Lewis acid, afforded acid derivative **62** in good yield as outlined in Scheme 4.1.[144]

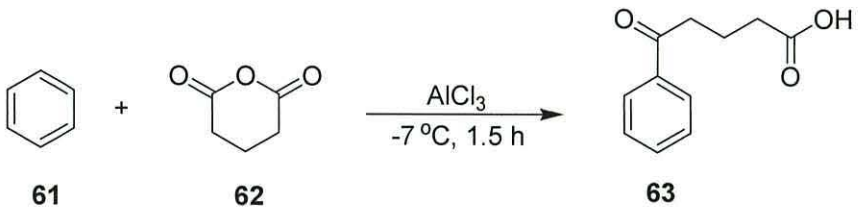

61 **62** **63**

Scheme 4.1. Synthesis of 4-benzoylbutyric acid **63**.

This reaction is extremely exothermic and needed to be kept at low temperature, -7 °C, throughout. The work-up was simple, as the acid product **63** could be separated by filtration from the aqueous phase. The crude product **63** was further purified by firstly dissolving it in basic media, followed by filtration. Isolation after re-acidification afforded acid **63** in 91.7 % yield. The acid derivative **63** was easily characterised by ^{1}H NMR spectral analysis, which shows the methylene groups as two different triplets, δ 3.09 and δ 2.52, due to the electronic effects conferred by the carbonyl and the carboxylic acid group, respectively, and one pentuplet at δ 2.10 due to similar splitting from the two methylenes. The aromatic protons appear in three different environments because of the electron-withdrawing effect of the carbonyl group at δ 7.97, δ 7.58 and δ 7.47. This data was also consistent with literature values.[145]

The reduction of acid derivative **63** was carried out using the Huang-Minlon modification of the Wolff-Kischner reaction as outlined in Scheme 4.2.[146]

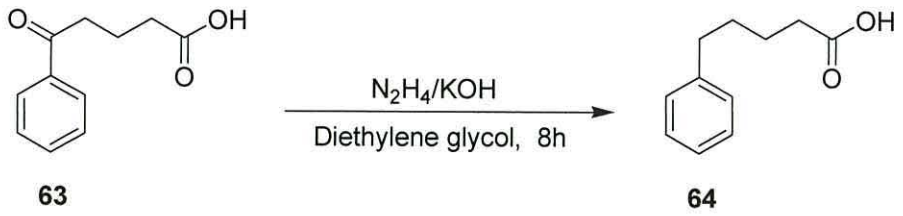

63 64

Scheme 4.2. Synthesis of 5-phenylvaleric acid **64**.

The acid product **64** was isolated simply by precipitation in acidic media to give a 71.6 % yield. It was well characterised by both ^{1}H and ^{13}C NMR spectral analysis. Comparing the ^{1}H NMR spectrum with that of the starting material **63,** the differences in the shift of the aromatic protons are smaller compared to the starting material **63** and they appear in two different environments at δ 7.30 and δ 7.21, instead of the three signals seen in the starting material **63**, δ 7.97, δ 7.58 and δ 7.47. This is due to the disappearance of the electron-withdrawing effect of the carbonyl group α to the ring. The product is also confirmed by ^{13}C NMR spectral analysis, where the peak at δ 199.35 due to the carbonyl has disappeared. The IR spectrum shows a broad and strong band at 2916 cm^{-1}, corresponding to the hydroxyl group, plus a strong and sharp band at 1711 cm^{-1}, corresponding to the carbonyl group, which combined together account for the presence of the acid group.

Esterification of acid derivative **64** was carried out by treatment in dry methanol with thionyl chloride as shown in Scheme 4.3.

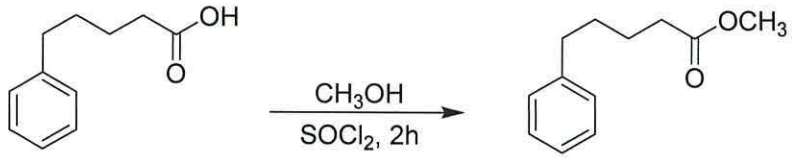

64 65

Scheme 4.3. Synthesis of 5-phenylvaleric acid methyl ester **65**.

The ester product **65** was identified by comparing its ^{1}H NMR spectrum with that of the parent compound. This revealed the appearance of a new peak at δ 3.7, which

integrates for three hydrogens and is consistent with the CH_3 signal of the methoxy group and literature data.[147]

A further, second Friedel-Crafts acylation was carried out at -7 °C using succinic anhydride **66** and aluminium chloride as the Lewis acid catalyst as described in Scheme 4.4.

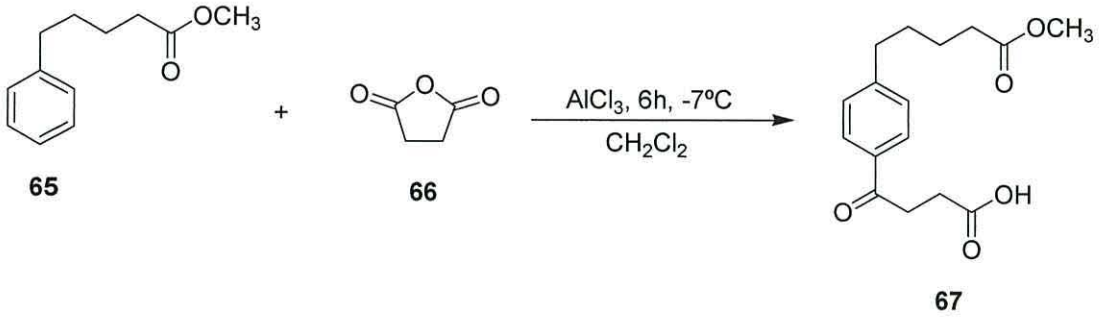

65 **66** **67**

Scheme 4.4. Synthesis of 3-[4-5-valerianyloxymethyl)-benzoyl]-propionic acid **67**.

Identification of the acid product **67** was determined by ^{1}H NMR spectral analysis. The aromatic protons appear in two distinctive environments, δ 7.91 and δ 7.27, as two doublets, due to the deshielding that the carbonyl group confers to the 4-carbon alkyl chain, compared to its absence in the 5-carbon alkyl chain. The ^{13}C NMR spectrum confirms the presence of three different carbonyl groups with the ketone group at δ 199.0, the carbonyl of the acid at δ 180.0 and the carbonyl of the ester at δ 175.5.

Further reduction of the carbonyl group at the α-position with respect to the phenyl ring of derivative **67** was carried out in acidic conditions using the Clemmensen reaction with amalgamated zinc in hydrochloric acid, as illustrated in Scheme 4.5. The Clemmensen reduction of compound **67** involved, firstly, the generation *in situ* of amalgamated zinc by reaction of zinc dust with mercury chloride in hydrochloric acid/water mixture. The reaction then proceeds over a long period of time, *ca.* 48 hours, with addition of aliquots of hydrochloric acid every ten hours, since the

acid is consumed during the course of the reaction. Under acidic conditions, hydrolysis of the ester group also occurs to afford diacid derivative **69**.

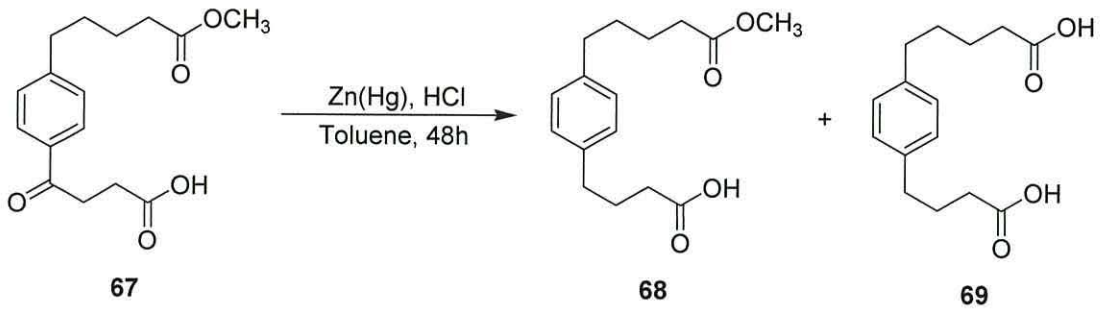

67 **68** **69**

Scheme 4.5. Synthesis of methyl δ-(4-γ-butyric acid)-phenylvalerate **68**.

The resulting product **68** was characterised by ^{1}H NMR spectral analysis. The aromatic protons appear as a singlet, in contrast to the parent compound **67**. This is due to the disappearance of the carbonyl group adjacent to the phenyl ring, which makes the electronic environment and hence, chemical shift, similar for the four protons.

A second esterification was carried out in methanol using excess of thionyl chloride as outlined in Scheme 4.6.

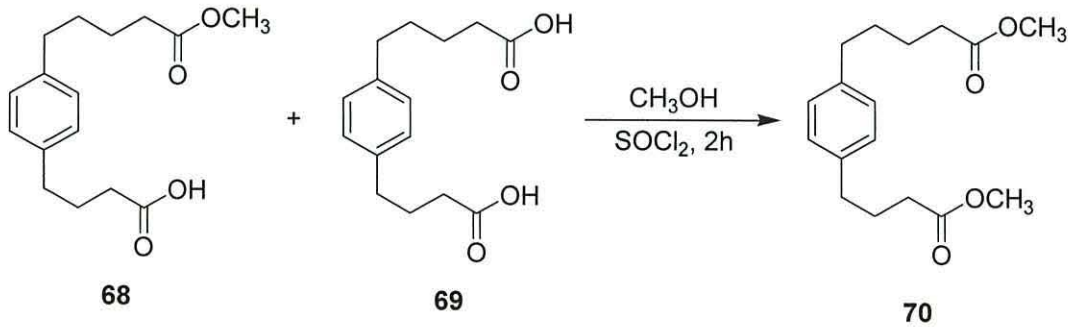

68 **69** **70**

Scheme 4.6. Synthesis of methyl δ-(4-γ-methylbutyrate)-phenylvalerate **70**.

The ester product **70** was characterised by its ^{1}H NMR spectrum, which shows a six hydrogen singlet, as two overlapping singlets, at δ 3.67 corresponding to the methoxy groups. The structure is almost symmetrical, therefore many signals of

both the alkyl chains overlap making it difficult to obtain coupling constants. One singlet at δ 7.10 corresponds to the hydrogens of the ring, whereas only two triplets, at δ 2.62 and δ 2.34, and two apparent pentuplets, at δ 1.95 and δ 1.67, account for both of the alkyl chains.

The ring closure was carried out using a modification of the acyloin condensation. The ene-diolate product was stabilised by trapping it using TMSCl as outlined in Scheme 4.7.

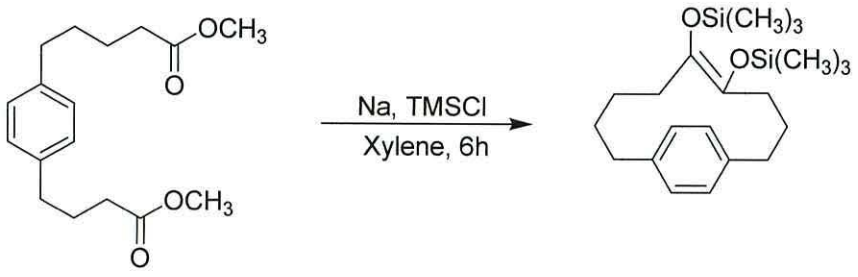

70 **71**

Scheme 4.7. Synthesis of 5,6-O-trimethylsilyl-bicyclo[9.2.2]pentadeca-1(14),5,11(15),12-tetraene **71**.

The solvent employed, xylene, had previously been dried, distilled under sodium and degassed under argon. This reaction was therefore carried under extreme dry conditions. The set-up required an atmosphere of argon and the use of mechanical overhead stirring in order to prepare the highly disperse suspension of sodium in refluxing xylene. After this dispersion had been achieved, the temperature was brought down to room temperature and the solvent was replaced by dry and degassed diethyl ether. A solution of the ester derivative **70** in dry ether was then added dropwise to the refluxing dispersion.

After work-up, the product **71** was isolated by simple distillation, since the presence of the silyl groups confers a higher boiling to the product **71** than that of its parent compound **70**. Characterisation of the product **71** was difficult since most of the features of the starting material **70** are present in the product. There are a few characteristics that differentiate the starting material from product. First of all, in the

^{1}H NMR spectrum, a signal at δ 0.35 corresponds to the methyl groups attached to the silicon, integrating for 18 protons. Secondly, the signal due to the protons of the methoxy group present in the starting material had disappeared. In the IR spectrum, the characteristic features of the ester group had disappeared and there were new peaks, at 1613 cm^{-1} corresponding to the double bond and at 843 cm^{-1} corresponding to the Si-O stretchings. Finally, the mass spectrum clearly showed a major peak at m/*z* 376 corresponding to the molecular mass of the desired product. However, the highest yield obtained for this reaction was only 5 %.

Other intramolecular cyclisation approaches were then carried out. Reduction of diester **70** using DIBAL as the reducing agent was attempted as shown in Scheme 4.8.

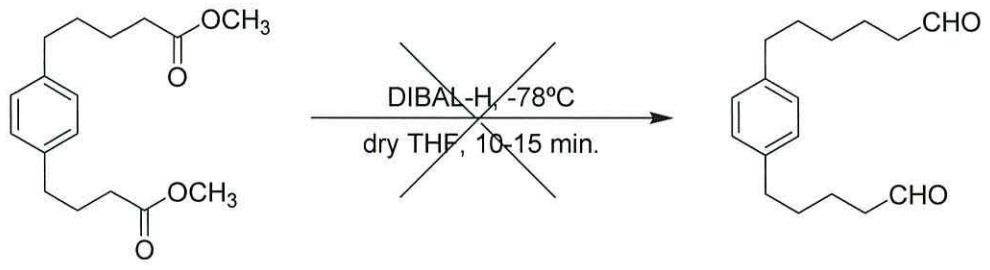

70 **72**

Scheme 4.8. Attempted reduction of diester **70** to dialdehyde **72**.

Purification of the crude oil resulting from the reaction by column chromatography afforded two main fractions, which were identified by GCMS as the product **72**, in 45 % yield, and the half reduced products **73** and **74**, in 55 % yield. Changing the reaction time to 20 minutes and three hours did not produce a significant difference in the outcome of the reaction.

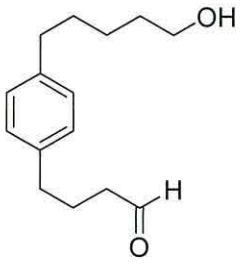

73

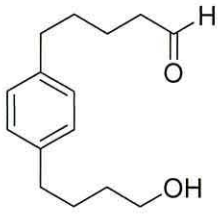

74

Figure 4.2. By-products resulting from the reduction of ester **70** with DIBAL.

Diester **70** was instead reduced to the corresponding alcohol derivative **75** in dry THF using lithium aluminium hydride as the reducing agent, as shown in Scheme 4.9. Isolation of the pure product was achieved by column chromatography.

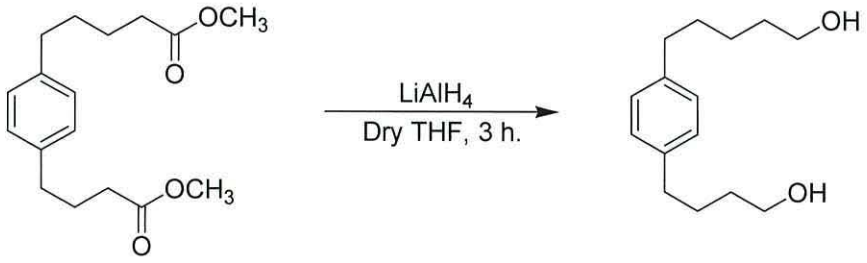

70 **75**

Scheme 4.9. Synthesis of 5-(4-(4-hydroxybutyl)phenyl)pentan-1-ol **75**.

Identification of the dialcohol **75** was achieved by spectroscopic analysis. The two alcohol groups appear as a broad singlet at δ 2.23 in the ^{1}H NMR spectrum. They were confirmed in the infrared spectrum as a broad band at 3350 cm^{-1}. Furthermore, the molecular ion was found by mass spectrometry at m/*z* 236 in addition to another peak due to the loss of a molecule of water derived from the alcohol group at m/*z* 218.

The dialcohol derivative **75** was subsequently fully oxidised to its corresponding aldehyde derivative **72** using an excess of pyridinium chlorochromate as the oxidising agent, as outlined in Scheme 4.10.

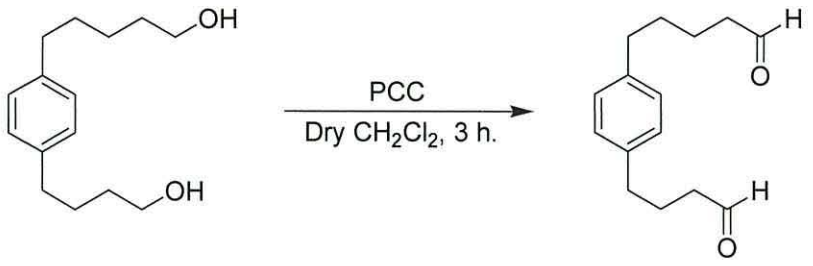

75 **72**

Scheme 4.10. Oxidation of the alcohol derivative **75** to the dialdehyde **72**.

Dialdehyde **72** was isolated by column chromatography by eluting with a mixture of diethyl ether and petroleum spirit and subsequently fully characterised. The aldehyde group was identified in the infrared spectrum at 1723 cm^{-1}. Further evidence of the conversion to the aldehyde came from the disappearance of the broad band of the alcohol group present in the parent compound **75**. The ^{13}C NMR spectrum showed the two carbonyl groups at δ 202.7 and δ 202.4 respectively. In addition, the molecular ion was found by mass spectrometry at m/*z* 232, plus the loss of a molecule of water at m/*z* 214.

Intramolecular McMurry coupling of dialdehyde **72** in dry THF using titanium chloride and the zinc-copper couple was attempted as outlined in Scheme 4.11.

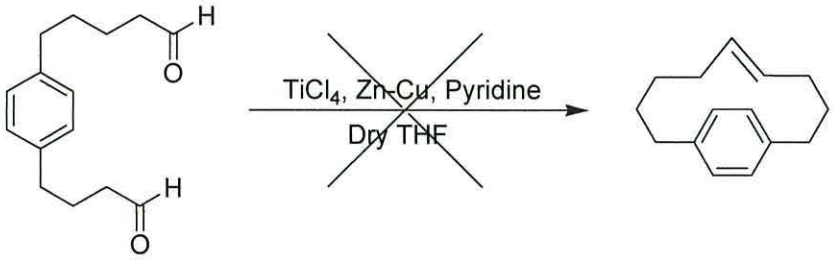

72 **76**

Scheme 4.11. McMurry synthesis applied to the synthesis of paracyclophanes.

Work-up of the McMurry coupling proved to be extremely difficult. Column chromatography was tried, although unsuccessfully, giving always a complicated mixture of bands visible by TLC. Identification of the product was tried by both

NMR and mass spectrometry. The ^{1}H NMR spectrum was very complicated with a range of overlapping peaks. However the peak corresponding to the aldehyde at δ 9.65 was found to be still present. A peak at δ 5.03 indicated that some type of alkene might have been formed. GCMS gave many different peaks always with high molecular mass. The appropriate ion at m/*z* 232 for the expected product could not be identified.

Intramolecular cyclisation of dialdehyde **72** was also attempted using samarium iodide in dry THF as outlined in Scheme 4.12.

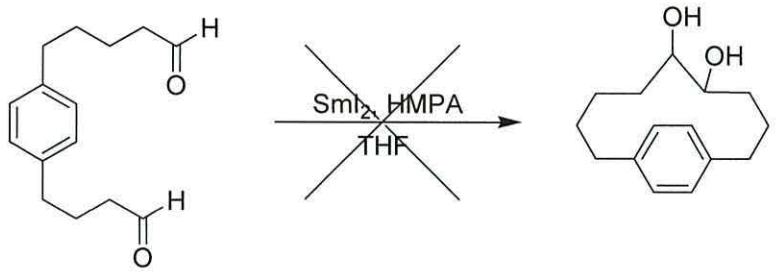

72 **77**

Scheme 4.12. Samarium iodide applied to the synthesis of paracyclophanes.

Various experimental conditions were applied to carry out this reaction. Common to all of them was the consistent use of extremely dry conditions and relatively high dilution ($7.3x10^{-3}$ M) under argon atmospheres. Samarium iodide was either used from commercial source (Aldrich) or made *in situ*. Generation of samarium iodide *in situ* proved to be much more reactive as it gave rise to a very deep, intense purple colour. The reaction was made both in the presence of HMPA/*tert*-butanol, without HMPA and without *tert*-butanol.

Isolation of the products of the reaction was difficult to achieve by column chromatography. Analysis of the reaction mixture by GCMS showed three compounds as the main products of the reaction, the starting material dialdehyde **72**, the fully reduced dialcohol **75** and the half reduced diester to the alcohols **73** and **74** (Figure 4.3).

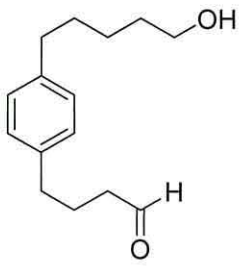

73

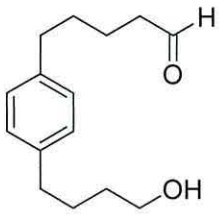

74

Figure 4.3. By-products derived from the reaction of dialdehyde **72** with samarium iodide.

Dialkene **78** was synthesised in 61 % yield from dialdehyde **72** following a typical Wittig reaction as shown in Scheme 4.13.

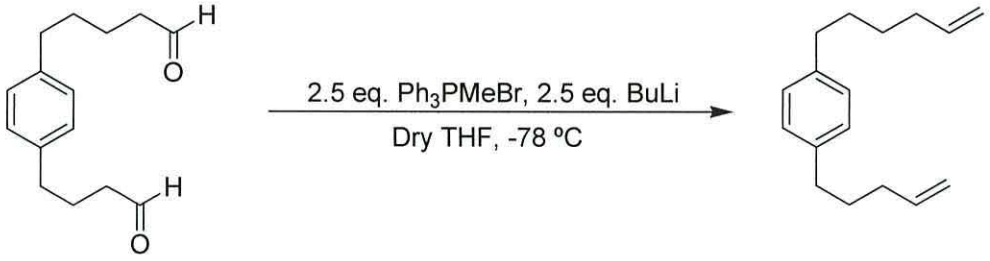

72 78

Scheme 4.13. Wittig reaction on dialdehyde **72**.

Product dialkene **78** was fully characterised. The ^{1}H NMR spectrum showed two unresolved multiplets at δ 5.87 (2H) and δ 5.06 (4H) that indicated the presence of the alkene protons. Analysis by GCMS gave further evidence of alkene formation, as the molecular ion was identified at m/*z* 228, which corresponds to the expected mass for the alkene **78**.

Ring closing metathesis (RCM) on dialkene **78** using 20 % of the first generation Grubbs catalyst was attempted as outlined in Scheme 4.14.

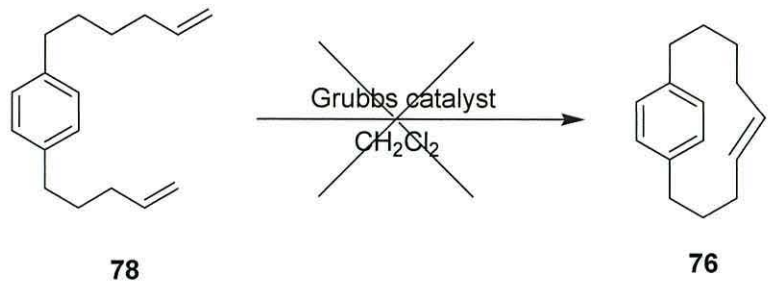

78 76

Scheme 4.14. RCM as tool for the synthesis of paracyclophanes.

This reaction was carried out both at room temperature and at reflux with identical results. Analysis by GCMS showed the presence of two main peaks. Mostly starting material was recovered plus an additional peak whose molecular mass was m/*z* 234, which could not be identified.

In order to form an alternative precursor, another set of reactions were attempted by introducing oxygen into the paracyclophane ring. The reaction of hydroquinone **79** with dibromo derivative **89** yielded paracyclophane **81** in 38 % yield as outlined in Scheme 4.15.[148]

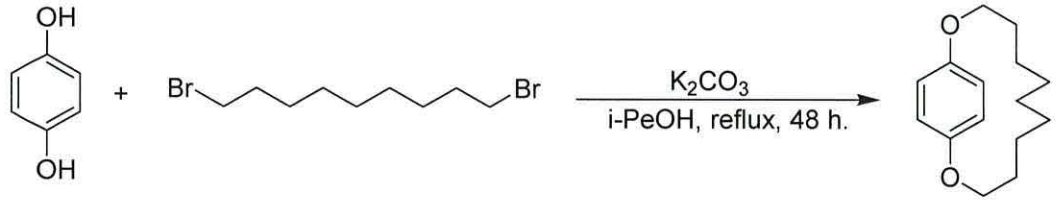

79 80 81

Scheme 4.15. Synthesis of 11-member ring oxo-paracyclophane **81**.

The product, paracyclophane ether **81**, was identified by spectral analysis. Two triplets at δ 3.90 and δ 3.42 accounted for the protons on the carbons attached to the oxygen. The ring closure to oxygen was confirmed by two peaks at δ 68.6 and δ 68.5 in the ^{13}C NMR spectrum. The molecular ion was also found by GCMS at m/*z* 234, consistent with the structure of the cyclised product **81**.[149]

To illustrate the applicability of the method for paracyclophane synthesis, the procedure described above was extended to the synthesis of a smaller paracyclophane ring containing only seven carbons and two oxygens in order to attain the nine-membered ring. Reaction of hydroquinone **79** with the dibromo derivative **82** yielded paracyclophane **83** in 7 % yield as outlined in Scheme 4.15.

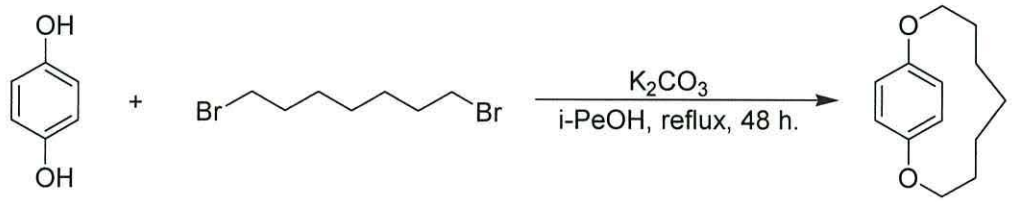

79 **82** **83**

Scheme 4.16. Synthesis of 9-member ring oxo-paracyclophane **83**.

The formation of product paracyclophane derivative **83** was identified by spectral analysis. This showed a highly symmetric product as the four aromatic protons appeared as a singlet at δ 6.64. The methylene protons adjacent to oxygen appeared as a triplet at δ 3.84. The molecular ion was identified by GCMS analysis at m/*z* 207.

Due to the problems involved in obtaining appropriate yields through ring closure, a new synthetic route towards the synthesis of paracyclophanes was envisaged. This route involved the Hoffmann elimination of two suitable amine hydroxide precursors.[150] The first precursor was obtained from 2-methylfuran **84**. This was reacted with formaldehyde and dimethylamine hydrochloride in absolute ethanol to give tertiary amine **85** and was subsequently converted to the quaternary amine **85** by exhaustive methylation as outlined in Scheme 4.18.[151]

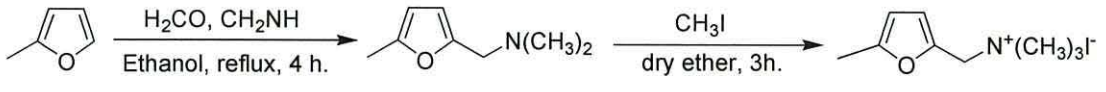

84 **85** **86**

Scheme 4.17. Synthesis of furan derivative **86** as the quaternary iodide salt.

The first reaction yielded the hydrochloride salt version of amine **85**, which was neutralised with sodium hydroxide and extracted with an organic solvent to give the free amine **85**. Exhaustive methylation of amine **85** with iodomethane afforded quaternary amine iodide salt **86**, which was isolated by simple filtration and dried under vacuum at 70 °C.

Subsequent conversion of amine **86** to its corresponding hydroxide salt **87** was accomplished by passing an aqueous solution of the amine salt through a Dowex ion-exchange column (Scheme 4.18). The resulting aqueous solution was freeze-dried to afford hydroxide **87** as a white solid.

86 **87**

Scheme 4.18. Conversion of amine **86** to its hydroxide salt **87**.

The second precursor required for the Hoffmann elimination was obtained from chloro-derivative **88**. This was converted to the iodide derivative **89** in dry acetone using sodium iodide at room temperature (Scheme 4.19) and was subsequently transformed to the quaternary amine iodide salt **90** using trimethylamine.

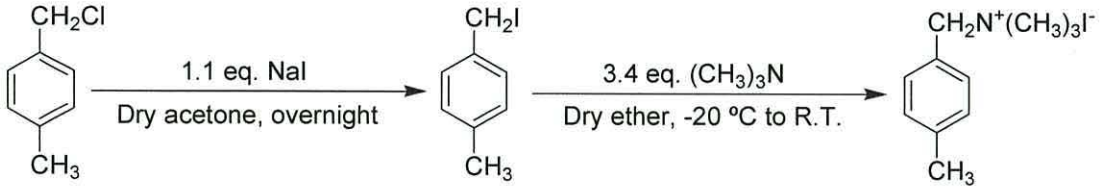

88 **89** **90**

Scheme 4.19. Synthesis of benzyl derivative **90** as the quaternary ammonium iodide salt.

Further conversion of amine **90** to its hydroxide version **91** was achieved by passing an aqueous solution of the iodide salt through a Dowex ion exchange column as shown in Scheme 4.20. The resulting aqueous solution was freeze-dried to afford hydroxide **91** as a white solid.

90 **91**

Scheme 4.20. Conversion of amine **90** to its hydroxide salt **91**.

The Hoffmann elimination reaction between amine hydroxides **87** and **91** afforded paracyclophane derivative **92**. The reaction (Scheme 4.21) was carried out using a Dean-Stark apparatus in order to distil the water derived from the reaction. Phenothiazine was also added to the reaction vessel in order to avoid polymerisation of the products.

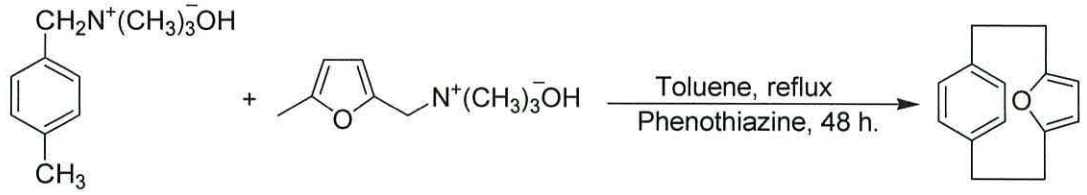

91 **87** **92**

Scheme 4.21. Hoffmann elimination of quaternary ammonium hydroxides **87** and **91**.

In addition to the desired product, two other expected products **93** and **94** were obtained from the reaction as shown in Figure 4.4. The ratio of the products was 2:1:1, as would have been expected from statistical coupling of hydroxides **87** and **91**.

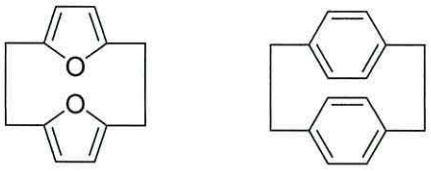

94 **93**

Figure 4.4. By-products **93** and **94** derived from the Hoffmann elimination.

Further reaction of paracyclophane **92** with potassium acetate and bromine opened the furan ring to afford paracyclophane derivative **95**.

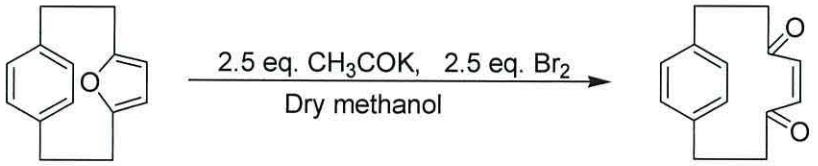

92 **95**

Scheme 4.22. Synthesis of alkene derivative **95**.

Another precursor that is suitable for the Hoffmann elimination was obtained from nitrobenzene derivative **96** using the same conditions as for benzene derivative **88**. Reaction of sodium iodide with nitro benzene derivative **96** in dry acetone afforded nitroderivative **97** in 76 % yield. This was further derivatised by exhaustive methylation with trimethylamine in dry ether to afford the iodide salt derivative **98**.

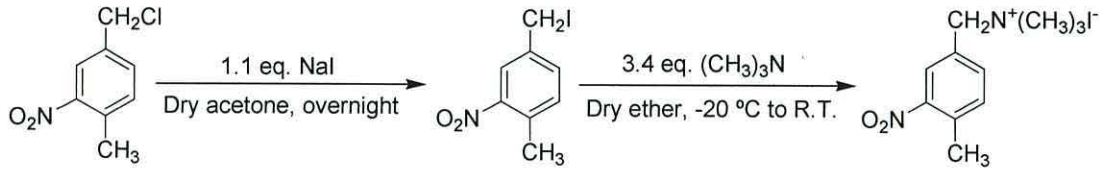

96 **97** **98**

Scheme 4.23. Synthesis of nitrobenzyl derivative **98** as its quaternary ammonium iodide salt.

The conversion of the iodide salt **98** into its corresponding hydroxide salt **99** was completed by ion exchange through a Dowex column. This iodide salt derivative **98** was quite insoluble in water solution and hence very difficult to convert to its hydroxide counterpart **99**. This conversion was aided by addition of some ethanol (Scheme 4.24).

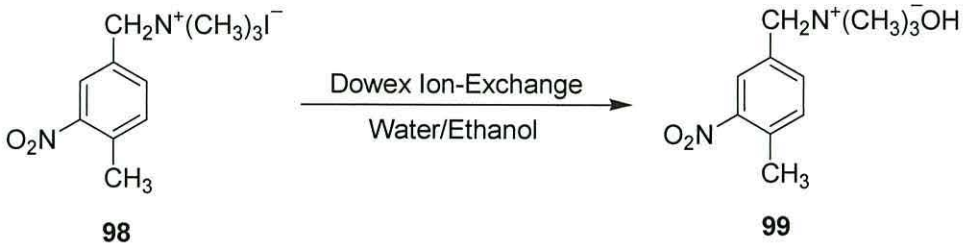

98 99

Scheme 4.24. Conversion of iodide salt **98** to hydroxide salt **99**.

The Hoffmann elimination between amine hydroxides **87** and **99** afforded paracyclophane derivative **100** as outlined in Scheme 4.25.

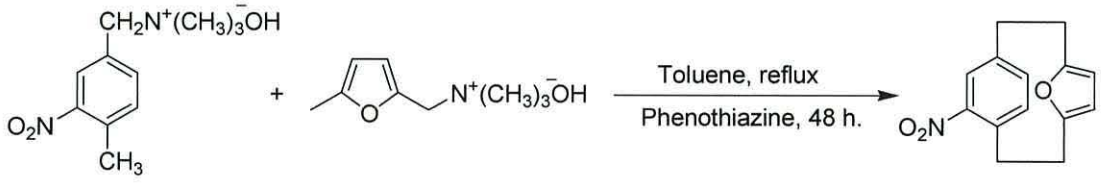

99 87 100

Scheme 4.25. Hoffmann elimination of quaternary ammonium hydroxides **87** and **100**.

The product, paracyclophane derivative **100**, was isolated in 13.8 % by column chromatography and spectral analysis confirmed its structure. The ^{1}H NMR spectrum showed the aromatic protons in three different environments as two doublets at δ 7.56 and δ 7.44, and one singlet at δ 7.98. In addition, the molecular ion was found by GCMS analysis at m/*z* 243.

Two other by-products were also collected. Furan derivative **94** in 7.1 % yield, which had been previously characterised, and paracyclophane derivative **101** in 8.5 % yield. Paracyclophane **101** was obtained as a yellow solid. The ^{1}H NMR spectrum showed high symmetry as the aromatic protons appear in two environments at δ 7.98 and δ 7.52. Additionally, the molecular ion was found by GCMS at m/*z* 298.

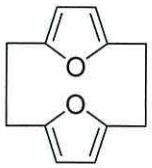

94

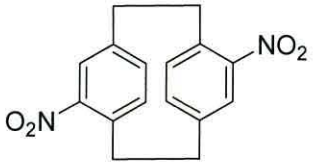

101

Figure 4.5. By-products from the Hoffmann elimination between hydroxides **87** and **99**.

Discussion

Various different methods can be applied in order to synthesise [9]-paracyclophanes. The most obvious choice is to build the two acyclic chains at the *para*-position of the benzene ring and then, by an intramolecular cyclisation reaction, close them up forming the paracyclophane ring. Within this type of approach falls the reaction known as the acyloin condensation. Although starting out with very cheap and available materials, this approach was found to be quite elaborate and time-consuming.

The sequence followed for the synthesis of [9]-paracyclophane **1** *via* acyloin condensation is outlined in Scheme 4.26. The synthetic route involves seven steps from cheap and readily available starting materials before the carbon-carbon bond formation leads to a ring closure, which constitutes the key step for the overall process due to fact that this cyclisation reaction is entropically unfavoured.

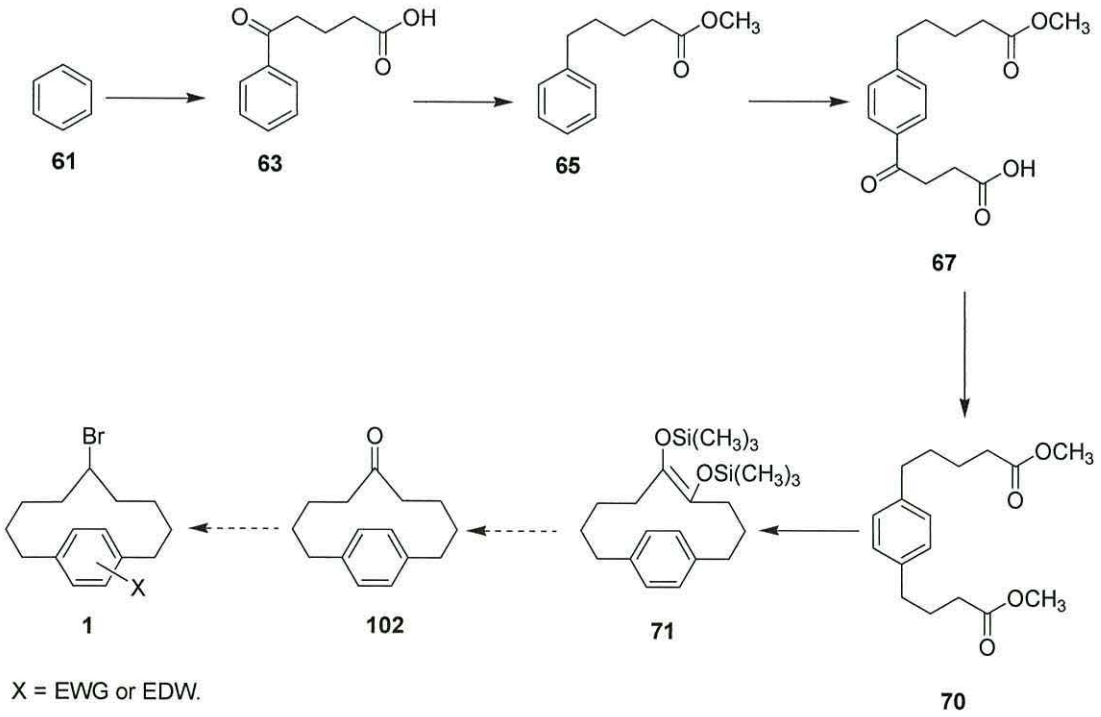

Scheme 4.26. Strategy for the synthesis of [9]-paracyclophanes of general structure **1** *via* intramolecular acyloin condensation.

The first step involves the Friedel-Crafts acylation of benzene **61** using succinic anhydride **62**. The resulting product **63** was reduced and esterified to obtain benzene derivative **65**. The reduction was achieved by the known Huang-Minlon process, which takes place in basic conditions provided by the presence of potassium hydroxide in high boiling diethylene glycol.[152] The mechanism of the reaction involves the initial formation of the corresponding hydrazone, whose decomposition at high temperature leads to the desired product. For that reason, after initial formation of the hydrazone at 140 °C for three hours, excess water and hydrazine are distilled to avoid the reverse reaction, and the final temperature is raised to about 180 °C, which favours hydrazone decomposition and formation of the product. This reduction is essential in order to direct a second Friedel-Crafts acylation to the *para*-position of the benzene ring. If the carbonyl group were present, its electron-withdrawing power would have favoured the *meta*-substituted product instead, with the carbocation intermediate being the least destabilised, as is the case in any electrophilic aromatic substitution.

The second acylation to generate derivative **67** proceeded with both high yield and selectivity. The favoured products were expected to be *ortho*-derivative **102** and *para*-substituted **67** in a statistical ratio of 2:1 (*ortho*/*para*) as illustrated in Figure 4.6. However, in practice, the alkyl chain is too bulky and steric interactions prevent the formation of the *ortho*-derivative **102**. Therefore the substitution mainly occurs in the *para*-position.

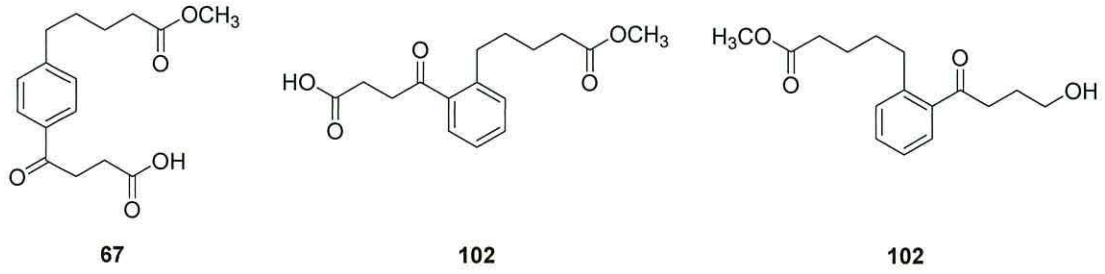

67 102 102

Figure 4.6. Expected products from the Friedel-Crafts acylation of derivative **64**.

Another reduction was then carried out in acidic conditions using the Clemmensen reduction. Although there has been some discrepancy as to what the exact mechanism of the Clemmensen reduction is, it is believed that the rate determining step is the coordination of the carbonyl atom to the metal surface.[153] It has been noted, however, that both ionic and non ionic reactions contribute to the global process in which a four electron transfer is required for the overall reaction (Scheme 4.27).[154,155]

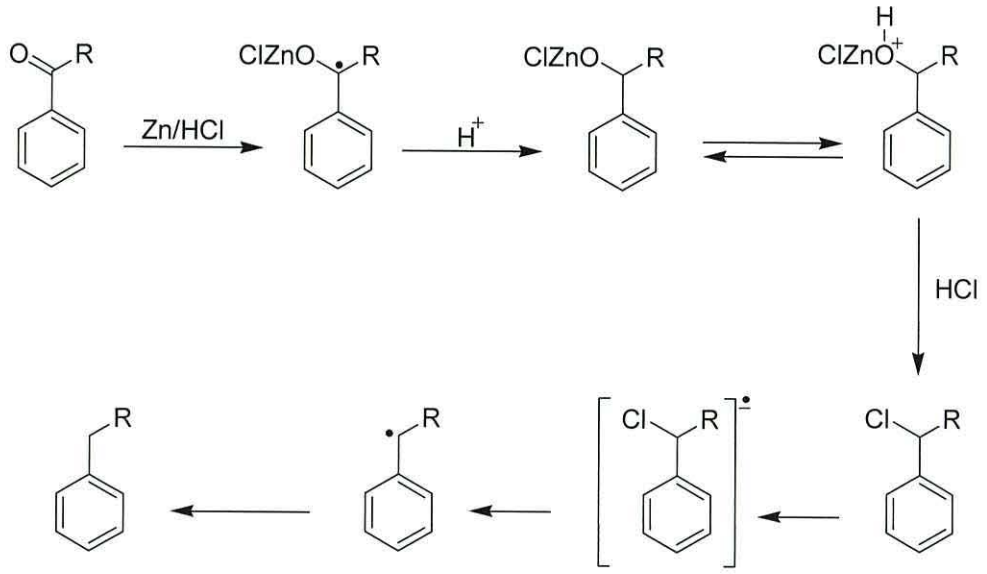

Scheme 4.27. Mechanism for the Clemmensen reduction.

It is certain that, in addition the expected product, hydrolysis of the ester group at the other alkyl chain also occurs. This presents no problem synthetically because both acid groups can be esterified in the subsequent step.

The key step for the success in the synthesis of [9]-paracyclophane derivatives **8** is the acyloin condensation. This has been regarded as the most useful method for the synthesis of medium- and large-ring ketones (9 to 15 member rings) from dicarboxylic esters.[156] Compared to other methods, the Dieckmann and Thorpe-Ziegler condensations are practically ineffective for rings in the 9-12 range, although on occasion, the yield of the acyloin product may be lowered by competing Dieckmann condensation.[157] The general conditions for the reactions are very

similar, *i.e.*, an alkali metal dispersed in an inert solvent. However, this is not usually a great problem since the acyloin condensation is more rapid than the Dieckmann reaction.

Acyloin condensation is a powerful method for the formation of carbon-carbon bonds resulting in an α-hydroxyketone.[158-161] A modified method of the acyloin condensation protects the α-hydroxyketone *in situ* with TMSCl, which has been reported to give better yields.[156,162,163] Another advantage of the modified method over the original method of synthesis reported by Cram[76] is that the latter requires the use of overhead mechanical stirring in a complicated set-up that contained dangerous sodium metal during a much more prolonged time, and was considered hazardous in our laboratory.

Mechanistically, the acyloin condensation involves the reductive dimerisation of a carboxylic ester. When, as in our case, an α,ω-diester is used, such dimerisation results in the production of a cyclic ene-diolate. The reducing agent is an alkali metal, for example sodium. Two moles of metal are required for each mole of ester with the concomitant precipitation of a mole of alkoxide and 1.5 mole of the ene-diolate. The accepted mechanism involves the production of the dianion of the diester either by coupling of two initially formed radical anions or by two-electron reduction of an ester to a dianion followed by its addition to a second molecule of ester.[157] As it has been pointed out above, the presence of TMSCl generally results in higher yields, easy isolation and storage, and freedom from side reactions.[164]

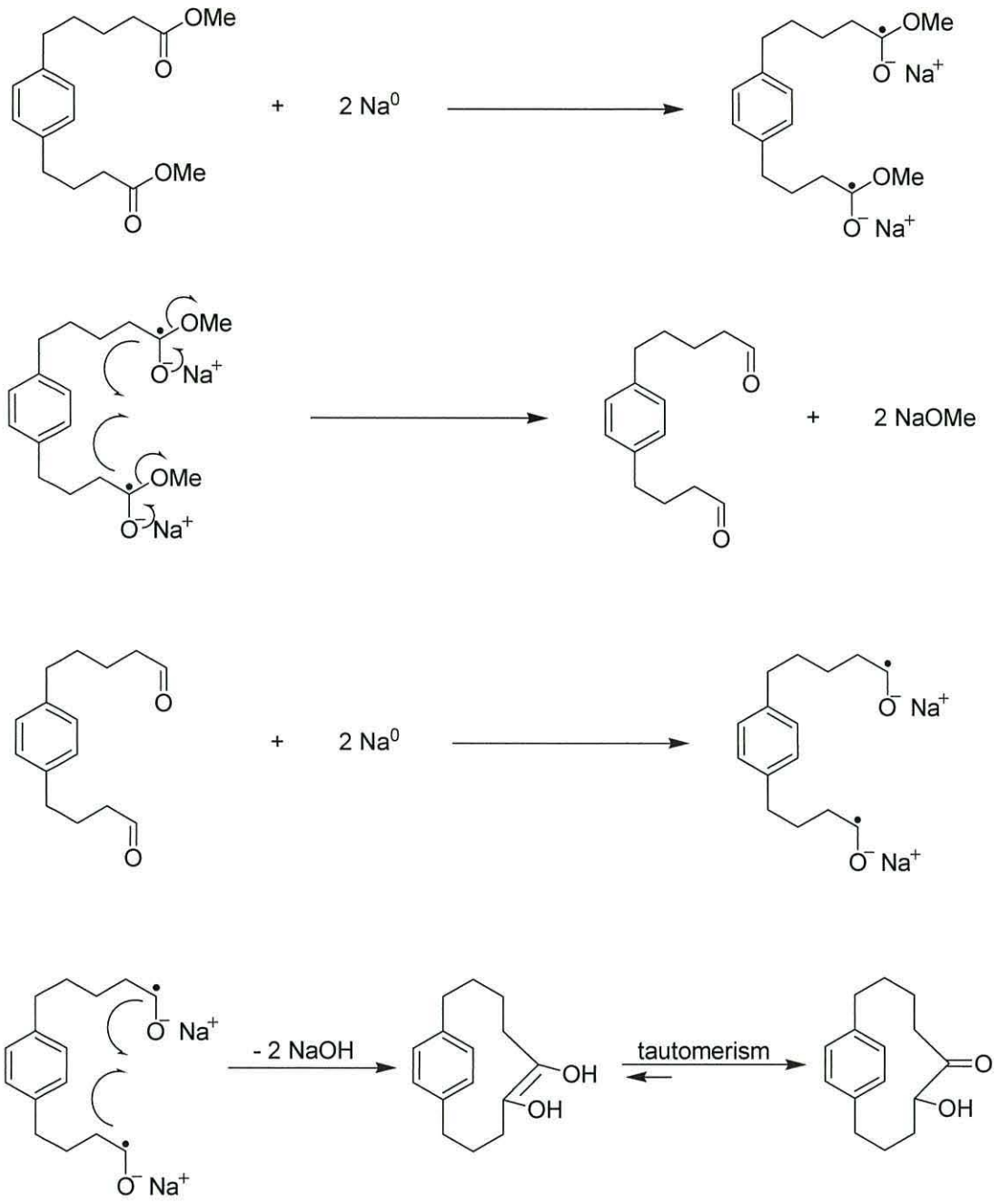

Scheme 4.28. Mechanism for the acyloin condensation.

Various factors were considered in order to carry out a successful intramolecular acyloin condensation. Firstly, sodium is the most commonly utilised metal for the acyloin condensation. Considering that the reaction rate is directly proportional to the available metal surface area, a large surface area of metal is needed. This was achieved through dispersion in a high boiling inert solvent such as xylene. Secondly, the high boiling solvent is necessary to keep the metal molten and to help break up

the cake that may have a tendency to form around the individual metal particles. When the high dispersion was achieved, the temperature of the reaction was lowered and the solvent was substituted by dry ether. Thirdly, complete exclusion of oxygen is also an essential factor. The small amount of oxygen present in commercial nitrogen is sufficient to transform the disodium enolate of the acyloin into the corresponding cyclic diketone and other secondary reaction-products. To overcome this, a stream of argon was passed through the solvent before and during the reaction to displace any remaining oxygen.

The experimental conditions necessary for a successful acyloin condensation made it very difficult for the reaction to be reproducible from one experiment to another. The factor that is likely to have had the most influence over reproducibility was that the area of metal varies considerably from one experiment to another. This irreproducibility, together with the fact that this is a highly entropically unfavoured reaction, made the acyloin condensation for the synthesis of 9-membered ring paracyclophane an unreliable method, which is also very laborious and in the best cases resulted in poor yields. Better yields are necessary in order to subsequently form a range of various substituents at the aromatic ring ranging from electron-donating to electron-withdrawing groups.

Other routes to the synthesis of [9]-paracyclophane derivatives **8**, which are reported to provide a more reliable methodology, were thus explored.[165-167] These methods involved the use of other intramolecular synthetic approaches. Having already synthesised diester **70**, further functionalisation led to the synthesis of other precursors **72** and **78**, suitable for other types of intramolecular reactions.

In order to obtain appropriate precursors, the reduction of diester **70** to dialdehyde **72** in a single step was attempted. The use of DIBAL has been demonstrated in previous work to facilitate the reduction of esters to aldehydes.[168-171]

In light of the failure to reduced diester **70** by using DIBAL, a different approach was taken comprising a two-step process (Scheme 4.29). Firstly, complete reduction

of dialdehyde **72** to dialcohol **75** was achieved with the powerful reducing agent lithium aluminium hydride resulting in the sole formation of the product **75**, which was easily isolated by column chromatography in 90.5 % yield.

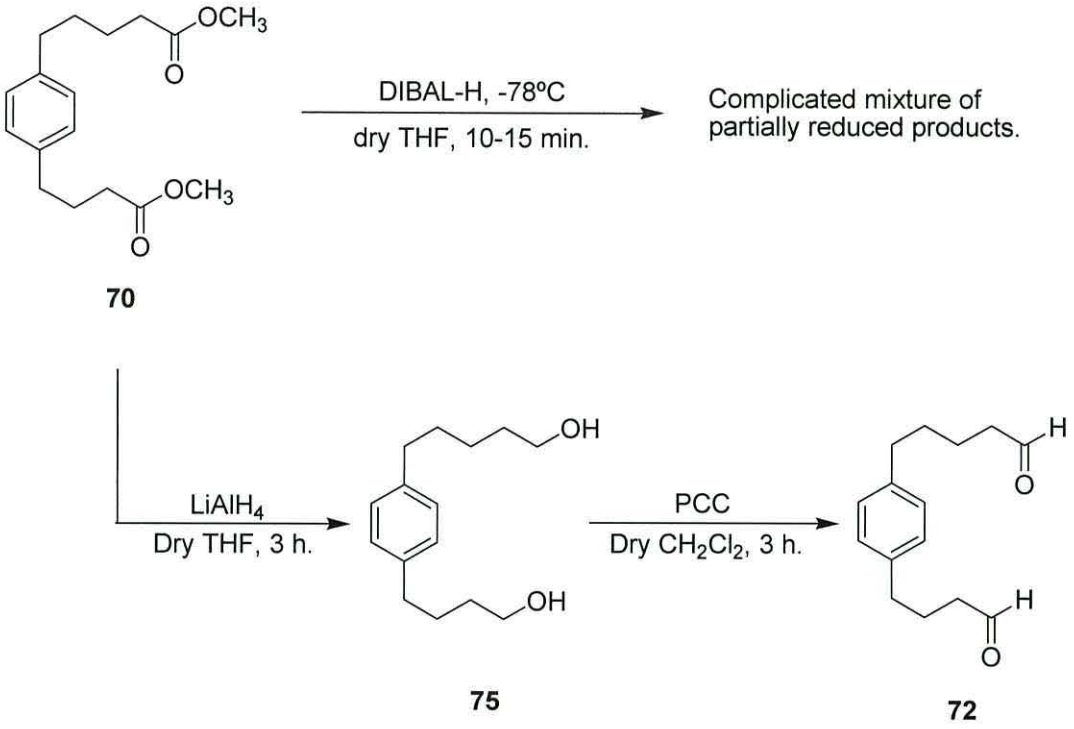

Scheme 4.29. Conversion of diester **70** into dialdehyde **72**.

Subsequent oxidation to dialdehyde **72** was attained using pyridinium chlorochromate (Scheme 4.29). Dialdehyde **72** was a suitable precursor for two intramolecular cyclisation procedures (Scheme 4.30).

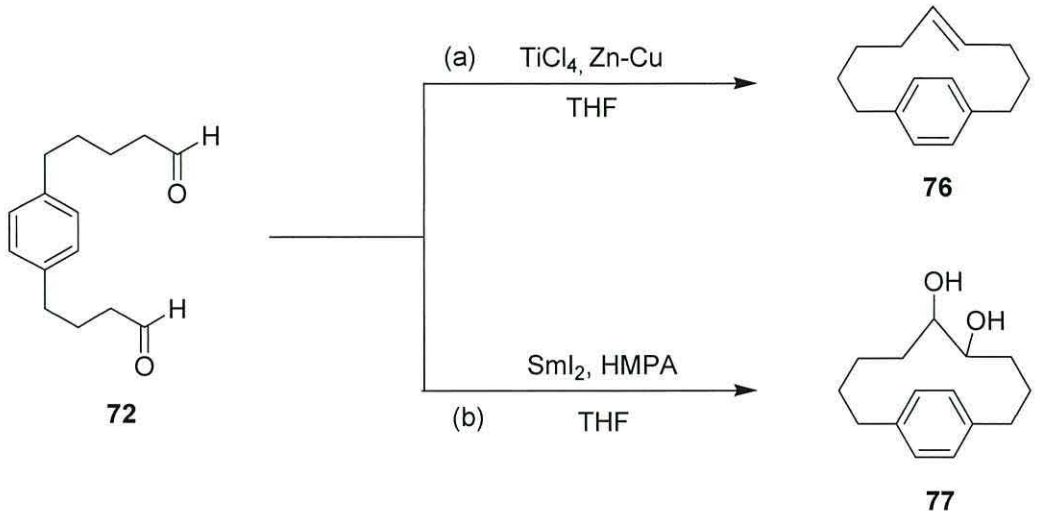

Scheme 4.30. Intramolecular cyclisation reactions *via* reductive coupling.

The pinacol coupling, also known as the McMurry coupling, is shown in Scheme 4.30 (a). The use of this approach was based on previous success in synthesising heterocyclic compounds,[172] strained olefins,[173] and macrocyclic ring systems,[174] and also unsaturated cyclophanes.[175,176]

The effectiveness of heterogeneous reactions depends largely on the available surface area of the solid being used. It is well known that the simplest way to activate any solid is to dissolve it in an organic solvent because the reaction rate is directly proportional to the available metal surface area. The McMurry reaction illustrates this. Commercially available titanium powder is unsuitable to carry out this reaction, but this highly reactive metal shows considerably different degrees of activity depending on its genesis. The McMurry coupling, in particular, is based upon the generation *in situ* of highly reducing Ti(0) species by reduction of $TiCl_4$ with Zn(Cu). Air is excluded by a stream of nitrogen, due to the high affinity of titanium for oxygen, which generates titanium oxides, plus the fact that the reaction proceeds *via* radical intermediates, which are highly sensitive towards oxygen. A large excess of titanium was used because, during the reaction, very stable titanium oxides are formed as by-products and they are unable to be reduced back to the active low valent titanium (LVT). In other words, LVT is consumed during the reaction without being regenerated. This is, in fact, the driving force of the titanium-

induced carbonyl coupling.[177] The large thermodynamic driving force provided by the formation of the titanium-oxygen bonds makes it possible to build a large amount of strain into the product during a carbonyl coupling reaction.[178] LVT is unable to promote acyloin condensation, but it does couple ketoesters into enol ethers.[179] This reaction requires high dilution conditions provided by the use of a syringe pump as a method of addition of the carbonyl substrate.[173] This high dilution is necessary in order to favour the intramolecular reaction over the intermolecular process.

Step 1. Carbon-carbon bond formation.

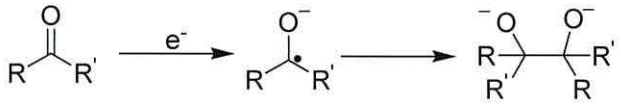

Step 1. Deoxygenation.

Scheme 4.31. Mechanism for the McMurry coupling.

The mechanism of the McMurry coupling is summarised in Scheme 4.31 and it takes place in two steps. The first step is the reductive dimerisation of the starting aldehyde to form the carbon-carbon bond, followed by deoxygenation of the 1,2-diolate intermediate to yield the alkene. This should have occurred in our case as well. Analysis of the reaction product proved to be overly complicated, since the formation of a mixture of oligomers took place rather than the anticipated clean two-step process. The failure of this reaction gives yet further evidence of the special characteristics of the paracyclophane system, which makes it so difficult for an intramolecular cyclisation method to succeed. The driving force of the McMurry reaction is not enough to overcome the high deficit in entropy and strain necessary to build the paracyclophane system. Instead, intermolecular addition of the reactive radical intermediates takes place.

The samarium iodide reductive coupling of dialdehyde **72** illustrated in Scheme 4.30 (b) was also attempted.[180] The use of samarium iodide to promote this type of intramolecular pinacol coupling is explained partly by the properties of samarium metal such as large ionic radius, flexible coordination and high oxophilicity (Scheme 4.32).[181]

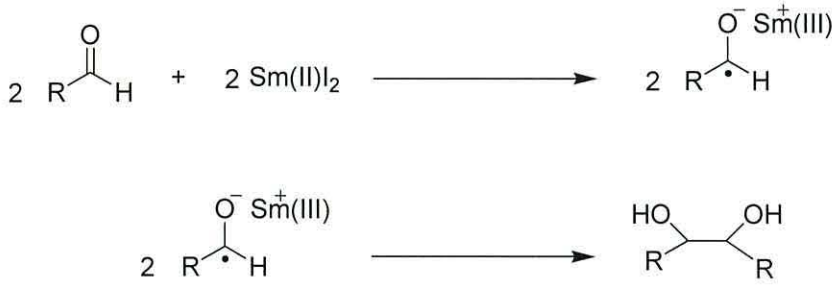

Scheme 4.32. Mechanism of the samarium iodide pinacol coupling.

Previous work by other researchers showed that, by using Samarium iodide, it was possible to overcome unfavourable entropy factors as well as transannular interactions, such as occurs in the synthesis of the oxonene ring.[182] Samarium iodide has also been employed, in the presence of HMPA, to promote efficient 8-endo radical cyclisations to give 8-membered rings.[165]

Medium rings (7-9) are more difficult to produce than large rings. The optimum conditions used in order to carry out the pinacol intramolecular reductive coupling of medium rings were found in the literature as follows: 2.2 eq. of SmI_2, 2.2 eq. of *t*-BuOH and 8.2 eq. of HMPA. The use of HMPA is justified by its ability to exclude proton sources from the coordination sphere of the Sm(III) ion, thereby resulting in a longer-lived reactive intermediate.[183] When the same procedure was applied to the paracyclophane system it was found that the presence of HMPA did not affect the outcome of the reaction. The expected product is illustrated in Figure 4.7.

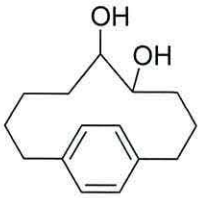

77

Figure 4.7. Expected product 77 of the samarium promoted intramolecular pinacol coupling.

The reaction carried out in the absence of *tert*-butanol in the reaction mixture did not appear to have a considerable effect on the outcome of the reaction, either qualitatively or quantitatively. The main factor affecting the course of the reaction was the use of *in situ* generated samarium iodide, in contrast to the commercially available samarium iodide. When the reaction was made using commercial samarium iodide in THF solution mostly starting material was recovered as an indication that this samarium was ineffective in the reductive process. However, the samarium iodide generated *in situ* by reaction of samarium metal with iodine afforded a deep purple colour that was indicative of the presence of the correct reductive species. Nonetheless, almost negligible desired product could be identified in the reaction mixture. Analysis by GCMS indicated the presence of a molecular ion corresponding to that of the expected product, plus the loss of a molecule of water. However, only traces of the material could be obtained and the structure could not be confirmed by any other spectroscopic method. Predominantly, the starting material was reduced partially and completely to the dialcohol analogue (Figure 4.8), indicating that the samarium species present in solution were active in reduction of the substrate.

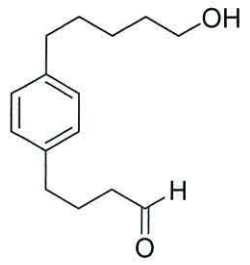

73

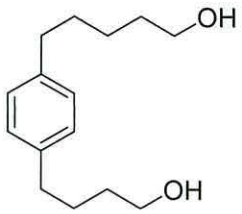

75

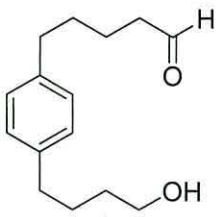

74

Figure 4.8. Products analysed from the treatment of dialdehyde **72** with samarium iodide.

A last attempt at an intramolecular cyclisation method was tried using ring closing metathesis (RCM). Examples of successful RCM for medium rings are present in the literature.[184,185] For instance, the skeleton of Eleutherobin **103** (9-membered ring) was constructed by RCM using Grubbs catalyst (10 %) under high dilution (0.003 M), although the yield was poor, 30 %, the rest being unreacted material and some cross metathesis product (Figure 4.9).[186]

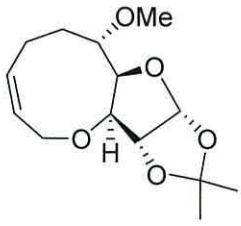

103

Figure 4.9. Eleutherobin **103**, a 9-member ring successfully synthesised by RCM.

In order to carry out a successful RCM, the appropriate precursor had to be obtained, which was synthesised following a typical Witting reaction from dialdehyde, as can be seen in Scheme 4.33.

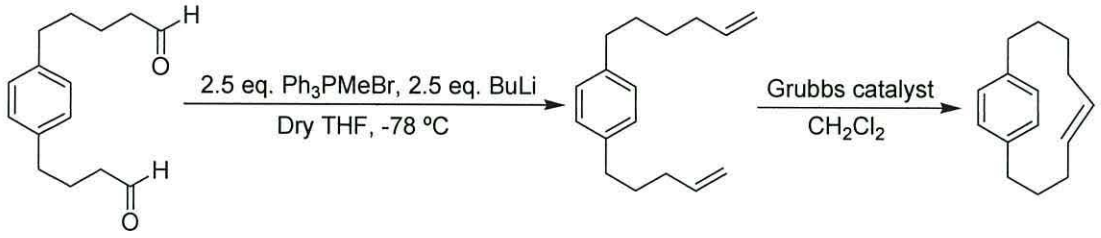

72 78 79

Scheme 4.33. RCM as an approach to synthesise paracyclophane derivatives.

The Wittig reaction with the dialdehyde **72** was used to extend the carbon chain length by one carbon on each arm to afford the α,ω-diene **79**. This was necessary to maintain the correct number of carbons in the macrocycle, since the RCM reaction proceeds with the loss of a molecule of ethylene. Many factors need to be taken into account in order to effect a successful RCM, some of which are described below.

First of all, there are many catalysts available for the RCM reaction. Some of these catalysts are comprised of tungsten or molybdenum alkylidene complexes, developed by Schrock and co-workers.[187] Nonetheless, the ruthenium carbene complexes introduced by Grubbs and co-workers[188] are undoubtedly the most popular and versatile ones with the advantage that they are commercially available. It was therefore decided to use the first generation Grubbs catalyst. The amount of catalyst required depends on the rate of the RCM reaction relative to that of any side reactions leading to destruction of the catalyst (10-25 %). Dilute solutions ($3x10^{-3}$ M) were used as they favour the intramolecular cyclisation with respect to the competing intermolecular reaction, which leads to dimer, trimer and higher polymers. The dilute conditions also disfavour ring opening metathesis polymerisation (ROMP) of the cyclic product because such reactions only proceed to a significant extent above a critical concentration of the cyclic compound, which is around $3x10^{-3}$ M.[166,185,189]

There are many other different types of metathesis processes. For instance, ring opening metathesis (ROM), ROMP or acyclic diene metathesis polymerisation (ADMET) may be in competition with RCM depending on the nature of the substrate

and the catalyst used. The intrinsic competition between RCM and acyclic diene metathesis polymerization (ADMET) can be controlled to some extent by adjusting the dilution of the reaction mixture. The inherent strain of medium-sized rings, eight- to eleven-membered cycloalkenes make them excellent substrates for ROMP because the release of ring strain provides a formidable driving force, but constitute particularly challenging targets for RCM. If pre-existing conformational constraints, however, force the substrates to adopt a favourable conformation for ring closure, even this class of compounds is within reach, as witnessed by a rapidly growing number of successful applications. In this context, a recent report describes the synthesis of an eight-membered ring incorporating an E-configured double bond that has been formed by RCM.[188] There was no certainty that our system would provide a successful RCM, but it was difficult to make adequate predictions as, in most of the cases reported, the outcome of the RCM reactions has not been systematically reviewed.

In the case of the cyclisation of starting material, alkene **79**, the deficit in enthalpy inherent to the system should be entropically counterbalanced because RCM cuts one substrate molecule into two products. RCM generates two molecules from one with volatile loss of ethylene, allowing for the desired cycloalkene to be accumulated in the reaction mixture.[188] This should provide a gain in entropy favouring the reaction, since the closing of the ring gives a negative entropy disfavouring the reaction.[177]

The difficulty encountered in the RCM synthetic approach towards the paracyclophane system **1** showed us that the strain, conformation and deficit in entropy are too significant to be counterbalanced by RCM using first generation Grubbs catalyst. However, this result does not imply that the use of a different catalyst in the future could not lead to a successful RCM, since the reaction is largely dependent on the type of catalyst and not every catalyst is applicable for every reaction.

The possibility of synthesising a 9-member paracyclophane ring by intramolecular nucleophilic substitution was explored using the Williamson synthesis. Mandolini[148]

achieved the synthesis of a 10-member ring paracyclophane derivative.[190] Due to the fact that the intermolecular reaction is second order, whereas the cyclisation is first order, high substrate concentrations favour polymerisation. Cyclisation can only occur in these reactions without competition and only at low concentrations. Therefore, it is clear that the use of the syringe pump was strictly necessary in order to ensure that high dilution was maintained at all times during the reaction. The effective molarity estimated for 9-member ring formation is indeed lower than $5x10^{-4}$ M.[149]

Mandolini's[149] findings were that the Williamson synthesis for the synthesis of medium ring cyclophanes is more effective for metacyclophanes than for paracyclophanes, probably due to the higher ring strain in the latter. Ring strain arises from a combination of bond opposition forces due to imperfect staggering (Pitzer strain), deformation of ring bond angles (Baeyer strain), and transannular strains due to repulsive interactions between atoms across the ring. In the case of medium rings, they are affected principally by Pitzer and Baeyer strain. Upon application of this methodology to the paracyclophane system, the 10-member ring product **81** was successfully synthesised in a 37.8 % yield compared to only 7.0 % yield for the 9-member ring product **83**. This result highlights the large dip in effectiveness in the use of the Williamson synthesis as the size of the ring decreases.

81 **83**

Figure 4.10. Paracyclophane derivatives **81** (37.8 %) and 9-oxo-paracyclophane **83** (7.0 %).

The Hoffmann elimination provides an alternative route leading to the formation of medium-sized paracyclophane rings. It requires, however, synthesis of the appropriate precursors, which must contain a quaternary ammonium hydroxide

functionality. These precursors were prepared in accordance with literature methodology, which was improved where necessary (Scheme 4.34).

Quaternary ammonium hydroxides **87** and **91** were obtained using a different strategy depending on the starting materials available. Hydroxide **97** was obtained from furan derivative **84**, using a Mannich type reaction to convert it into tertiary free amine **85**.[191] Amine **85** was subsequently methylated to the iodide salt **86**. Hydroxide **91** was obtained using a slightly different approach, starting out from the chloro derivative **88**, which was transformed into its iodide derivative **89** and subsequently methylated into its iodide salt **90**. Both of the iodide salts, **86** and **90**, were converted to the hydroxide corresponding derivatives, **87** and **91** respectively, by using an ion exchange resin. This is one of the main drawbacks of this procedure. Since none of the salts are very soluble in water, large quantities of water were required in order to dissolve the iodide salts. The water was then removed with the assistance of a freeze-drier. This was especially a problem in the case of iodide salt **90**, which, due to its more apolar nature conferred by the benzene ring, was harder to dissolve in water than the more polar furan derivative **86**.

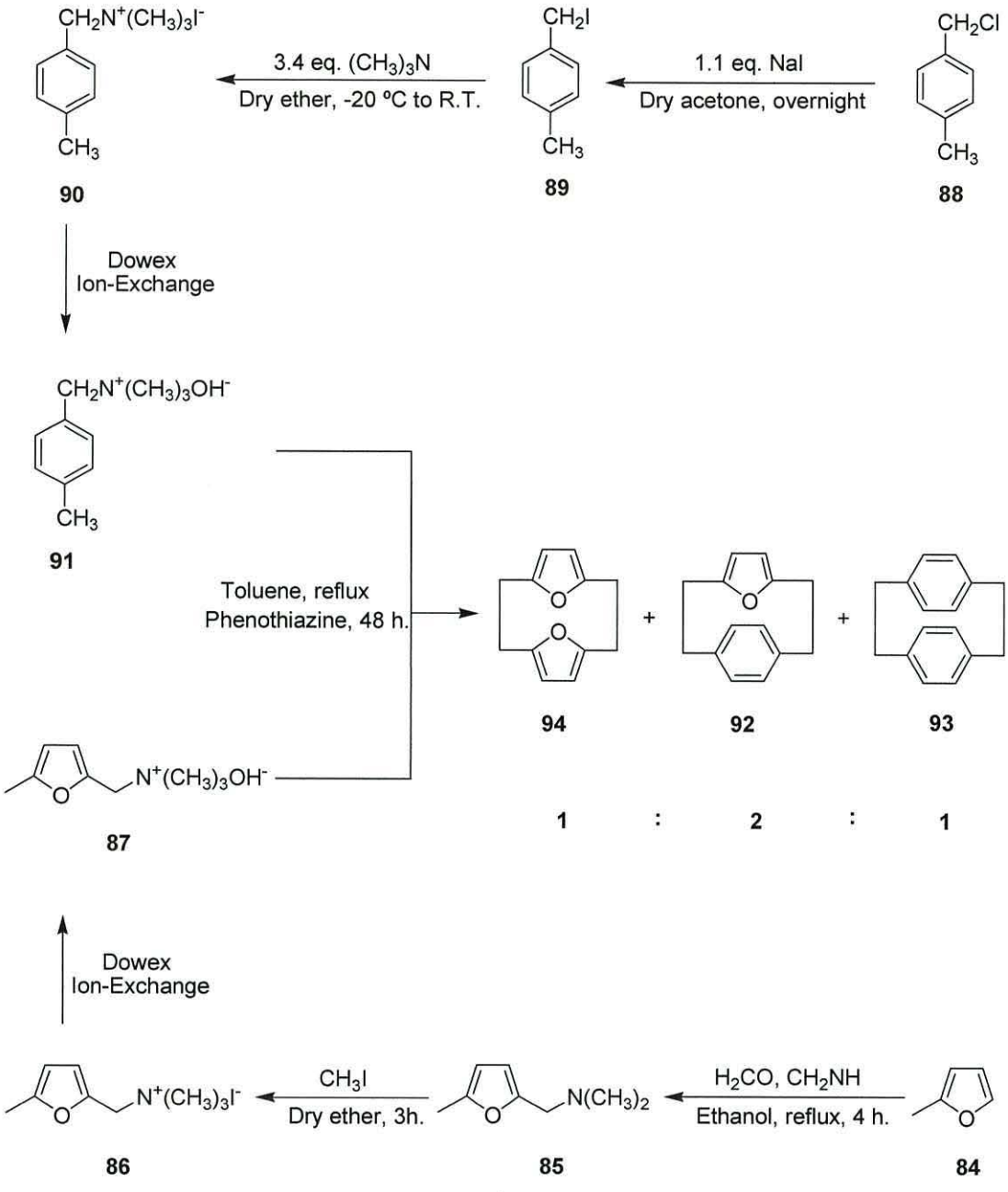

Scheme 4.34. Synthesis of paracyclophane derivatives **92**, **93** and **94** *via* Hoffmann elimination.

Reaction between hydroxide salts **87** and **91** was initiated by the Hoffmann degradation and gave three main products whose ratio can be explained statistically.[150,192] The Hoffmann degradation is driven by the stable formation of a tertiary amine and a molecule of water, and produces two very reactive alkenes **104** and **105**, which react in a 1,6-cycloaddition fashion (Scheme 4.35).[71,193]

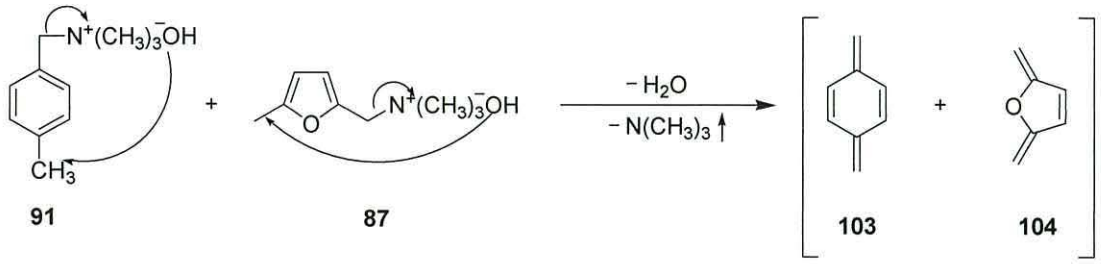

Scheme 4.35. Intermediate formation in the coupling reaction of quaternary ammonium hydroxides **87** and **91**.

Because one equivalent of each of the hydroxide salts **87** and **91** was used, there is a 25 % probability of two furan rings reacting to form product **94** and two benzene rings to react to form product **93**. However, statistically it is twice as likely that one benzene ring and one furan ring react to form the product derivative **92**, the synthetic target.

Paracyclophane **92** is the only product resulting from the Hoffmann elimination that is susceptible to further derivatisation by opening up the furan ring into an alkyl chain. Further derivatisation could then be achieved by functionalisation of the alkene group. This was achieved by using addition of bromine at the double bond of the furan ring (Scheme 4.36).

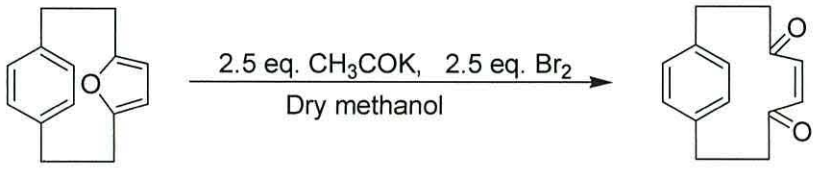

92 **95**

Scheme 4.36. Synthesis of paracyclophane derivative **95**.

Successful synthesis of paracyclophane derivative **95** demonstrates that the Hoffmann elimination as a key step is a valid route in order for the synthesis of an 8-membered ring paracyclophane derivative **95**. This route could be taken further in order to obtain a 9-member ring paracyclophane derivative (Scheme 4.34).[192] However it is beyond the scope of this Chapter.

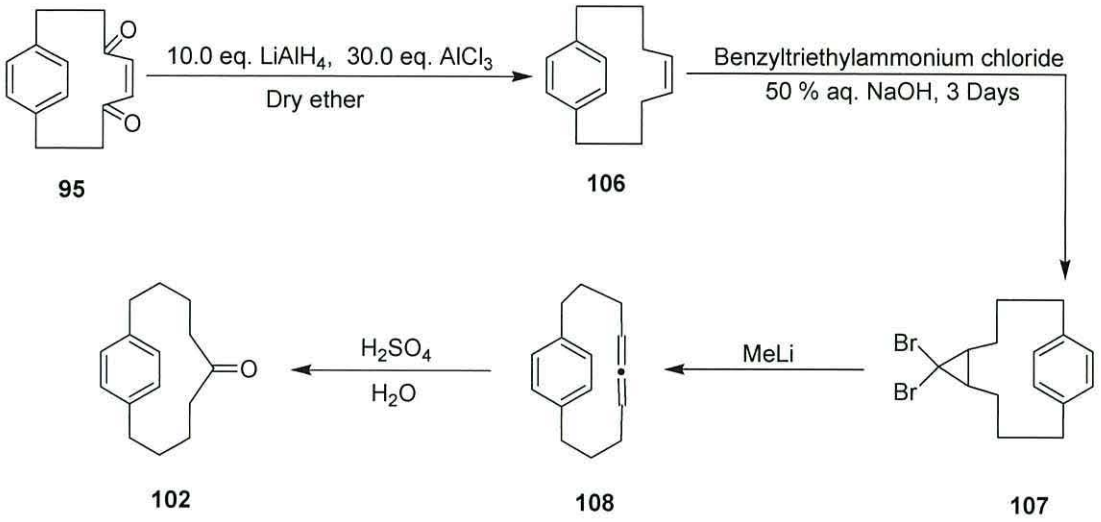

Scheme 4.37. Further derivatisation route to obtain a 9-membered ring paracyclophane derivative **102**.

A key requirement for the model studies is the ability to vary the electronic character of the aromatic ring. For this reason, the route to intermediate **100** was attempted from a different, commercially-available starting material, illustrated in Scheme 4.38, which utilises derivative **96**, already possessing a nitro group at the benzene ring.

The introduction of a nitro group in the benzene ring of the paracyclophane was possible by starting from benzene derivative **96**. This material was subjected to the same procedure as for derivative **88**, and the resulting hydroxide derivative **99** was reacted by Hoffmann elimination to yield paracyclophane derivative **100** in 13.8 % yield. One important observation is that hydroxide derivative **99** is thermally less stable than hydroxide derivative **91** and therefore reacts much more readily as the temperature increases above 30 °C possibly due to the more acidic nature of the hydrogen in the methyl substituent, which is induced by the electron withdrawing power of the nitro group. Paracyclophane derivative **100** could be subject to further derivatisation as outlined for the case of paracyclophane derivative **92** (Scheme 4.37).

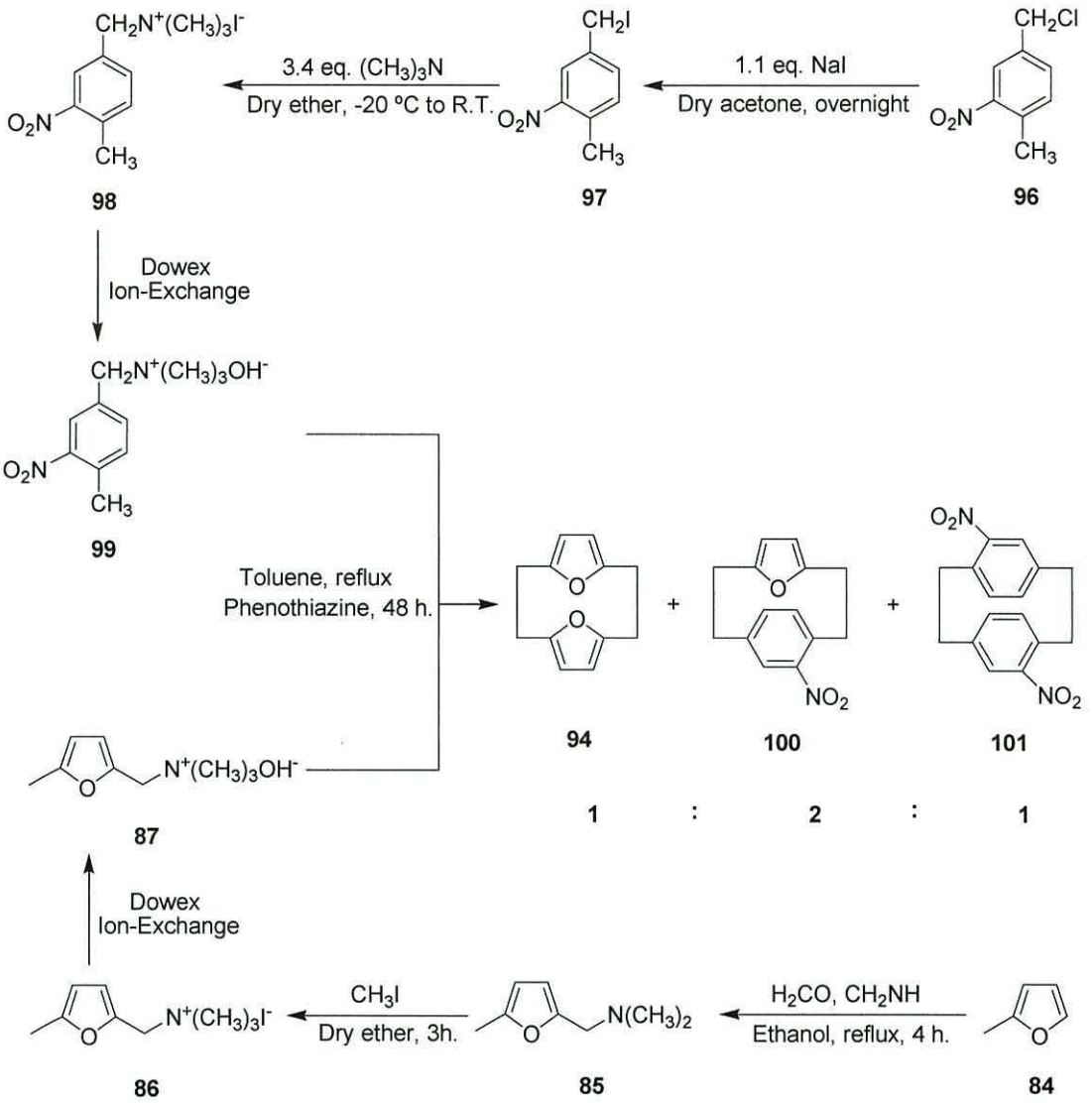

Scheme 4.38. Synthesis of substituted paracyclophane derivatives **94**, **100** and **101** *via* Hoffmann elimination.

Finally it is important to remark on a few considerations that must be made when using the Hoffmann reaction in order to produce paracyclophane derivatives. The hazard of using free amines in the laboratory, the need for using large quantities of starting material in order to get enough material, since a lot of steps are necessary, and the much elaborated procedure makes this a long time-consuming strategy. Yet this process provides a much simpler and more reliable methodology to give access to the difficult medium-sized rings, especially paracyclophanes. Moreover, the resulting product, which contains the alkene group at the middle of the alkyl chain allows further functionalisation, leading to a number of derivatives appropriate for

generating radicals of interest. This method, therefore, shows the most promise for developing a route towards substituted paracyclophane models.

In addition, it was possible to purchase a sample of 20 mg of paracyclophane derivative **109** (Figure 4.11) from the Aldrich Rare Chemical Catalogue.

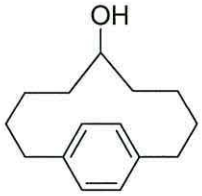

109

Figure 4.11. Structure of paracyclophane derivative **109**.

Derivative **109** has been spectroscopically characterised in order to be used for comparative purposes. Analysis of derivative **109** by ^{1}H NMR clearly shows the shielding of the protons that are located above the aromatic ring at δ 0.91, 0.75, 0.65, 0.52, 0.16 and 0.00, indicating the influence of the ring current effect.

As it has been shown in this chapter, the synthesis of [9]-paracyclophane derivatives is not a straightforward task. The high deficit in entropy and strain that has to be overcome to bring together two alkyl chains in a *para*-substituted benzene to form a medium ring makes intramolecular cyclisation methods difficult to successfully carry out in most cases. The intramolecular reactions that actually give a positive result are often not reproducible. The acyloin condensation, in particular, gives a very low, almost negligible, yield of product. The reasons for low reproducibility have already been discussed in this chapter. Other intramolecular cyclisation reactions, such as cyclisation promoted by samarium iodide, McMurry coupling and RCM afford products other than the cyclised paracyclophane as the major components. All these intramolecular approaches also have the disadvantage that they are very laborious and time-consuming. However, it has been possible to produce a paracyclophane ring using different methodology rather than through intramolecular coupling. The Hoffmann elimination provides a method to prepare [8]-paracyclophanes.

Functionalisation at the benzene ring has been achieved by introducing a nitro group into the starting material. Further work on these compounds could give an entry to [9]-paracyclophane derivatives and they are likely to provide a better model to study the interaction between aromatics and radicals than anthracenes because of their rigid geometry.

Conclusions and future work

Synthetic models such as anthracene derivatives **2** and the acyclic derivative **3** have been synthesised. The skeleton structure of acyclic model **3** has been constructed by Grignard reaction of benzyl bromide **37** with heptaldehyde, to give alcohol derivative **39**, which was subsequently converted into bromo derivative **41** by nucleophilic substitution. Substitution at the aromatic ring was accomplished by introduction of the nitro group into the aromatic ring by direct nitration. The nitro group was reduced to the amino derivative **44** by reaction with hydrazine monohydrate and graphite. Sandmeyer reaction of amino derivative **41** with copper (II) bromide achieved bromo derivative **45**.

Anthracene models of general structure **2** have been synthesised following a general three step sequence. Diels Alder reaction of the appropriate 2,6-substituted anthracene with ethyl acrylate, has been followed by reduction of the resulting ester derivatives and then conversion of the corresponding alcohols into bromide derivatives. The main challenge in the synthesis of anthracene derivatives has been to produce a range of substituted 2,6-substituted anthracene derivatives suitable for Diels Alder reaction. Substituents at the aromatic ring of the anthracene moiety have been obtained using different strategies. Derivatisation of diaminoanthracene **12** to functional groups such as bromo, has failed due to the high sensitivity of the 9,10-position at the anthracene ring towards typical chemical reagents used in Sandmeyer reactions. 2,6-Substituted anthraquinones can be synthesised followed by reduction of the quinone moiety in order to achieve the corresponding 2,6-anthracene derivatives. The 2,6-dimethyl anthraquinone **7** has been synthesised by Diels Alder reaction of benzoquinone **5** with isoprene **6**. The Sandmeyer reaction has proven useful in the synthesis of 2,6-bromo anthraquinone **11** and 2,6-dihydroxy anthraquinone **10** from 2,6-diamino anthraquinone **12**. Since there is no general method that could be applicable to the reduction of substituted anthraquinones, 2,6-substituted anthraquinones had to be reduced using different procedures for each

functional group. Zinc reductions are applicable to the reduction of methyl substituted anthraquinone **7** and diamino anthraquinone **12**, however they are incompatible with halogen substituted anthraquinones. The bromo-substituted anthracene **14** was synthesised by partial reduction of anthraquinone **11** to diol **15** with sodium borohydride followed by dehydration using tin chloride in acid medium. The hydroxy substituted anthraquinone **10** was incompatible with zinc reduction, but could be reduced using aluminium amalgam. The 2,6-nitro anthracene derivative **35** has been synthesised by direct nitration of the anthracene moiety using trifluoroacetic anhydride and ammonium nitrate. This reaction produced isomers **35** and **36**, which were separated by column chromatography. The successful introduction of the nitro derivative into the anthracene moiety at the 2,6-position provides a breakthrough in the synthesis of 2,6-substituted anthracene adducts as it can be further derivatised into a whole range of other functional groups, which could be subject of further work.

The relative rates of reaction towards *tri*-butyl tin hydride of anthracenes **2** and acyclic derivatives **3** have been measured. Electron withdrawing groups at the aromatic ring increase the reactivity of the substrate, suggesting that a lower electron density at the aromatic ring stabilises the intermediate of the bromine abstraction. This trend follows a Hammett relationship giving further evidence for an electronic effect. In addition, high level computational studies have shown that RSEs of radicals derived from anthracene derivatives **33**, **34**, **35** and **47** are all within ± 1 $kJmol^{-1}$ implying that stabilisation in negligible for these particular radicals, and therefore indicating that the substituent effect shown in the radical abstraction of bromine by Bu_3SnH is principally due to polar effects through a δ^- transition state and not because of radical stabilisation.

The ESR spectrum of anthracene derivative **33** has shown interaction of the radical with the α-protons (13.5 G) and the β-protons (1.3 G). The fact that the interaction between the radical and the aromatic ring could not be identified, may provide another evidence that the stabilisation of the free radicals generated in the bromine abstraction reaction by Bu_3SnH is insignificant.

Cyclic voltammetry has been used to study the electroreduction of the carbon-bromine bond in anthracene and acyclic models of general structures **2** and **3**, respectively. The broadness and shape of the observed reduction peaks indicates that the reduction is governed by the kinetics of an electron transfer step. In addition, the transfer coefficient of the rate controlling electron transfer provides evidence that the electrochemical reductive cleavage of the investigated derivatives follows a concerted mechanism without formation of a radical anion as intermediate. Furthermore, the connection between the potential of reduction of the carbon-halogen bond and the stabilisation of the δ^- transition state has been established by linear correlation with Hammett plots. Electrochemistry results are consistent with the relative rate studies, supporting the fact that electron donating groups destabilise the intermediate, whereas electron withdrawing groups have a stabilising effect. Low values of the reaction constant calculated by Hammett plots of 0.15 in the case of anthracene derivatives and 0.06 for acyclic derivatives plus some deviation from linearity indicates a small influence of the polar effect in the electrochemical reduction of the carbon-bromine bond compared to that observed in the bromine abstraction reaction with Bu_3SnH. This indicates less degree of polarization in the δ^- transition state. Therefore, the electrochemical reduction of the carbon-bromine bond for these systems is more likely to be governed by the radical stability of the intermediate rather than polar effects. In addition, anthracene models **2** have shown a greater contribution of the electron density at the aromatic ring on the rate of reaction than acyclic, which denotes the influence of their more restrictive geometry in comparison with acyclic derivatives.

The synthesis of substituted [9]-paracyclophanes of general type **1** has been investigated. The high deficit in entropy and strain, which has to be overcome to bring together two alkyl chains in para-substituted benzene to form a medium ring, makes intramolecular cyclisation methods difficult to successfully carry out in most of the cases examined. The acyloin condensation gives a very low, almost negligible, yield of product and results are difficult to reproduce. Other intramolecular cyclisation reactions, such as cyclisation promoted by samarium iodide, McMurry coupling and RCM afford products other than the cyclised

paracyclophane as the major components. All these intramolecular approaches have also the disadvantages that are very laborious and time-consuming. A different alternative to the synthesis of paracyclophanes is the cycloaddition of quaternary ammonium hydroxides initiated by the Hoffmann. This method affords [8]-paracyclophane **99**, which could be further derivatised to [9]-paracyclophane as part of further work. In addition, derivatisation at the aromatic ring of the paracyclophane system has been achieved by the cycloaddition of quaternary ammonium hydroxides **91** and **104** already containing a nitro group.

There are a few key points that could be developed further. For example, the regiochemistry of the dinitration of anthracene derivatives gives two main isomers. This specific preference for the 2,6- and 2,7-derivatives should be studied in more detail.

Other 2,6-disubstituted anthracene derivatives can be synthesised in order to obtain a wider range of functional groups suitable for both relative rates and cyclic voltammetry studies. These new derivative could be correlated using a Hammett plot. For example, the amino derivative could be obtained by reduction of the corresponding nitro analogue. This would afford a diazonium intermediate that could readily be converted into its phenol analogue, which could then be transformed into the corresponding methoxy derivative. The dimethyl derivative could also be oxidised to its corresponding acid analogue and the latter transformed into an ester group.

In relation to the relative rates of reaction, it would be quite interesting to explore the individual contribution of the entropic factor. This could be achieved by carrying out bromine abstraction at different temperatures.

Another very important issue that should be looked into is the fact that the radical being formed at the top of the aromatic ring is not completely aligned with the aromatic π-cloud. The interaction could thus be strengthen by extending the aliphatic chain with a methyl group to obtain a structure whereby the radical would better

interact with the electron cloud of the aromatic introducing another element of rigidity.

The Hoffmann degradation as a route leading to the synthesis of paracyclophane should also be taken further in order to obtain a whole range of substituted paracyclophane derivatives. It is anticipated that paracyclophane derivatives would provide a better model to study the interaction of radical intermediates with the aromatic moiety. This is because of their more restrictive geometry and the ability of the paracyclophane system to hold the radical just above the aromatic ring.

Experimental

General experimental

All reactions that required an inert atmosphere were carried out under Schlenk conditions using dry nitrogen or dry argon as the inert gas through a standard nitrogen line. The solvents were distilled and dried by standard methods unless otherwise stated.[194] All precursors were obtained from commercial sources (eg. Aldrich, Lancaster, Avocado) and were used without further purification unless otherwise stated.

NMR spectra for routine samples were recorded on a Bruker AC-250 Spectrometer (^{1}H 250 MHz, ^{13}C 63 MHz) (s = singlet, bs = broad singlet, d = doublet, t = triplet, pt = pseudotriplet, q = quartet, dd = doublet of doublets, dt = doublet of triplets, p = pentuplet, s = sextet, sp = septet, m = multiplet). More specialised NMR spectra for pure compounds were recorded on a Bruker Avance 500 (^{1}H 500 MHz, ^{13}C 125 MHz, DEPT, COSY and HMQC). All of the coupling constants (*J*) were recorded in Hz.

Column chromatography was generally done with Davisil silica gel (40-60 microns). Aluminium oxide Brockmann I (150 mesh) was also used as stated.

IR spectra were recorded on a Bruker Tensor 27 spectrometer. Liquid compounds were recorded as a liquid film. Solids were recorded as a KBr disc or using Nujol mull.

GCMS was carried out with a Micromass GCT model for the mass spectrometer. The chromatography column used was an Agilent 6890N DB-SMS, length (30 m), internal diameter (0.25 mm), thickness of the film (0.25 μm), temperature range (-60-325 °C), constant flow of Helium (1.5 ml/min), purge flow (20 ml/min), injector

temperature (250 °C). The GCMS standard program used was: initial temperature (40 °C), initial time (2 min.), rate (10 °C/min), final temperature (260 °C) and final time (2 min.). For routine analysis, the GCMS apparatus used was a Jones Chromatography JCL6000. The column used was a Chrompak CP-SIL5 DB, length (30 m), internal diameter (0.32 mm), thickness of the film (0.25 μm), temperature range (-60-325 °C), constant flow of Helium (1.5 ml/min), purge flow (20 ml/min), injector (250 °C). The program used was: initial temperature (50 °C), initial time (2 min.), rate (10 °C/min), final temperature (250 °C) and final time (10 min.).

LCMS was carried out with a TOF LC Bruker Daltonics by direct insertion using dichloromethane as the solvent of choice.

Microanalysis was obtained from a Carlo Elba Elemental Analyser MOD 1106 (with helium as carrier gas) CHNS-O EA1108.

Electrochemistry was done using an Autolab Model PG30.

Crystal structures were provided by the EPSRC National Crystallography Service at the Department of Chemistry, University of Southampton.

ESR spectra were collected at the University of York in collaboration with Professor Bruce Gilbert.

Synthetic experiments

Synthesis of 2,6 and 2,7-dimethylanthraquinone (13 and 14)

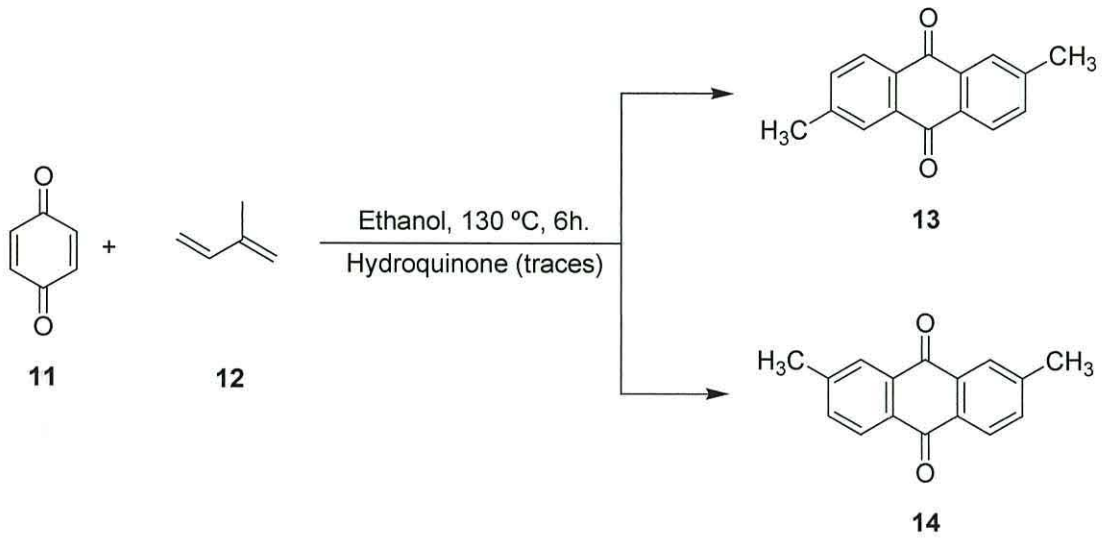

Benzoquinone **11** (5.0 g, 46 mmol, 1.0 eq.), isoprene **12** (11.4 g, 139 mmol, 3.0 eq.) and traces of hydroquinone, were suspended in absolute ethanol (20 ml) in a beaker which was then placed in an autoclave, and heated at 130 °C under pressure for 6h. The autoclave was allowed to reach room temperature and the resulting mixture was dissolved in potassium hydroxide solution in ethanol (400 ml, 5 %) and heated for 8h at 40 °C under air. Stirring was continued for 12h at room temperature under air. The mixture was then heated again at 50 °C for 1h before it was filtered to give an insoluble white cream solid. The remaining filtrate was distilled to give a mixture (1:1) of the *title compounds* as a white-cream solid **13** and **14** (8.5 g, 36 mmol, 78 %) mp 225-226 °C (lit.,[195] 226-227 °C) for **13** and mp 159-160 °C (lit.,[196] 160-161 °C) for **14**; δ_H 8.20 (2H, d, *J* 7.9), 8.09 (2H, s), 7.58 (2H, d, *J* 7.9), 2.54 (6H, s); δ_C 183.0, 145.2, 134.8, 134.7, 133.5, 131.4, 127.5, 21.88; GCMS (Rt = 17.28 min.) 236 (100 %), 212 (24), 208 (28), 193 (11), 178 (18), 165 (62), 151 (8), 139 (5), 104 (9), 89 (20), 77 (11), 63 (10).

Analysis of 2,6-diaminoanthraquinone (15)

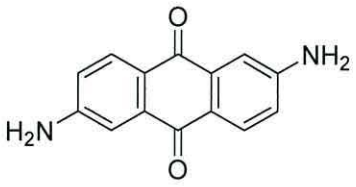

15

mp 312-313 °C, (lit.,[197] 310-320 °C,); δ_H (DMSO-d_6) 7.85 (2H, d, *J* 8.5), 7.23 (2H, s), 6.84 (2H, d, *J* 8.5), 6.57 (4H, s, -NH_2); δ_C 180.9, 154.7, 135.8, 129.3, 121.3, 116.9, 109.6.

Synthesis of 2,6-dihydroxyanthraquinone (16)

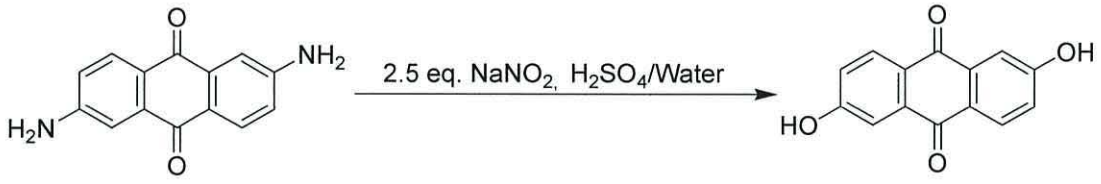

15 **16**

2,6-Diaminoanthraquinone **15** (12.0 g, 58 mmol, 1.0 eq.) was suspended in sulphuric acid (20.0 g) diluted in water (100 ml) in a three-necked round-bottom flask equipped with a mechanical stirrer and a reflux tube. Sodium nitrite (9.9 g, 140 mmol, 2.5 eq.) was added in portions at 0 °C. The mixture was warmed up to room temperature and then brought to reflux for 20 min. The yellowish-brown solid was filtered whilst hot, boiled with barium hydroxide (17.0 g) in water (250 ml). The precipitate was extracted with boiling water (200 ml). Acidification of the combined filtrates with hydrochloric acid gave a golden yellow precipitate that was filtered, washed with water and air dried to afford the *title compound* **16** as a yellow solid (5.5 g, 26 mmol, 45 %) mp 355 °C, decomposes (lit.,[101] 360 °C, decomposes); ν_{max} cm^{-1} 3233, 2924, 2854, 1702, 1672, 1446; δ_H (DMSO-d_6) 10.5 (2H, s), 7.72 (2H,

d, *J* 8.5), 7.15 (2H, s), 6.70 (2H, d, *J* 8.5); δ_C 181.2, 163.1, 135.5, 129.7, 126.5, 120.8, 112.2.

Synthesis of 2,6-dibromoanthraquinone (17)

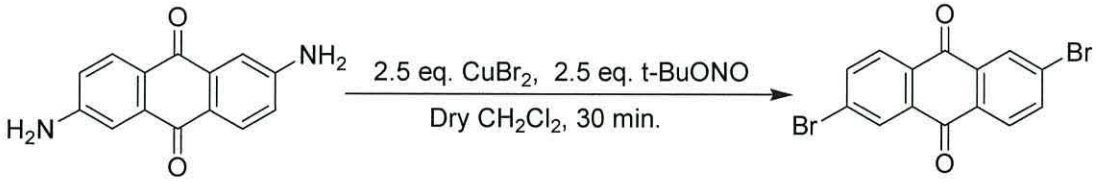

15 **17**

2,6-Diaminoanthraquinone **15** (5.0 g, 24 mmol, 1.0 eq.) was added in portions to a suspension of copper (II) bromide (13.4 g, 60 mol, 2.5 eq.) and *tert*-butyl nitrite (6.2 g, 60 mmol, 2.5 eq.) in dry acetonitrile (200 ml) at 50-60 °C in a three-necked round-bottom flask under a positive pressure of nitrogen. The mixture was stirred at reflux for 30 minutes until all gas evolution had ceased. It was cooled down to room temperature and poured over an aqueous solution of hydrochloric acid (100 ml, 20 %). The resulting precipitate was filtered, washed with water, and air dried to give a brown-yellowish solid. This solid was extracted by successive recrystallisations from hot toluene to afford the *title compound* **17** as a yellow powder (6.4 g, 17 mmol, 80 %) mp 286-287 °C (lit.,[198] 289-290 °C); ν_{max} cm^{-1} 2924, 1677, 1573, 1461, 1377, 1307, 1285, 732; δ_H 8.37 (2H, d, *J* 1.9), 8.10 (2H, d, *J* 8.2), 7.88 (2H, dd, *J* 1.9, *J* 8.2); δ_C 137.4, 130.4, 129.2; m/z 363 (1 %), 365 (3), 367 (1), 284 (1), 207 (15), 201 (100), 166 (12), 150 (21), 116 (33), 98 (9), 75 (20); GCMS (Rt = 23.49 min.) 366 (100 %), 338 (24), 310 (22), 287 (30), 259 (18), 229 (28), 150 (75), 75 (62).

Synthesis of 2,6-diaminoanthracene (18)

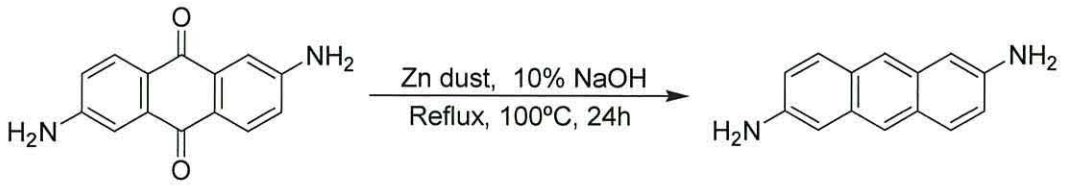

15 **18**

2,6-Diaminoanthraquinone **15** (13.1 g, 55 mmol, 1.0 eq.) was suspended in an aqueous sodium hydroxide solution (125 ml, 10 %) in a three-necked round-bottom flask equipped with a mechanical stirrer and a refluxing tube. Zinc powder (10.0 g, 150 mmol, 2.8 eq.) was added at room temperature, and the mixture was brought to reflux under continuous stirring. Ethanol (10 ml) was added to prevent violent foaming. After 30 and 60 minutes, respectively, two more portions of zinc powder (10.0 g, 150 mmol, 2.8 eq.) were added. The resulting mixture was stirred under reflux for a total time of 24h. The resulting mixture was filtered whilst hot and washed with hot water until the filtrate became clear. The grey residue was air dried and continuously extracted with acetone using a soxhlet unit to afford the *title compound* **18** as a yellow powder (3.5 g, 17 mmol, 31 %) (green fluorescent). Note: The reaction goes through different stages of reduction, changing colour from red, passing through purple and yellow. Although it is a yellow precipitate after 3h of mechanical stirring, the reduction is not complete at that stage, but after 24h when it becomes green the reaction is complete. mp 230 °C decomposed (lit.,[82] 234 °C decomposes); ν_{max} cm^{-1} 3398, 3305, 3204, 2924, 2854, 2360, 1476, 889; δ_H 7.82 (2H, s), 7.63 (2H, d, *J* 9.2), 6.92 (2H, d, *J* 9.2), 6.79 (2H, s), 5.22 (4H, s, $-NH_2$); δ_C 144.0, 130.6, 127.9, 127.2, 121.3, 120.4, 103.7.

Synthesis of 2,6-dimethylanthracene (19)

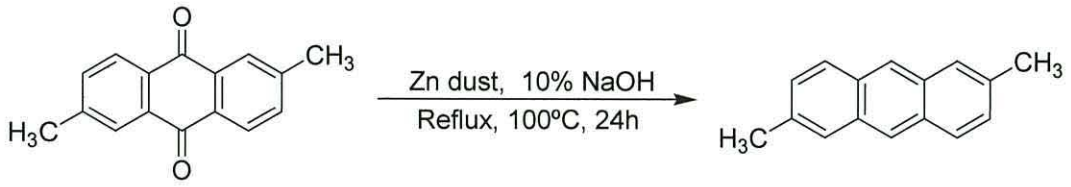

13 **19**

2,6-Dimethylanthraquinone **13** (5.0 g, 21 mmol, 1.0 eq.) was suspended in an aqueous sodium hydroxide solution (125 ml, 10 %) in a three-necked round-bottom flask equipped with a mechanical stirrer and a reflux tube. Zinc powder (10.0 g, 150 mmol, 7.1 eq.) was added at room temperature and the mixture was brought to reflux under continuous mechanical stirring. Ethanol (10 ml) was added to prevent violent foaming. After 30 and 60 minutes two more portions of zinc powder (10.0 g, 150 mmol, 7.1 eq.) were added respectively. The resulting mixture was stirred under reflux for a total time of 24h. The mixture was filtered whilst hot and washed with hot water. The grey solid residue was air dried and extracted with hot toluene (200 ml) portions until the solution did not show any fluorescent spot under UV light. The combined solutions were evaporated to afford the *title compound* **19** as a yellowish powder (1.9 g, 9 mmol, 45 %) (green fluorescent) mp 230-231 °C (lit.,[199] 224-225 °C); ν_{max} cm^{-1} 3019, 2854, 1215, 902, 755, 699; δ_H 8.19 (2H, d, *J* 7.9), 8.09 (2H, s), 7.59 (2H, d, *J* 7.9), 7.27 (2H, s), 2.54 (6H, s); δ_C 128.5, 128.4, 128.0, 126.9, 126.8, 126.3, 125.5, 124.7, 30.9; HRMS-EI (calculated m/z 206.1091; required m/z 206.1091) m/z 206.1091 (100 %), 189.07 (8), 178.07 (2), 103.05 (4), 95.54 (3), 89.04 (8), 76.03 (4); GCMS (Rt = 21.49 min.) 206 (100 %), 189 (28), 89 (10).

Synthesis of 2,6-dibromoanthracene (20)

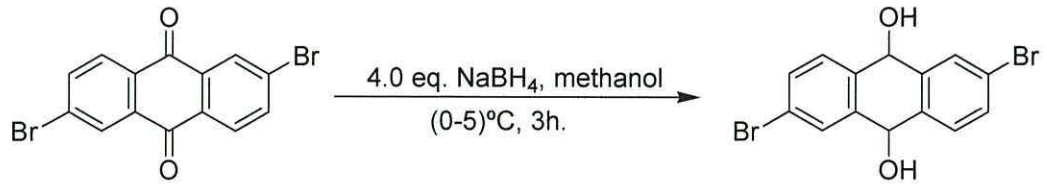

17 **25**

Sodium borohydride (4.0 g, 109 mmol, 4.0 eq.) was added portion-wise during 30 minutes, to avoid rapid increase in temperature, to a suspension of 2,6-dibromoanthraquinone **17** (10.0 g, 27 mmol, 1.0 eq.) in methanol, kept between 0-5 °C using and ice/water bath, in a three-necked round-bottom flask under a positive pressure of nitrogen. The mixture was stirred for 3h, maintaining the temperature between 0-5 °C. After that time, the mixture had turned into an homogeneous dark orange solution. It was poured over of a mixture ice/water (200 ml) and formation of a white precipitate occurred, which was collected by filtration, washed with water and air dried; δ_H (DMSO-d_6) 7.89 (2H, d, *J* 1.9), 7.70 (2H, d, *J* 8.2), 7.52 (2H, dd, *J* 8.2 *J* 1.9), 5.70 (2H, d, *J* 6.3), 5.50 (2H, d, *J* 5.1); δ_C 206.2, 142.5, 139.1, 130.3, 127.2, 126.4, 121.3, 67.3; GCMS (Rt = 26.68 min.) 370 (10 %), 352 (26), 336 (100), 273 (62), 255 (18), 210 (14), 176 (65), 163 (36), 87 (24), 74 (24), 51 (20).

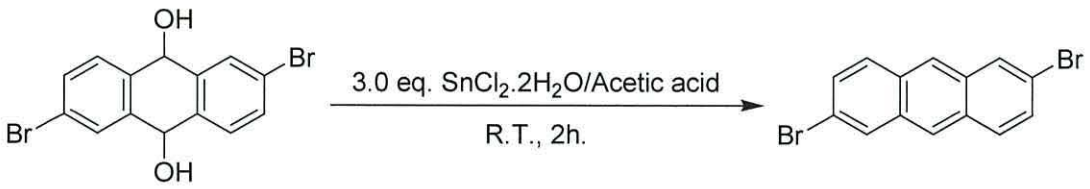

25 **20**

The white precipitate **25** obtained from the above procedure was placed into a flask with glacial acetic acid (200 ml), under a positive pressure of nitrogen. Tin (II) chloride dihydrate (18.5 g, 82 mmol, 3.0 eq.) was added to the resulting suspension and the mixture was stirred at room temperature for 2h. After that time, water

(100 ml) was added. A precipitate was formed, collected by filtration, washed thoroughly with water and air dried. The product was finally dried under high vacuum to eliminate any remaining traces of water and acetic acid to afford the *title compound* **20** as a bright yellow powder (2.8 g, 8 mmol, 76 %) mp 195-196 °C; ν_{max} cm^{-1} 2934, 2360, 1586, 1462, 1377, 899, 794, 757, 725; δ_H 8.32 (2H, s), 8.18 (2H, s), 7.89 (2H, d, *J* 9.2), 7.54 (2H, d, *J* 9.2); δ_C 206.3, 150.1, 132.4, 131.7, 128.8, 126.5, 125.9, 122.3; HRMS-EI (calculated m/z 333.8991; required m/z 333.8993) m/z 334 (28 %), 335 (100), 333 (31), 256 (9), 176 (88), 167 (10), 150 (9), 88 (98), 75 (18); GCMS (Rt = 23.78 min.) 336 (100 %), 255 (18), 176 (65), 150 (14), 88 (32).

Reaction of 2,6-diaminoanthraquinone (15) with hydriodic acid in acetic acid

2,6-Diaminoanthraquinone **15** (1.0 g, 4 mmol, 1.0 eq.) was suspended in acetic acid (75 ml) in a three-necked round-bottom flask equipped with a mechanical stirrer and a reflux tube. Hydriodic acid (4.0 g, 31 mmol, 7.5 eq.) was added at room temperature and the mixture was brought to reflux under continuous stirring for 16h. The hot solution was poured into sodium bisulfite aqueous solution (1 %). The resulting precipitate was separated by filtration, washed with water and air dried to give an orange solid. The same procedure was repeated using acetone as a co-solvent with identical result. The starting material was characterised by NMR as a brown-red solid; δ_H (DMSO-d_6) 7.85 (2H, d, *J* 8.5), 7.25 (2H, s), 6.85 (2H, d, *J* 8.5), 6.57 (4H, s); δ_C 181.0, 154.7, 135.8, 129.3, 121.3, 116.9, 109.6; GCMS and NMR characterisation did not show any other peaks that could indicate the formation of diaminoanthracene **18**.

Reaction of 2,6-dihydroxyanthraquinone (16) with zinc in aqueous sodium hydroxide solution

2,6-Dihydroxyanthraquinone **16** (5.0 g, 21 mmol, 1.0 eq.) was suspended in an aqueous sodium hydroxide solution (125 ml, 10 %) in a three-necked round-bottom flask equipped with a mechanical stirrer and a reflux tube. Zinc powder (11.8 g, 180 mmol, 8.6 eq.) was added at room temperature and the mixture was brought to reflux under continuous mechanical stirring. Ethanol (10 ml) was added to prevent violent foaming. After 30 and 60 minutes, two more portions of zinc powder (10.0 g, 180 mmol, 8.6 eq.) were added, respectively. The resulting mixture was stirred under reflux for a total time of 24h. The resulting mixture was filtered whilst hot and washed with hot water. The grey solid residue was air dried and extracted with hot toluene (200 ml) and hot acetone (200 ml). The combined solutions were evaporated to afford a yellowish powder (green fluorescent). The solution was reacidified to give a green solid (0.2 g). NMR did not show any significant peak apart from the solvent. No peak could be observed by GCMS.

Reaction of 2,6-dimethylanthraquinone (13) with zinc and ammonia

2,6-Dimethylanthraquinone **13** (5.0 g, 21 mmol, 1.0 eq.) was added to a mixture of liquid ammonia (25 ml), water (13 ml), pyridine, (13 ml), a spatula of copper sulphate and zinc (13.9 g, 212 mmol, 10.0 eq.) in a three-necked round-bottom flask under nitrogen. The mixture was brought to reflux for 15h. Portions of liquid ammonia (25 ml) were added every 5h. The solution was filtered whilst hot, washed several times with hydrochloric acid (2N) and water. The solid was air dried and extracted with hot toluene. The solvent was evaporated to give a yellowish solid (green fluorescent) (1.3 g, 6 mmol, 30 %) mp 230-231 °C (lit.,[199] 224-225 °C); δ_H 8.19 (2H, d, *J* 7.9), 8.09 (2H, s), 7.59 (2H, d, *J* 7.9), 7.27 (2H, s), 2.54 (6H, s); δ_C 128.5, 128.4, 128.0, 126.9, 126.8, 125.5, 124.7, 30.9; m/z 206 (100 %), 189 (8),

178 (2), 103 (4), 95 (3), 89 (8), 76 (4); GCMS (Rt = 21.49 min.) 206 (100 %), 189 (28), 89 (10).

Reaction of 2,6-dibromoanthraquinone (17) with zinc in aqueous sodium hydroxide solution

2,6-Dibromoanthraquinone **17** (13.0 g, 39 mmol, 1.0 eq.) was suspended in an aqueous sodium hydroxide solution (125 ml, 10 %) in a three-necked round-bottom flask equipped with a mechanical stirrer and a reflux tube. Zinc powder (10.0 g, 180 mmol, 4.2 eq.) was added at room temperature, and the mixture was brought to reflux under continuous mechanical stirring. Ethanol (10 ml) was added to prevent violent foaming. After 30 and 60 minutes two more portions of zinc powder (10.0 g, 180 mmol, 4.2 eq.) were added consecutively. The resulting mixture was stirred under reflux for a total time of 24h. The mixture was filtered whilst hot and washed with hot water. The grey solid residue was air dried and extracted with hot toluene (200 ml) portions until the solution did not show any fluorescent spot under UV light. The combined solutions were evaporated to give a yellowish powder (green fluorescent) (5.3 g, 28 mmol, 76 %); δ_H 8.32 (2H, s), 8.09 (4H, m), 7.58 (4H, m); δ_C 131.7, 128.3, 126.3, 125.4; GCMS (Rt = 16.14 min., anthracene **24**) 178 (100 %), 152 (11), 89 (12), 76 (13), 63 (9).

Reaction of 2,6-dibromoanthraquinone (17) with mercury amalgam in cyclohexanol

Aluminium powder (7.0 g, 260 mmol, 14.3 eq.) and mercury chloride (0.2 g, 6 mmol, 0.1 eq.) were suspended in cyclohexanol (120 ml) and carbon tetrachloride (4 ml) in a three-necked round-bottom flask equipped with a refluxing tube under a positive pressure of nitrogen. The suspension was heated cautiously, until a vigorous reaction set in at 150-160 °C, and then the mixture was refluxed for 2h. 2,6-

Dibromoanthraquinone **17** (6.0 g, 18 mmol, 1.0 eq.) was added portion-wise, then it was refluxed for 2.5h. The mixture was cooled down to room temperature and poured over ice cold hydrochloric acid (100 ml, 2N), then extracted with dichloromethane (3 x 100 ml). The product slowly precipitated from the organic solvent to give a yellow solid hardly soluble in any organic solvent (0.6 g, 3 mmol, 16 %) GCMS (Rt = 21.84 min., $C_{14}H_{10}O$, 10H-anthracen-9-one **22**) 194 (100 %), 165 (48), 97 (4).

Reaction of 2,6-dibromoanthraquinone (17) with zinc and ammonia

2,6-Dibromoanthraquinone **17** (5.0 g, 15 mmol, 1.0 eq.) was added to a mixture of liquid ammonia (25 ml), water (13 ml), pyridine, (13 ml), a spatula of copper sulphate and zinc (9.7 g, 150 mmol, 10.0 eq.) in a three-necked round-bottom flask under nitrogen. The mixture was brought to reflux for 15h. Portions of liquid ammonia (25 ml) were added every 5h. The solution was filtered whilst hot, washed several times with hydrochloric acid (2N) and then water. The solid was air-dried and extracted with hot toluene. The solvent was evaporated to give a yellowish solid (green fluorescent) (1.1 g, 4 mmol, 24 %); GCMS (Rt = 14.84 min., 10.2 %, 9,10-dihydroanthracene **21**) 179 (100 %), 165 (18), 153 (14), 115 (4), 89 (20), 77 (16), 63 (10); (Rt = 16.14 min., 55.4 %, anthracene **24**) 178 (100 %), 152 (11), 89 (12), 76 (13), 63 (9); (Rt = 17.85 min., 31.5 %, 10H-anthracen-9-one **22**) 194 (100 %), 165 (98), 115 (10), 82 (17), 63 (13); (Rt = 19.48 min., 2.9 %, 2-bromoanthracene **23**) 256 (100 %), 176 (62), 150 (23), 129 (14), 88 (37), 77 (16), 55 (13).

Synthesis of 2,6-dihydroxyanthracene (26)

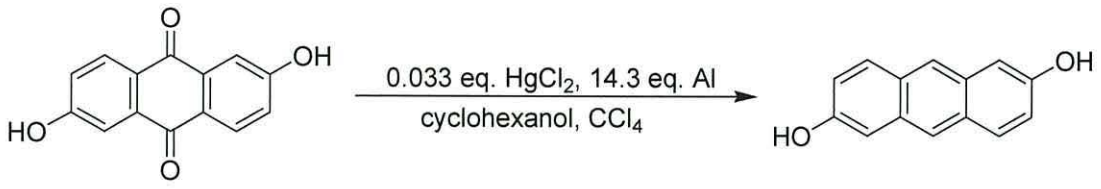

16 **26**

Aluminium powder (9.2 g, 340 mmol, 14.3 eq.) and mercury chloride (0.2 g, 0.8 mmol, 0.1 eq.) were suspended in cyclohexanol (120 ml) and carbon tetrachloride (4 ml) in a three-necked round-bottom flask equipped with a refluxing tube under a positive pressure of nitrogen. The suspension was heated cautiously until a vigorous reaction set in at around 150-160 °C, then the mixture was refluxed for 2h. 2,6-Dihydroxyanthraquinone **16** (5.0 g, 24 mmol, 1.0 eq.) was added portion-wise, then it was refluxed for 2.5h. The mixture was cooled down to room temperature and poured over ice cold hydrochloric acid (100 ml, 2N). It was extracted with dichloromethane (3 x 100 ml) and the solvent was evaporated to afford the *title compound* **26** as a yellow powder (0.5 g, 2 mmol, 12 %); mp 293-295 °C (lit.,[84] 294-297 °C); δ_H 10.51 (2H, s), 8.32 (2H, s), 8.18 (2H, s), 7.89 (2H, d, *J* 8.6), 7.54 (d, 2H, *J* 8.6).

Reaction of 2,6-diaminoanthracene (18) with nitrosylsulphuric acid

2,6-Diaminoanthraquinone **18** (5.0 g, 24 mmol, 1.0 eq.) was dissolved in concentrated sulphuric acid (100 ml) under a nitrogen atmosphere in a three-necked round-bottom flask. To the well stirred solution, nitrosylsulphuric acid (6.7 g, 53 mmol, 2.2 eq.) was added slowly and the mixture was allowed to react for 30 minutes. Afterwards, the reaction mixture was slowly added to an ice/water bath. Tetrafluoroboric acid was added in excess to the resulting solution until a precipitate appeared. The solution was then filtered, the precipitate air dried to give a dark red

blackish solid **27** (10.0 g), which could not be characterised by NMR or GCMS, and was used as recovered.

Reaction of 2,6-diaminoanthracene tetrafluoroborate diazonium salt (27) with copper (II) bromide

2,6-Tetrafluoroboratediazonium salt **27** (5.0 g, 12 mmol, 1.0 eq.) recovered from the above reaction was added in portions to a suspension of copper (II) bromide (6.1 g, 27 mmol, 2.2 eq.) in dry dichloromethane (100 ml) in a three-necked round-bottom flask under a positive pressure of nitrogen. The mixture was stirred for 1h until all gas evolution had ceased. It was cooled down to room temperature and water (50 ml) was added. It was extracted twice with dichloromethane (75 ml), dried over magnesium sulphate and evaporated. No peaks relating to the desired product by either NMR spectral analysis or GCMS.

Reaction of 2,6-diaminoanthracene (18) with copper bromide and sodium nitrite

2,6-Diaminoanthracene **18** (1.0 g, 5 mmol, 1.0 eq.) was added portion-wise to a suspension of copper bromide (2.7 g, 12 mmol, 2.5 eq.) and sodium nitrite (0.8 g, 12 mmol, 2.5 eq.) in dry acetonitrile (100 ml) in a three-necked round-bottom flask under a positive pressure of nitrogen. The mixture was stirred for 30 minutes until all gas evolution had ceased. It was cooled down to room temperature and poured over an aqueous hydrochloric acid solution (100 ml, 20 %). It was extracted twice with dichloromethane (75 ml), washed with an aqueous hydrochloric acid solution (75 ml, 20 %), dried over magnesium sulphate and evaporated. No peaks relating to the desired product by either NMR spectral analysis or GCMS.

Reaction of 2,6-diaminoanthracene (18) with sodium nitrite in acid/aqueous solution

Sodium nitrite (0.8 g, 12 mmol, 2.5 eq.) was added to a suspension of 2,6-diaminoanthracene **18** (1.0 g, 5 mmol, 1.0 eq.) in an aqueous hydrochloric acid solution (100 ml, 20 %) at 0 °C in a three-necked round-bottom flask under a positive pressure of nitrogen. The mixture was stirred for 30 minutes. Copper (II) bromide (2.7 g, 12 mmol, 2.5 eq.) was added and the solution was warmed until all gas evolution had ceased. It was cooled down to room temperature and poured over an aqueous hydrochloric acid solution (100 ml, 20 %). The mixture was extracted with dichloromethane (2 x 75 ml), washed with an aqueous hydrochloric acid solution (50 ml, 20 %), dried over magnesium sulphate and evaporated. No peaks relating to the desired product by either NMR spectral analysis or GCMS.

Reaction of 2,6-diaminoanthracene (18) with copper bromide and *tert*-butyl nitrite

2,6-Diaminoanthracene **18** (1.0 g, 5 mmol, 1.0 eq.) was added portion-wise to a suspension of copper (II) bromide (2.7 g, 12 mmol, 2.5 eq.) and *tert*-butyl nitrite (1.2 g, 12 mmol, 2.5 eq.) in dry acetonitrile (100 ml) in a three-necked round-bottom flask under a positive pressure of nitrogen. The mixture was stirred for 1h until all gas evolution had ceased. It was cooled down to room temperature and poured over an aqueous hydrochloric acid solution (100 ml, 20 %). The solution was then extracted with dichloromethane (2 x 75 ml), washed with an aqueous hydrochloric acid solution (50 ml, 20 %), dried over magnesium sulphate and evaporated. No peaks relating to the desired product by either NMR spectral analysis or GCMS.

Synthesis of anthracene derivative (28)

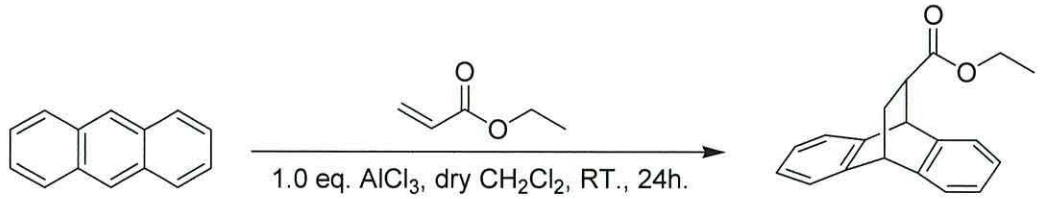

24 **28**

Ethyl acrylate (10.6 g, 106 mmol, 1.0 eq.) was added to a suspension of aluminium chloride (14.1 g, 106 mmol, 1.0 eq.) in dry dichloromethane (200 ml), in a three-necked round-bottom flask under a positive pressure of nitrogen. After 1h of stirring, anthracene **24** (18.4 g, 106 mmol, 1.0 eq.) was added portion-wise. The resulting mixture was stirred at room temperature for 24h. The mixture was then poured over ice, the organic layer separated, washed with water, dried over magnesium sulphate, and the solvent evaporated. The resulting powder was dissolved in dichloromethane, absorbed onto silica gel and purified by column chromatography. The product was eluted with petrol/ether 90:10 to afford the *title compound* **28** as a white powder (25.2 g, 91 mmol, 88 %) mp 100-101 °C (lit.,[200] 98-99 °C); ν_{max} cm^{-1} 2924, 2854, 2359, 1728, 1459, 1191, 758; δ_H 7.32 (4H, m), 7.15 (4H, m), 4.74 (1H, d, *J* 2.6), 4.39 (1H, pt, *J* 2.6, *J* 2.5), 4.09 (2H, m), 2.92 (1H, ddd, *J* 10.4, *J* 4.6, *J* 2.6), 2.23 (1H, ddd, *J* 12.6, *J* 4.6, *J* 2.5), 2.04 (1H, ddd, *J* 12.6, *J* 10.4, *J* 2.6), 1.24 (3H, pt, *J* 7.3, *J* 6.9); δ_C 173.5, 144.0, 143.7, 142.5, 140.0, 126.2, 126.1, 125.7, 125.6, 124.8, 123.7, 123.5, 123.3; m/z 301.1191 ($M + Na^+$), 579.2485 ($2M + Na^+$), 265.0 (14 %), 170.1 (27), 84.0 (23), 73.1 (65), 49.1 (21); GCMS (Rt = 22.44 min.) 278 (5 %), 202 (10), 178 (100), 152 (7), 55 (9).

Synthesis of anthracene derivative (29)

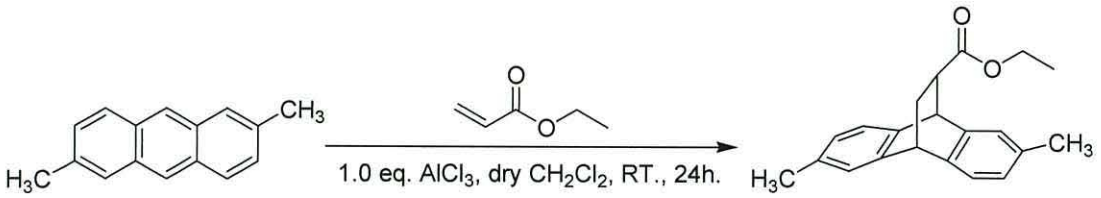

19 **29**

Ethyl acrylate (0.6 g, 6 mmol, 1.0 eq.) was added to a suspension of aluminium chloride (0.8 g, 5.8 mmol, 1.0 eq.) in dry dichloromethane (200 ml), in a three-necked round-bottom flask under a positive pressure of nitrogen. After 1h of stirring, 2,6-dimethyl anthracene **19** (1.2 g, 6 mmol, 1.0 eq.) was added portion-wise. The resulting mixture was stirred at room temperature for 24h. The mixture was then poured over ice, the organic layer separated, washed with water, dried over magnesium sulphate, and the solvent evaporated. The resulting powder was dissolved in dichloromethane, absorbed onto silica gel and purified by column chromatography. The product was eluted with petrol:ether 90:10 to afford the *title compound* **29** as a yellowish oil that, upon cooling in the freezer, gave a white-yellowish powder (1.1 g, 4 mmol, 74 %) mp 78-79 °C; R_f values: petrol 100 % (0.00), petrol/ether 90:10 (0.56), petrol/ether 50:50 (0.79); Found: C, 81.68, H, 7.20. $C_{21}H_{24}O_2$ requires C, 82.32, H, 7.24 %; ν_{max} cm^{-1} 2924, 1733, 1482, 1185, 1027, 736, 818; δ_H 7.27 (4H, m), 7.01 (2H, m), 4.74 (1H, m), 4.37 (1H, m), 4.20 (1H, m), 4.13 (1H, m), 2.98 (1H, ddd, *J* 2.9, *J* 4.8, *J* 10.4), 2.42 (6H, s), 2.30 (1H, m), 2.08 (1H, m), 1.32 (3H, dd, *J* 7.0, *J* 14.2); δ_C 173.7, 144.5, 144.2, 140.9, 140.4, 135.7, 135.3, 126.7, 126.5, 126.1, 125.7, 124.2, 123.5, 60.7, 53.5, 46.7, 44.4, 30.9, 21.4, 14.4; HRMS-EI (calculated m/z 329.1564, M + Na^+; required m/z 329.1527, M + Na^+); m/z 329.1527 and 330.1564, and adduct 635.3156; GCMS (Rt = 24.75 min.) 306 (4 %), 233 (6), 206 (100), 189 (17), 165 (3), 55 (9).

Synthesis of anthracene derivative (31)

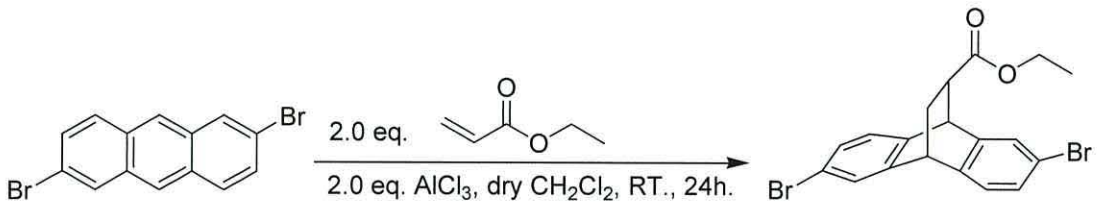

20 **31**

Ethyl acrylate (0.6 g, 6 mmol, 2.0 eq.) was added to a suspension of aluminium chloride (0.8 g, 6 mmol, 2.0 eq.) in dry dichloromethane (200 ml), in a three-necked round-bottom flask under a positive pressure of nitrogen. After 1h of stirring, 2,6-dibromoanthracene **20** (1.0 g, 3 mmol, 1.0 eq.) was added portion-wise. The resulting mixture was stirred at room temperature for 48h. The mixture was then poured over ice, the organic layer separated, washed with water, dried over magnesium sulphate, and the solvent evaporated. The resulting powder was dissolved in dichloromethane (75 ml), absorbed onto silica gel and purified by column chromatography. The product was eluted with petrol/ether 80:20 to afford the *title compound* **31** as a red oil, which under high vacuum became an yellow-reddish solid (0.7 g, 2 mmol, 54 %) mp 62-63 °C; R_f values: petrol 100 % (0.00), petrol/ether 80:20 (0.60), petrol/ether 70:30 (0.63); ν_{max} cm^{-1} 3018, 2978, 2361, 1704, 1456, 1370, 1215, 1032, 754, 668; δ_H 7.53 (2H, d, *J* 7.9), 7.43 (2H, d, *J* 2.2), 7.15 (2H, dd, *J* 7.9 *J* 2.2), 5.30 (1H, d, *J* 2.9), 4.24 (1H, pt, *J* 2.6), 4.09 (2H, m), 2.84 (1H, ddd, *J* 1.6 *J* 4.8, *J* 10.7), 2.42 (6H, s), 2.25 (1H, m), 2.17 (1H, m), 1.32 (3H, m); δ_C 173.6, 143.9, 143.6, 140.6, 139.9, 129.5, 129.1, 126.2, 125.9, 124.7, 124.6, 61.7, 47.7, 47.5, 41.9, 31.6, 14.0; GCMS (Rt = 31.98 min.) 436 (4 %), 352 (62), 273 (100), 243 (20), 163 (60), 113 (11), 82 (19).

Reaction of 2,6-dibromoanthracene (20) with ethyl acrylate and aluminium trichloride

Ethyl acrylate (0.6 g, 5.5 mmol, 1.2 eq) was added to a suspension of aluminium chloride (0.6 g, 5.5 mmol, 1.2 eq.) in dry dichloromethane (200 ml), in a three-necked round-bottom flask under a positive pressure of nitrogen. After 1h of stirring, 2,6-dibromoanthracene **20** (1.0 g, 3.0 mmol, 1.0 eq.) was added portion-wise. The resulting mixture was stirred at room temperature for 24h. The mixture was then poured over ice, the organic layer separated, washed with water, dried over magnesium sulphate, and the solvent evaporated. The resulting powder was dissolved in dichloromethane, absorbed onto silica and purified by column chromatography to afford the *title compound* as a yellow solid (0.2 g, 0.4 mmol, 11 %) mp 62-63 °C; R_f values: petrol 100 % (0.00), petrol/ether 80:20 (0.60), petrol/ether 70:30 (0.63); ν_{max} cm^{-1} 3018, 2978, 2361, 1704, 1456, 1370, 1215, 1032, 754, 668; δ_H 7.53 (2H, d, *J* 7.9), 7.43 (2H, d, *J* 2.2), 7.15 (2H, dd, *J* 7.9 *J* 2.2), 5.30 (1H, d, *J* 2.9), 4.24 (1H, pt, *J* 2.6), 4.09 (2H, m), 2.84 (1H, ddd, *J* 1.6 *J* 4.8, *J* 10.7), 2.42 (6H, s), 2.25 (1H, m), 2.17 (1H, m), 1.32 (3H, m); δ_C 173.6, 143.9, 143.6, 140.6, 139.9, 129.5, 129.1, 126.2, 125.9, 124.7, 124.6, 61.7, 47.7, 47.5, 41.9, 31.6, 14.0; HRMS-EI (calculated m/z 349.8946/351.8915/353.8904; required m/z 349.8916/351.8909/353.8902); GCMS (Rt = 31.98 min.) 436 (4 %), 352 (62), 273 (100), 243 (20), 163 (60), 113 (11), 82 (19).

Synthesis of anthracene derivative (32)

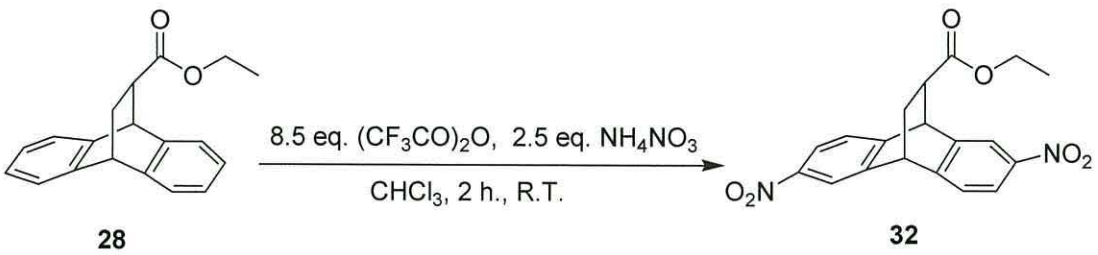

28 32

Ester derivative **28** (1.0 g, 3.6 mmol, 1.0 eq.) was added to a three-necked round-bottom flask equipped with a condenser containing a suspension of ammonium nitrate (0.7 g, 9.0 mmol, 2.5 eq.) and trifluoroacetic anhydride (4.3 ml, 30.6 mmol, 8.5 eq.) in chloroform (10 ml) under a positive pressure of nitrogen. After 2h of continuous stirring at room temperature, the mixture had become a homogenous yellow solution. Then water (50 ml) was added and the mixture was extracted with chloroform (2 x 100 ml), dried over magnesium sulphate, filtered and the organic solvent evaporated under reduced pressure to give an yellow oil. This oil was absorbed onto silica and purified by column chromatography by eluting with petrol/ether 50:50 to afford the *title compound* **32** and anthracene derivative **33** as thick yellow oil, which under high vacuum became a yellow solid with a combined mass and yield of (1.2 g, 3.3 mmol, 91 %).

Analysis of the 2,6-derivative **32**

(0.6 g, 1.7 mmol, 44 %) mp 65-66 °C; Found: C, 61.96, H, 4.41, N, 6.70. $C_{21}H_{24}O_2$ requires C, 61.95, H, 4.38, N, 7.61 %; R_f values: petrol 100 % (0.00), petrol/ether 50:50 (0.55); ν_{max} cm^{-1} 3024, 2981, 1730, 1521, 1465, 1344, 1214, 1193, 1080, 1024, 755, 667; δ_H 8.21 (2H, d, *J* 1.9), 8.12 (2H, ddd, *J* 8.2 *J* 3.8 *J* 1.6), 7.51 (2H, dd, *J* 8.2, *J* 1.6), 4.97 (1H, bs), 4.66 (1H, bs), 4.09 (2H, m), 2.96 (1H, ddd, *J* 10.5, *J* 4.8, *J* 2.9), 2.27 (1H, ddd, *J* 12.9, *J* 4.8, *J* 2.9), 2.12 (1H, ddd, *J* 12.9, *J* 10.4, *J* 2.5), 1.24 (3H, pt, *J* 7.3, *J* 7.0); δ_H 8.21 (1H, d, *J* 1.6), 8.17 (1H, d, *J* 1.9), 8.08 (2H, dd, *J* 8.2, *J* 2.2), 7.49 (2H, d, *J* 8.2), 4.98 (1H, d, *J* 2.2), 4.66 (1H, s), 4.09 (2H, m), 2.96 (1H, ddd, *J* 10.4, *J* 4.8, *J* 2.9), 2.27 (1H, ddd, *J* 12.9, *J* 4.8, *J* 2.9), 2.11 (1H, ddd, *J* 12.9, *J* 10.4, *J* 2.5), 1.24 (3H, pt, *J* 7.3, *J* 7.0); δ_C 172.1, 149.1, 146.6, 142.7, 140.6, 124.6, 124.5, 122.6, 122.5, 120.3, 119.5, 61.4, 46.5, 43.9, 43.0, 29.7, 14.2; HRMS-EI (calculated m/z 391.0855, M + Na^+; required m/z 391.0901, M + Na^+) m/z 391.0855 (M + Na^+, 100 %), 392.091 (M + Na^+, 10 %), 759.1900 (2M + Na^+); GCMS (Rt = 28.42 min.) 268 (18 %), 223 (100), 193 (22), 177 (41), 150 (19), 121 (10), 94 (9), 71 (20), 55 (92).

Analysis of the 2,7-derivative **33**

(0.6 g, 1.8 mmol, 46 %) mp 110-111 °C; R_f values: petrol 100 % (0.00), petrol/ether 50:50 (0.45); ν_{max} cm^{-1} 2959, 1730, 1530, 1465, 1312, 1192, 1079, 1023, 901, 878, 858, 809, 737, 560; δ_H 8.21 (1H, d, *J* 1.6), 8.17 (1H, d, *J* 1.9), 8.08 (2H, dd, *J* 8.2, *J* 2.2), 7.49 (2H, d, *J* 8.2), 4.98 (1H, d, *J* 2.2), 4.66 (1H, s), 4.09 (2H, m), 2.96 (1H, ddd, *J* 10.4, *J* 4.8, *J* 2.9), 2.27 (1H, ddd, *J* 12.9, *J* 4.8, *J* 2.9), 2.11 (1H, ddd, *J* 12.9, *J* 10.4, *J* 2.5), 1.24 (3H, pt, *J* 7.3, *J* 7.0); δ_C 172.1, 149.8, 148.3, 146.6, 146.3, 143.7, 140.1, 126.1, 124.6, 122.7, 122.1, 120.5, 119.1, 61.4, 46.5, 43.8, 42.9, 29.9, 14.2; m/z 391.0855 ($M + Na^+$, 100 %), 392.091 ($M + Na^+$, 10 %), 759.1900 ($2M + Na^+$); GCMS (Rt = 28.42 min.) 268 (18 %), 223 (100), 193 (22), 177 (41), 150 (19), 121 (10), 94 (9), 71 (20), 55 (92).

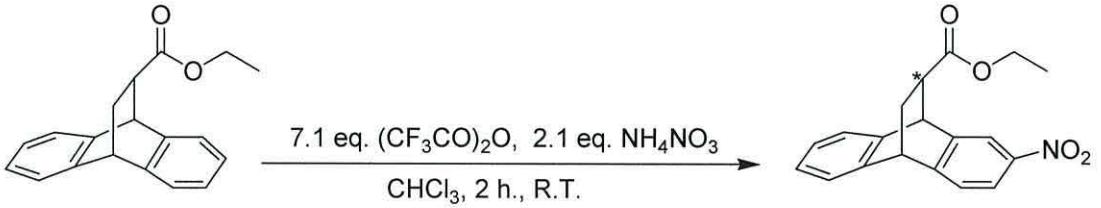

28 **34**

The same procedure had been done previously using 2.1 equivalents of ammonium nitrate and 7.1 equivalents of trifluroacetic anhydride to give a mixture of the products **32** and **33** (characterised above) and mono-nitro derivative **34** (0.6 g, 2.0 mmol 41 %); mp 84-85 °C; R_f values: petrol 100 % (0.00), petrol/ether 50:50 (0.62); ν_{max} cm^{-1} 3024, 2981, 1730, 1530, 1460, 1312, 1192, 1215, 1081, 1027, 757, 667; δ_H 8.02 (1H, dd, *J* 1.6, *J* 9.8), 7.89 (1H, m), 7.29 (1H, d, *J* 8.2), 7.5 (2H, m), 7.20 (1H, m), 7.05 (1H, m), 4.69 (1H, s), 4.36 (1H, s), 3.95 (2H, m), 2.81 (1H, ddd, *J* 10.4, *J* 4.8, *J* 2.6), 2.05 (1H, m), 1.96 (1H, m), 1.9 (3H, m); δ_C 172.9, 151.2, 147.8, 141.2, 126.4, 126.5, 124.0, 123.9, 123.8, 122.0, 120.0, 61.0, 46.8, 43.9, 43.6, 30.4, 14.3; HRMS-EI (calculated m/z 346.1063, $M + Na^+$; required m/z 346.1072, $M + Na^+$) m/z 346.1063 ($M + Na^+$), 362.0803 ($M + K^+$), 699.2211 ($2M + Na^+$);

GCMS (Rt = 20.74 min.) 223 (82 %), 194 (15), 176 (85), 165 (100), 151 (18), 126 (7), 88 (9), 55 (11).

Reaction of anthracene derivative (28) with potassium nitrate and sulphuric acid

Ester derivative **28** (1.0 g, 3.6 mmol, 1.0 eq.) was dissolved in dry dichloromethane (75 ml) in a three-necked round-bottom flask along with potassium nitrate (0.7 g, 7.2 mmol, 2.0 eq.) under nitrogen. The suspension was cooled down to 0 °C using an ice/salt bath. Sulphuric acid (1.4 g, 14.0 mmol, 4.0 eq.) was added dropwise and the solution was stirred for 3h. The resulting solution was extracted with dichloromethane (100 ml), washed with saturated sodium bicarbonate solution until gas evolution ceased, washed with water to eliminate any remaining traces of acid, dried over magnesium sulphate and evaporated to give a yellow oil. This oil was absorbed onto silica and purified by column chromatography to afford the mono-nitro product **34** as a yellow solid upon cooling (0.9 g, 2.5 mmol 57 %); mp 84-85 °C; R_f values: petrol 100 % (0.00), petrol/ether 50:50 (0.62); ν_{max} cm^{-1} 3024, 2981, 1730, 1530, 1460, 1312, 1192, 1215, 1081, 1027, 757, 667; δ_H 8.02 (1H, dd, *J* 1.6, *J* 9.8), 7.89 (1H, m), 7.29 (1H, d, *J* 8.2), 7.5 (2H, m), 7.20 (1H, m), 7.05 (1H, m), 4.69 (1H, s), 4.36 (1H, s), 3.95 (2H, m), 2.81 (1H, ddd, *J* 10.4, *J* 4.8, *J* 2.6), 2.05 (1H, m), 1.96 (1H, m), 1.9 (3H, m); δ_C 172.9, 151.2, 147.8, 141.2, 126.4, 126.5, 124.0, 123.9, 123.8, 122.0, 120.0, 61.0, 46.8, 43.9, 43.6, 30.4, 14.3; GCMS (Rt = 20.74 min.) 223 (82 %), 194 (15), 176 (85), 165 (100), 151 (18), 126 (7), 88 (9), 55 (11).

Reaction of 2,6-diaminoanthracene (18) with ethyl acrylate in dry benzene at reflux

2,6-Diaminoanthracene **18** (1.0 g, 5 mmol, 1.0 eq.) and ethyl acrylate (0.7 g, 7 mmol, 1.5 eq.) were dissolved in dry benzene (150 ml) in a two-necked round-bottom flask under a nitrogen atmosphere. The solution was heated to reflux for 24h, after which time it was poured over ice, extracted with dichloromethane, dried over magnesium sulphate and evaporated to give a yellow-orange solid. The ^{1}H NMR showed a complicated mixture of products, which could not be separated by column chromatography.

Reaction of 2,6-diaminoanthracene (18) with ethyl acrylate in dry benzene at reflux

Ethyl acrylate (1.9 g, 19 mmol, 2.0 eq.) was added to a suspension of aluminium chloride (5.1 g, 38 mmol, 4.0 eq.) in dry dichloromethane (200 ml), in a three-necked round-bottom flask under a positive pressure of nitrogen. After 1h stirring, 2,6-diaminoanthracene **18** (2.0 g, 10 mmol, 1.0 eq.) was added portion-wise. The resulting mixture was stirred at reflux for 24h. The mixture was then poured over ice, the organic layer separated, washed with water, dried over magnesium sulphate, and the solvent evaporated. The resulting powder was dissolved in dichloromethane, absorbed onto silica and purified by column chromatography. No peaks relating to the desired product by either NMR spectral analysis or GCMS.

Reaction of 2,6-diaminoanthracene (18) with ethyl acrylate in dry benzene in an autoclave

2,6-Diaminoanthracene **18** (1.0 g, 4.8 mmol, 1.0 eq.) and ethyl acrylate (0.7 g, 7.2 mmol, 1.5 eq.) were dissolved in dry benzene (20 ml) in a beaker, which was placed into an autoclave. The solution was heated at 150 °C for 24h, after which it was poured over ice, extracted with dichloromethane, dried over magnesium sulphate and evaporated to give a yellow-orange solid. ^{1}H NMR and GCMS indicated only the presence of starting material.

Synthesis of anthracene derivative (36)

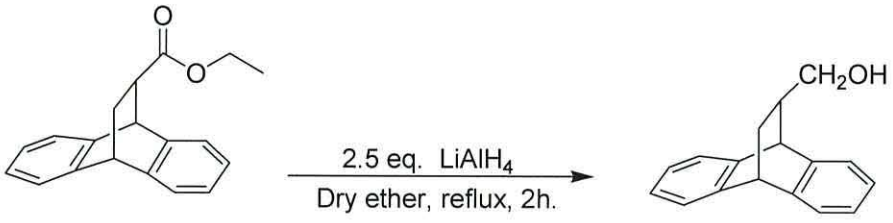

28 **36**

A solution of anthracene **28** (5.0 g, 18 mmol, 1.0 eq.) in dry ether (75 ml) was added slowly to a suspension of lithium aluminium hydride (1.7 g, 45 mol, 1.2 eq.) in dry ether (100 ml), in a three-necked round-bottom flask under a positive pressure of nitrogen. The mixture was brought to reflux and stirred for 2h. Once that time was completed, the reaction was stopped, by firstly adding dropwise ethyl acetate (40 ml) and secondly an aqueous, saturated sodium metabisulfite solution (50 ml). The residue was filtered through a magnesium sulphate pad and the solution evaporated to give a white solid. This white solid was dissolved in dichloromethane, absorbed onto silica and purified by column chromatography. The product was eluted with a mixture of petroleum spirit/ether (70:30) to afford the *title compound* **36** as a white solid (3.4 g, 14 mmol, 80 %) mp 110-111 °C (lit.,[201] 105-108 °C); ν_{max} cm^{-1} 3193, 2923, 1463, 1377, 1028, 749, 534, 456; δ_H 7.34 (2H, m), 7.30 (2H, m), 7.14 (4H, m),

4.46 (1H, d, *J* 2.3), 4.30 (1H, pt, *J* 2.9, *J* 2.5), 3.37 (1H, m), 3.01 (1H, m), 2.18 (1H, m), 1.97 (1H, dpt, *J* 12.3, *J* 10.1, *J* 2.9), 1.55 (1H, s, -OH), 1.11 (2H, ddd, *J* 12.3, *J* 4.8, *J* 2.5); δ_C 143.8, 140.5, 125.9, 125.8, 125.7, 125.6, 125.3, 123.6, 123.4, 123.1, 66.1, 45.6, 44.0, 40.9, 31.0; GCMS (Rt = 15.52 min.) 178 (100 %), 152 (9).

Synthesis of anthracene derivative (37)

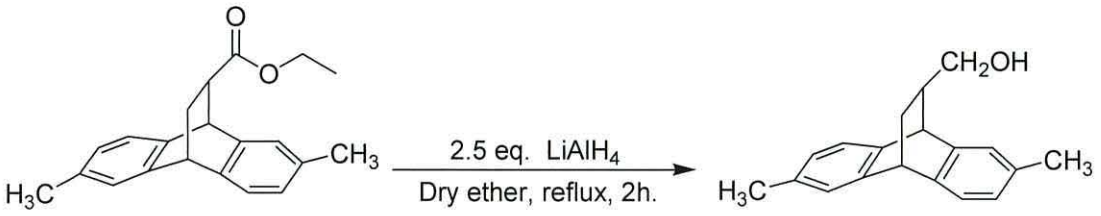

29 **37**

A solution of the ester **29** (1.0 g, 3.3 mmol, 1.0 eq.) in dry ether (75 ml) was added slowly to a suspension of lithium aluminium hydride (0.3 g, 8.2 mmol, 2.5 eq.) in dry ether (75 ml), in a three-necked round-bottom flask under a positive pressure of nitrogen. The mixture was brought to reflux and stirred for 2h. Once that time was completed, the reaction was stopped by, firstly adding dropwise ethyl acetate (40 ml) and secondly an aqueous, saturated sodium metabisulfite solution. The residue was filtered through a magnesium sulphate pad and the solution evaporated to give a white solid. This white solid was dissolved in dichloromethane, absorbed onto silica and purified by column chromatography. The product was eluted with a mixture of petroleum spirit/ether (50:50) to give an oil, which upon cooling in the freezer afforded the *title compound* **37** as a white solid (0.7 g, 2.7 mmol, 81 %); R_f values 100 % petrol (0.00), petrol/ether 90:10 (0.09), petrol/ether 50:50 (0.42); (Found: C, 84.62, H, 7.83). $C_{19}H_{20}O$ requires C, 86.36, H, 7.58 %; ν_{max} cm^{-1} 3355, 2941, 1481, 1031, 803, 737, 553, 432; δ_H 7.18 (4H, m), 6.97 (2H, d), 4.39 (1H, m), 4.23 (1H, dd, *J* 5.4, *J* 2.5), 3.39 (1H, m), 3.06 (1H, pt, *J* 9.8, *J* 9.5), 2.19 (1H, m), 1.97 (1H, m), 1.78 (1H, s, -OH), 1.12 (1H, m); δ_C 143.3, 141.3, 137.8, 135.1, 126.4, 125.1, 124.4, 124.0, 123.3, 122.9, 66.2, 45.2, 44.8, 44.1, 31.3; HRMS-EI (calculated

m/z 303.1142, M + K^+; required m/z 303.1146, M + K^+); m/z 287.14 (M + Na^+, 100 %), 288.14 (20); 551.28 (2M + Na^+, 79 %); 303.11 (M+ K^+); GCMS (Rt = 22.67 min.) 247 (25 %), 206 (100 %), 189 (18).

Synthesis of anthracene derivative (38)

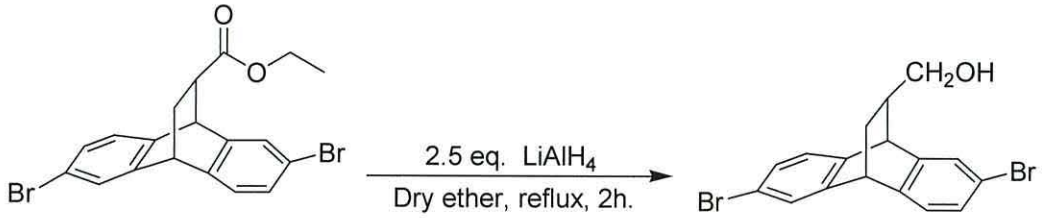

31 **38**

A solution of the ester **31** (1.0 g, 2.3 mmol, 1.0 eq.) in dry ether (75 ml) was added slowly to a suspension of lithium aluminium hydride (0.2 g, 5.7 mmol, 2.5 eq.) in dry ether (100 ml), in a three-necked round-bottom flask under a positive pressure of nitrogen. The mixture was brought to reflux and stirred for 2h. Once that time was completed, the reaction was stopped by, firstly adding dropwise ethyl acetate (40 ml) and secondly an aqueous, saturated sodium metabisulfite solution. The residue was filtered through a magnesium sulphate pad and the solution evaporated to give a yellow oil. This yellow oil was dissolved in dichloromethane, absorbed onto silica and purified by column chromatography. The product was eluted with a mixture of petroleum spirit/ether (50:50) to give an oil, which upon cooling in the freezer afforded the *title compound* **38** as a yellow solid (0.9 g, 2.2 mmol, 95 %) mp 100-101 °C; R_f values 100 % petrol (0.00), petrol/ether 50:50 (0.67), 100 % ether (0.93); ν_{max} cm^{-1} 3381, 3014, 2952, 2871, 1455, 1404, 1078, 1017, 822, 756, 667; δ_H 7.51 (2H, d, *J* 7.9), 7.29 (2H, bs), 7.12 (2H, d, *J* 7.9), 4.15 (1H, bs), 3.69 (1H, bs), 3.08 (1H, m), 2.25 (1H, m), 2.16 (1H, bs, -OH), 2.03 (1H, m), 0.97 (1H, ddd, *J* 12.6, *J* 4.4, *J* 2.9); δ_C 146.8, 144.7, 143.5, 142.9, 141.3, 139.5, 129.0, 126.0, 125.3, 124.5, 123.9, 122.3, 65.5, 42.3, 41.8, 31.4, 15.3.

Synthesis anthracene derivative (39)

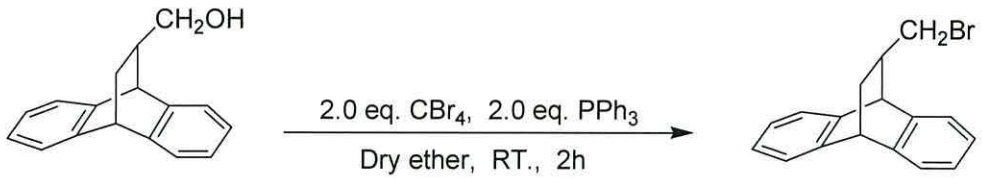

36 **39**

In a three-necked round-bottom flask, the alcohol **36** (1.0 g, 3.6 mmol, 1.0 eq.), along with carbon tetrabromide (2.4 g, 7.2 mmol, 2.0 eq.), was dissolved in dry diethyl ether (50 ml). Triphenylphosphine (1.9 g, 7.2 mmol, 2.0 eq.) was added portion-wise with formation of a white precipitate. After 3h stirring, the resulting suspension was filtered to separate insoluble triphenylposphine oxide. The remaining solution was absorbed onto silica and purified by column chromatography. The product was eluted using a mixture of petroleum spirit/ether 90:10 to afford the *title compound* **39** as a white solid, which was crystallised by slow evaporation (1.0 g, 3.2 mmol, 89 %) mp 138-139 °C (lit.,[88] 141-144 °C); R_f values: petrol/ether 90:5 (0.75); ν_{max} cm^{-1} 3092, 2894, 1495, 1280, 750, 722; δ_H 7.38 (2H, m), 7.33 (2H, m), 7.18 (4H, m), 4.55 (1H, bd, *J* 1.9), 4.33 (1H, bd, *J* 2.5), 3.14 (1H, dd, *J* 9.8, *J* 6.4), 2.87 (1H, pt, *J* 9.8), 2.40 (1H, m), 2.13 (1H, ddd, *J* 12.8, *J* 9.8, *J* 2.9), 1.24 (1H, ddd, *J* 12.6, *J* 4.4, *J* 2.9); δ_C 143.5, 143.4, 143.2, 139.6, 126.3, 126.0, 125.9, 125.8, 125.7, 123.9, 123.5, 123.3, 47.3, 44.2, 41.1, 38.0, 34.9; GCMS (Rt = 22.40 min.) 300/298 (1:1) (2 %), 219 (20), 178 (100), 152 (12), 89 (3).

Synthesis of anthracene derivative (40)

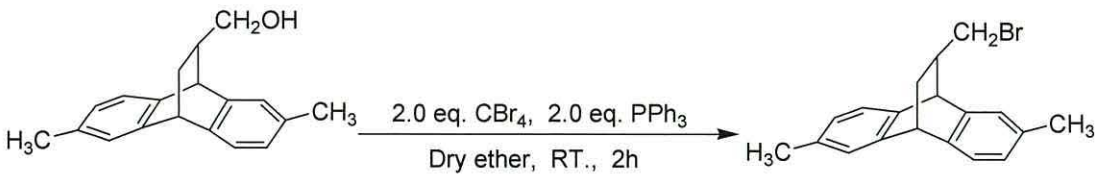

37 **40**

In a three-necked round-bottom flask, the alcohol derivative **37** (1.0 g, 3.8 mmol, 1.0 eq.), along with carbon tetrabromide (2.5 g, 7.6 mmol, 2.0 eq.), was dissolved in dry dichloromethane (50 ml). Triphenylphosphine (2.0 g, 7.6 mmol, 2.0 eq.) was added portion-wise, and the formation of white precipitate was observed. After 3h stirring, the resulting suspension was filtered to separate insoluble triphenylposphine oxide. The remaining solution was absorbed onto silica and purified by column chromatography. The product was eluted using a mixture of petrol/ether 90:10 to afford the *title compound* **40** as a yellow oil (0.7 g, 2.1 mmol, 57 %); R_f values: petrol 100 % (0.25), petrol/ether 90:10 (0.79), petrol/ether 50:50 (0.92); ν cm^{-1} 3007, 2947, 2861, 1481, 1218, 822, 757, 647, 554; δ_H 7.11 (2H, m), 7.02 (2H, m), 6.82 (2H, m), 4.55 (1H, dd, *J* 5.7 *J* 1.9), 4.33 (1H, dd, *J* 5.4 *J* 2.5), 2.99 (1H, m), 2.74 (1H, ddd, *J* 9.8 *J* 5.7 *J* 2.9), 2.21 (1H, m), 2.20 (6H, bs), 1.95 (1H, m), 1.07 (1H, ddd, *J* 12.3, *J* 4.5, *J* 2.9); δ_C 143.9, 140.5, 139.9, 135.8, 135.5, 135.3, 126.2, 125.4, 124.6, 124.3, 124.1, 123.2, 46.9, 43.9, 41.3, 38.3, 35.1, 35.0, 21.3; m/z 328/326 (4 %), 247 (98), 206 (100), 189 (72), 178 (5); GCMS (Rt = 26.75 and 27.68 min. two peaks (two regioisomers), the same chromatogram) 247/249 (22 %), 206 (100), 189 (10), 152 (2), 101 (3), 89 (5).

Synthesis of anthracene derivative (41)

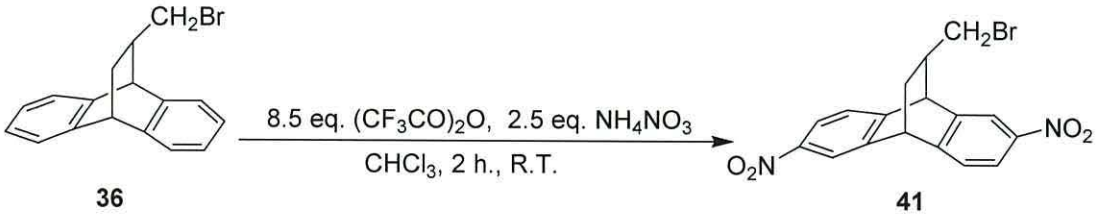

36 41

Anthracene derivative **36** (1.0 g, 3.3 mmol, 1.0 eq.) was added to a three-necked round-bottom flask equipped with a condenser containing a suspension of ammonium nitrate (0.7 g, 8.4 mmol, 2.5 eq.) and trifluoroacetic anhydride (4.0 ml, 28.4 mmol, 8.5 eq.) in chloroform (10 ml) under a positive pressure of nitrogen. After 2h of continuous stirring at room temperature, the mixture had become a

homogenous yellow solution. Then water (50 ml) was added and the mixture was extracted with chloroform (2 x 100 ml), dried over magnesium sulphate, filtered and the organic solvent evaporated under reduced pressure to give a yellow oil. This oil was absorbed onto silica and purified by column chromatography eluting with petrol/ether 50:50 to afford the *title compound* **41** and anthracene derivative **42** as a thick yellow oil, which under high vacuum became a yellow solid (1.2 g, 3.1 mmol, 92 %).

Characterisation of the 2,7 derivative **42**

(0.7 g, 1.8 mmol, 54 %) mp 165-166 °C; Found: C, 52.27, H, 3.22, N, 6.78. $C_{21}H_{24}O_2$ requires C, 52.44, H, 3.34, N, 7.20 %; R_f values: petrol 100 % (0.00), petrol/ether 50:50 (0.35); petrol/ether 40:60 (0.30); δ_H 8.15 (1H, d, *J* 2.2), 8.12 (1H, d, *J* 2.2), 8.01 (1H, dd, *J* 8.2, *J* 2.2), 7.97 (1H, dd, *J* 8.2, *J* 2.2), 7.39 (2H, pt, *J* 8.5), 4.72 (1H, d, *J* 2.2), 4.50 (1H, t, *J* 2.5), 3.05 (1H, dd, *J* 10.1, *J* 6.3), 2.69 (1H, pt, *J* 10.1), 2.35 (1H, m), 2.09 (1H, m), 1.24 (1H, m); δ_C 149.1, 148.8, 146.7, 146.6, 143.5, 140.1, 124.7, 124.6, 122.8, 122.5, 120.8, 119.3, 47.2, 44.2, 40.2, 36.1, 34.5; HRMS-EI (calculated m/z 388.0142; required m/z 388.0059) m/z 388.0142/390.0143 (very weak signal), 372/374 (5 %), 309 (60), 268 (100), 263 (91), 239 (80), 222 (100), 210 (98), 192 (33), 176 (100), 164 (100), 150 (76); GCMS (Rt = 22.40 min.) 300/298 (1:1) (2 %), 219 (20), 178 (100), 152 (12), 89 (3).

Characterisation of the 2,6 derivative **41**

(0.5 g, 1.3 mmol, 39 %) mp 93-94 °C; R_f values: petrol 100 % (0.00), petrol/ether 50:50 (0.50); petrol/ether 40:60 (0.45); δ_H 8.24 (2H, m), 8.12 (2H, m), 7.54 (2H, m), 4.85 (1H, bs), 4.60 (1H, bs), 3.18 (1H, m), 2.71 (1H, t, *J* 10.1), 2.45 (1H, m), 2.19 (1H, m), 1.34 (1H, m); δ_C 149.4, 142.9, 147.0, 146.8, 142.9, 139.6, 124.5, 124.4, 122.4, 122.3, 119.5, 118.9, 47.1, 44.2, 40.1, 35.8, 33.6; m/z 388.0142/390.0143 (very weak signal), 372/374 (5 %), 309 (60), 268 (100), 263 (91), 239 (80), 222 (100),

210 (98), 192 (33), 176 (100), 164 (100), 150 (76); GCMS (Rt = 22.40 min.) 300/298 (1:1) (2 %), 219 (20), 178 (100), 152 (12), 89 (3).

Synthesis of 4-bromo-decane (10)

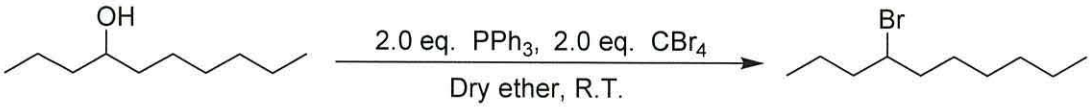

52 **10**

In a three-necked round-bottom flask, 4-decanol **52** (1.0 g, 6.3 mmol, 1.0 eq.), along with carbon tetrabromide (4.2 g, 13.0 mmol, 2.0 eq.), was dissolved in dry diethylether (50 ml). Triphenylphosphine (3.3 g, 13.0 mmol, 2.0 eq.) was added portion-wise with formation of a white precipitate. After 1h of stirring, the resulting suspension was filtered to separate insoluble triphenylposphine oxide and the solution was concentrated in the rotary evaporator. The resulting mixture was filtered through a silica pad to eliminate any remaining trace of triphenylphosphine oxide. The final solution was concentrated to give a colourless liquid. This liquid was further purified from traces of bromoform and carbon tetrabromide by distillation to afford the *title compound* **10** as a colourless liquid (1.4 g, 6.1 mmol, 97 %) bp 52-54 °C at 0.4 mmHg; R_f value in petrol 100 % (0.78); ν_{max} cm^{-1} 2958, 2858, 2732, 1464; δ_H 4.06 (1H, m,), 1.81 (4H, m), 1.57 (2H, m), 1.46 (2H, m), 1.34 (6H, m), 0.95 (3H, t, *J* 7.3), 0.91 (3H, t, *J* 7.0); δ_C 58.57, 41.26, 39.22, 31.71, 28.75, 27.55, 22.60, 20.82, 14.07, 13.49. GCMS (Rt = 8.61 min.) 141 (18 %), 99 (16), 85 (65), 71 (68), 57 (100).

Synthesis of 1-phenyl-decan-4-ol (44)

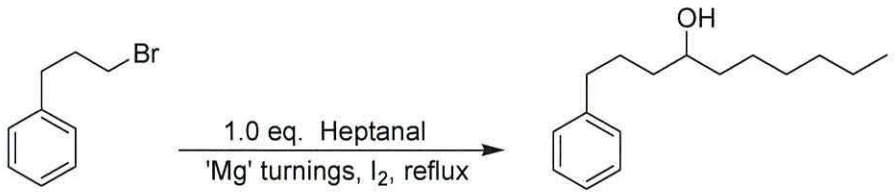

43 **44**

In a three-necked round-bottom flask equipped with a condenser and a positive pressure of nitrogen were placed, dry ether (75 ml), magnesium turnings (0.7 g, 30.0 mmol, 3.0 eq.) and one crystal of iodine. The suspension was warmed up for about 10 minutes until the colour of the iodine disappeared, and then brought to reflux. A solution of 3-bromopropyl benzene **43** (2.0 g, 10.0 mmol, 1.0 eq.) dissolved in dry ether (30 ml) was added dropwise maintaining reflux for 2h further. Heptanal (1.1 g, 10.0 mmol, 1.0 eq.) dissolved in dry ether (50 ml) was added dropwise keeping gentle reflux. The solution was refluxed for further 2h, then cooled down to room temperature and poured over a mixture of ice (20 g) and concentrated hydrochloric acid (10 ml). The organic layer was separated and the aqueous layer was extracted with ether (3 x 100 ml). The combined organic layers were washed with aqueous sodium bicarbonate solution (2 x 20 ml, 5 %) and water (20 ml), dried over magnesium sulphate and concentrated in the rotary evaporator to give light yellow oil. This oil was absorbed onto silica gel and purified by column chromatography eluting with petrol/ether 50:50 to afford the *title compound* **44** as a colourless oil (1.8 g, 7.7 mmol, 77 %); bp 128-130 °C at 0.7 mmHg; R_f values: petrol 100 % (0.02), petrol/ether 90:10 (0.17), petrol/ether 90:20 (0.33), petrol/ether 50:50 (0.63); Found: C, 80.88, H, 11.34; $C_{19}H_{20}O$ requires C, 81.99, H, 11.18 %; ν_{max} cm^{-1} 3350, 2929, 2856, 1496, 747, 698; δ_H 7.08 (2H, m), 6.98 (3H, m), 3.39 (1H, m), 2.44 (2H, m), 1.59 (1H, m), 1.52 (1H, s, -OH), 1.46 (1H, m), 1.27 (4H, m), 1.10 (8H, m), 0.71 (3H, t, *J* 6.9); δ_C 142.3, 128.2, 128.1, 125.5, 71.5, 37.3, 36.8, 35.7, 31.7, 29.2, 27.3, 25.4, 22.4, 13.9; m/z 234 (2 %), 216 (5), 131 (10), 104 (100), 91 (30), 55 (15). GCMS (Rt = 13.85 min.) 216 (9 %), 147 (3), 131 (18), 104 (100), 91 (31), 77 (4), 55 (12).

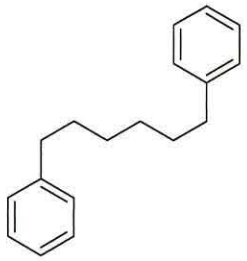

46

The diaromatic **46** was obtained as a colourless oil; bp 344-347 °C (lit.,[202] 346 °C); R_f values: petrol 100 % (0.21) (eluted with this mixture); petrol/ether 90:10 (0.64); petrol/ether 50:50 (0.95); bp 345-347 °C at 760 mmHg (lit,. 346 °C at 760 mmHg); δ_H 7.41 (4H, m), 7.32 (6H, m), 2.74 (4H, m), 1.76 (4H, m), 1.52 (4H, m); δ_C 142.9, 128.7 (x2 carbons), 125.9 (x2 carbons), 125.9, 36.1, 31.6, 29.2; HRMS-EI (calculated m/z 238.1723; required m/z 238.1722) m/z 238 (5 %), 201 (8), 116 (2), 105 (3), 92 (41), 91 (100), 65 (2); GCMS (Rt = 14.67 min.) 238 (45 %), 144 (8), 117 (7) 104 (12), 91 (100), 77 (6).

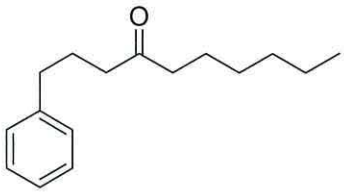

45

Carbonyl derivative **45** was obtained as a colourless oil; R_f values: petrol 100 % (0.07); petrol/ether 90:10 (0.57) (eluted with this mixture); petrol/ether 90:20 (0.72); petrol/ether 50:50 (0.88); ν_{max} cm^{-1} 3026, 3026, 2929, 2857, 1713, 1454, 1372, 746, 699; δ_H 7.10 (2H, m), 6.90 (3H, m), 2.44 (2H, t, *J* 7.6), 2.21 (2H, t, *J* 7.3), 2.17 (2H, t, *J* 7.3), 1.72 (2H, p, *J* 7.3), 1.35 (2H, t, *J* 7.0), 1.10 (6H, m), 0.70 (3H, t, *J* 6.5); δ_C 210.8, 141.5, 128.3, 128.2, 125.7, 42.7, 41.6, 34.9, 31.4, 28.7, 25.0, 23.6, 22.3, 13.8; HRMS-EI (calculated m/z 232.1854; required m/z 232.1827) m/z 232 (2 %), 230 (7), 214 (32), 147 (15), 141 (5), 128 (3), 113 (7), 104 (21), 91 (40), 85 (48), 77 (51), 71 (77), 58 (100); GCMS (Rt = 13.64 min.) 232 (2 %), 214(2), 104 (100), 91 (50), 58 (23).

Synthesis of (4-Bromo-decyl)-benzene (47)

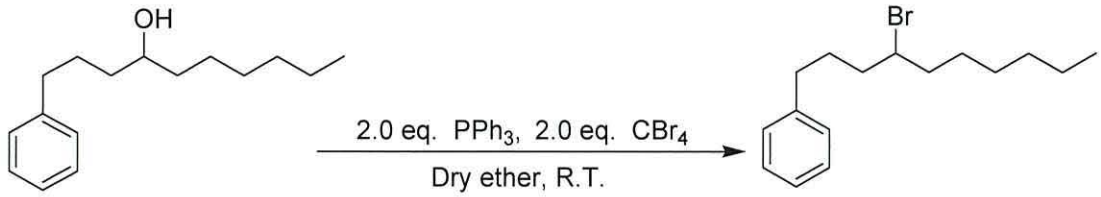

44 **47**

In a three-necked round-bottom flask, 1-phenyl-decan-4-ol **44** (1.0 g, 4.3 mmol, 1.0 eq.), along with carbon tetrabromide (2.8 g, 8.5 mmol, 2.0 eq.), was dissolved in dry diethylether (50 ml). Triphenylphosphine (2.2 g, 8.5 mmol, 2.0 eq.) was added portion-wise, and the formation of a white precipitate was observed. After 1h of stirring, the resulting suspension was filtered to separate triphenylphosphine oxide and the solution was concentrated under reduced pressure. The resulting mixture was filtered through a silica pad, eluting with pure petroleum spirit. The final solution was concentrated to give a colourless liquid. This liquid was further purified from traces of bromoform and carbon tetrabromide by distillation to afford the *title compound* **47** as a colourless liquid (1.2 g, 4.0 mmol, 95 %) bp 125-127 °C at 0.3 mmHg; R_f value petrol 100 % (0.51); ν_{max} cm^{-1} 3026, 2928, 2857, 1942, 1869, 1802, 1745, 1454, 784, 698; δ_H 7.29 (5H, m), 4.10 (1H, m), 2.68 (2H, m), 1.66 (14H, m), 0.91 (3H, m); δ_C 142.0, 128.4, 125.9, 58.6, 39.2, 38.7, 35.3, 31.7, 29.2, 28.8, 27.6, 22.7, 14.4; HRMS-EI (calculated m/z 298.1121/296.1128; required m/z 298.1121/296.1140) m/z 296 (15 %), 216 (82), 131 (100), 117 (65), 105 (69), 92 (62), 841 (60), 69 (49), 55 (42). Molecular peak is at 296 (100) and 298 (100) indicative of Br; GCMS (Rt = 14.55 min.) 296 (4 %), 216 (13), 147 (3), 131 (18), 117 (11), 104 (50), 91 (100), 77 (4), 55 (12).

Synthesis of 1-(4-Bromo-decyl)-4-nitro-benzene (48)

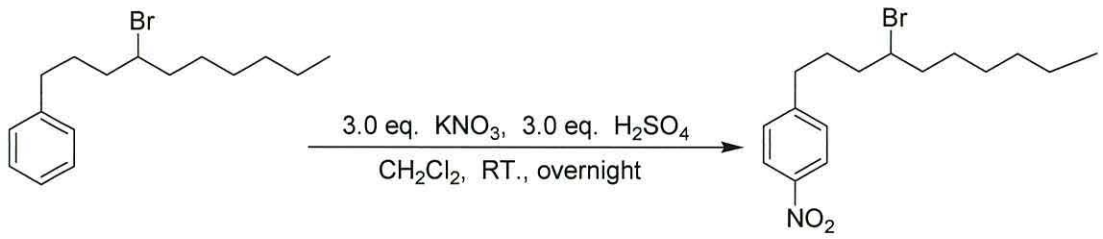

47 **48**

(4-Bromo-decyl)-benzene **47** (1.0 g, 3.4 mmol, 1.0 eq.) was dissolved in dry dichloromethane (50 ml) in a three-necked round-bottom flask along with potassium nitrate (1.2 g, 12.0 mmol, 3.0 eq.) under nitrogen. The suspension was cooled down to 0 °C using an ice/salt bath. Sulphuric acid (2.2 g, 22.0 mmol, 3.0 eq.) was added dropwise and the solution was stirred for 3h. The resulting mixture was extracted with dichloromethane (100 ml), washed with saturated sodium bicarbonate solution until gas evolution ceased, washed with water to eliminate the remaining traces of acid, dried over magnesium sulphate and evaporated to give a yellow oil which was a mixture of *ortho*- **49** and *para*-nitro-product **48** (0.9 g, 2.6 mmol, 78 %). This oil was absorbed onto silica gel and purified by column chromatography eluting with petrol/ether 95:5 to afford the *title compound* **48** as a yellow oil. The same procedure had been done before using one equivalent of nitrating agent, but the yield of the reaction was very poor, and mostly starting material was recovered.

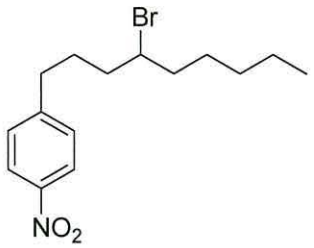

48

The *para*-isomer **48** was recovered as a light yellow oil (0.5 g, 1.6 mmol, 48 %); R_f values: petrol 100 % (0.00); petrol/ether 95:4 (0.32); petrol/ether 50:50 (0.88); ν_{max} cm^{-1} 2929, 2857, 1604, 1520, 1345, 735; δ_H 8.16 (2H, d, *J* 8.5), 7.36 (2H, d,

J 8.5), 4.04 (1H, m), 2.77 (2H, m), 1.96 (2H, m), 1.83 (4H, m), 1.53 (1H, m), 1.40 (1H, m), 1.30 (6H, m), 0.89 (3H, t, *J* 6.8); δ_C 149.82, 131.8, 129.2, 123.6, 51.94, 39.2, 38.4, 35.1, 31.9, 29.4, 29.3, 22.6, 27.5, 13.9; HRLCS-EI (calculated m/z 366.0832/364.0848, M + Na^+; required m/z 366.0801/364.0883, M + Na^+) m/z (364.0848 and 366.0832, M + Na^+); GCMS (Rt = 20.60 min.) 262 (58 %), 244 (7), 216 (20), 192 (33), 178 (29), 164 (32), 149 (100), 137 (88), 117 (27), 106 (25), 91 (38), 78 (34), 55 (62).

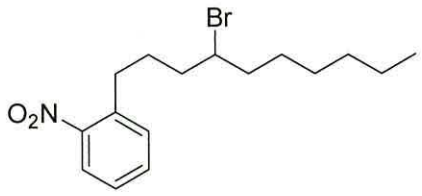

49

The *ortho*-isomer **49** was recovered as a yellow oil (0.4 g, 1.1 mmol, 30 %) R_f values: petrol 100 % (0.00); petrol/ether 95:4 (0.41); petrol/ether 50:50 (0.88); δ_H 7.65 (1H, dd, *J* 8.2, *J* 0.95), 7.28 (1H, ddd, *J* 7.6, *J* 7.3, *J* 1.3), 7.11 (2H, m), 3.81 (1H, m), 2.66 (2H, m), 1.67 (3H, m), 1.56 (3H, m), 1.28 (1H, m), 1.18 (1H, m), 1.05 (6H, m), 0.65 (3H, t, *J* 6.9); δ_C 149.1, 136.7, 132.7, 131.5, 126.8, 57.8, 38.9, 38.6, 32.0, 31.4, 28.4 (x2 carbons), 27.3, 22.3, 13.8; m/z (364.0848 and 366.0832, M + Na^+); GCMS (Rt = 18.36 min.) 341 8 (2 %), 326 (68), 262 (48 %), 244 (72), 226 (40), 216 (30), 178 (29), 160 (42), 146 (100), 132 (98), 119 (98), 106 (45), 91 (90), 77 (74), 55 (100).

Synthesis of 4-(4-Bromo-decyl)-phenylamine (50)

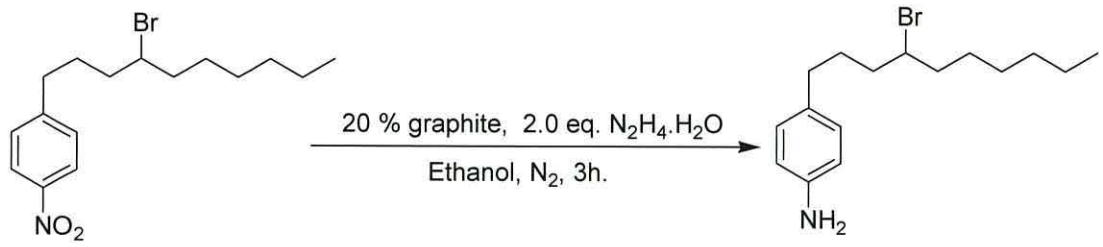

48 **50**

1-(4-Bromo-decyl)-4-nitro-benzene **48** (3.4 g, 10 mmol, 1.0 eq.) was dissolved in absolute ethanol (100 ml) in a three-necked round-bottom flask equipped with a condenser under nitrogen. To this solution, hydrazine monohydrate (1.0 g, 20 mmol, 2.0 eq.) and graphite (3.0 g, 10 %) were added and the mixture brought to reflux for 2h. The reaction mixture was cooled down to room temperature, filtered and washed with absolute ethanol (100 ml). The organic solvent was evaporated to give an orange/yellow oil. This oil was purified by column chromatography using neutral alumina and eluting with petroleum spirit/ether 50:50 to afford the *title compound* **50** as a yellow oil (2.3 g, 7 mmol, 72 %) R_f values: petrol 100 % (0.00); petrol/ether 50:50 (0.61); ν_{max} cm^{-1} 3364, 3216, 2927, 2855, 1621, 1516, 1458, 1275, 822, 749; δ_H 7.00 (2H, d, *J* 8.2), 6.66 (2H, d, *J* 8.2), 4.07 (1H, m), 3.56 (2H, bs, $-NH_2$), 2.55 (2H, m), 1.85 (4H, m), 1.73 (1H, m), 1.53 (1H, m), 1.42 (1H, m), 1.33 (7H, m), 0.92 (3H, t, *J* 6.9); δ_C 144.1, 132.2, 129.2, 115.4, 58.7, 39.2, 38.6, 34.4, 31.7, 29.5, 28.7, 27.5, 22.6, 14.1; HRLCS-EI (calculated m/z 314.1318/312.1332, $M + H^+$; required m/z 314.1302/312.1321, $M + H^+$) m/z (312.1332 and 314.1318, $(M + H^+)$; GCMS (Rt = 21.07 min.) 231 (100 %), 146 (11), 132 (12), 119 (21), 106 (100), 77 (9), 55 (5).

Synthesis of 1-bromo-(4-bromo-decyl)-phenyl amine (51)

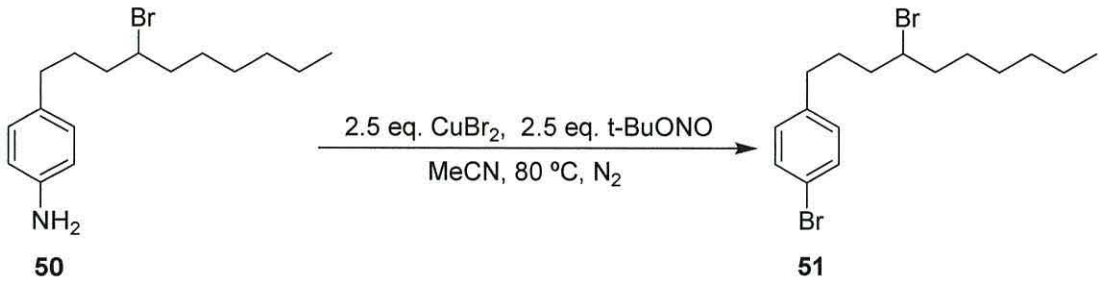

50 **51**

A solution of 4-(4-bromo-decyl)-phenyl amine **50** (1.0 g, 3 mmol, 1.0 eq.) in acetonitrile (20 ml) was added dropwise to a suspension of copper (II) bromide (1.8 g, 8 mmol, 2.5 eq.) and tert-butyl nitrite (0.8 g, 8 mmol, 2.5 eq.) in dry acetonitrile (200 ml) at 50-60 °C in a two-necked round-bottom flask under a positive pressure of nitrogen. The mixture was stirred at reflux for 30 min. until all gas evolution had ceased. It was cooled down to room temperature and poured over an aqueous hydrochloric acid solution (100 ml, 20 %). It was extracted with ether (2 x 100 ml), washed with aqueous sodium bicarbonate solution (100 ml, 10 %), washed with water (50 ml), dried over magnesium sulphate and evaporated under reduced pressure. The resulting oil was absorbed onto silica gel and purified by column chromatography, eluting with pure petrol, to afford the *title compound* **51** as a yellow oil (0.8 g, 2 mmol, 62 %) R_f value: petrol 100 % (0.75); ν_{max} cm^{-1} 2925, 2853, 1536, 1462, 1386, 1013, 1111, 813, 740; δ_H 7.52 (2H, d, *J* 8.2), 7.01 (2H, d, *J* 8.2), 3.10 (1H, m), 2.55 (2H, m), 1.62 (4H, m), 1.34 (10H, m), 0.92 (3H, t, *J* 6.9); δ_C 142.5, 131.3, 126.8, 56.7, 37.2, 36.7, 34.2, 31.5, 29.2, 27.9, 27.7, 21.6, 13.6; GCMS (Rt = 23.80 min.) 376 (14 %), 294 (3), 211 (8), 182 (48), 171 (100), 104 (10), 90 (21), 55 (19).

Synthesis of 4-benzoylbutyric acid (63)

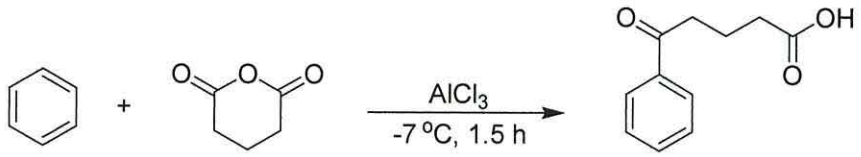

61 **62** **63**

A suspension of aluminium chloride (29.2 g, 220 mmol, 2.5 eq.) was prepared as a solution in benzene **61** (25 ml) and then cooled to -7 °C with an ice-salt bath. A solution of glutaric anhydride **62** (10.0 g, 88 mmol, 1.0 eq.) in benzene (29 ml) was added slowly over ten minutes, and the mixture was then stirred for 1.5h, maintaining the temperature at -7 °C. After this time, water (50 ml) was added dropwise, followed by hydrochloric acid (15 ml). The excess solvent was removed under reduced pressure and the resulting yellow precipitate was dissolved in a aqueous saturated sodium carbonate solution (50 ml) and the impurities removed by filtration. Following filtration, the solution was decolourised with activated charcoal, and reacidified with concentrated hydrochloric acid to afford the *title compound* **63** as a white solid (15.5 g, 81 mmol, 92 %) mp 122-124 °C (lit.,[145] 123-125 °C); ν_{max} cm^{-1} 3500, 2850, 1691, 1673, 1453, 1377, 1291, 735, 691; δ_H 7.97 (2H, d, *J* 7.3), 7.58 (1H, t, *J* 7.3), 7.47 (2H, t, *J* 7.3), 3.09 (2H, t, *J* 7.2), 2.52 (2H, t, *J* 7.2), 2.10 (2H, p, *J* 7.2); δ_C 199.4, 179.1, 136.7, 133.1, 128.6, 127.9, 37.3, 33.0, 18.9.

Synthesis of 5-phenylvaleric acid (64)

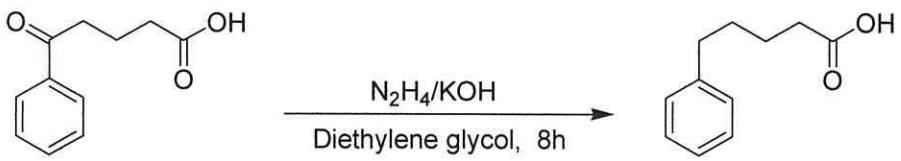

63 **64**

In a three-necked round-bottom flask, equipped with a condenser and thermometer, γ-benzoylbutyric acid **63** (15.0 g, 0.1 mol, 1.0 eq.), along with hydrazine monohydrate (12.5 g, 0.4 mol, 5.0 eq.) and potassium hydroxide (17.5 g, 0.3 mol, 4.0 eq), was dissolved in diethylene glycol (100 ml) and heated at reflux (140 °C) for 3h. After this time, the excess hydrazine and water were removed by distillation and the temperature of the mixture was then raised to 180 °C and refluxed for a further 7h. The mixture was then cooled to room temperature. Water (50 ml) was added and the solution was decolourised with activated charcoal and filtered. Afterwards, hydrochloric acid (4N) was added until the solution became acid to afford the *title compound* **64** as colourless crystals (9.8 g, 0.1 mol, 71 %) mp 57-59 °C (lit.,[203] 58-62 °C); ν_{max} cm^{-1} 2916, 1711, 1462, 1376, 1315, 1254, 928, 749, 699; δ_H 7.30 (2H, m), 7.21 (3H, m), 2.66 (2H, m), 2.41 (2H, m), 1.70 (4H, m); δ_C 180.4, 142.0, 128.4, 128.3, 125.8, 35.6, 33.9, 30.8, 24.3.

Synthesis of 5-phenylvaleric acid methyl ester (65)

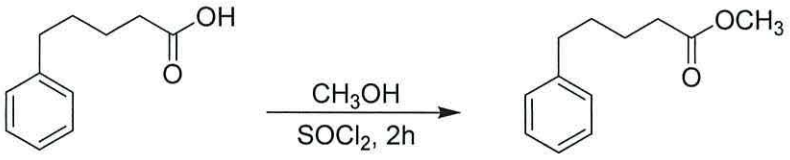

64 **65**

Dry methanol (75 ml) was placed in a three-necked round-bottom flask under a nitrogen atmosphere. Thionyl chloride (9.3 g, 80 mmol, 2.0 eq.) was added dropwise at room temperature and allowed to stir for *ca.* 25 minutes. After this time, 5-phenylvaleric acid **64** (7.0 g, 40 mmol, 1.0 eq.) was added and the mixture was stirred further for 2h. The excess solvent was then evaporated under high vacuum and the residue dissolved in dichloromethane, dried over magnesium sulphate and evaporated again to afford the *title compound* **65** as an orange oil (7.4 g, 39 mmol, 98 %) bp 108 °C at 2 mmHg (lit.,[204] 110 °C at 2 mmHg); ν_{max} cm^{-1} 3025, 2946, 2858, 1947, 1738, 1603, 1496, 1439, 1361, 1199, 1085, 846, 749, 699; δ_H 7.28 (2H, m),

7.20 (3H, m), 3.69 (3H, s), 2.65 (2H, t, *J* 7.0), 2.36 (2H, t, *J* 7.0), 1.68 (4H, t, *J* 3.7); δ_C 174.0, 142.1, 128.4, 128.3, 125.8, 51.5, 35.6, 33.9, 30.9, 24.6.

Synthesis of 3-[4-5-valerianyloxymethyl)-benzoyl]-propionic acid (67)

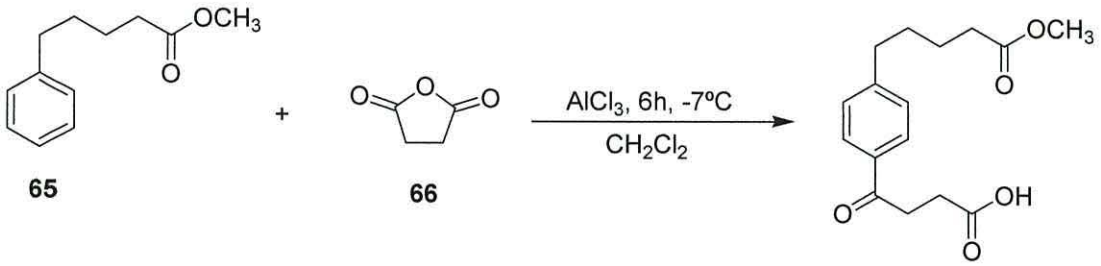

65 **66** **67**

5-Phenylvaleric acid methyl ester **65** (4.0 g, 21 mmol, 1.0 eq.) and succinic anhydride **66** (2.1 g, 21 mmol, 1.0 eq.) were dissolved in dry dichloromethane (100 ml) in a three-necked round-bottom flask and the solution was cooled to -7 °C using an salt ice bath. Aluminum chloride (8.3 g, 63 mmol, 3.0 eq.) was added in small portions over 2h, maintaining the temperature below 0 °C. The mixture was then stirred for a further 4h. The reaction mixture was poured cautiously over a beaker containing ice (160 g), while agitating vigorously. The resulting opaque solution was extracted with a portion of diethyl ether (50 ml) and dichloromethane (50 ml). The combined organic layers were dried over magnesium sulphate and the solvent was evaporated with a high vacuum pump to afford the *title compound* **67** as a white solid (5.8 g, 19 mmol, 95 %) mp 98-100 °C (lit.,[68] 98-100 °C); δ_H 9.81 (1H, s), 7.91 (2H, d, *J* 8.2), 7.27 (2H, d, *J* 8.2), 3.64 (3H, s), 3.27 (2H, t, *J* 6.6), 2.77 (2H, t, *J* 6.6), 2.66 (2H, t, *J* 5.5), 2.33 (2H, t, *J* 7.0), 1.65 (4H, dt, *J* 7.0, *J* 3.5); δ_C 199.0, 180.0, 175.5, 149.7, 135.7, 130.1, 129.7, 53.1, 37.0, 35.3, 34.5, 31.9, 29.5, 25.9.

Synthesis of methyl δ-(4-γ-Butyric Acid)-phenylvalerate (68)

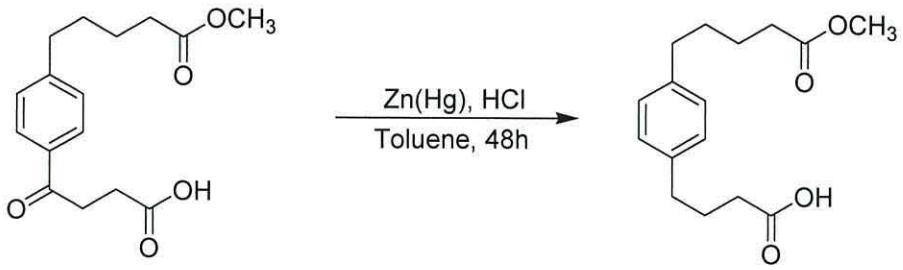

67 **68**

Amalgamated zinc was prepared *in situ* as follows: Zinc (8.8 g) and mercury chloride (0.7 g) were dissolved in water (12.0 ml) and hydrochloric acid (0.5 ml). The excess water was decanted and the amalgamated zinc covered with hydrochloric acid (12.7 ml). To this freshly-prepared amalgamated zinc was added 5-phenyl-valeric acid methyl ester **67** (6.2 g, 21 mmol) dissolved in toluene (150 ml). The mixture was then stirred at reflux for 48h, during which more hydrochloric acid (3.8 ml) was added every ten h. Afterwards, the reaction was cooled down to room temperature and the aqueous layer was extracted with two portions of diethyl ether (100 ml). The combined organic layers were dried over magnesium sulphate and the solvent evaporated under reduce pressure to afford the *title compound* **68** as a dark orange/brown solid (4.6 g, 16 mmol, 78 %) mp 79-80 °C (lit.,[76] 79-80 °C); δ_H 7.11 (4H, s), 3.68 (3H, s), 2.65 (4H, m), 2.37 (4H, m), 1.96 (2H, m), 1.68 (4H, m).

Synthesis of 5-[4-(3-methoxycarbonyl-propyl)-phenyl]-valeric acid methyl ester (70)

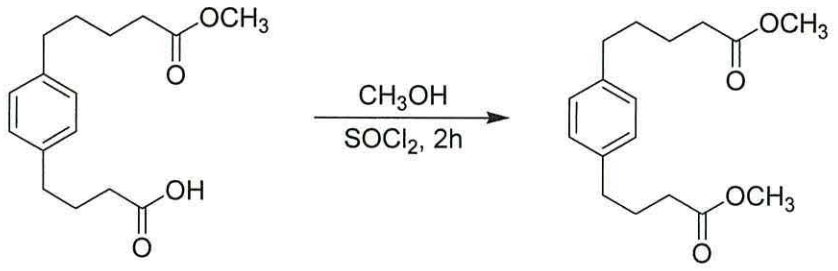

68 **70**

Dry methanol (75 ml) was placed in a three-necked round-bottom flask under nitrogen atmosphere. To this, thionyl chloride (4.6 g, 39 mmol, 2.0 eq.) was added dropwise at room temperature and allowed to stir for *ca.* 25 minutes. After this time, 5-phenylvaleric acid **68** (6.0 g, 22 mmol, 1.0 eq.) was added and the mixture was stirred for a further 2h. The excess solvent was then evaporated under high vacuum, the residue was dissolved in dichloromethane (100 ml), dried over magnesium sulphate and evaporated to afford the *title compound* **70** as an orange oil (6.1 g, 21 mmol, 95 %) 163-169 °C at 0.4 mmHg (lit.,[76] 165-170 °C at 0.4 mmHg); ν_{max} cm^{-1} 2948, 2859, 1738, 1514, 143.6, 1363, 1173, 1040, 797, 770, 692; δ_H 7.10 (4H, s), 3.67 (6H, s), 2.62 (4H, t, *J* 7.5), 2.34 (4H, t, *J* 7.5), 1.95 (2H, p, *J* 7.5), 1.67 (4H, dt, *J* 7.5); δ_C 173.96, 173.87, 139.65, 138.70, 128.39, 128.34, 51.74, 51.37, 35.42, 34.65, 33.85, 33.32, 30.90, 26.51, 24.54. m/*z* 292 (10 %), 260 (31), 229 (31), 186 (48), 158 (12), 130 (32), 117 (100), 91 (30), 74 (23), 59 (29).

Synthesis of 5,6-OTrimethylsilyl-bicyclo[9.2.2]pentadeca-1(14),5,11(15),12-tetraene (71)

70 **71**

Dry and degassed xylene (200 ml) was placed in a three-necked round-bottom flask under an argon atmosphere. Sodium metal (0.7 g, 30 mmol, 4.2 eq.) was added into the flask portion-wise. The solution was heated under reflux and stirred at full power using a mechanical stirrer until all the sodium was dispersed, for about 30 minutes. After this time, the solution was cooled down to room temperature, maintaining the stirring. Then, the mechanical stirrer was replaced by a powerful magnetic stirrer, and an addition funnel containing a dry, degassed solution of 5-[4-(3-methoxycarbonyl-propyl)-phenyl]-valeric acid methyl ester **70** (2.0 g, 7 mmol, 1.0 eq.) and TMSCl (3.1 g, 30 mmol, 4.2 eq.) in xylene was inserted onto the round-bottom flask and argon was bubbled through the solution to maintain an inert argon atmosphere. The solution was heated under reflux whilst adding the solution containing the methyl ester and TMSCl dropwise over 2h. A purple colour was observed after a few minutes, but faded later. The mixture was stirred for a further 6h. Then, the solution was filtered and the residue washed with diethyl ether. The solvent was evaporated under reduced pressure, and the xylene was distilled to afford the *title compound* **71** as the product (0.1 g, 4 mmol, 5 %) ν_{max} cm^{-1} 2923, 1613, 1454, 1250, 1095, 843, 796, 768, 691 (m); δ_H 7.09 (4H, s), 3.80 (4H, m), 2.81 (4H, m), 1.83 (2H, m), 1.64 (4H, m), 0.35 (18H, s); δ_C 137.86, 134.77, 130.07, 129.08, 128.32, 126.23, 62.75, 62.62, 35.75, 35.13, 30.84, 30.60, 25.63, 21.09, 19.87; m/*z* 376 (80 %), 288 (2), 258 (6), 231 (48), 147 (26), 117 (20), 91 (8), 73 (100), 57 (4).

Analysis of bicyclo[9.2.2]pentadeca-1(14),11(15),12-trien-6-ol (109)

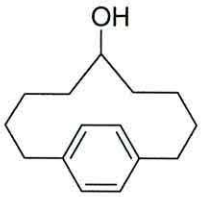

109

A pure sample of paracyclophane derivative **109** was obtained from Sigma Aldrich Rare Chemical Library (20 mg). δ_H 6.90 (4H, m), 2.57 (2H, m), 2.23 (3H, m), 1.44 (2H, m), 1.24 (1H, m), 1.04 (1H, m), 0.91 (3H, m), 0.75 (1H, s, -OH), 0.65 (2H, m), 0.52 (1H, m), 0.16 (1H, m), 0.00 (1H, m); δ_C 140.2 139.8, 130.4, 130.1, 129.4, 128.9, 70.2, 35.3, 35.0, 34.2, 31.9, 29.7, 25.8, 23.8, 23.2; GCMS (Rt = 13.5 min.) 218 (36 %), 200 (15), 189 (10), 171 (21), 157 (19), 144 (24), 129 (32), 117 (79), 104 (95), 91 (100), 77 (32), 65 (19), 57 (33).

Reaction of 5-[4-(3-methoxycarbonyl-propyl)-phenyl]-valeric acid methyl ester (70) with DIBAL

DIBAL (7.6 ml, 7.6 mmol, 2.2 eq.) was added dropwise to a stirred solution of 5-[4-(3-methoxycarbonyl-propyl)-phenyl]-valeric acid methyl ester **70** (1.0 g, 3.4 mmol, 1.0 eq.) in dry THF (100 ml) at -78 °C. The stirring was maintained for 1h at -78 °C. After this time, methanol (20 ml) and a saturated sodium carbonate solution (20 ml) were added successively. The mixture was extracted with diethyl ether (2 x 100 ml), dried over magnesium sulphate, filtered and the solvent removed under reduced pressure to give a yellowish oil. This oil was absorbed onto silica and purified by chromatography column to give two main fractions, eluting with petrol/ether (80:20), R_f = 0.85 and R_f = 0.70. The same procedure was repeated changing the reaction times to 20 minutes and 3h with no change (0.2 g, 0.9 mmol, 28 %); δ_H 9.72 (1H, s), 7.08 (4H, s), 3.64 (3H, s), 2.60 (4H, m), 2.42 (2H, m), 2.31 (2H, t, *J* 7.3), 1.93 (2H,

m), 1.64 (4H, m); GCMS (Rt = 14.35 min., 55.5 %) 262 (7 %), 244 (15), 231 (12), 188 (24), 131 (18), 117 (100), 105 (18), 91 (40); (Rt = 13.69 min., 44.5 %) 232 (3 %), 214 (12), 188 (70), 170 (15), 144 (15), 117 (100), 91 (40).

Synthesis of 5-[4-(4-Hydroxy-butyl)-phenyl]-pentan-1-ol (75)

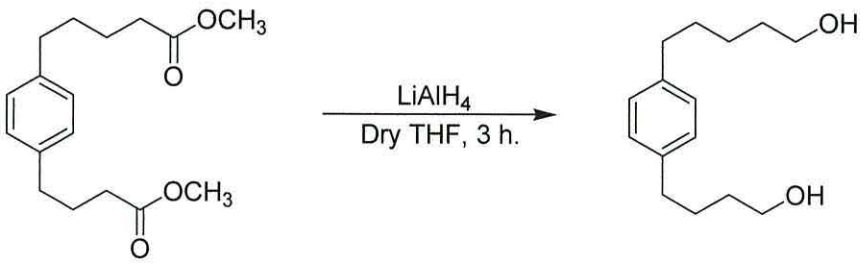

70 **75**

5-[4-(3-Methoxycarbonyl-propyl)-phenyl]-valeric acid methyl ester **70** (5.0 g, 17 mmol, 1.0 eq.) was added portion-wise to a stirred suspension of lithium aluminium hydride (1.4 g, 37 mmol, 2.2 eq.) in dry THF (200 ml). The reaction was stirred at reflux for 3h. The reaction mixture was cooled down to room temperature, then ethyl acetate (20 ml) and a saturated solution of sodium metabisulfite (50 ml) were added consecutively. The mixture was extracted three times with dichloromethane (100 ml), dried over magnesium sulphate, filtered and the solvent evaporated under reduced pressure to give a pale orange oil. This oil was absorbed onto silica and purified by column chromatography. The product was eluted with diethyl ether to afford the *title compound* **75** as an oil (3.6 g, 15 mmol, 91 %) $\nu_{max}(cm^{-1})$ 3349, 2932, 2857, 1720, 1512, 1458, 1265, 1053, 737, 702; δ_H 7.09 (4H, s), 3.50 (4H, m), 2.50 (4H, m), 2.23 (2H, bs, -OH), 1.34 (2H, m), 1.61 (8H, m). δ_C 128.4, 62.7, 62.6, 35.5, 35.2, 32.6, 32.3, 31.3, 27.8, 25.4; GCMS (Rt = 15.73 min.) 236 (6 %), 218 (10), 190 (8), 172 (20), 145 (50), 131 (60), 117 (100), 91 (65).

Synthesis of 5-[4-(4-Oxo-butyl)-phenyl]-pentanal (72)

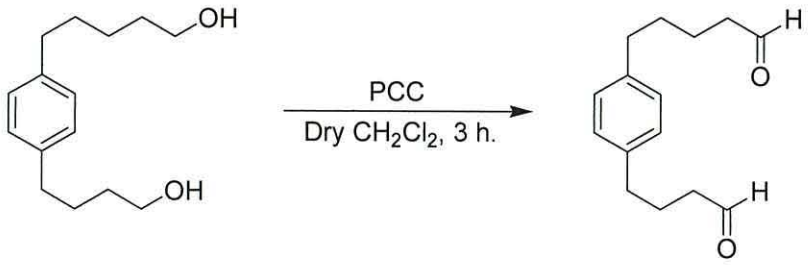

75 **72**

A solution of 5-[4-(4-hydroxy-butyl)-phenyl]-pentan-1-ol **75** (2.0 g, 9 mmol, 1.0 eq.) in dry dichloromethane (50 ml) was added dropwise to a stirred suspension of pyridinium chlorochromate (6.5 g, 30 mmol, 3.5 eq.) and celite (50 g) in dry dichloromethane. After 3h stirring at room temperature, diethyl ether (100 ml) was added to the resulting gum. The solution was decanted and a further two portions of ether (100 ml) were added and subsequently decanted. The organic extract was dried over magnesium sulphate, filtered, and the solvent evaporated to give an oil, which was further purified by a chromatography column eluting with petroleum spirit/diethyl ether 50:50 to afford the *title compound* **72** as an marmalade orange oil (1.4 g, 6 mmol, 70 %); Found: C, 76.50; H, 8.43. $C_{15}H_{20}O_2$ requires C, 77,55; H. 8,68 %; ν_{max} cm^{-1} 2936, 2722, 1723, 1513, 1241, 735; δ_H 9.65 (2H, s), 7.09 (4H, s), 2.62 (4H, m), 2.44 (4H, pt, *J* 6.4, *J* 6.7), 1.94 (2H, p, *J* 7.6), 1.06 (4H, m); δ_C 202.7, 202.4, 139.7, 138.7, 128.4, 43.7, 43.1, 35.2, 34.6, 30.9, 23.7, 21.6; GCMS (Rt = 13.69 min.) 232 (3 %), 214 (12), 188 (70), 170 (15), 144 (15), 117 (100), 91 (40).

Synthesis of 1-hex-5-enyl-4-pent-4-enyl-benzene (78)

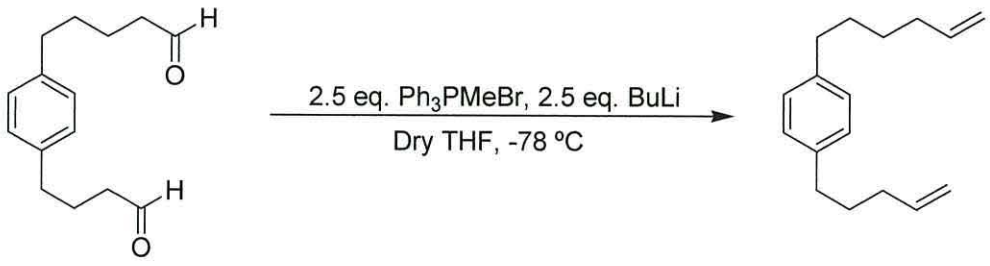

72 **78**

Butyl lithium (10.3 ml, 26.0 mmol, 2.5 eq.) was added dropwise to a stirred suspension of methyl triphenylphosphonium bromide (7.8 g, 26.0 mmol, 2.5 eq.) in dry THF (200 ml) at -78 °C. The resulting mixture was warmed up gradually to room temperature at which point it became a deep orange colour. It was cooled down to -78 °C again, then a solution of 5-[4-(4-oxo-butyl)-phenyl]-pentanal **72** (2.0 g, 8.6 mmol, 1.0 eq.) in dry THF (50 ml) was added dropwise. The reaction mixture was warmed up progressively to room temperature and stirred for 1h longer. After this time, an aqueous solution of ammonium chloride (75 ml) was added. It was extracted with diethyl ether (3 x 100 ml). The organic solvent was dried over magnesium sulphate, filtered and evaporated under reduced pressure to afford the *title compound* **78** as an orange oil (1.2 g, 5.3 mmol, 61 %) δ_H 7.11 (4H, s), 5.87 (2H, m), 5.06 (4H, m), 2.63 (4H, m), 2.12 (4H, m), 1.68 (4H, m), 1.48 (2H, m); δ_C 139.9, 139.7, 138.9, 138.7, 128.4, 128.3, 114.7, 114.4, 35.4, 34.9, 33.7, 33.4, 31.1, 30.7, 28.6; GCMS (Rt = 13.02 min.) 228 (60 %), 215 (10), 199 (8), 186 (9), 172 (10), 154 (12), 143 (30), 130 (80), 117 (100), 105 (40), 91 (50), 69 (40), 55 (60).

Reaction of 5-[4-(4-Oxo-butyl)-phenyl]-pentanal (72) with titanium tetrachloride

A solution of 5-[4-(4-Oxo-butyl)-phenyl]-pentanal **72** (0.3 g, 1.1 mmol, 1.0 eq.) in dry THF (100 ml) was added *via* syringe pump over the period of 36h to a refluxing

solution containing a mixture of titanium tetrachloride (8.6 ml, 8.6 mmol, 8.0 eq.), pyridine (0.1 g, 1.1 mmol, 1.0 eq.) and magnesium (0.2 g, 8.6 mmol, 8.0 eq.) under an argon atmosphere. After the addition was completed, the solution was stirred for further 2h, cooled down to room temperature and then an aqueous solution of potassium carbonate (75 ml) was added. The mixture was extracted with ether and then the solvent was dried over magnesium sulphate, filtered and evaporated under reduced pressure to give an orange oil (0.1 g, 0.5 mmol, 59 %). The crude product was subjected to ^{1}H NMR analysis. δ_H 9.65 (s), 7.09 (s), 5.05 (s), 3.80-3.31 (m), 1.94-1.05 (m); GCMS: High molecular peaks.

Reaction of 1-hex-5-enyl-4-pent-4-enyl-benzene (78) with Grubbs catalyst

1-Hex-5-enyl-4-pent-4-enyl-benzene **78** (0.4 g, 1.8 mmol, 1.0 eq.) was dissolved in dry and degassed dichloromethane (700 ml) under an argon atmosphere in a three-necked round-bottom flask at room temperature. Grubbs catalyst of second generation (20 % w/w) was added to the solution. After stirring for 3h, water (200 ml) was added. The mixture was extracted with dichloromethane (100 ml), dried over magnesium sulphate, filtered and the solvent removed to give a yellowish oil. Note: This reaction was also repeated at reflux; GCMS: (Rt = 13.02 min., 60 %) identified as starting material. (Rt = 15.64 min., 40 %) 234 (12 %), 193 (86), 179 (25), 165 (16), 115 (100), 91 (24).

Reaction of 5-[4-(4-Oxo-butyl)-phenyl]-pentanal (72) with samarium iodide

Active samarium iodide solution was prepared as follows: In dry and degassed THF (300 ml), samarium powder (1.6 g, 11 mmol, 5.0 eq.) and iodine (0.1 g, 0.1 eq.) were stirred at room temperature under argon for ten minutes. A solution of diiodomethane (1.8 g, 7 mmol, 3.1 eq.) in THF (50 ml) was added dropwise over five minutes. The mixture was stirred for 30 minutes (green colour) and then heated at

reflux for 2h to give a deep purple colour (indicative of active samarium iodide). To the fresh samarium iodide solution, HMPA (5.80 g, 30 mmol, 13.6 eq.) was added. A solution of 5-[4-(4-Oxo-butyl)-phenyl]-pentanal **72** (0.5 g, 2 mmol, 1.0 eq.) and *tert*-butanol (0.4 g, 5 mmol, 2.2 eq.) were added dropwise over a period of 2h. The mixture was cooled down to room temperature and a saturated aqueous ammonium chloride solution (100 ml) was added. It was extracted with ether (2 x 100 ml), dried over magnesium sulphate and evaporated to yield a yellow oil (0.2 g, 1 mmol, 50 %). Note: The same procedure was repeated using commercial samarium iodide. It was repeated without HMPA and without *tert*-butanol. Different experiments were tested. Commercially available samarium iodide was used in the first instance. The generation of samarium iodide *in situ* recognised by its distinctive deep purple colour has been proven to be the most effective method. A relatively high dilution of at least $6x10^{-3}$ M was desirable. There was a very little amount of product obtained, and the product with one hydroxyl less, plus the alkene were both identifiable by GCMS. The identified amount was too little material to be isolated. The major products of reaction were: starting material, aldehyde reduced to the dialcohol and ester half reduced to the alcohol.

Synthesis of 2,12-dioxa-bicyclo[11.2.2]heptadeca-1(16),13(17),14-triene (81)

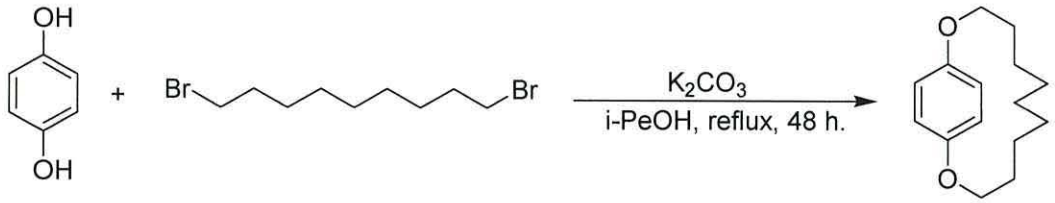

79 **80** **81**

Potassium carbonate (6.3 g, 45 mmol, 5.0 eq.) was suspended in isopentanol (600 ml) under nitrogen and the mixture was brought to reflux. A solution of hydroxyquinone **79** (1.0 g, 9 mmol, 1.0 eq.) and dibromononane **80** (3.1 g, 11 mmol, 1.2 eq.) in isopentanol (100 ml) was added dropwise over a period of 48h. The mixture was cooled down to room temperature, water (200 ml) was added and the

solution was extracted three times with ether (100 ml). The organic phase was washed with sodium hydroxide solution (150 ml, 20 %), washed again with saturated sodium chloride solution (100 ml), dried over magnesium sulphate and evaporated. The resulting white solid was absorbed onto silica and purified by column chromatography. The product was eluted with petrol/ethyl acetate 50:1 to afford the *title compound* **81** as a white solid (0.8 g, 3 mmol, 38 %) mp 56-57 °C (lit.,[149] mp 56 °C); δ_H 6.78 (4H, s), 3.90 (2H, t, *J* 6.4), 3.42 (2H, t, *J* 6.7), 1.86 (2H, m), 1.79 (2H, m), 1.35 (10H, bs); δ_C 150.0, 121.4, 115.9, 115.5, 68.6, 68.5, 34.0, 32.8, 29.5, 29.2, 28.7, 28.6, 28.1, 28.0; GCMS (Rt = 11.71 min.) 234 (22 %), 149 (5), 110 (100), 94 (4), 81 (7), 69 (10), 55 (27).

Synthesis of oxo-paracyclophane (83)

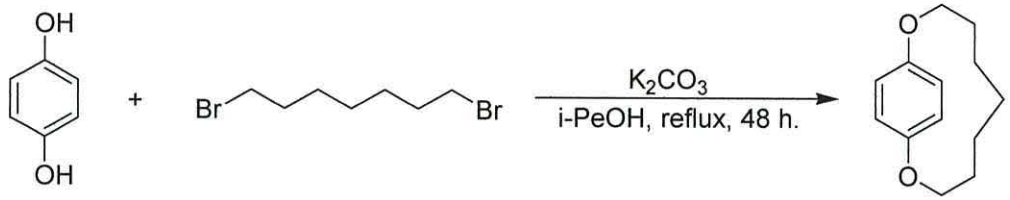

79 **82** **83**

Potassium carbonate (6.3 g, 45.0 mmol, 5.0 eq.) was suspended in isopentanol (600 ml) under nitrogen and it was brought to reflux. A solution of hydroxyquinone **83** (1.0 g, 9.1 mmol, 1.0 eq.) and dibromoheptane **82** (2.3 g, 8.9 mmol, 1.0 eq.) in isopentanol (100 ml) was added dropwise over a period of 48h. The mixture was cooled down to room temperature, water (200 ml) was added and the solution was extracted with ether (3 x 100 ml). The organic phase was washed with sodium hydroxide solution (150 ml, 20 %), washed again with saturated sodium chloride solution (100 ml), dried over magnesium sulphate and evaporated. The resulting white solid was dissolved in dichloromethane, absorbed onto silica gel and purified by column chromatography. The product was eluted with petrol/ethyl acetate 50:1 to afford the *title compound* **83** as a white solid (0.1 g, 0.6 mmol, 7 %); mp 40-41 °C;

δ_H 6.64 (4H, s), 3.84 (4H, t, *J* 3.2), 1.70 (4H, p, *J* 3.2), 1.34 (2H, m), 1.19 (2H, m), 0.81 (2H, m); δ_C 153.2, 115.9, 68.3, 34.0, 32.7, 26.7; GCMS (Rt = 9.81 min.) 207 (82 %), 186 (55), 117 (100), 91 (34).

Synthesis of dimethyl-(5-methyl-furan-2-ylmethyl)-amine (85)

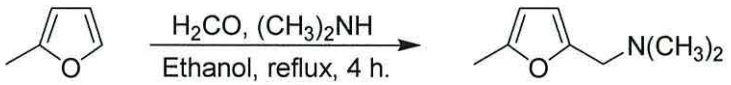

84 **85**

Dimethylamine hydrochloride (59.8 g, 0.7 mol, 1.5 eq.) and paraformaldehyde (22.0 g, 0.7 mol, 1.5 eq.) were suspended in absolute ethanol (200 ml) in a three-necked round-bottom flask equipped with a stirrer and reflux condenser. 2-methyl furan **84** (40.0 g, 0.5 mol, 1.0 eq.) was added and the mixture was stirred at reflux for 4h. After that time, the ethanol was evaporated, leaving a yellow solid as the hydrochloride salt. This solid was neutralised with sodium hydroxide (24 g) dissolved in water (100 ml). The aqueous solution was extracted twice with ether (100 ml), the combined organic layers were dried over magnesium sulphate and evaporated to afford the *title compound* **85** as a colourless liquid (26.7 g, 0.2 mol, 39 %) bp 159-163 °C (lit.,[191] 161-164 °C); ν_{max} cm^{-1} 3346, 3105, 2943, 2858, 2816, 2768, 1567, 1454, 1365, 1221, 1019, 848; δ_H 5.98 (1H, m), 5.79 (1H, m), 3.30 (2H, s), 2.21 (3H, s), 2.18 (6H, s); δ_C 149.8, 148.8, 109.3, 105.8, 54.2, 43.4, 11.8.

Synthesis of trimethyl-(5-methyl-furan-2-ylmethyl)-ammonium iodide (86)

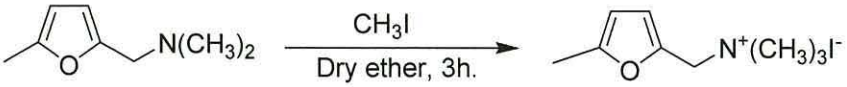

85 **86**

Dimethyl-(5-methyl-furan-2-ylmethyl)-amine **85** (10.0 g, 72 mmol, 1.0 eq.) was dissolved in dry diethyl ether (100 ml) in a two-necked round-bottom flask under nitrogen atmosphere. Methyl iodide (15.3 g, 110 mmol, 1.5 eq.) was added slowly with the instant formation of a yellow precipitate. The mixture was allowed to stir for 3h. After that time, it was filtered, washed with dry ether and dried at 70 °C under vacuum to afford the *title compound* **86** as a yellow solid (19.0 g, 68 mmol, 94 %) mp 159-160 °C (lit.,[205] 161-162 °C); ν_{max} cm^{-1} 2924, 1552, 1463, 1376, 806; δ_H 6.81 (1H, d, *J* 2.8), 5.92 (1H, d, *J* 2.8), 4.83 (2H, s), 3.27 (9H, s), 2.22 (3H, s); δ_C 155.9, 140.4, 118.8, 107.7, 62.4, 53.3, 13.8.

Synthesis of trimethyl-(5-methyl-furan-2-ylmethyl)-ammonium hydroxide (87)

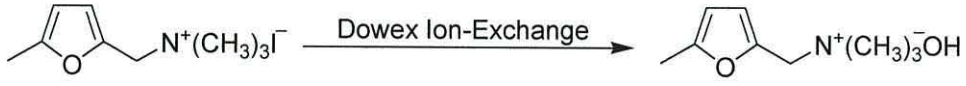

86 **87**

Trimethyl-(5-methyl-furan-2-ylmethyl)-ammonium iodide **86** (20.2 g, 72 mmol, 1.0 eq.) salt was dissolved in the minimum amount of water and passed through a column of DOWEX (200 g). The water was eliminated using a freeze drier to afford the *title compound* **87** as a white powder (7.6 g, 44 mmol, 62 %); ν_{max} cm^{-1} 2924, 1719, 1605, 1555, 1463, 1376, 950, 876, 806; δ_H (DMSO-d_6) 4.96 (1H, bs), 4.92 (1H, bs), 3.31 (9H, s), 3.27 (3H, s), 2.26 (2H, s); δ_C 155.9, 140.4, 118.8, 107.7, 62.4, 53.3, 13.8.

Synthesis of 1-iodomethyl-4-methyl-benzene (89)

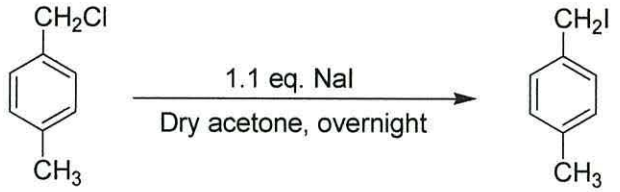

88 **89**

Sodium iodide (47.0 g, 0.3 mol, 1.1 eq.) was dissolved in dry acetone (200 ml) in a two-necked round-bottom flask under a nitrogen atmosphere. α-Chloro-*p*-xylene **88** (40.0 g, 0.3 mol, 1.0 eq.), dissolved in dry acetone (100 ml), was added slowly and the mixture was left stirring overnight. Afterwards, the suspension was filtered to collect the sodium chloride residue as a precipitate. The solution was evaporated to afford the *title compound* **89** as a orange/yellow oil which crystallised upon cooling to room temperature as orange needle crystals (62.5 g, 0.3 mol, 95 %) mp 47-49 °C (lit.,[206] 47-48) °C; ν_{max} cm^{-1} 1612, 1512, 1150, 814, 555, 480; δ_H 7.32 (2H, d, *J* 7.2), 7.12 (2H, d, *J* 7.2), 4.50 (2H, s), 2.38 (3H, s); δ_C 137.4, 136.0, 129.8, 128.6, 65.9, 20.8.

Synthesis of trimethyl-(4-methyl-benzyl)-ammonium iodide (90)

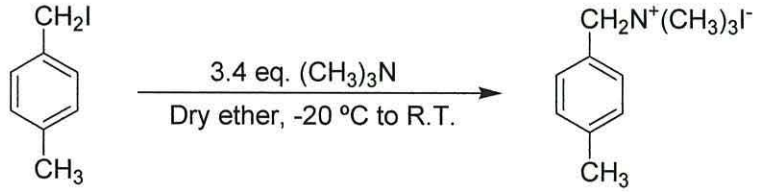

89 **90**

A solution of trimethylamine in dry diethyl ether was prepared as follows: dry ether (100 ml) was placed in a three-necked round-bottom flask under nitrogen atmosphere. The solvent was cooled down to -20 °C using a bath of methylated spirit and liquid nitrogen. Trimethylamine (57.1 g, 1.0 mol, 3.4 eq.) was bubbled into the

solution. To this solution, 1-(iodomethyl)-4-methylbenzene **89** (66.0 g, 0.3 mol, 1.0 eq.) was added dissolved in dry ether (100 ml) over a period of 1h, always maintaining the temperature below 0 °C. The formation of a yellow precipitate was observed almost immediately. The mixture was then allowed to reach room temperature and the excess of trimethylamine was lost by evaporation. The resulting suspension was filtered, washed with dry ether and dried at 70 °C under vacuum to afford the *title compound* **90** as a yellow solid (78.4 g, 0.3 mol, 95 %) mp 202-203 °C (lit.,[207] 210-212 °C); ν_{max} cm^{-1} 3424, 3000, 2972, 1489, 1458, 1382, 984, 930, 890, 817, 753, 450; δ_H 7.46 (2H, d, *J* 7.9), 7.15 (2H, d, *J* 7.9), 4.90 (2H, s), 3.31 (9H, s), 2.29 (3H, s); δ_C 141.2, 132.9, 129.9, 124.2, 65.8, 52.8, 21.3, 15.2.

Synthesis of trimethyl-(4-methyl-benzyl)-ammonium hydroxide (91)

90 **91**

Trimethyl-(4-methyl-benzyl)-ammonium iodide **90** (20.0 g, 69 mmol, 1.0 eq.) was dissolved in the minimum amount of water and passed through a column of DOWEX (200 g). The water was evaporated using a freeze drier to afford the *title compound* **91** as a white powder (6.8 g, 38 mmol, 55 %); ν_{max} cm^{-1} 3392, 2924, 2854, 2360, 1460, 1377; δ_H (DMSO-d_6) 7.41 (2H, d *J* 7.9), 7.17 (2H, d, *J* 7.9), 4.74 (2H, s), 3.80 (1H, s), 3.21 (9H, s), 2.23 (3H, s); δ_C 138.7, 131.1, 127.7, 122.9, 77.3, 68.7, 52.4, 21.2.

Synthesis of 15-oxa-tricyclo[8.2.2.14,7]pentadeca-1(13),4,6,10(14),11-pentaene (92)

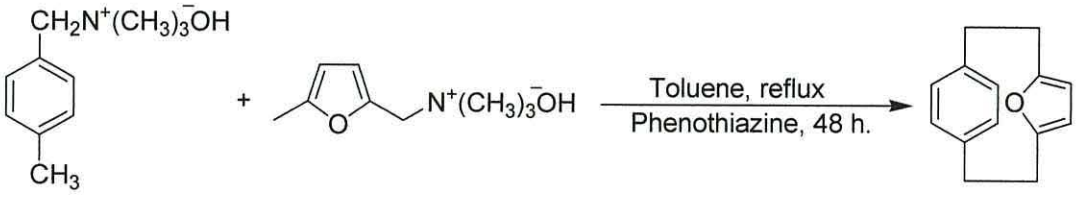

91 **87** **92**

Trimethyl-(4-methyl-benzyl)-ammonium hydroxide **91** (10.1 g, 56 mmol, 1.0 eq.) and trimethyl-(5-methyl-furan-2-ylmethyl)-ammonium hydroxide **87** (9.5 g, 56 mmol, 1.0 eq.) were suspended in toluene (200 ml) into a three-necked round-bottom flask equipped with a condenser and a Dean-Stark apparatus. The solution was brought to reflux and phenothiazine (0.1 g) was also added. After all the water was removed, the Dean-Stark apparatus was dismantled and the mixture was stirred under reflux for further 48h to ensure completion of the reaction. The reaction mixture was then cooled and filtered to remove insoluble polymeric material. The toluene solution was evaporated leaving a purple residue, then extracted with diethyl ether, which was evaporated and the residue purified by column chromatography. The product was collected by eluting with hexane/ether (90:10) to afford the *title compound* **92** as a white solid (1.9 g, 10 mmol, 17 %); R_f = 0.70; mp 67-68 °C (lit.,[150] 67-68 °C); δ_H 6.45 (4H, s), 5.56 (2H, s), 2.82 (4H, t, *J* 6.9), 2.43 (4H, t, *J* 6.9); δ_C 154.7, 133.0, 129.02, 106.7, 36.9, 28.9; GCMS (Rt = 10.12 min.) 198 (55 %), 104 (100), 94 (22), 78 (15), 66 (8).

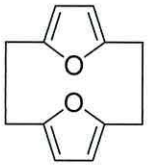

94

Difuran derivative **94** was collected by eluting with ether to give a white solid (1.1 g, 6 mmol, 10 %); R_f = 0.60; mp 188-190 °C (lit.,[151] 189-190 °C); δ_H 4.60 (4H, s), 2.42 (8H, s); δ_C 71.6, 15.4; GCMS (Rt = 8.63 min.) 188 (35%), 94 (100), 77 (5), 66 (12).

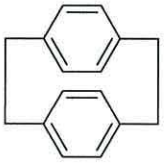

93

Diaromatic derivative **93** was collected by eluting with hexane to give the a white solid (0.9 g, 4 mmol, 8 %); R_f = 0.80; mp 286-287 °C (lit.,[78] 285-287 °C); δ_H 6.45 (8H, s), 2.82 (8H, t, *J* 7.0), 2.43 (4H, t, *J* 7.0); GCMS (Rt = 11.63 min.) 208 (22 %), 104 (100), 89 (3), 78 (12).

Synthesis of bicyclo[8.2.2]tetradeca-1(13),5,10(14),11-tetraene-4,7-dione (95)

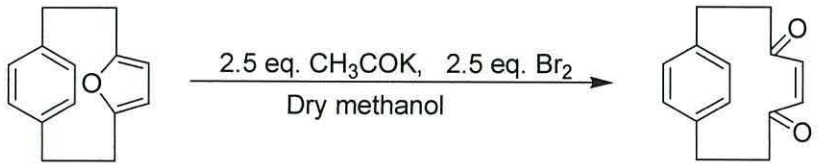

92 **95**

A solution of bromine (2.0 g, 13 mmol, 2.5 eq.) in dry methanol (30 ml) was added to a suspension of 15-oxa-tricyclo[8.2.2.14,7]pentadeca-1(13),4,6,10(14),11-pentaene **92** (1.0 g, 5 mmol, 1.0 eq.) and anhydrous potassium acetate (1.2 g,

13 mmol, 2.5 eq.) in dry methanol at 0 °C over 4h. The mixture was stirred vigorously. A very fine precipitate crashed out from the solution. When addition of bromine was finished, the mixture was added to sulphuric acid (2N) and was left standing for one day. Afterwards, it was extracted with dichloromethane (3 x 200 ml), washed with sodium bicarbonate solution (100 ml, 20 %), then water, and then dried and evaporated. It was recrystallised from methanol to afford the *title compound* **95** as a white powder (0.4 g, 2 mmol, 37 %) mp 160-161 °C (lit.,[150] 162-163 °C); ν_{max} cm^{-1} 2924, 2854, 1693, 1461, 1377, 423; δ_H 7.11 (4H, s), 5.54 (2H, s), 2.94 (4H, t, *J* 6.4), 2.70 (4H, t, *J* 6.4); δ_C 201.1, 137.0, 127.6, 126.9, 43.6, 29.2; HRMS-EI (calculated m/z 214.0994; required m/z 214.0994) m/*z* 214 (38 %), 118 (85), 117 (100), 104 (22), 91 (21), 77 (5); GCMS (Rt = 12.87 min.) 214 (82 %), 117 (100), 104 (24), 91 (33), 78 (15).

Synthesis of 4-iodomethyl-1-methyl-2-nitro-benzene (97)

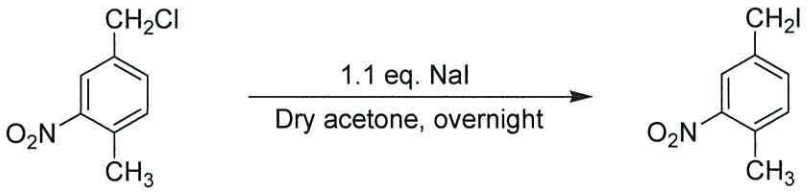

96 **97**

Sodium iodide (22.2 g, 0.2 mol, 1.1 eq.) was dissolved in dry acetone (200 ml) in a two-necked round-bottom flask under nitrogen atmosphere. 4-Chloromethyl-1-methyl-2-nitrobenzene **96** (25.0 g, 0.1 mol, 1.0 eq.), dissolved in dry acetone (100 ml), was added slowly and the mixture was left stirring overnight. Afterwards, the suspension was filtered to collect the sodium chloride residue as a precipitate. The filtrate was evaporated to give a yellowish oil which crystallised upon cooling to room temperature to afford the *title compound* **97** as white needles (28.2 g, 0.1 mol, 76 %) mp 84-85 °C; ν_{max} cm^{-1} 3026, 2362, 1618, 1522, 1489, 1342, 1164, 930, 838, 815; δ_H 8.01 (1H, d, *J* 1.8), 7.53 (1H, dd, *J* 7.9, *J* 1.8), 7.31 (1H, d, *J* 7.9), 4.47 (2H, s), 2.59 (3H, s); δ_C 137.6, 133.4, 133.2, 132.9, 128.7, 124.6, 20.3, 12.8; HRMS-EI

(calculated m/z 276.9612; required m/z 276.9600) m/*z* 276.9612 (52 %), 260 (15), 234 (17), 219 (48), 205 (100), 189 (24).

Synthesis of trimethyl-(4-methyl-3-nitro-benzyl)-ammonium iodide (98)

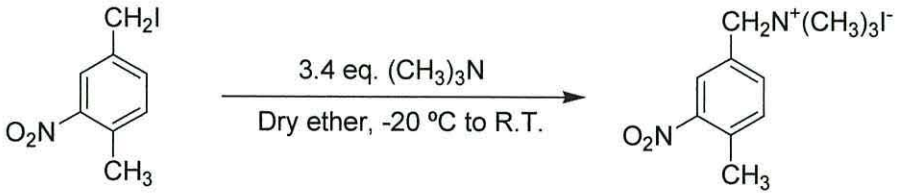

97 **98**

A solution of trimethylamine in dry diethyl ether was prepared as follows: dry ether (100 ml) was placed in a three-necked round-bottom flask under nitrogen atmosphere. The solvent was cooled down to -20 °C using a bath of methylated spirit and liquid nitrogen. Trimethylamine (26.8 g, 0.5 mol, 3.4 eq.) was passed into the solution. To this solution, 4-iodomethyl-1-methyl-2-nitro-benzene **97** (37.0 g, 0.1 mol, 1.0 eq.) was added dissolved in dry ether (100 ml) over a period of 1h, always maintaining the temperature below 0 °C. The formation of a yellow precipitate was observed almost immediately. The mixture was then allowed to reach room temperature, the excess of trimethylamine was lost by evaporation. The resulting suspension was filtered, washed with dry ether and dried at 70 °C under vacuum to afford the *title compound* **98** as a yellow solid (41.2 g, 0.1 mol, 92 %) mp 199-200 °C; ν_{max} cm^{-1} 2999, 2362, 1622, 1529, 1495, 1409, 1352, 915, 884, 847, 820, 743; δ_H (DMSO-d_6) 8.17 (1H, d, *J* 1.6), 7.76 (1H, dd, *J* 7.9, *J* 1.9), 7.63 (1H, d, *J* 7.9), 4.62 (2H, s), 3.02 (9H, s), 2.46 (3H, s); δ_C 148.9, 137.3, 134.9, 133.4, 128.6, 127.6, 66.0, 51.9, 19.5; HRLCS-EI (calculated m/z 209.1285, M-I^-; required m/z 209.1276, M-I^-) m/*z* 209.1285 (M-I^-,100 %).

Synthesis of trimethyl-(4-methyl-3-nitro-benzyl)-ammonium hydroxide (99)

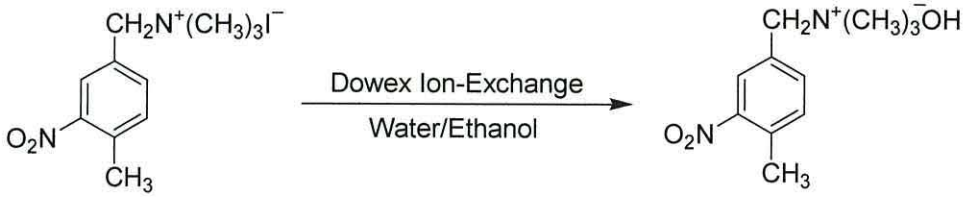

98 **99**

Trimethyl-(4-methyl-3-nitro-benzyl)-ammonium iodide salt **98** (20.0 g, 60 mmol, 1.0 eq.) was dissolved in the minimum amount of water and passed through a column of DOWEX (200 g). The water was eliminated using a freeze drier to afford the *title compound* **99** as a white powder (7.2 g, 32 mmol, 54 %) mp 120-121 °C (decomposes into a polymer); ν_{max} cm^{-1} 3372, 2925, 2854, 1583, 1462, 1376, 1215, 760.

Synthesis of 15-oxa-tricyclo[8.2.2.14,7]pentadeca-1(13),4,6,10(14),11-pentaene (100)

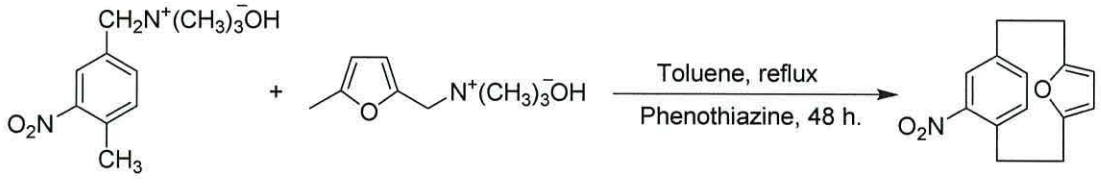

99 **87** **100**

Trimethyl-(4-methyl-3-nitro-benzyl)-ammonium hydroxide **99** (4.2 g, 19 mmol, 1.0 eq.) and trimethyl-(5-methyl-furan-2-ylmethyl)-ammonium hydroxide **87** (3.2 g, 19 mmol, 1.0 eq.) were suspended in toluene (200 ml) into a three-necked round-bottom flask equipped with a condenser and a Dean-and-Stark apparatus. The solution was brought to reflux, and phenothiazine (0.1 g) was also added. After all the water was removed, the Dean-and-Stark apparatus was dismantled and the mixture was stirred at reflux for a further 48h to ensure completion of the reaction.

The reaction mixture was then cooled and filtered to remove the insoluble polymeric material. The toluene solution was evaporated leaving a purple residue, then extracted with diethyl ether (2 x 100 ml), which was evaporated and the residue was purified by column chromatography. The product was collected when eluting with hexane/ether 90:10 to afford the *title compound* **100** as a yellowish solid (0.6 g, 3 mmol, 14 %) mp 276-277 °C; δ_H 7.98 (1H, s), 7.56 (1H, d, *J* 7.3), 7.44 (1H, d, *J* 7.3), 5.36 (2H, s), 2.87 (4H, m), 2.43 (4H, m); δ_C 153.0, 148.7, 137.4, 133.6, 132.3, 128.4, 122.0, 106.7, 36.5, 28.3; GCMS (Rt = 15.24 min.) 243 (33 %), 149 (5), 104 (7), 94 (100), 77 (1).

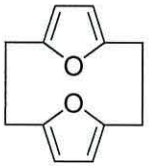

94

Difuran derivative **94** was collected by eluting with ether to give a white solid (0.3 g, 1 mmol, 7 %) mp 188-190 °C (lit.,[151] 189-190 °C); δ_H 4.60 (4H, s), 2.42 (8H, s); δ_C 71.6, 15.4; GCMS (Rt = 8.63 min.) 188 (35 %), 94 (100), 77 (5), 66 (12).

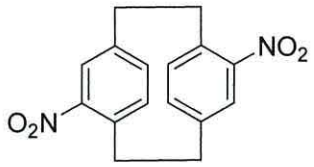

101

Paracyclophane derivative **101** was collected by eluting with hexane/ether 90:10 to give a yellow solid (0.3 g, 1 mmol, 9 %) mp 298-299 °C; δ_H 7.98 (1H, s), 7.52 (4H, m), 2.85 (4H, m), 2.41 (4H, m); δ_C 148.8, 137.7, 134.0, 132.8, 128.5, 123.0, 106.7, 34.5, 27.3; GCMS (Rt = 25.53 min.) 298 (18 %), 104 (100), 89 (3), 78 (12).

Electrochemistry experiments

Experimental set up

All the electrochemical experiments were performed in the three-electrode cell (Figure e.12) using a platinum wire as the working electrode, a platinum net as the counter electrode, and the standard calomel electrode (SCE) as the reference electrode.

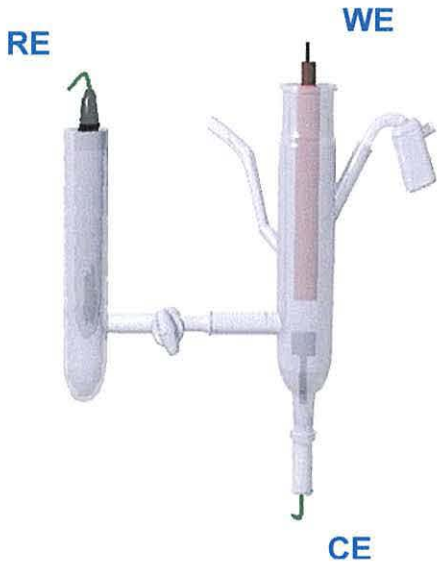

Figure e.12. Schematic diagram of an electrochemical cell. RE (reference electrode), WE (working electrode) and CE (counter electrode).

Tetra-butyl ammonium tetrafluoroborate ($TBABF_4$) (purity > 98 %, AVOCADO Research Chemicals Ltd) was employed as the supporting electrolyte. This was purified by recrystallisation from ethyl acetate and diethyl ether and subsequent drying at 60 °C under high vacuum pump. The electrolyte solution was made up of $TBABF_4$ (0.1 M) in dry dichloromethane. The concentration of the analyte solutions studied was 10 mM. The electrochemical cell was left overnight in an acid bath (mixture 1:1 v/v of concentrated nitric and sulphuric acids), washed with distilled

water, steamed in a vapour bath and dried in the oven. The rest of the glassware employed to make up the solutions were dried from the oven (100 °C) and cooled down to room temperature by blowing nitrogen through it. All measurements were performed using an AUTOLAB ECO CHEMIE IME663.

Experimental procedure

Both the electrochemical cell and the electrodes were rinsed with dry dichloromethane. The electrochemical cell was purged with nitrogen for 30 minutes prior to each experiment (for each analyte and for the electrolyte in order to obtain the background voltammogram).

The working electrode was filled up with analyte solution (10 mM) and the reference was filled up with electrolyte solution (Figure e.12). Each measurement consisted only of one voltammetric cycle. Between each of the measurements, the working electrode was always rinsed with ethanol, flamed and rinsed with dry dichloromethane, flamed again and then introduced into the electrochemical cell. All experiments were performed at room temperature. The data obtained for each experiment are presented in Appendix J.

Competitive studies experiments

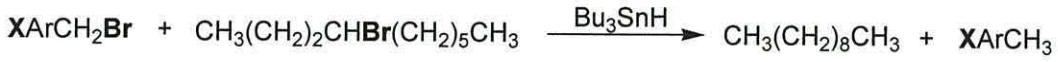

In a typical competitive study experiment, standard solutions of two bromide derivatives and mesitylene were prepared in deuterated chloroform according to the equations listed in Appendix E. For each of the standard solutions, a given volume calculated from the equations listed in Appendix E was pipetted into a NMR tube (one equivalent for each of the analytes). The ^{1}H NMR and the GCMS spectra were both recorded for the resulting mixed solution. Afterwards, one equivalent of *tri*-butyl tin hydride was added along with AIBN (0.1 g). The solution was left standing for 2h. After that time, the ^{1}H NMR and GCMS spectra were recorded again and the spectra analysed. The data thus obtained are presented in Appendix F.

References

1. T. Bugg, *An Introduction to Enzyme and Coenzyme Chemistry*, 1997, Blackwell Science, London.
2. B. C. Gates, *Catalytic Chemistry*, 1992, John Wiley & Sons, New York.
3. R. B. Silverman, *The Organic Chemistry of Enzyme-Catalysed Reactions*, 2000, Academic Press, London.
4. W. Buckel and B. T. Golding, *FEMS. Microbiol. Rev.*, 1999, **22**, 5, 523-541.
5. M. Ormo, K. Regnström, Z. Wang, L. Que, Jr, M. Sahlin and B. M. Sjoberg, *J. Biol. Chem.*, 1995, **270**, 12, 6570-6576.
6. N. Maiti, L. Widjaja and R. Banerjee, *J. Biol. Chem.*, 1999, **274**, 46, 32733-32737.
7. J. T. Jarrett, M. Amaratunga, C. L. Drennan, J. D. Scholten, R. H. Sands, M. L. Ludwig and R. G. Matthews, *Biochemistry*, 1996, **35**, 7, 2464-2475.
8. J. T. Jarrett, C. L. Drennan, M. Amaratunga, J. D. Scholten, M. L. Ludwig and R. G. Matthews, *Bio. Med. Chem.*, 1996, **4**, 8, 1237-1246.
9. A. Becker, K. Fritz-Wolf, W. Kabsch, J. Knappe, S. Schultz and A. F. Volker Wagner, *Nat. Struct. Biol.*, 1999, **6**, 10, 969-975.
10. V.-M. Leppanen, M. C. Merckel, D. L. Ollis, K. K. Wong, J. W. Kozarich and A. Goldman, *Struct. Fold. Des.*, 1999, **7**, 7, 733-744.
11. R. Reitzer, K. Gruber, G. Jogl, U. Wagner, H. Bothe, W. Buckel and C. Kratky, *Struct. Fold. Des.*, 1999, **7**, 8, 891-902.
12. U. Ermler, W. Garabarse, S. Shima, M. Goubeaud and R. K. Thauer, *Science*, 1997, **278**, 5342, 1457-1462.
13. B. Halliwell and J. M. C. Gutteridge, *Free radicals in Biology and Medicine*, 1998, Oxford University Press, Oxford.
14. J. Stubbe and W. A. Van der Donk, *Chem. Rev.*, 1998, **98**, 2, 705-762.
15. J. Stubbe and P. Riggs-Gelaso, *TIBS*, 1998, **23**, 11, 438-443.
16. P. A. Frey, *Annu. Rev. Biochem.*, 2001, **70**, 121-148.
17. R. Banerjee, *Biochemistry*, 2001, **40**, 21, 6191-6196.

18. W. A. Fenton and L. E. Rosenberg, *The metabolic and Molecular Bases of Inhereted Disease*, 1995, Mc Graw Hill, New York.
19. N. H. Thoma, T. W. Meier, P. R. Evans and P. F. Leadly, *Biochem.*, 1998, **37**, 41, 14386-14393.
20. F. Mancia, N. H. Keep, A. Nakagawa, P. F. Leadlay, S. McSweeney, B. Rasmussen, P. Bosecke, O. Diat and P. R. Evans, *Structure*, 1996, **4**, 3, 339-350.
21. A. Jordan and P. Reichard, *Annu. Rev. Biochem.*, 1998, **67**, 71-98.
22. D. T. Logan, J. Andersson, B.-M. Sjoberg and P. Nordlund, *Science*, 1999, **283**, 5407, 1499-1504.
23. E. Elleningand, C. Gerez, M. Knupling, G. Lu, J. Salem, H. Rubin, S. Sauge-Merle, J.-P. Laulhere and M. Fontecave, *Eur. J. Biochem.*, 1998, **258**, 2, 485-490.
24. J. Du Bois, T. J. Mizoguchi and S. J. Lippard, *Coord. Chem. Rev.*, 2000, **200**, 443-485.
25. A. Ehrenberg, *BioSystems*, 2001, **62**, 1, 9-12.
26. A. Becker and W. Kabsch, *J. Biol. Chem.*, 2002, **277**, 42, 40036-40042.
27. A. Gugger, R. Batra, P. Rzadek, G. Rist and B. Giese, *J. Am. Chem. Soc.*, 1997, **119**, 38, 8740-8741.
28. H. A. Headlam, A. Mortimer, C. J. Easton and M. J. Davies, *Chem. Res. Toxicol.*, 2000, **13**, 11, 1087-1095.
29. M. J. Perkins, *Radical chemistry*, 1994, Ellis Horwood Limited, London.
30. N. S. Isaacs, *Reactive Intermediates in Organic Chemistry*, 1973, John Wiley & Sons, London.
31. M. B. Smith and J. March, *Advanced Organic Chemistry*, 2001, John Wiley & Sons, New York.
32. C. J. Moody and G. H. Whitham, *Reactive Intermediates*, 1992, Oxford University Press, Oxford.
33. H. Lund and M. M. Baizer, *Organic Electrochemistry*, 1990, Marcel Dekker, Inc., New York.
34. J. Casanova and L. Eberson, *The Chemistry of the Carbon-Halogen Bond*, 1973, John Wiley and Sons, New York.

35. A. J. Bard and L. R. Faulkner, *Electrochemical Methods: Fundamentals and Applications*, 2000, John Wiley & Sons, New York.
36. P. T. Kissinger and W. R. Heineman, *J. Chem. Educ.*, 1983, **60**, 702.
37. J. Wang, *Analytical Electrochemistry*, 2000, Wiley-Vch, New York.
38. D. e. a. Pletcher, *Instrumental Methods in Electrochemistry*, 1985, Halsted Press, Southampton.
39. A. Charlton, *Electrochemistry*, 1994, University of Wales, Bangor.
40. H. G. Kuivila, *Acc. Chem. Res.*, 1968, **1**, 10, 299-305.
41. A. F. Parsons, *An Introduction to Free Radical Chemistry*, 2000, Blackwell Science, Cambridge.
42. M. L. Poutsma and J. K. Kochi, *Free Radicals*, 1973, John Wiley and Sons, London.
43. D. Griller and K. U. Ingold, *Acc. Chem. Res.*, 1980, **13**, 9, 317-323.
44. J. E. Wertz and J. R. Bolton, *Electron Spin Resonance: Elementary Theory and Practical Applications*, 1986, Chapman and Hall, London.
45. D. C. Nonhebel, J. M. Tedder and J. C. Walton, *Radicals*, 1979, Cambridge University Press, Cambridge.
46. Z. Wen, Z. Li, Z. Shang and J.-P. Cheng, *J. Org. Chem.*, 2001, **66**, 4, 1466-1472.
47. R. Arnaud, A. Grand and R. Subra, *J. Mol. Structure-Theochem*, 1993, **283**, 1, 101-109.
48. G. Leroy, *J. Mol. Structure-Theochem*, 1985, **120**, 1, 91-106.
49. D. J. Pasto, *J. Am. Chem. Soc.*, 1988, **110**, 24, 8164-8175.
50. R. L. Blankespoor, R. L. De Jong, R. Dykstra, D. A. Hamstra, D. B. Rozema, D. P. Van Meurs and P. Vink, *J. Am. Chem. Soc.*, 1991, **113**, 9, 3507-3513.
51. D. J. R. Brook, R. C. Haltiwanger and T. H. Koch, *J. Am. Chem. Soc.*, 1991, **113**, 15, 5910-5911.
52. M. Negareche, Y. Badrudin, Y. Berchadsky, A. Friedmann and P. Tordo, *J. Org. Chem.*, 1986, **51**, 3, 342-346.
53. H. Minoux and C. Chipot, *J. Am. Chem. Soc.*, 1999, **121**, 44, 10366-10372.
54. S. K. Burley and G. A. Petsko, *FEBS. Lett*, 1986, **203**, 2, 139-143.
55. J. C. Ma and D. A. Dougherty, *Chem. Rev.*, 1997, **97**, 5, 1303-1324.

56. J. Sunner, K. Nishizawa and K. Kebarle, *J. Phys. Chem.*, 1981, **85**, 13, 1814-1820.

57. S. L. De Wall, L. J. Barbour and G. W. Gokel, *J. Am. Chem. Soc.*, 1999, **121**, 37, 8405-8406.

58. C. A. Deakine and M. Mautner, *J. Am. Chem. Soc.*, 1985, **107**, 2, 474-479.

59. J. P. Gallivan and D. A. Dougherty, *Proc. Natl. Acad. Sci.*, 1999, **96**, 17, 9459-9464.

60. M. M. Flocco and S. L. Mowbray, *J. Mol. Biol.*, 1994, **235**, 2, 709-717.

61. J. B. Mitchell, C. L. Nandi, I. K. McDonald, J. M. Thornton and S. L. Price, *J. Mol. Biol.*, 1994, **239**, 2, 315-331.

62. D. A. Dougherty, *Science*, 1996, **271**, 5246, 163-168.

63. J. L. Sussman, M. Harel, F. Frolow, C. Oefner, A. Goldman, L. Toker and I. Silman, *Science*, 1991, **253**, 5022, 872-877.

64. M. Dennis, J. Giradaut, F. Kotzyba-Hibert, M. Goeldner, C. Hirth, J.-Y. Chang, C. Lazure, M. Chretien and J.-P. Changeux, *Biochemistry*, 1988, **27**, 7, 2346-2357.

65. C. Weise, H.-J. Kreienkamp, R. Raba, A. Pedak, A. Aaviksaar and F. Hucho, *EMBO J.*, 1990, **9**, 12, 3885-3888.

66. J.-L. Galzi, F. Revah, D. Black, M. Goeldner, C. Hirth and J.-P. Changeux, *J. Biol. Chem.*, 1990, **265**, 18, 10430-10437.

67. C. A. Lesburg, G. Zhai, D. E. Cane and D. W. Christianson, *Science*, 1997, **277**, 5333, 1820-1825.

68. D. J. Cram and M. Goldstein, *J. Am. Chem. Soc.*, 1963, **85**, 8, 1063-1074.

69. D. J. Cram and M. Goldstein, *J. Am. Chem. Soc.*, 1963, **85**, 1063-1074.

70. D. J. Cram and H. U. Daeniker, *J. Am. Chem. Soc.*, 1954, **76**, 10, 2743-2751.

71. D. J. Cram, C. S. Montgomery and G. R. Knox, *J. Am. Chem. Soc.*, 1965, **88**, 3, 515-525.

72. G. A. Russell, *J. Am. Chem. Soc.*, 1958, **80**, 18, 4987-4996.

73. G. A. Russell, *J. Am. Chem. Soc.*, 1958, **80**, 18, 4997-5001.

74. K. D. Raner, J. Lusztyk and K. U. Ingold, *J. Am. Chem. Soc.*, 1989, **111**, 10, 3652-3658.

75. N. J. Bunce, K. U. Ingold, J. P. Landers, J. Lusztyk and J. C. Scaiano, *J. Am. Chem. Soc.*, 1985, **107**, 19, 5464-5472.
76. D. J. Cram and M. F. Antar, *J. Am. Chem. Soc.*, 1958, **80**, 12, 3109-3114.
77. D. J. Cram and M. Cordon, *J. Am. Chem. Soc.*, 1955, **77**, 7, 1810-1811.
78. D. J. Cram and S. Steinberg, *J. Am. Chem. Soc.*, 1951, **73**, 12, 5691-5703.
79. N. L. Allinger and T. J. Walter, *J. Am. Chem. Soc.*, 1972, **94**, 26, 9267-9268.
80. D. J. Cram and M. F. Antar, *J. Am. Chem. Soc.*, 1958, **80**, 12, 3103-3109.
81. D. A. Dougherty and D. A. Stauffer, *Science*, 1990, **250**, 4987, 1558-1560.
82. M. A. Rabjohns and P. Hodge, *Polymer*, 1997, **38**, 13, 3395-3407.
83. L. A. Errede and J. P. Cassisy, *J. Am. Chem. Soc.*, 1960, **82**, 14, 3653-3657.
84. M. A. Petti, T. J. Shepodd, R. E. Barrans and D. A. Dougherty, *J. Am. Chem. Soc.*, 1988, **110**, 20, 6825-6840.
85. M. P. Doyle, B. Siegfried and J. F. Dellaria, *J. Org. Chem.*, 1977, **42**, 14, 2426-2430.
86. S. Terabe and R. Konaka, *J. Am. Chem. Soc.*, 1973, **95**, 15, 4976-4986.
87. H. Tanida and H. Ishitobi, *Tet. Lett.*, 1964, **5**, 15, 807-811.
88. A. De Meijere, D. Faber, U. Heinecke, R. D. Walsh, T. Muller and Y. Apeloig, *Eur. J. Org. Chem.*, 2001, **2001**, 4, 663-680.
89. I. Fleming, *Pericyclic Reactions*, 1999, Oxford University Press, Oxford.
90. M. Sainsbury, *Aromatic Chemistry*, 1992, Oxford University Press, Oxford.
91. K. L. Williamson and Y.-F. L. Hsu, *J. Am. Chem. Soc.*, 1970, **92**, 25, 7385-7389.
92. J. A. Berson, R. D. Reynolds and W. M. Jones, *J. Am. Chem. Soc.*, 1956, **78**, 23, 6049-6052.
93. J. C. C. Atherton and S. Jones, *Tetrahedron*, 2003, **59**, 46, 9039-9057.
94. P. Yates and P. Eaton, *J. Am. Chem. Soc.*, 1960, **82**, 16, 4436-4437.
95. M. Konieczny and R. G. Harvey, *J. Org. Chem.*, 1979, **44**, 26, 4813-4816.
96. C. Galli, *Chem. Rev.*, 1988, **88**, 5, 765-792.
97. T. Cohen, A. G. Dietz and J. R. Miser, *J. Org. Chem.*, 1976, **42**, 12, 2053-2058.
98. A. G. Giumanini, G. Verardo, P. Geatti and P. Strazzolini, *Tetrahedron*, 1996, **52**, 20, 7137-7148.

99. J. G. Lee and H. T. Cha, *Tet. Lett.*, 1992, **33**, 22, 3167-3168.

100. G. Valkanas and H. Hopff, *J. Org. Chem.*, 1962, **27**, 10, 3680-3682.

101. L. H. Briggs and G. A. Nicholls, *J. Chem. Soc.*, 1951, 1138-1139.

102. D. Marquardt and F. A. McCormick, *Tet. Lett.*, 1994, **35**, 8, 1131-1134.

103. D. S. Bapat, B. C. S. Rao and K. Venkataraman, *Tet. Lett.*, 1960, **5**, 1, 15-19.

104. T. R. Criswell and B. H. Klanderman, *J. Org. Chem.*, 1974, **39**, 6, 770-774.

105. N. Shyamasundar and P. Caluwe, *J. Org. Chem.*, 1981, **46**, 4, 809-811.

106. R. W. Rimmer, R. G. Christiansen, R. K. Brown and R. B. Sandin, *J. Am. Chem. Soc.*, 1950, **72**, 5, 2298-2299.

107. C. Hansch, A. Leo and R. W. Taft, *Chem. Rev.*, 1991, **91**, 2, 165-195.

108. M. D. Bartberger, W. R. Dolbier Jr., J. Lusztyk and K. U. Ingold, *Tetrahedron*, 1997, **53**, 29, 9857-9880.

109. K. Maruyama and T. Katagiri, *J. Phys. Chem.*, 1986, **108**, 20, 6263-6270.

110. J. Hooz and S. H. Gilani, *Can. J. Chem.*, 1968, **46**, 1, 86-87.

111. J. M. Mellor, S. Mittoo, R. Parkes and R. W. Millar, *Tetrahedron*, 2000, **56**, 40, 8019-8024.

112. S. Braverman, T. Pechenick and Y. Zafrani, *Tetrahedron*, 2001, **42**, 7, 1391-1393.

113. N. J. Hales, H. Heany, J. H. Hollinshead and S. V. Ley, *Tetrahedron*, 1995, **51**, 28, 7741-7754.

114. B. H. Han, D. H. Shin and S. Y. Cho, *Tet. Lett.*, 1985, **26**, 50, 6233-6234.

115. S. Gowda and D. C. Gowda, *Tetrahedron*, 2002, **58**, 11, 2211-2213.

116. Byung Hee Han, Dae Hyun Shin and Sung Yun Cho, *Tet. Lett.*, 1985, **26**, 50, 6233-6234.

117. J. W. Larsen, M. Freund, K. Y. Kim, M. Sidovar and J. L. Stuart, *Carbon*, 2000, **38**, 655-661.

118. C. Couture and A. J. Paine, *Can. J. Chem.*, 1984, **63**, 1, 111-120.

119. A. K. Croft, C. J. Easton and L. Radom, *J. Am. Chem. Soc.*, 2003, **125**, 14, 4120-4124.

120. P. F. Wood, D. J. Henry and L. Radom, *J. Phys. Chem. A*, 2003, **107**, 39, 7985-7990.

121. W. J. Hehre, R. Ditchfield, L. Radom and J. A. Pople, *J. Am. Chem. Soc.*, 1970, **92**, 16, 4796-4801.

122. L. Menapace and H. G. Kuivila, *J. Am. Chem. Soc.*, 1964, **86**, 15, 3047-3051.

123. N. S. Isaacs, *Physical Organic Chemistry*, 1987, Longman, New York.

124. E. V. Blackburn and D. D. Tanner, *J. Am. Chem. Soc.*, 1980, **103**, 12, 4100-4104.

125. C. Chatgilialoglu, K. U. Ingold and J. C. Scaiano, *J. Org. Chem.*, 1986, **52**, 5, 938-940.

126. D. J. Henry, C. J. Parkinson, P. M. Mayer and L. Radom, *J. Phys. Chem. A*, 2001, **105**, 27, 6750-6756.

127. A. K. Croft and C. J. Easton, *Aust. J. Chem.*, 2004, **57**, 7, 651-654.

128. C. J. Easton and M. C. Merrett, *J. Am. Chem. Soc.*, 1996, **118**, 12, 3035-3036.

129. H. M. Walborsky and C. Hamdouchi, *J. Am. Chem. Soc.*, 1993, **115**, 14, 6406-6408.

130. C. P. Andrieux, A. Gorande and J. M. Saveant, *J. Am. Chem. Soc.*, 1992, **114**, 17, 6893-6904.

131. J. Simonet, *Electrochem. Commun.*, 2005, **7**, 1, 74-80.

132. C. P. Andrieux, J.-M. Saveant and K. B. Su, *J. Phys. Chem.*, 1986, **90**, 16, 3815-3823.

133. C. P. Andrieux, I. Gallardo, J.-M. Saveant and K. B. Su, *J. Am. Chem. Soc.*, 1986, **108**, 4, 638-649.

134. A. A. Isse, M. G. Ferlin and A. Gennaro, *J. Electroanal. Chem.*, 2005, **581**, 1, 38-45.

135. C. P. Andrieux, M. Grzeszczuk and J.-M. Saveant, *J. Am. Chem. Soc.*, 1991, **113**, 23, 8811-8817.

136. A. J. Fry and R. L. Krieger, *J. Org. Chem.*, 1976, **41**, 1, 54-58.

137. J. A. Cleary, M. S. Mubark, K. L. Vieira, A. G. Anderson and D. G. Peters, *J. Electroanal. Chem.*, 1986, **198**, 1, 107-124.

138. M. S. Mubarak, *J. Org. Chem.*, 1990, **55**, 3, 1065-1070.

139. C. P. Andrieux, A. Merz and J.-M. Saveant, *J. Am. Chem. Soc.*, 1985, **107**, 21, 6097-6103.

140. M. A. Prasad and M. V. Sangaranarayanan, *Tetrahedron*, 2004, **60**, 51, 10967-10972.

141. C. P. Andrieux, L. Gelis, M. Medebielle, J. Pinson and J.-M. Saveant, *J. Am. Chem. Soc.*, 1990, **112**, 9, 3509-3520.

142. D. Bethell and J.-M. Saveant, *Advances in Physical Organic Chemistry*, 1990, Academic Press UK, London.

143. C. M. A. Brett and A. M. O. Brett, *Electrochemistry: Principles, Methods and Applications*, 1993, Oxford University Press, Oxford.

144. A. G. Anderson, A. F. Montana, A. A. MacDonald and G. M. Masada, *J. Org. Chem.*, 1973, **38**, 8, 1445-1450.

145. Y.-S. Hon, S.-W. Lin, L. Lu and Y.-J. Chen, *Tetrahedron*, 1995, **51**, 17, 5019-5034.

146. J. H. Klemm and G. M. Bower, *J. Am. Chem. Soc.*, 1958, **80**, 2, 344-347.

147. A. T. Blomquist, R. E. Stahl, Y. C. Meinwald and B. H. Smith, *J. Org. Chem.*, 1961, **26**, 6, 1687-1691.

148. G. Illuminati and L. Mandolini, *Acc. Chem. Res.*, 1981, **14**, 4, 95-102.

149. A. Dalla Cort, L. Mandolini and B. Masci, *J. Org. Chem.*, 1980, **45**, 19, 3923-3925.

150. D. J. Cram and G. R. Knox, *J. Am. Chem. Soc.*, 1961, **83**, 9, 2204-2205.

151. H. E. Winberg, F. S. Fawcett, W. E. Mochel and C. W. Theobald, *J. Am. Chem. Soc.*, 1960, **82**, 6, 1428-1435.

152. H. Minlon, *J. Am. Chem. Soc.*, 1946, **68**, 8, 2487-2488.

153. J. H. Brewster, *J. Am. Chem. Soc.*, 1954, **76**, 2, 6364-6367.

154. M. L. Di Vona and V. Rosnati, *J. Org. Chem.*, 1991, **56**, 13, 4269-4273.

155. M. L. Di Vona, B. Floris, L. Luchetti and V. Rosnati, *Tet. Lett.*, 1990, **31**, 42, 6081-6084.

156. K. T. Finley, *Chem. Rev.*, 1964, **64**, 5, 573-581.

157. J. J. Bloomfield and D. C. Owsley, *J. Org. Chem.*, 1975, **40**, 4, 393-402.

158. A. T. Blomquist, R. E. Burge Jr. and A. C. Sucsy, *J. Am. Chem. Soc.*, 1952, **74**, 14, 3636-3642.

159. S. M. McElvain, *Org. Reactions*, 1948, **4**, 256-304.

160. A. T. Blomquist and A. Goldstein, *Org. Synth. Coll. Vol. 4*, 1963, **4**, 216.

161. A. C. Cope, J. W. Barthel and R. D. Smith, *Org. Synth. Coll. Vol. 4*, 1963, **4**, 218.

162. J. J. Bloomfield, J. M. Nelke and Z. Valenta, *Org. Synth. Coll. Vol. 6*, 1973, **57**, 167-171.

163. T. S. Daynard, P. S. Eby and J. H. Hutchinson, *Can. J. Chem.*, 1993, **71**, 7, 1022-1028.

164. J. P. Schaefer and J. J. Bloomfield, *Org. Reactions*, 1967, **15**, 40-42.

165. L. Yet, *Chem. Rev.*, 2000, **100**, 8, 2963-3007.

166. K. J. Ivin, *J. Mol. Catal. A.*, 1998, **133**, 1, 1-16.

167. S. K. Armstrong, *J. Chem. Soc. Perk. Trans. 1*, 1998, **1998**, 2, 371-388.

168. D. M. Kalvin and R. W. Woodard, *Tetrahedron*, 1984, **40**, 18, 3387-3389.

169. S. Chandrasekhar, M. S. Kumar and B. Muralidhar, *Tet. Lett.*, 1998, **39**, 6, 909-910.

170. A. Wada, N. Fujioka, Y. Tanaka and M. Ito, *J. Org. Chem.*, 2000, **65**, 8, 2438-2443.

171. D. H. Rich, E. T. Sun and A. S. Boparai, *J. Org. Chem.*, 1978, **43**, 18, 3624-3643.

172. J. Hu, X. Jiang, T. He, J. Zhou, Y. Hu and H. Hu, *J. Chem. Soc. Perk. Trans. 1*, 2001, **2001**, 15, 1820-1825.

173. F. Grutzmacher and G. Nolte, *Chem. Ber.*, 1994, **127**, 1157-1162.

174. M. R. Johnson, D. C. Miller, K. Bush and J. A. I. Becker, *J. Org. Chem.*, 1992, **57**, 16, 4414-4417.

175. T. Yamato, K. Fujita and H. Tsuzuki, *J. Chem. Soc. Perk. Trans. 1*, 2001, **2001**, 17, 2089-2097.

176. S. Rele, S. Talukdar, A. Banerji and S. Chattopadhyay, *J. Org. Chem.*, 2001, **66**, 9, 2990-2994.

177. A. Furstner and K. Langemann, *J. Org. Chem.*, 1996, **61**, 12, 3942-3943.

178. J. E. McMurry, *Chem. Rev.*, 1989, **89**, 7, 1513-1524.

179. A. Furstner, *Angew. Chem., Int. Ed. Engl.*, 1993, **32**, 2, 164-189.

180. J. L. Namy, J. Souppe and H. B. Kagan, *Tet. Lett.*, 1983, **24**, 8, 765-766.

181. J. Inanaga, Y. Yokoyama, Y. Handa and M. Yamaguchi, *Tet. Lett.*, 1991, **32**, 44, 6371-6374.

182. M. Inoue, M. Sasaki and K. Tachibana, *Tet. Lett.*, 1997, **38**, 9, 1611-1614.
183. G. A. Molander, *J. Org. Chem.*, 1994, **59**, 11, 3186-3192.
184. K. R. Buszek, N. Sato and Y. Jeong, *Tet. Lett.*, 2002, **43**, 2, 181-184.
185. F. D. Boyer, I. Hanna and S. P. Nolan, *J. Org. Chem.*, 2001, **66**, 11, 4094-4096.
186. K. P. Kaliappan and N. Kumar, *Tet. Lett.*, 2003, **44**, 2, 379-381.
187. R. R. Schrock, J. S. Murdzek, G. C. Bazan, J. Robbins, M. DiMare and M. O'Reagan, *J. Am. Chem. Soc.*, 1990, **112**, 10, 3875-3886.
188. A. Furstner, *Angew. Chem., Int. Ed. Engl.*, 2000, **39**, 17, 3012-3043.
189. T. M. Trnka and R. H. Grubbs, *Acc. Chem. Res.*, 2001, **34**, 1, 18-29.
190. L. Mandolini, B. Masci and S. Roelens, *J. Org. Chem.*, 1977, **42**, 23, 3733-3736.
191. R. F. Holdren and R. M. Hixon, *J. Am. Chem. Soc.*, 1946, **68**, 7, 1198-1201.
192. K.-L. Noble, H. Hopf and L. Ernst, *Chem. Ber.*, 1984, **117**, 474-488.
193. D. J. Cram, C. K. Dalton and G. R. Knox, *J. Am. Chem. Soc.*, 1963, **85**, 8, 1088-1093.
194. B. S. Furniss, A. J. Hannaford, P. W. G. Smith and A. R. Tatchell, *Textbook of Practical Organic Chemistry*, 1989, Longman, London.
195. H. A. Staab and M. Sauer, *Liebigs. Ann.*, 1983, 743-759.
196. L. H. Klemm and K. B. Desai, *J. Org. Chem.*, 1963, **28**, 3, 625-630.
197. K. K. Zasshi, *Chemical Abstracts*, 1957, **60**, 1048-1049.
198. K. Imhoff, *Chem. Ber.*, 1904, **37**, 4707-4710.
199. K. Sisido, Y. Udo, T. Nakamura and H. Nozaki, *J. Org. Chem.*, 1960, **26**, 8, 1368-1369.
200. Y. Chung, B. F. Duerr, T. A. McKelvey, P. Nanjappan and A. W. Czarnik, *J. Org. Chem.*, 1989, **54**, 5, 1018-1032.
201. M. Kolobielski, *J. Org. Chem.*, 1963, **28**, 7, 1883-1885.
202. K. T. Serijan and P. H. Wise, *J. Am. Chem. Soc.*, 1951, **73**, 5191-5193.
203. M. W. Cronyn, *J. Am. Chem. Soc.*, 1952, **74**, 5, 1225-1230.
204. A. T. Blomquist, R. E. Stahl, Y. C. Meinwald and B. H. Smith, *J. Org. Chem.*, 1961, **26**, 6, 1687-1691.

205. J. E. Gready, T. W. Hambley, K. Kakiuchi, K. Kobiro, S. Sternhell, C. W. Tansey and Y. Tobe, *J. Am. Chem. Soc.*, 1990, **112**, 21, 7537-7540.

206. G. H. Daub and R. N. Castle, *J. Org. Chem.*, 1954, **19**, 10, 1571-1573.

207. M. J. S. Dewar and A. P. Marchand, *J. Am. Chem. Soc.*, 1966, **88**, 2, 354-358.

Appendices

Index

Appendix A. Crystal structure of anthracene 39

University of Southampton · School of Chemistry
EPSRC National Crystallography Service

Table 1. Crystal data and structure refinement.

Identification code	**05src0137**	
Empirical formula	$C_{17}H_{15}Br$	
Formula weight	299.20	
Temperature	120(2) K	
Wavelength	0.71073 Å	
Crystal system	Monoclinic	
Space group	$P2_1/c$	
Unit cell dimensions	$a = 8.4575(6)$ Å	$\alpha = 90°$
	$b = 25.0260(15)$ Å	$\beta = 106.485(5)°$
	$c = 6.5393(5)$ Å	$\gamma = 90°$
Volume	1327.20(16) $Å^3$	
Z	4	
Density (calculated)	1.497 Mg / m^3	
Absorption coefficient	3.076 mm^{-1}	
F(000)	608	
Crystal	Cut Shard; Colourless	
Crystal size	0.22 × 0.14 × 0.03 mm^3	
θ range for data collection	2.99 – 27.48°	
Index ranges	$-10 \le h \le 10$, $-32 \le k \le 32$, $-8 \le l \le 8$	
Reflections collected	14309	
Independent reflections	3033 [$R_{int} = 0.0468$]	
Completeness to $\theta = 27.48°$	99.5 %	
Absorption correction	Semi–empirical from equivalents	
Max. and min. transmission	0.9134 and 0.5510	
Refinement method	Full-matrix least-squares on F^2	
Data / restraints / parameters	3033 / 0 / 164	
Goodness-of-fit on F^2	1.015	
Final R indices [$F^2 > 2\sigma(F^2)$]	$R1 = 0.0464$, $wR2 = 0.0873$	
R indices (all data)	$R1 = 0.0883$, $wR2 = 0.1032$	
Extinction coefficient	0.0033(7)	
Largest diff. peak and hole	0.376 and –0.570 e $Å^{-3}$	

Diffractometer: *Nonius KappaCCD* area detector (ϕ scans and ω scans to fill *asymmetric unit* sphere). **Cell determination:** DirAx (Duisenberg, A.J.M.(1992). J. Appl. Cryst. 25, 92-96.) **Data collection:** Collect (Collect: Data collection software, R. Hooft, Nonius B.V., 1998). **Data reduction and cell refinement**: *Denzo* (Z. Otwinowski & W. Minor, *Methods in Enzymology* (1997) Vol. **276**: *Macromolecular Crystallography*, part A, pp. 307–326; C. W. Carter, Jr. & R. M. Sweet, Eds., Academic Press). **Absorption correction**: *SORTAV* (R. H. Blessing, Acta Cryst. A**51** (1995) 33–37; R. H. Blessing, J. Appl. Cryst. **30** (1997) 421–426). **Structure solution**: *SHELXS97* (G. M. Sheldrick, Acta Cryst. (1990) A**46** 467–473). **Structure refinement**: *SHELXL97* (G. M. Sheldrick (1997), University of Göttingen, Germany). **Graphics:** *ORTEP3 for Windows* (L. J. Farrugia, J. Appl. Crystallogr. 1997, 30, 565).
Special details: All hydrogen atoms were fixed.

Table 2. Atomic coordinates [$\times 10^4$], equivalent isotropic displacement parameters [$Å^2 \times 10^3$] and site occupancy factors. U_{eq} is defined as one third of the trace of the orthogonalized U^{ij} tensor.

Atom	*x*	*y*	*z*	U_{eq}	*S.o.f.*
C1	2201(4)	4086(1)	6564(5)	48(1)	1
C2	815(4)	3939(1)	4618(4)	39(1)	1
C3	567(4)	3323(1)	4607(5)	44(1)	1
C4	765(3)	3081(1)	2510(5)	40(1)	1
C5	2444(3)	3245(1)	2333(4)	39(1)	1
C6	3689(4)	2910(1)	2137(5)	48(1)	1
C7	5134(4)	3129(2)	1899(5)	55(1)	1
C8	5339(4)	3674(2)	1895(5)	52(1)	1
C9	4102(4)	4013(1)	2130(4)	44(1)	1
C10	2641(3)	3799(1)	2313(4)	36(1)	1
C11	1147(3)	4105(1)	2475(4)	37(1)	1
C12	−304(3)	3905(1)	702(4)	38(1)	1
C13	−1368(4)	4213(1)	−849(5)	49(1)	1
C14	−2622(4)	3964(2)	−2397(5)	58(1)	1
C15	−2816(4)	3421(2)	−2394(5)	60(1)	1
C16	−1759(4)	3110(1)	−837(5)	51(1)	1
C17	−501(3)	3352(1)	707(5)	40(1)	1
Br1	2572(1)	4853(1)	6874(1)	81(1)	1

Table 3. Bond lengths [Å] and angles [°].

C1–C2	1.511(4)
C1–Br1	1.946(3)
C1–H1A	0.9900
C1–H1B	0.9900
C2–C3	1.554(4)
C2–C11	1.562(4)
C2–H2	1.0000
C3–C4	1.551(4)
C3–H3A	0.9900
C3–H3B	0.9900
C4–C17	1.510(4)
C4–C5	1.515(4)
C4–H4	1.0000
C5–C6	1.379(4)
C5–C10	1.398(4)
C6–C7	1.388(4)
C6–H6	0.9500
C7–C8	1.373(5)
C7–H7	0.9500
C8–C9	1.389(5)
C8–H8	0.9500
C9–C10	1.382(4)
C9–H9	0.9500
C10–C11	1.506(4)
C11–C12	1.514(4)
C11–H11	1.0000
C12–C13	1.383(4)
C12–C17	1.395(4)
C13–C14	1.388(4)
C13–H13	0.9500
C14–C15	1.370(5)
C14–H14	0.9500
C15–C16	1.387(5)
C15–H15	0.9500
C16–C17	1.382(4)
C16–H16	0.9500
C2–C1–Br1	113.1(2)
C2–C1–H1A	109.0
Br1–C1–H1A	109.0
C2–C1–H1B	109.0
Br1–C1–H1B	109.0
H1A–C1–H1B	107.8
C1–C2–C3	108.5(2)
C1–C2–C11	113.4(2)
C3–C2–C11	108.5(2)
C1–C2–H2	108.8
C3–C2–H2	108.8
C11–C2–H2	108.8
C4–C3–C2	110.2(2)
C4–C3–H3A	109.6
C2–C3–H3A	109.6
C4–C3–H3B	109.6
C2–C3–H3B	109.6
H3A–C3–H3B	108.1
C17–C4–C5	106.9(2)

C17–C4–C3	106.5(2)
C5–C4–C3	107.4(2)
C17–C4–H4	111.9
C5–C4–H4	111.9
C3–C4–H4	111.9
C6–C5–C10	120.4(3)
C6–C5–C4	126.8(3)
C10–C5–C4	112.8(2)
C5–C6–C7	119.4(3)
C5–C6–H6	120.3
C7–C6–H6	120.3
C8–C7–C6	120.5(3)
C8–C7–H7	119.7
C6–C7–H7	119.7
C7–C8–C9	120.4(3)
C7–C8–H8	119.8
C9–C8–H8	119.8
C10–C9–C8	119.6(3)
C10–C9–H9	120.2
C8–C9–H9	120.2
C9–C10–C5	119.8(3)
C9–C10–C11	126.7(3)
C5–C10–C11	113.5(2)
C10–C11–C12	107.0(2)
C10–C11–C2	107.2(2)
C12–C11–C2	106.6(2)
C10–C11–H11	111.9
C12–C11–H11	111.9
C2–C11–H11	111.9
C13–C12–C17	120.1(3)
C13–C12–C11	126.5(3)
C17–C12–C11	113.4(2)
C12–C13–C14	119.3(3)
C12–C13–H13	120.4
C14–C13–H13	120.4
C15–C14–C13	120.7(3)
C15–C14–H14	119.6
C13–C14–H14	119.6
C14–C15–C16	120.4(3)
C14–C15–H15	119.8
C16–C15–H15	119.8
C17–C16–C15	119.5(3)
C17–C16–H16	120.2
C15–C16–H16	120.2
C16–C17–C12	120.1(3)
C16–C17–C4	127.0(3)
C12–C17–C4	112.9(2)

Symmetry transformations used to generate equivalent atoms:

Table 4. Anisotropic displacement parameters [$Å^2 \times 10^3$]. The anisotropic displacement factor exponent takes the form: $-2\pi^2[h^2a^{*2}U^{11} + \cdots + 2\ h\ k\ a^*\ b^*\ U^{12}]$.

Atom	U^{11}	U^{22}	U^{33}	U^{23}	U^{13}	U^{12}
C1	60(2)	45(2)	37(2)	−1(1)	13(2)	3(2)
C2	44(2)	39(2)	34(2)	−1(1)	12(1)	3(1)
C3	51(2)	38(2)	47(2)	3(1)	19(2)	−2(1)
C4	43(2)	30(2)	49(2)	−1(1)	18(1)	−1(1)
C5	41(2)	41(2)	34(2)	−1(1)	12(1)	−2(1)
C6	48(2)	49(2)	49(2)	−5(2)	14(2)	4(2)
C7	43(2)	73(2)	49(2)	−2(2)	15(2)	8(2)
C8	36(2)	80(3)	41(2)	2(2)	11(1)	−7(2)
C9	44(2)	53(2)	31(2)	1(1)	4(1)	−14(2)
C10	37(2)	44(2)	26(1)	0(1)	7(1)	−7(1)
C11	47(2)	31(2)	32(1)	2(1)	9(1)	−3(1)
C12	40(2)	43(2)	34(2)	−2(1)	14(1)	−1(1)
C13	49(2)	56(2)	41(2)	5(2)	13(2)	−1(2)
C14	46(2)	85(3)	39(2)	7(2)	6(2)	4(2)
C15	45(2)	88(3)	43(2)	−15(2)	9(2)	−14(2)
C16	44(2)	55(2)	55(2)	−17(2)	20(2)	−14(2)
C17	36(2)	43(2)	44(2)	−8(1)	18(1)	−6(1)
Br1	101(1)	54(1)	72(1)	−19(1)	−1(1)	−12(1)

Table 5. Hydrogen coordinates [$\times 10^4$] and isotropic displacement parameters [$Å^2 \times 10^3$].

Atom	x	y	z	U_{eq}	*S.o.f.*
H1A	3228	3911	6471	57	1
H1B	1944	3947	7851	57	1
H2	−220	4117	4715	46	1
H3A	1390	3163	5843	53	1
H3B	−546	3241	4734	53	1
H4	625	2683	2467	47	1
H6	3558	2534	2166	58	1
H7	5987	2901	1737	65	1
H8	6333	3819	1731	63	1
H9	4259	4389	2164	53	1
H11	1301	4500	2389	44	1
H13	−1243	4590	−854	59	1
H14	−3353	4173	−3470	70	1
H15	−3679	3256	−3463	72	1
H16	−1899	2733	−834	61	1

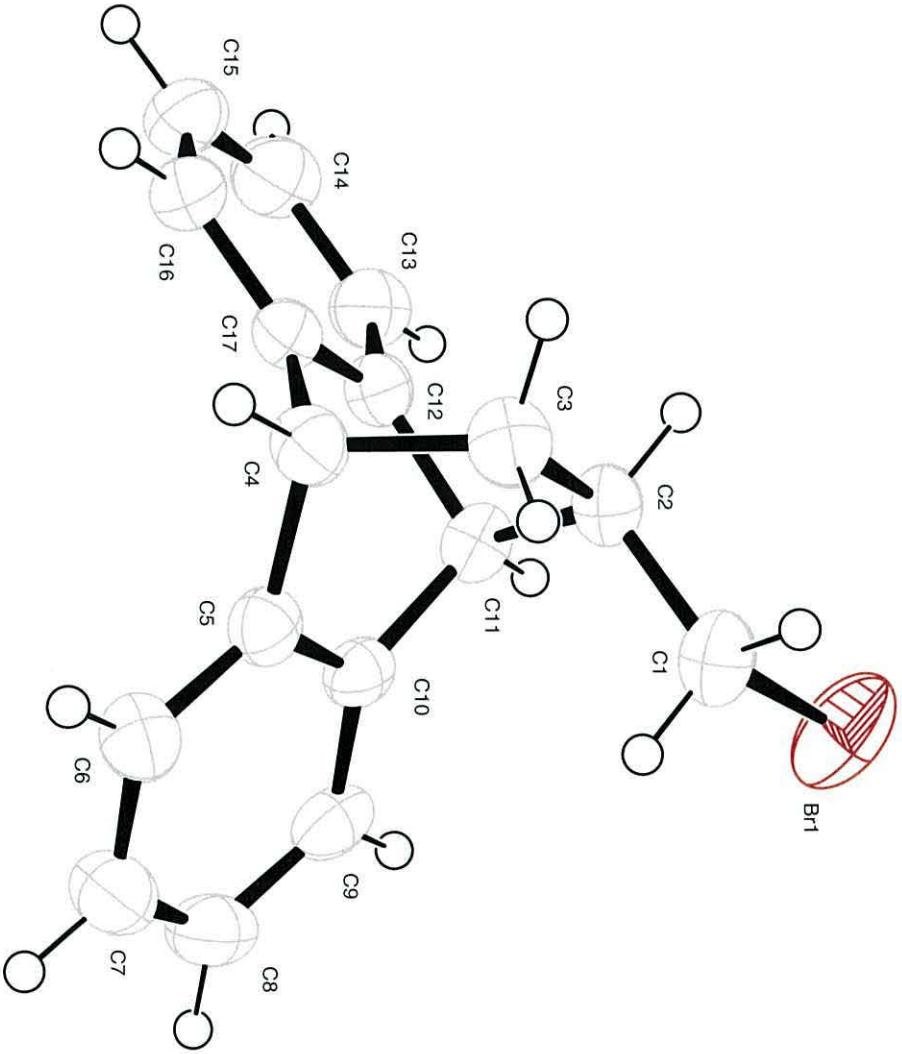
C15
C14
C16
C13
C17
C12
C3
C4
C2
C11
C5
C1
C10
C6
Br1
C9
C7
C8

Appendix B. Crystal structure of anthracene 29

University of Southampton · School of Chemistry
EPSRC National Crystallography Service

Table 1. Crystal data and structure refinement.

Identification code	**05src0006**	
Empirical formula	$C_{21}H_{22}O_2$	
Formula weight	306.39	
Temperature	120(2) K	
Wavelength	0.71073 Å	
Crystal system	Triclinic	
Space group	*P*–1	
Unit cell dimensions	a = 6.2520(17) Å	α = 70.84(7)°
	b = 9.968(8) Å	β = 85.92(6)°
	c = 14.606(6) Å	γ = 72.33(6)°
Volume	818.8(8) Å^3	
Z	2	
Density (calculated)	1.243 Mg / m^3	
Absorption coefficient	0.078 mm^{-1}	
F(000)	328	
Crystal	Rod; Colourless	
Crystal size	0.09 × 0.03 × 0.02 mm^3	
θ range for data collection	3.77 – 27.48°	
Index ranges	$-8 \le h \le 7$, $-12 \le k \le 12$, $-18 \le l \le 18$	
Reflections collected	16188	
Independent reflections	3718 [R_{int} = 0.0801]	
Completeness to θ = 27.48°	99.5 %	
Absorption correction	Semi–empirical from equivalents	
Max. and min. transmission	0.9984 and 0.9930	
Refinement method	Full-matrix least-squares on F^2	
Data / restraints / parameters	3718 / 363 / 277	
Goodness-of-fit on F^2	1.094	
Final *R* indices [$F^2 > 2\sigma(F^2)$]	*R1* = 0.0792, *wR2* = 0.1531	
R indices (all data)	*R1* = 0.1431, *wR2* = 0.1754	
Extinction coefficient	0.066(10)	
Largest diff. peak and hole	0.215 and –0.203 e Å^{-3}	

Diffractometer: *Nonius KappaCCD* area detector (ϕ scans and ω scans to fill *asymmetric unit* sphere). **Cell determination:** DirAx (Duisenberg, A.J.M.(1992). J. Appl. Cryst. 25, 92-96.) **Data collection:** Collect (Collect: Data collection software, R. Hooft, Nonius B.V., 1998). **Data reduction and cell refinement**: *Denzo* (Z. Otwinowski & W. Minor, *Methods in Enzymology* (1997) Vol. **276**: *Macromolecular Crystallography*, part A, pp. 307–326; C. W. Carter, Jr. & R. M. Sweet, Eds., Academic Press). **Absorption correction**: *SORTAV* (R. H. Blessing, Acta Cryst. A**51** (1995) 33–37; R. H. Blessing, J. Appl. Cryst. **30** (1997) 421–426). **Structure solution**: *SHELXS97* (G. M. Sheldrick, Acta Cryst. (1990) A**46** 467–473). **Structure refinement**: *SHELXL97* (G. M. Sheldrick (1997), University of Göttingen, Germany). **Graphics:** *ORTEP3 for Windows* (L. J. Farrugia, J. Appl. Crystallogr. 1997, 30, 565).

Special details:
All hydrogen atoms were fixed. There is some disorder within the crystal.

Table 2. Atomic coordinates [× 10^4], equivalent isotropic displacement parameters [$Å^2$ × 10^3] and site occupancy factors. U_{eq} is defined as one third of the trace of the orthogonalized U^{ij} tensor.

Atom	*x*	*y*	*z*	U_{eq}	*S.o.f.*
C1	7702(4)	4737(3)	8358(2)	42(1)	1
C2	8592(4)	3447(3)	9264(2)	39(1)	1
C3	7347(4)	2842(3)	10012(2)	43(1)	1
C4	8432(4)	1624(3)	10787(2)	43(1)	1
C5	10734(4)	1010(3)	10832(2)	41(1)	1
C6	11973(4)	1635(2)	10074(2)	40(1)	1
C7	10916(4)	2845(2)	9296(2)	37(1)	1
C8	12032(4)	3629(3)	8420(2)	42(1)	1
C9	11116(18)	3580(30)	7530(11)	39(2)	0.593(6)
C10	12353(11)	2996(12)	6860(6)	38(2)	0.593(6)
C11	11169(10)	2990(9)	6096(5)	38(2)	0.593(6)
C12	8856(10)	3516(9)	6019(5)	36(2)	0.593(6)
C13	7684(11)	4127(9)	6708(5)	35(2)	0.593(6)
C14	8790(18)	4160(20)	7501(10)	39(2)	0.593(6)
C18	7609(8)	3443(5)	5195(3)	51(1)	0.593(6)
C31	8320(30)	4280(30)	7513(14)	48(4)	0.407(6)
C32	6822(17)	4444(14)	6817(8)	42(3)	0.407(6)
C33	7746(16)	3919(12)	6065(7)	44(2)	0.407(6)
C34	10025(16)	3267(12)	6042(6)	40(3)	0.407(6)
C35	11442(16)	3160(16)	6772(8)	43(3)	0.407(6)
C36	10630(20)	3640(40)	7565(17)	44(4)	0.407(6)
C37	10928(14)	2690(8)	5214(5)	62(2)	0.407(6)
C15	8827(4)	5945(3)	8341(2)	41(1)	1
C16	11395(4)	5282(3)	8375(2)	43(1)	1
C17	11885(5)	−328(3)	11672(2)	54(1)	1
C19	7972(5)	7298(3)	7469(2)	45(1)	1
C20	4671(6)	9198(3)	6717(2)	65(1)	1
C21	3830(6)	8683(4)	6010(3)	81(1)	1
O1	9029(3)	7762(2)	6793(2)	62(1)	1
O2	5778(3)	7935(2)	7543(1)	57(1)	1

Table 3. Bond lengths [Å] and angles [°].

C1–C31	1.440(10)
C1–C2	1.506(4)
C1–C15	1.561(3)
C1–C14	1.574(7)
C1–H1	1.0000
C2–C3	1.376(4)
C2–C7	1.391(3)
C3–C4	1.386(4)
C3–H3	0.9500
C4–C5	1.379(4)
C4–H4	0.9500
C5–C6	1.390(4)
C5–C17	1.507(4)
C6–C7	1.380(4)
C6–H6	0.9500
C7–C8	1.511(4)
C8–C9	1.478(7)
C8–C16	1.552(3)
C8–C36	1.570(10)
C8–H8	1.0000
C9–C10	1.374(7)
C9–C14	1.390(7)
C10–C11	1.385(7)
C10–H10	0.9500
C11–C12	1.380(6)
C11–H11	0.9500
C12–C13	1.395(7)
C12–C18	1.512(6)
C13–C14	1.404(7)
C13–H13	0.9500
C18–H18A	0.9800
C18–H18B	0.9800
C18–H18C	0.9800
C31–C32	1.369(9)
C31–C36	1.387(8)
C32–C33	1.384(8)
C32–H32	0.9500
C33–C34	1.378(8)
C33–H33	0.9500
C34–C35	1.391(8)
C34–C37	1.508(7)
C35–C36	1.401(8)
C35–H35	0.9500
C37–H37A	0.9800
C37–H37B	0.9800
C37–H37C	0.9800
C15–C19	1.503(4)
C15–C16	1.537(4)
C15–H15	1.0000
C16–H16A	0.9900
C16–H16B	0.9900
C17–H17A	0.9800
C17–H17B	0.9800
C17–H17C	0.9800
C19–O1	1.192(3)
C19–O2	1.338(3)
C20–O2	1.453(4)

C20–C21	1.482(5)
C20–H20A	0.9900
C20–H20B	0.9900
C21–H21A	0.9800
C21–H21B	0.9800
C21–H21C	0.9800
C31–C1–C2	110.3(12)
C31–C1–C15	109.4(12)
C2–C1–C15	106.3(2)
C31–C1–C14	9.5(9)
C2–C1–C14	104.8(7)
C15–C1–C14	104.5(7)
C31–C1–H1	104.0
C2–C1–H1	113.4
C15–C1–H1	113.4
C14–C1–H1	113.4
C3–C2–C7	120.0(2)
C3–C2–C1	126.6(2)
C7–C2–C1	113.4(2)
C2–C3–C4	119.3(3)
C2–C3–H3	120.4
C4–C3–H3	120.4
C5–C4–C3	121.6(2)
C5–C4–H4	119.2
C3–C4–H4	119.2
C4–C5–C6	118.5(2)
C4–C5–C17	121.0(2)
C6–C5–C17	120.5(2)
C7–C6–C5	120.5(2)
C7–C6–H6	119.7
C5–C6–H6	119.7
C6–C7–C2	120.1(2)
C6–C7–C8	126.5(2)
C2–C7–C8	113.5(2)
C9–C8–C7	109.8(10)
C9–C8–C16	107.9(10)
C7–C8–C16	106.7(2)
C9–C8–C36	10.5(10)
C7–C8–C36	101.7(14)
C16–C8–C36	104.8(14)
C9–C8–H8	110.8
C7–C8–H8	110.8
C16–C8–H8	110.8
C36–C8–H8	120.9
C10–C9–C14	125.3(7)
C10–C9–C8	125.5(8)
C14–C9–C8	109.2(7)
C9–C10–C11	116.8(6)
C9–C10–H10	121.6
C11–C10–H10	121.6
C12–C11–C10	121.8(6)
C12–C11–H11	119.1
C10–C11–H11	119.1
C11–C12–C13	119.0(6)
C11–C12–C18	120.5(6)
C13–C12–C18	120.5(5)
C12–C13–C14	121.7(5)
C12–C13–H13	119.2
C14–C13–H13	119.2
C9–C14–C13	115.3(6)

C9–C14–C1	117.0(7)
C13–C14–C1	127.6(7)
C32–C31–C36	128.3(9)
C32–C31–C1	124.2(11)
C36–C31–C1	107.5(10)
C31–C32–C33	115.5(8)
C31–C32–H32	122.3
C33–C32–H32	122.3
C34–C33–C32	121.2(8)
C34–C33–H33	119.4
C32–C33–H33	119.4
C33–C34–C35	119.9(7)
C33–C34–C37	118.7(8)
C35–C34–C37	121.4(7)
C34–C35–C36	122.4(7)
C34–C35–H35	118.8
C36–C35–H35	118.8
C31–C36–C35	112.8(8)
C31–C36–C8	119.3(10)
C35–C36–C8	127.8(10)
C34–C37–H37A	109.5
C34–C37–H37B	109.5
H37A–C37–H37B	109.5
C34–C37–H37C	109.5
H37A–C37–H37C	109.5
H37B–C37–H37C	109.5
C19–C15–C16	112.9(2)
C19–C15–C1	109.8(2)
C16–C15–C1	109.5(2)
C19–C15–H15	108.2
C16–C15–H15	108.2
C1–C15–H15	108.2
C15–C16–C8	110.0(2)
C15–C16–H16A	109.7
C8–C16–H16A	109.7
C15–C16–H16B	109.7
C8–C16–H16B	109.7
H16A–C16–H16B	108.2
C5–C17–H17A	109.5
C5–C17–H17B	109.5
H17A–C17–H17B	109.5
C5–C17–H17C	109.5
H17A–C17–H17C	109.5
H17B–C17–H17C	109.5
O1–C19–O2	123.1(3)
O1–C19–C15	126.7(3)
O2–C19–C15	110.1(2)
O2–C20–C21	110.2(3)
O2–C20–H20A	109.6
C21–C20–H20A	109.6
O2–C20–H20B	109.6
C21–C20–H20B	109.6
H20A–C20–H20B	108.1
C20–C21–H21A	109.5
C20–C21–H21B	109.5
H21A–C21–H21B	109.5
C20–C21–H21C	109.5
H21A–C21–H21C	109.5
H21B–C21–H21C	109.5
C19–O2–C20	116.5(2)

Table 4. Anisotropic displacement parameters [Å^2× 10^3]. The anisotropic displacement factor exponent takes the form: $-2\pi^2[h^2a^{*2}U^{11} + \cdots + 2\,h\,k\,a^*\,b^*\,U^{12}]$.

Atom	U^{11}	U^{22}	U^{33}	U^{23}	U^{13}	U^{12}
C1	44(2)	35(1)	44(2)	−4(1)	−3(1)	−18(1)
C2	48(2)	33(1)	38(1)	−11(1)	0(1)	−17(1)
C3	47(2)	38(1)	48(2)	−12(1)	5(1)	−19(1)
C4	61(2)	35(1)	37(1)	−8(1)	5(1)	−24(1)
C5	58(2)	29(1)	39(1)	−11(1)	−3(1)	−18(1)
C6	47(2)	29(1)	48(2)	−13(1)	−1(1)	−14(1)
C7	51(2)	30(1)	37(1)	−15(1)	3(1)	−17(1)
C8	47(2)	32(1)	45(2)	−13(1)	7(1)	−13(1)
C9	48(4)	26(4)	41(5)	−4(3)	5(4)	−18(4)
C10	45(4)	30(3)	39(3)	−10(2)	3(3)	−13(4)
C11	43(4)	29(3)	39(3)	−9(2)	3(3)	−9(3)
C12	43(6)	26(5)	33(3)	−2(3)	−6(5)	−10(5)
C13	33(4)	33(4)	38(4)	−6(2)	0(3)	−11(3)
C14	62(5)	29(4)	30(4)	−6(3)	−8(4)	−21(5)
C18	61(3)	56(3)	37(3)	−13(2)	−5(2)	−20(2)
C31	61(7)	31(8)	51(8)	3(5)	−3(5)	−30(6)
C32	57(7)	32(5)	33(4)	−1(3)	2(5)	−19(5)
C33	63(7)	30(5)	38(5)	−6(4)	−9(5)	−14(5)
C34	56(10)	31(7)	31(4)	−10(4)	4(8)	−10(10)
C35	56(7)	28(4)	41(6)	−9(4)	18(5)	−13(6)
C36	73(9)	33(6)	31(6)	−15(5)	22(7)	−21(9)
C37	90(6)	51(4)	46(4)	−21(3)	16(4)	−19(4)
C15	51(2)	31(1)	42(2)	−12(1)	5(1)	−15(1)
C16	51(2)	35(1)	48(2)	−14(1)	5(1)	−20(1)
C17	74(2)	37(1)	47(2)	−6(1)	−7(1)	−18(1)
C19	55(2)	33(1)	46(2)	−12(1)	7(1)	−15(1)
C20	71(2)	44(2)	57(2)	3(1)	2(2)	−5(2)
C21	79(2)	72(2)	76(2)	13(2)	−6(2)	−38(2)
O1	64(1)	53(1)	58(1)	1(1)	13(1)	−23(1)
O2	59(1)	40(1)	52(1)	1(1)	7(1)	−3(1)

Table 5. Hydrogen coordinates [× 10^4] and isotropic displacement parameters [$Å^2$ × 10^3].

Atom	*x*	*y*	*z*	U_{eq}	*S.o.f.*
H1	6025	5114	8307	50	1
H3	5762	3256	9998	52	1
H4	7568	1200	11298	52	1
H6	13560	1227	10092	48	1
H8	13699	3170	8477	50	1
H10	13944	2612	6919	46	0.593(6)
H11	11972	2615	5611	46	0.593(6)
H13	6097	4534	6638	43	0.593(6)
H18A	7571	4304	4620	76	0.593(6)
H18B	6070	3451	5384	76	0.593(6)
H18C	8378	2526	5048	76	0.593(6)
H32	5253	4887	6847	50	0.407(6)
H33	6792	4009	5557	53	0.407(6)
H35	13014	2745	6731	52	0.407(6)
H37A	10529	1781	5294	94	0.407(6)
H37B	12566	2469	5211	94	0.407(6)
H37C	10275	3444	4600	94	0.407(6)
H15	8388	6240	8936	49	1
H16A	12040	5350	8952	52	1
H16B	12027	5855	7790	52	1
H17A	11118	−258	12271	81	1
H17B	13453	−361	11732	81	1
H17C	11834	−1234	11559	81	1
H20A	5744	9752	6402	78	1
H20B	3401	9880	6941	78	1
H21A	5096	8035	5774	121	1
H21B	3061	9545	5463	121	1
H21C	2777	8130	6326	121	1

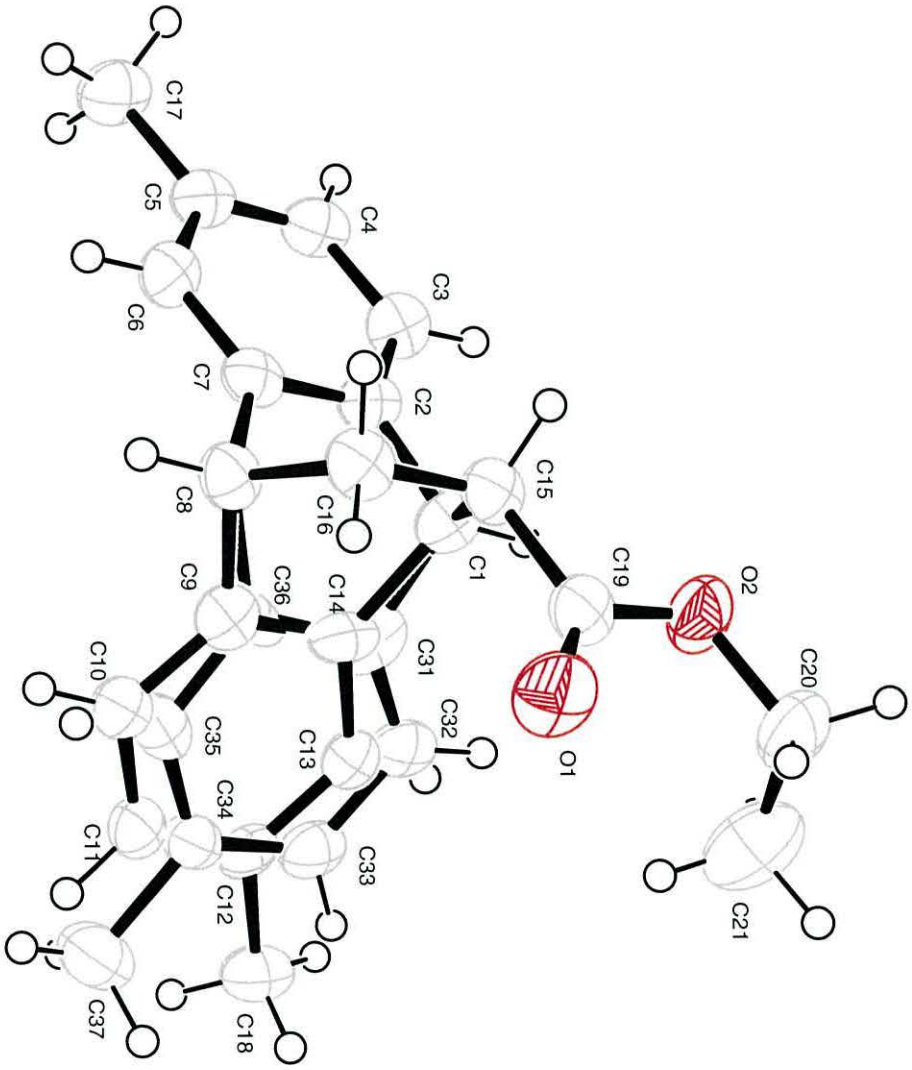
C17
C5
C4
C3
C6
C7
C2
C15
C8
C16
C1
C19
O2
C9
C36
C14
C31
C20
C10
C35
C32
C13
O1
C34
C11
C33
C12
C21
C37
C18

Appendix C. Crystal structure of anthracene 42

University of Southampton · School of Chemistry
EPSRC National Crystallography Service

Table 1. Crystal data and structure refinement.

Identification code	**2005src0441**	
Empirical formula	$C_{17}H_{13}BrN_2O_4$	
Formula weight	389.20	
Temperature	120(2) K	
Wavelength	0.71073 Å	
Crystal system	Monoclinic	
Space group	*C2/c*	
Unit cell dimensions	a = 18.884(5) Å	α = 90°
	b = 9.725(3) Å	β = 112.90(3)°
	c = 18.447(3) Å	γ = 90°
Volume	3120.7(14) Å^3	
Z	8	
Density (calculated)	1.657 Mg / m^3	
Absorption coefficient	2.659 mm^{-1}	
F(000)	1568	
Crystal	Blade; Colourless	
Crystal size	0.10 × 0.04 × 0.03 mm^3	
θ range for data collection	3.05 – 27.48°	
Index ranges	$-24 \le h \le 24$, $-12 \le k \le 12$, $-23 \le l \le 23$	
Reflections collected	30574	
Independent reflections	3570 [R_{int} = 0.0859]	
Completeness to θ = 27.48°	99.6 %	
Absorption correction	Semi–empirical from equivalents	
Max. and min. transmission	0.9245 and 0.7769	
Refinement method	Full-matrix least-squares on F^2	
Data / restraints / parameters	3570 / 0 / 236	
Goodness-of-fit on F^2	1.169	
Final R indices [$F^2 > 2\sigma(F^2)$]	$R1$ = 0.0898, $wR2$ = 0.1724	
R indices (all data)	$R1$ = 0.1506, $wR2$ = 0.1940	
Largest diff. peak and hole	0.520 and –0.304 e Å^{-3}	

Diffractometer: *Nonius KappaCCD* area detector (ϕ scans and ω scans to fill *asymmetric unit* sphere). **Cell determination:** DirAx (Duisenberg, A.J.M.(1992). J. Appl. Cryst. 25, 92-96.) **Data collection:** Collect (Collect: Data collection software, R. Hooft, Nonius B.V., 1998). **Data reduction and cell refinement**: *Denzo* (Z. Otwinowski & W. Minor, *Methods in Enzymology* (1997) Vol. **276**: *Macromolecular Crystallography*, part A, pp. 307–326; C. W. Carter, Jr. & R. M. Sweet, Eds., Academic Press). **Absorption correction**: *SORTAV* (R. H. Blessing, Acta Cryst. A**51** (1995) 33–37; R. H. Blessing, J. Appl. Cryst. **30** (1997) 421–426). **Structure solution**: *SHELXS97* (G. M. Sheldrick, Acta Cryst. (1990) A**46** 467–473). **Structure refinement**: *SHELXL97* (G. M. Sheldrick (1997), University of Göttingen, Germany). **Graphics:** *ORTEP3 for Windows* (L. J. Farrugia, J. Appl. Crystallogr. 1997, 30, 565).

Special details:

All hydrogen atoms were fixed.
The methylene bromide arm is disordered over two possible sites.

Table 2. Atomic coordinates [× 10^4], equivalent isotropic displacement parameters [$Å^2$ × 10^3] and site occupancy factors. U_{eq} is defined as one third of the trace of the orthogonalized U^{ij} tensor.

Atom	*x*	*y*	*z*	U_{eq}	*S.o.f.*
C1	1129(3)	3671(7)	1393(4)	59(2)	1
C2	519(3)	2574(6)	1050(3)	47(1)	1
C3	−72(4)	2587(7)	314(4)	54(2)	1
C4	−595(3)	1516(7)	116(3)	53(2)	1
C5	−541(4)	409(6)	605(4)	53(2)	1
C6	72(3)	384(6)	1345(4)	48(1)	1
C7	591(3)	1460(6)	1568(3)	46(1)	1
C8	1260(3)	1613(6)	2334(4)	52(2)	1
C9	1171(3)	2971(7)	2676(4)	54(2)	1
C10	1171(4)	3160(8)	3425(4)	67(2)	1
C11	1056(4)	4464(8)	3658(5)	68(2)	1
C12	971(3)	5544(7)	3158(4)	59(2)	1
C13	998(3)	5408(7)	2406(4)	61(2)	1
C14	1087(3)	4083(6)	2160(4)	53(2)	1
C16	2003(3)	1724(7)	2161(4)	55(2)	1
N1	−1245(4)	1541(7)	−655(4)	70(2)	1
N11	840(3)	6950(7)	3408(5)	79(2)	1
O1	−1766(4)	739(6)	−782(3)	84(2)	1
O2	−1236(3)	2416(7)	−1136(3)	101(2)	1
O11	732(3)	7045(6)	4023(4)	92(2)	1
O12	844(3)	7926(6)	2977(4)	98(2)	1
C15	1922(4)	2980(8)	1596(5)	75(2)	0.607(9)
C17	2151(5)	2701(10)	985(5)	47(3)	0.607(9)
Br1	2394(1)	4346(4)	508(2)	61(1)	0.607(9)
C20	1922(4)	2980(8)	1596(5)	75(2)	0.393(9)
C21	2491(9)	3729(17)	1696(9)	54(4)	0.393(9)
Br21	2460(2)	4971(8)	803(3)	76(1)	0.393(9)

Table 3. Bond lengths [Å] and angles [°].

C1–C14	1.502(9)
C1–C2	1.516(9)
C1–C15	1.549(9)
C1–H1	1.0000
C2–C3	1.382(9)
C2–C7	1.415(8)
C3–C4	1.382(9)
C3–H3	0.9500
C4–C5	1.383(9)
C4–N1	1.475(8)
C5–C6	1.404(8)
C5–H5	0.9500
C6–C7	1.382(8)
C6–H6	0.9500
C7–C8	1.492(8)
C8–C9	1.501(9)
C8–C16	1.558(8)
C8–H8	1.0000
C9–C10	1.394(9)
C9–C14	1.407(9)
C10–C11	1.383(10)
C10–H10	0.9500
C11–C12	1.365(10)
C11–H11	0.9500
C12–C13	1.416(9)
C12–N11	1.493(9)
C13–C14	1.397(9)
C13–H13	0.9500
C16–C15	1.574(9)
C16–H16A	0.9900
C16–H16B	0.9900
N1–O1	1.205(8)
N1–O2	1.234(8)
N11–O11	1.232(8)
N11–O12	1.240(9)
C15–C17	1.382(11)
C15–H15	1.0000
C17–Br1	1.963(9)
C17–H17A	0.9900
C17–H17B	0.9900
C21–Br21	2.024(16)
C21–H21A	0.9900
C21–H21B	0.9900
C14–C1–C2	105.7(4)
C14–C1–C15	106.8(6)
C2–C1–C15	107.6(6)
C14–C1–H1	112.1
C2–C1–H1	112.1
C15–C1–H1	112.1
C3–C2–C7	119.9(6)
C3–C2–C1	126.5(5)
C7–C2–C1	113.5(5)
C2–C3–C4	118.2(6)
C2–C3–H3	120.9
C4–C3–H3	120.9
C5–C4–C3	123.4(6)
C5–C4–N1	117.7(6)

C3–C4–N1	118.9(6)
C4–C5–C6	118.0(6)
C4–C5–H5	121.0
C6–C5–H5	121.0
C7–C6–C5	119.8(6)
C7–C6–H6	120.1
C5–C6–H6	120.1
C6–C7–C2	120.5(5)
C6–C7–C8	126.7(5)
C2–C7–C8	112.7(5)
C7–C8–C9	107.1(5)
C7–C8–C16	108.2(5)
C9–C8–C16	106.3(5)
C7–C8–H8	111.7
C9–C8–H8	111.7
C16–C8–H8	111.7
C10–C9–C14	121.6(6)
C10–C9–C8	125.2(6)
C14–C9–C8	113.2(5)
C11–C10–C9	119.4(7)
C11–C10–H10	120.3
C9–C10–H10	120.3
C12–C11–C10	119.1(7)
C12–C11–H11	120.4
C10–C11–H11	120.4
C11–C12–C13	123.4(6)
C11–C12–N11	119.1(7)
C13–C12–N11	117.4(7)
C14–C13–C12	117.3(6)
C14–C13–H13	121.4
C12–C13–H13	121.4
C13–C14–C9	119.1(6)
C13–C14–C1	127.5(6)
C9–C14–C1	113.4(5)
C8–C16–C15	109.0(5)
C8–C16–H16A	109.9
C15–C16–H16A	109.9
C8–C16–H16B	109.9
C15–C16–H16B	109.9
H16A–C16–H16B	108.3
O1–N1–O2	123.1(7)
O1–N1–C4	119.2(6)
O2–N1–C4	117.7(7)
O11–N11–O12	125.3(7)
O11–N11–C12	117.3(7)
O12–N11–C12	117.5(7)
C17–C15–C1	118.0(7)
C17–C15–C16	114.0(7)
C1–C15–C16	109.4(5)
C17–C15–H15	104.7
C1–C15–H15	104.7
C16–C15–H15	104.7
C15–C17–Br1	114.0(7)
C15–C17–H17A	108.8
Br1–C17–H17A	108.8
C15–C17–H17B	108.8
Br1–C17–H17B	108.8
H17A–C17–H17B	107.6
Br21–C21–H21A	107.7
Br21–C21–H21B	107.7

H21A–C21–H21B	107.1

Table 4. Anisotropic displacement parameters [Å^2× 10^3]. The anisotropic displacement factor exponent takes the form: $-2\pi^2[h^2a^{*2}U^{11} + \cdots + 2\ h\ k\ a^*\ b^*\ U^{12}\ ]$.

Atom	U^{11}	U^{22}	U^{33}	U^{23}	U^{13}	U^{12}
C1	54(4)	58(4)	82(5)	22(3)	45(3)	7(3)
C2	49(3)	53(4)	54(4)	8(3)	36(3)	11(3)
C3	68(4)	49(4)	62(4)	12(3)	44(4)	19(3)
C4	49(3)	70(5)	44(3)	−2(3)	23(3)	20(3)
C5	53(4)	51(4)	60(4)	−8(3)	28(3)	2(3)
C6	51(3)	43(3)	56(4)	3(3)	27(3)	3(3)
C7	48(3)	52(4)	46(3)	−1(3)	26(3)	0(3)
C8	54(4)	54(4)	56(4)	7(3)	28(3)	−3(3)
C9	37(3)	68(4)	63(4)	−3(3)	25(3)	−15(3)
C10	62(4)	79(5)	67(4)	−7(4)	34(4)	−22(4)
C11	51(4)	77(5)	80(5)	−17(4)	30(4)	−21(4)
C12	33(3)	58(4)	84(5)	−20(4)	22(3)	−12(3)
C13	28(3)	64(4)	91(5)	1(4)	23(3)	−5(3)
C14	35(3)	47(4)	84(5)	−2(3)	30(3)	−6(3)
C16	48(3)	56(4)	61(4)	5(3)	21(3)	3(3)
N1	72(4)	77(4)	66(4)	1(3)	32(4)	26(4)
N11	40(3)	68(4)	113(6)	−24(4)	11(4)	1(3)
O1	94(4)	75(4)	61(3)	−7(3)	8(3)	3(3)
O2	85(4)	143(6)	72(4)	46(4)	27(3)	29(4)
O11	79(4)	111(5)	94(4)	−39(4)	41(3)	0(3)
O12	96(4)	70(4)	109(5)	−5(3)	19(4)	16(3)
C15	60(4)	78(5)	111(6)	30(4)	60(4)	15(4)
C17	38(5)	60(7)	52(6)	7(5)	26(5)	0(4)
Br1	49(1)	80(2)	61(1)	14(1)	27(1)	−7(1)
C20	60(4)	78(5)	111(6)	30(4)	60(4)	15(4)
C21	44(9)	61(10)	57(10)	−7(8)	20(7)	−1(8)
Br21	61(1)	97(3)	71(2)	0(2)	27(1)	−37(1)

Table 5. Hydrogen coordinates [$\times 10^4$] and isotropic displacement parameters [$Å^2 \times 10^3$].

Atom	*x*	*y*	*z*	U_{eq}	*S.o.f.*
H1	1050	4470	1029	71	1
H3	−118	3313	−46	65	1
H5	−908	−314	446	64	1
H6	131	−371	1690	58	1
H8	1291	835	2699	63	1
H10	1248	2401	3771	80	1
H11	1036	4606	4159	81	1
H13	959	6186	2081	73	1
H16A	2078	866	1911	66	1
H16B	2456	1857	2659	66	1
H15	2302	3671	1928	90	0.607(9)
H17A	1737	2185	572	57	0.607(9)
H17B	2611	2102	1183	57	0.607(9)
H20	1849	2508	1090	90	0.393(9)
H21A	2946	3125	1830	65	0.393(9)
H21B	2576	4316	2161	65	0.393(9)

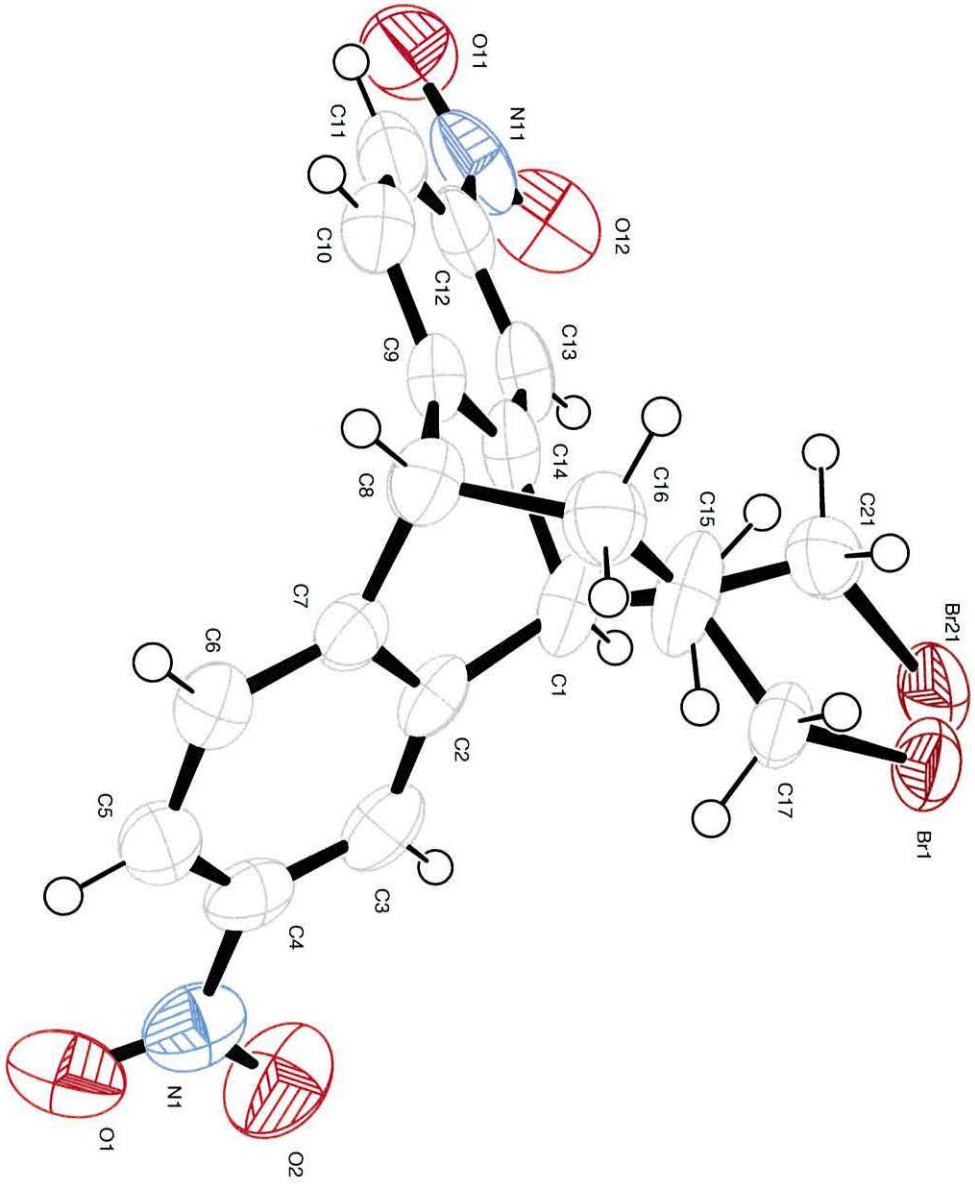
O11
N11
C11
O12
C10
C12
C13
C9
C14
C16
C8
C15
C21
C7
Br21
C6
C1
C2
C17
C5
Br1
C3
C4
N1
O1
O2

Appendix D. ESR spectrum of anthracene 33

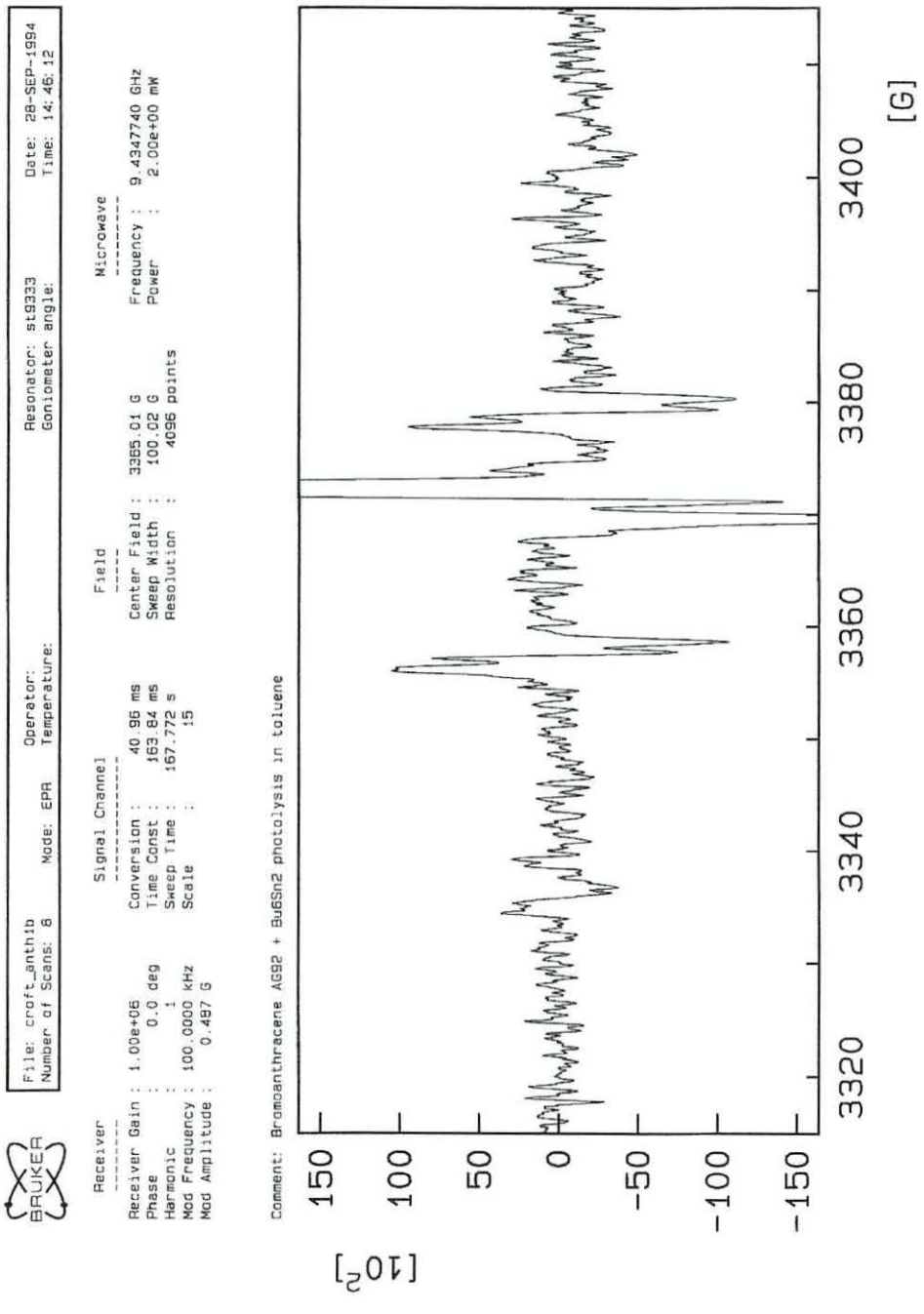

Appendix E. Calculations for competitive studies

Density of tri-butyl tin hydride: 1.082 g/ml.

Total volume in NMR tube: 0.75 ml.

Molecular weight of **10**: 221 g/mol.

Molecular weight of the reference (mesitylene): 177 g/mol.

Molecular weight of *tri*-butyltin hydride: 291 g/mol.

Number of equivalents of a given compound: 1.0 eq.

Number of equivalents of **10**: 1.0 eq.

Number of equivalents of *tri*-butyltin hydride: 1.0 eq.

Number of equivalents of the reference (mesitylene): 0.2 eq.

Number of moles of a given compound: 7.5×10^{-5} moles.

Number of moles of **10**: 7.5×10^{-5} moles.

Number of moles of *tri*-butyltin hydride: 7.5×10^{-5} moles.

Number of moles of the reference (mesitylene): 1.5×10^{-5} moles.

Molarity of a given compound inside the NMR tube: 0.1 M.

Molarity of **10** inside the NMR tube: 0.1 M.

Molarity of the reference (mesitylene) inside the NMR tube: 0.02 M.

Where,

TotalVolume (l): Total volume of the standard solution (l).

TotalVolume (ml): Total volume of the standard solution (ml).

Mass (A): Mass of the given compound used to make up the standard solution (g).

MW (A): Molecular weight of the given compound (g/mol).

Volume (A) = Volume of a given compound pipetted from the standard solution (µl).

Volume (B) = Volume of **10** pipetted from the standard solution (µl).

Mass (B) = Mass of **10** used to make up the standard solution (g).

Volume (C) = Volume of the reference (mesitylene) pipetted from the standard solution (µl).

Mass (C) = Mass of the reference (mesitylene) used to make up the standard solution (g).

$$Volume(A) = 75 \times MW(A) \times TotalVolume(l) \div Mass(A)$$

$$Volume(A) = 0.075 \times MW(A) \times TotalVolume(ml) \div Mass(A)$$

$$Volume(B) = 16575 \times TotalVolume(l) \div Mass(B)$$

$$Volume(B) = 16.575 \times TotalVolume(ml) \div Mass(B)$$

$$Volume(C) = 1800 \times TotalVolume(l) \div Mass(C)$$

$$Volume(C) = 1.8 \times TotalVolume(ml) \div Mass(C)$$

$$\text{Volume (Bu3SnH)} = 7.5 \times 10^{-5} \text{ moles} \times 291 \text{ g/mol} \times 10^{3} \text{ µl/ml} \div 1.082 \text{ g/ml} = 20.17 \text{ µl}$$

	MW (g/mol)	Mass (g)	Total Volume (ml)	Volume (µl)
47	297	0.4919	5	230
10	221	1.0225	10	160
Mesytilene	120	0.2779	25	160
Tin hydride	291	--------	--------	20
Added volume ($CDCl_3$)	--------	--------	--------	200

	MW (g/mol)	Mass (g)	Total Volume (ml)	Volume (µl)
39	299	0.5053	5	220
10	221	1.0225	10	160
Mesytilene	120	0.2779	25	160
Tin hydride	291	--------	--------	20
Added volume ($CDCl_3$)	--------	--------	--------	210

	MW (g/mol)	Mass (g)	Total Volume (ml)	Volume (µl)
40	327	0.9507	5	130
10	221	1.0225	10	160
Mesytilene	120	0.2779	25	160
Tin hydride	291	--------	--------	20
Added volume ($CDCl_3$)	--------	--------	--------	300

	MW (g/mol)	Mass (g)	Total Volume (ml)	Volume (µl)
41	389	0.7336	5	200
10	221	1.0225	10	160
Mesytilene	120	0.2779	25	160
Tin hydride	291	--------	--------	20
Added volume ($CDCl_3$)	--------	--------	--------	230

Appendix F. Relative rates of reaction

Anthracene 39 vs. acyclic derivative 10

Compound	**39**	**10**
^{1}H NMR signal	(2.80 + 3.10) 2H	4.06 1H
t_0	3,411	3,571
t_1	1,677	2,083
$\log(t_0/t_1)$	0,308	0,234
% reaction	51%	42%
% final	49%	58%
Krel(Bu_3SnH)	1,3	1,0

Compound	**39**	**10**
^{1}H NMR signal	(2.80 + 3.10) 2H	4.06 1H
t_0	6,695	7,317
t_1	4,598	5,556
$\log(t_0/t_1)$	0,163	0,120
% reaction	31%	24%
% final	69%	76%
Krel(Bu3SnH)	1,4	1,0

Compound	**39**	**10**
^{1}H NMR signal	(2.80 + 3.10) 2H	4.06 1H
t_0	9,776	10,345
t_1	5,016	6,522
$\log(t_0/t_1)$	0,290	0,200
% reaction	49%	37%
% final	51%	63%
Krel(Bu_3SnH)	1,4	1,0

Compound	**39**	**10**
^{1}H NMR signal	(2.80 + 3.10) 2H	4.06 1H
t_0	6,679	7,143
t_1	4,933	5,769
$\log(t_0/t_1)$	0,132	0,093
% reaction	26%	19%
% final	74%	81%
Krel(Bu_3SnH)	1,4	1,0

Compound	**39**	**10**
^{1}H NMR signal	(2.80 + 3.10) 2H	4.06 1H
t_0	9,435	9,677
t_1	4,976	6,000
$\log(t_0/t_1)$	0,278	0,208
% reaction	47%	38%
% final	53%	62%
Krel(Bu_3SnH)	1,3	1,0

Compound	**39**	**10**
^{1}H NMR signal	(2.80 + 3.10) 2H	4.06 1H
t_0	3,016	3,125
t_1	2,556	2,778
$\log(t_0/t_1)$	0,072	0,051
% reaction	15%	11%
% final	85%	89%
Krel(Bu_3SnH)	1,4	1,0

Compound	**39**	**10**
^{1}H NMR signal	(2.80 + 3.10) 2H	4.06 1H
t_0	1,600	1,667
t_1	1,249	1,408
$\log(t_0/t_1)$	0,108	0,073
% reaction	22%	16%
% final	78%	84%
Krel(Bu_3SnH)	1,5	1,0

Average (x)	1,39
Standard deviation (σ)	0,06
Sample size (n)	7
Confidence level (α)	0,05
t (95 %)	1,96
eem	0,02
eem by t	0,04
s/average	0,04
Value	$\mu = 1,39 \pm 0,04$
Relative standard deviation (RSD, %)	4,00

Anthracene 40 vs. acyclic derivative 10

Compound	**40**	**10**
^{1}H NMR signal	(2.80 + 3.10) 2H	4.06 1H
t_0	0,201	0,177
t_1	0,144	0,130
$\log(t_0/t_1)$	0,145	0,134
% reaction	28%	27%
% final	72%	73%
Krel(Bu_3SnH)	1,1	1,0

Compound	**40**	**10**
^{1}H NMR signal	(2.80 + 3.10) 2H	4.06 1H
t_0	0,197	0,180
t_1	0,135	0,130
$\log(t_0/t_1)$	0,164	0,141
% reaction	31%	28%
% final	69%	72%
Krel(Bu_3SnH)	1,2	1,0

Compound	**40**	**10**
^{1}H NMR signal	(2.80 + 3.10) 2H	4.06 1H
t_0	0,212	0,182
t_1	0,141	0,126
$\log(t_0/t_1)$	0,177	0,160
% reaction	33%	31%
% final	67%	69%
Krel(Bu_3SnH)	1,1	1,0

Average (x)	1,12
Standard deviation (σ)	0,04
Sample size (n)	3
Confidence level (α)	0,05
t (95 %)	1,96
eem	0,02
eem by t	0,05
s/average	0,04
Value	$\mu = 1,12 \pm 0,05$
Relative standard deviation (RSD, %)	3,67

Anthracene 41 vs. acyclic derivative 10

Compound	**41**	**10**
^{1}H NMR signal	(2.80 + 3.10) 2H	4.06 1H
t_0	1,860	1,754
t_1	1,621	1,724
$\log(t_0/t_1)$	0,060	0,007
% reaction	13%	2%
% final	87%	98%
Krel(Bu_3SnH)	8,0	1,0

Compound	**41**	**10**
^{1}H NMR signal	(2.80 + 3.10) 2H	4.06 1H
t_0	1,848	1,786
t_1	1,613	1,754
$\log(t_0/t_1)$	0,059	0,008
% reaction	13%	2%
% final	87%	98%
Krel(Bu_3SnH)	7,5	1,0

Compound	**41**	**10**
^{1}H NMR signal	(2.80 + 3.10) 2H	4.06 1H
t_0	1,802	1,724
t_1	1,576	1,695
$\log(t_0/t_1)$	0,058	0,007
% reaction	13%	2%
% final	87%	98%
Krel(Bu_3SnH)	7,9	1,0

Compound	**41**	**10**
^{1}H NMR signal	(2.80 + 3.10) 2H	4.06 1H
t_0	1,855	1,818
t_1	1,598	1,786
$\log(t_0/t_1)$	0,065	0,008
% reaction	14%	2%
% final	86%	98%
Krel(Bu_3SnH)	8,4	1,0

Compound	**41**	**10**
^{1}H NMR signal	(2.80 + 3.10) 2H	4.06 1H
t_0	1,717	1,667
t_1	1,534	1,644
$\log(t_0/t_1)$	0,049	0,006
% reaction	11%	1%
% final	89%	99%
Krel(Bu_3SnH)	8,1	1,0

Average (x)	7,98
Standard deviation (σ)	0,32
Sample size (n)	5
Confidence level (α)	0,05
t (95 %)	1,96
eem	0,14
eem by t	0,28
s/average	0,04
Value	$\mu = 7,98 \pm 0,28$
Relative standard deviation (RSD, %)	4,00

Acyclic derivative 47 vs. acyclic 10

Compound	**47**	**10**
GCMS signal	18,79	9,31
t_0	30,057	16,474
t_1	8,500	6,130
$\log(t_0/t_1)$	0,549	0,429
% reaction	72%	63%
% final	28%	37%
Krel(Bu_3SnH)	1,3	1,0

Compound	**47**	**10**
GCMS signal	18,79	9,31
t_0	29,604	22,390
t_1	6,990	7,073
$\log(t_0/t_1)$	0,627	0,500
% reaction	76%	68%
% final	24%	32%
Krel(Bu_3SnH)	1,3	1,0

Compound	**47**	**10**
GCMS signal	18,79	9,31
t_0	26,496	15,622
t_1	9,008	6,917
$\log(t_0/t_1)$	0,469	0,354
% reaction	66%	56%
% final	34%	44%
Krel(Bu_3SnH)	1,3	1,0

Compound	**47**	**10**
GCMS signal	18,79	9,31
t_0	26,805	18,223
t_1	7,045	5,901
$\log(t_0/t_1)$	0,580	0,490
% reaction	74%	68%
% final	26%	32%
Krel(Bu_3SnH)	1,2	1,0

Compound	**47**	**10**
GCMS signal	18,79	9,31
t_0	38,314	22,742
t_1	7,644	5,823
$\log(t_0/t_1)$	0,700	0,592
% reaction	80%	74%
% final	20%	26%
Krel(Bu_3SnH)	8,1	1,0

Average (x)	1,24
Standard deviation (σ)	0,06
Sample size (n)	5
Confidence level (α)	0,05
t (95 %)	1,96
eem	0,03
eem by t	0,05
s/average	0,05
Value	$\mu = 1,24 \pm 0,05$
Relative standard deviation (RSD, %)	4,89

Appendix G. Statistical equations to calculate errors

$$x = \sum_i x_i / n$$

$$\sigma = \sqrt{\frac{\sum_i x_i^2}{(n-1)} - \frac{\left(\sum_i x_i^2\right)}{n(n-1)}}$$

$$sem = \left(\frac{\sigma}{\sqrt{n}}\right)$$

$$\mu = x \pm t\left(\frac{\sigma}{\sqrt{n}}\right), \text{ where t = 1.96 (95 \% confidence level).}$$

$$RSD(\%) = 100 \cdot \frac{\sigma}{x}$$

Where,

x = Average value.

σ = Standard deviation.

sem = Standard error of the mean.

n = Number of repetitions.

μ = True value with interval of confidence.

RSD = Relative standard deviation.

Appendix H. Energies from computational studies

Calculated energies using B3LYP/6-31G*

Anthracene	Energy (Hartrees)	ZPE (Hartrees)
59a	-657,46320	0,282303
59b	-736,09865	0,337224
59c	-1066,46840	0,287538
59d	-5799,67350	0,262025

Radical	Energy (Hartrees)	ZPE (Hartrees)
60a	-656,79106	0,267286
60b	-735,42651	0,322151
60c	-1065,79600	0,272432
60d	-5799,00130	0,247065

Calculated energies using RMP2/6-31G*

Anthracene	Energy (Hartrees)	Radical	Energy (Hartrees)
59a	-655,28067	**60a**	-654,62023
59b	-733,62215	**60b**	-732,96179
59c	-1063,30300	**60c**	-1062,64230
59d	-5794,12760	**60d**	-5793,46700

Appendix I. Computational structures optimised using B3LYP/6-31G*

Anthracene X = H (59a)

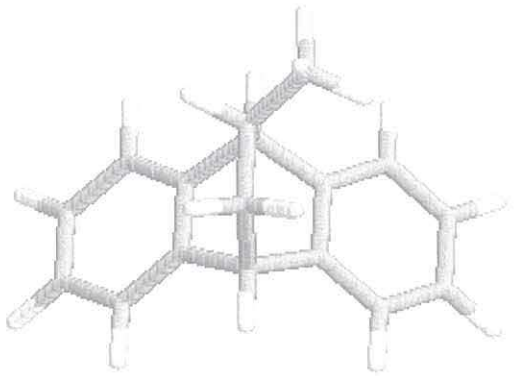

1\1\GINC-NODE03\SP\RMP2-FC\6-31G(d)\C17H16\CHS60A\02-Sep-2005\0\\#P RM
P2/6-31G* SP GUESS=CHECK GEOM=CHECK\\anthracene (H) B3LYP/6-31G* optim
ised single point RMP2\\0,1\H,0,1.6357318114,-0.7018842221,-2.95161809
18\C,0,1.200337209,0.2003270813,-2.5272508468\C,0,0.0809575865,2.52871
3229,-1.4332258021\C,0,0.7814772427,0.2182525664,-1.200221852\C,0,1.05
37447733,1.3492707248,-3.313912615\C,0,0.4973413678,2.5075192146,-2.76
98279837\C,0,0.2208631322,1.3855251614,-0.6522348856\C,0,0.8883192019,
-0.918485138,-0.1981377163\H,0,1.373697436,1.3369775075,-4.3525864369\
H,0,0.3842719002,3.3964406038,-3.3849616809\C,0,-0.1579891788,1.230888
7807,0.8105001884\H,0,-0.3521801078,3.4318603975,-1.008562044\C,0,1.81
98637175,-0.3936144353,0.9589391386\H,0,1.3048144696,-1.826579417,-0.6
468064913\C,0,-0.4930484514,-1.1486437704,0.3875030459\C,0,-1.18756720
93,-2.3540753343,0.4372947771\C,0,-1.0642627113,0.0177462566,0.9276312
844\C,0,-2.3254655062,-0.027134463,1.514295398\H,0,-0.6219250737,2.134
8714674,1.2176603097\C,0,1.1540466922,0.8724481563,1.5854776964\C,0,-2
.4594364188,-2.3965226408,1.0209999599\H,0,-0.7459331239,-3.2564252635
,0.0199142974\H,0,-3.0073127796,-3.3346203027,1.0544489719\C,0,-3.0253
104267,-1.2389667444,1.5568758598\H,0,-4.0139011684,-1.2761307459,2.00
70543985\H,0,-2.7663941326,0.8751296273,1.9327715013\H,0,2.7624928421,
-0.0975419769,0.4833947388\H,0,0.902012332,0.691707232,2.6369222432\H,
0,1.8402855513,1.7256325337,1.5559853508\C,0,2.1282867499,-1.474475919
8,2.0001156812\H,0,2.7985276782,-1.0857243256,2.7759748298\H,0,2.61883
66428,-2.3408917432,1.5394969945\H,0,1.2140290996,-1.8254577219,2.4919
831382\\Version=x86-Linux-G03RevB.04\State=1-A\HF=-653.0970378\MP2=-65
5.2806734\RMSD=8.884e-09\PG=C01 [X(C17H16)]\\@

Anthracene X = CH_3 (59b)

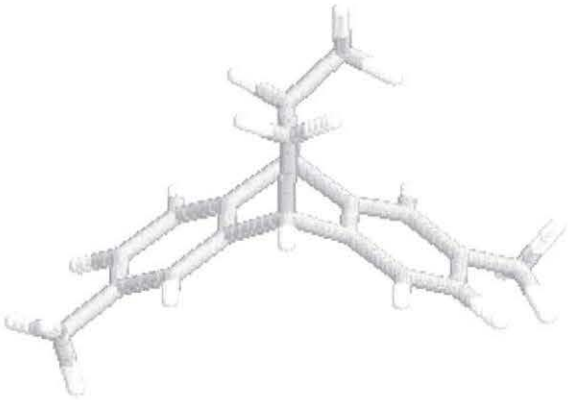

1\1\GINC-NODE01\SP\RMP2-FC\6-31G(d)\C19H20\CHS60A\02-Sep-2005\0\\#P RM
P2/6-31G* SP GUESS=CHECK GEOM=CHECK\\dimethyl anthracene B3LYP/6-31G*
optimised single point RMP2\\0,1\H,0,-1.0793330884,-0.5925240376,-3.17
44441973\C,0,-1.3028459748,0.148713304,-2.4099396879\C,0,-1.8947134372
,2.0628450621,-0.4593050297\C,0,-0.4544188532,0.3119395981,-1.32168391
89\C,0,-2.4525548844,0.9411566329,-2.5180699055\C,0,-2.7648850869,1.90
36151602,-1.5525513021\C,0,-0.7558739603,1.2759974273,-0.3426160272\C,
0,0.842898932,-0.4300486797,-1.0501329756\H,0,-3.1171139468,0.80598134
36,-3.3684774557\C,0,-4.0086056405,2.7549352219,-1.6701618588\C,0,0.28
18387947,1.3391640746,0.764899568\H,0,-2.1195367396,2.8073391397,0.303
3068293\C,0,1.9763870047,0.663343736,-1.0359003072\H,0,1.0505783348,-1
.1913468803,-1.8096408369\C,0,0.7505204912,-1.0200390316,0.3458601383\
C,0,0.9503342989,-2.3487055919,0.7018716766\C,0,0.4395535738,-0.062166
0289,1.3282459179\C,0,0.3346486219,-0.4492606275,2.6589408799\H,0,0.02
13748269,2.0695794367,1.5375986378\C,0,1.6473383449,1.6958318489,0.088
5670284\C,0,0.8362012408,-2.7557001919,2.0428047875\H,0,1.1922840701,-
3.083868475,-0.0643855849\C,0,1.0249100355,-4.2071337144,2.4207408953\
C,0,0.5303670138,-1.7908436398,3.0084878037\H,0,0.4410121658,-2.090946
2308,4.0502067202\H,0,0.0987829733,0.284486568,3.4269246939\H,0,1.9248
93934,1.1709303969,-2.0066798242\C,0,3.3757354511,0.0568934237,-0.8887
698953\H,0,2.4308738772,1.6897196989,0.8552728189\H,0,1.5983902444,2.7
11120518,-0.3199374628\H,0,3.5944296309,-0.6412375492,-1.7063653627\H,
0,3.4756224518,-0.4885845296,0.0564724255\H,0,1.9548869666,-4.61442245
83,2.0055460659\H,0,0.2048868316,-4.830580408,2.0406235532\H,0,1.05896
84217,-4.3365074923,3.5073117924\H,0,-3.7643386267,3.8247328194,-1.683
8680111\H,0,-4.6882444193,2.5934737536,-0.8236604525\H,0,-4.5623381631
,2.5291340265,-2.5870889007\H,0,4.1429044586,0.8402924561,-0.906442172
9\\Version=x86-Linux-G03RevB.04\State=1-A\HF=-731.1704402\MP2=-733.622
1485\RMSD=1.270e-10\PG=C01 [X(C19H20)]\\@

Anthracene X = Br (59c)

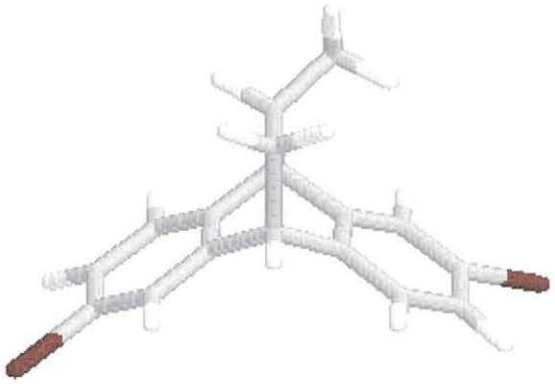

1\1\GINC-NODE07\SP\RMP2-FC\6-31G(d)\C17H14Br2\CHS60A\02-Sep-2005\0\\#P
RMP2/6-31G* SP GUESS=CHECK GEOM=CHECK\\dibromo anthracene B3LYP/6-31G
* optimised single point RMP2\\0,1\H,0,-2.520356726,-2.1629247645,0.56
20287024\C,0,-2.3044445043,-1.3789733596,-0.1600106706\C,0,-1.76162396
25,0.6476465207,-2.0287084727\C,0,-0.9896590483,-1.0658016985,-0.48896
96069\C,0,-3.3601463662,-0.6799535029,-0.7568699043\C,0,-3.075073846,0
.3210061227,-1.6814792328\C,0,-0.7216835402,-0.050953823,-1.4243623844
\C,0,0.265918758,-1.7382634355,0.0375393393\H,0,-4.3891816975,-0.91068
69907,-0.5042299372\C,0,0.762420269,0.1465233356,-1.6798726725\H,0,-1.
5662250904,1.4324466155,-2.7525939355\C,0,0.9843172555,-2.3661514702,-
1.2162002037\H,0,0.0413810923,-2.5086580761,0.7820163219\C,0,1.1677574
604,-0.6494040943,0.5906124679\C,0,1.7234756227,-0.6075836894,1.865640
6294\C,0,1.4302089575,0.3754047048,-0.335878696\C,0,2.249375277,1.4424
570742,0.0182702289\H,0,0.9584017536,0.9602349392,-2.3844580521\C,0,1.
316296824,-1.2152926956,-2.2180443657\C,0,2.5387040066,0.4754921347,2.
2042655996\H,0,1.5289772152,-1.3929438145,2.5891768046\C,0,2.808540000
9,1.4992837985,1.3001087259\H,0,3.4430488086,2.3293600782,1.5907915303
\H,0,2.4565800767,2.2379613502,-0.6935950123\H,0,0.2532975385,-3.03796
8453,-1.6812299968\C,0,2.2175557581,-3.1913347018,-0.8346342078\H,0,2.
4003399995,-1.1237158478,-2.349802773\H,0,0.88342136,-1.4210500434,-3.
2026611705\H,0,2.6772000904,-3.634587433,-1.7257827088\H,0,1.953079416
3,-4.0102840395,-0.1547114518\Br,0,3.3013166822,0.5510130126,3.9595164
377\Br,0,-4.5186475261,1.2784396916,-2.4990327486\H,0,2.9749821676,-2.
57263549,-0.3403168787\\Version=x86-Linux-G03RevB.04\State=1-A\HF=-579
1.7119799\MP2=-5794.1275542\RMSD=8.795e-09\PG=C01 [X(C17H14Br2)]\\@

Anthracene X = NO_2 (59d)

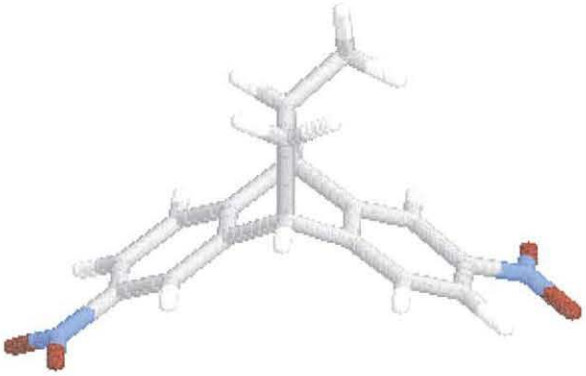

1\1\GINC-NODE05\SP\RMP2-FC\6-31G(d)\C17H14N2O4\CHS60A\02-Sep-2005\0\\#
P RMP2/6-31G* SP GUESS=CHECK GEOM=CHECK\\dinitroanthracene B3LYP/6-31G
* optimised single point RMP2\\0,1\H,0,0.5909550993,-3.1356229849,1.09
01757347\C,0,1.1636658659,-2.2150412041,1.0161378655\C,0,2.6441808193,
0.1737936921,0.825526079\C,0,0.515028859,-0.9827420615,0.9690875684\C,
0,2.5577929048,-2.2670478146,0.9631482636\C,0,3.2717352877,-1.07452613
12,0.8703192886\C,0,1.2579037047,0.2099511285,0.8732565683\C,0,-0.9815
251178,-0.7466141611,1.0445253006\H,0,3.0945289292,-3.2070911201,0.991
3504867\C,0,0.3888299065,1.4549521448,0.8523824007\H,0,3.2451243011,1.
07283595,0.7541214621\C,0,-1.221726894,0.1209671643,2.3385860179\H,0,-
1.5462379562,-1.682307785,1.0931702875\C,0,-1.3673385682,0.0951606703,
-0.1579995154\C,0,-2.35189279,-0.2027223957,-1.0902512094\C,0,-0.61961
93499,1.2840445112,-0.267553693\C,0,-0.8585445462,2.1751359219,-1.3117
162051\H,0,0.9772900971,2.3703861419,0.7450848412\C,0,-0.4353786581,1.
4604180576,2.1842217913\C,0,-2.5693660654,0.7037480574,-2.1317564524\H
,0,-2.945710263,-1.1076026607,-1.0354118672\C,0,-1.8415574244,1.884645
4789,-2.2594033248\H,0,-2.0494484004,2.5503397041,-3.0877974409\H,0,-0
.2813234642,3.0920632084,-1.3950199544\H,0,-0.7911418056,-0.4474392062
,3.1711214342\C,0,-2.7106605359,0.3378021784,2.6275586454\H,0,-1.12603
95691,2.3106715492,2.1642196432\H,0,0.2447166593,1.6121438461,3.028448
4049\H,0,-2.8433394451,0.9195946256,3.5468290972\H,0,-3.2330415202,-0.
6170713847,2.7597312583\N,0,-3.6047314389,0.3965069041,-3.130435545\N,
0,4.7405834892,-1.1287717505,0.8176588577\O,0,-4.2326737941,-0.6544234
839,-2.9975417806\O,0,-3.7842502665,1.2070924764,-4.0391067343\O,0,5.3
492700006,-0.0611428146,0.7385828628\O,0,5.2758611493,-2.2364429342,0.
8572241664\H,0,-3.2021181167,0.8827366699,1.8137289742\\Version=x86-Li
nux-G03RevB.04\State=1-A\HF=-1060.0331488\MP2=-1063.3029682\RMSD=4.879
e-09\PG=C01 [X(C17H14N2O4)]\\@

Radical X = H (60a)

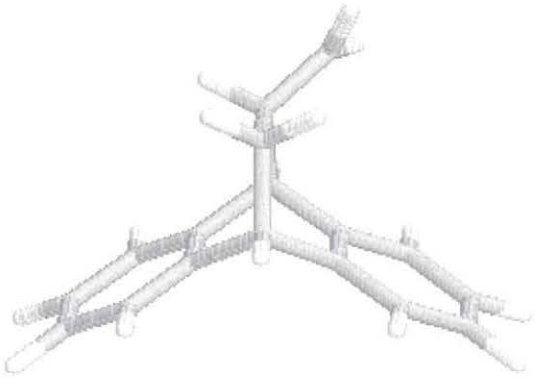

1\1\GINC-NODE04\SP\ROMP2-FC\6-31G(d)\C17H15(2)\CHS60A\02-Sep-2005\0\\#
P ROMP2/6-31G* SP GUESS=CHECK GEOM=CHECK\\anthracene (H) radical B3LYP
/6-31G* optimised single point RMP2\\0,2\H,0,0.6488220439,-0.605179824
4,3.3309995385\C,0,1.2295403836,-0.1912585532,2.5094135054\C,0,2.72686
09136,0.8794315039,0.3918742177\C,0,0.6103948016,0.1225248009,1.302625
6437\C,0,2.6050618466,0.0228388738,2.6561714162\C,0,3.3499631325,0.555
400633,1.6030155062\C,0,1.3606288858,0.6611288169,0.2422979655\C,0,-0.
8642807745,-0.016589363,0.98056856\H,0,3.0935734718,-0.2285047263,3.59
39913313\H,0,4.4179742484,0.7185074541,1.7215099613\C,0,0.5186921004,0
.9712102201,-0.9823801971\H,0,3.3072879944,1.2964225663,-0.4283414666\
C,0,-1.3848963304,1.4673557123,0.6736303173\H,0,-1.4332235746,-0.45237
1938,1.8068912716\C,0,-0.9968807006,-0.8142212277,-0.300578881\C,0,-1.
7797692287,-1.9487383269,-0.4955626571\C,0,-0.2388835416,-0.2885432005
,-1.3617366037\C,0,-0.2651570034,-0.9003796761,-2.6117406761\H,0,1.118
6421962,1.3591833925,-1.8117269379\C,0,-0.564294992,2.0123147281,-0.54
17694887\C,0,-1.7995827893,-2.5675867355,-1.7508770103\H,0,-2.36888225
05,-2.3533162417,0.3244565499\H,0,-2.4034345976,-3.4581160149,-1.90460
4407\C,0,-1.0457902212,-2.0463533183,-2.8034788224\H,0,-1.0627492264,-
2.5316850381,-3.7758574597\H,0,0.3201393565,-0.4921191976,-3.432935530
3\H,0,-1.1334666245,2.0498890972,1.567768802\H,0,-1.2281701246,2.21180
67995,-1.3897967974\H,0,-0.0804423132,2.9582977718,-0.2770230706\C,0,-
2.8570273099,1.5213033435,0.4649648122\H,0,-3.2916032283,1.244284694,-
0.4909475172\H,0,-3.5319424061,1.6438718191,1.3069900842\\Version=x86-
Linux-G03RevB.04\State=2-A\HF=-652.4603287\MP2=-654.6202278\RMSD=4.032
e-09\PG=C01 [X(C17H15)]\\@

Radical X = CH_3 (60b)

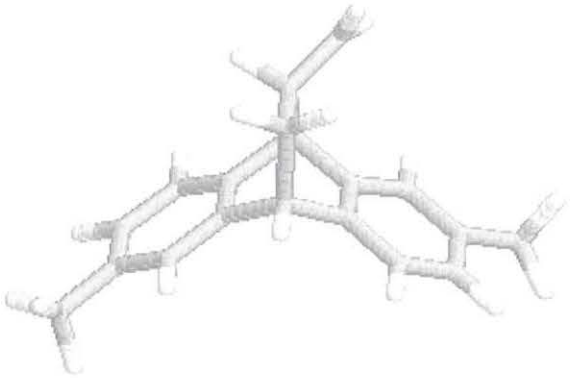

1\1\GINC-NODE02\SP\ROMP2-FC\6-31G(d)\C19H19(2)\CHS60A\02-Sep-2005\0\\#
P ROMP2/6-31G* SP GUESS=CHECK GEOM=CHECK\\dimethyl anthracene radical
B3LYP/6-31G* optimised single point RMP2\\0,2\H,0,-2.3042506994,-1.588
4513193,1.9487707771\C,0,-2.2594777713,-0.6371673973,1.4225987724\C,0,
-2.1711067968,1.8104201599,0.0731308896\C,0,-1.2929457132,-0.419275129
5,0.4471536134\C,0,-3.1760976211,0.3756761868,1.7286240877\C,0,-3.1455
431579,1.6076054369,1.0660831457\C,0,-1.2537351818,0.812102553,-0.2310
755371\C,0,-0.2455611587,-1.4030478117,-0.0354556725\H,0,-3.9267722406
,0.2029859847,2.4966977955\C,0,-4.1206075454,2.7077184524,1.4186374623
\C,0,-0.1640974745,0.8722141073,-1.286761236\H,0,-2.1354853417,2.75988
10538,-0.4592712069\C,0,-0.5613847951,-1.6503034696,-1.5860791812\H,0,
-0.2766428963,-2.3495940506,0.5119732147\C,0,1.1086803389,-0.727689866
,0.046673866\C,0,2.2438362114,-1.2225583314,0.677832862\C,0,1.15065289
88,0.5096830755,-0.620448452\C,0,2.3338383869,1.2385651893,-0.64629530
63\H,0,-0.1216881037,1.8458965557,-1.7852748757\C,0,-0.4605267367,-0.2
699279591,-2.3151613498\C,0,3.4437227094,-0.4902514454,0.6690997812\H,
0,2.2040195734,-2.1840710214,1.187488362\C,0,4.6671251223,-1.016156383
4,1.3849263974\C,0,3.4705756156,0.737891965,-0.0003777063\H,0,4.392921
4672,1.3143159685,-0.0178388534\H,0,2.3789889631,2.1942820343,-1.16435
4571\H,0,-1.6013366529,-1.9969905418,-1.6141463018\C,0,0.3079901304,-2
.6988363856,-2.1850838487\H,0,0.3423179758,-0.2920092547,-3.0599734132
\H,0,-1.393194386,-0.0544538196,-2.8471476161\H,0,1.313977239,-2.46149
04583,-2.5183861713\H,0,4.851784413,-2.0701854507,1.1452599369\H,0,4.5
526010937,-0.9505710408,2.4750583331\H,0,5.5634782446,-0.4486398139,1.
1145540824\H,0,-4.5217470238,3.1927667797,0.5209285496\H,0,-3.64010845
84,3.4915706768,2.0193211965\H,0,-4.9656808336,2.3228953315,1.99873789
38\H,0,0.0347928983,-3.7481152973,-2.1205326594\\Version=x86-Linux-G03
RevB.04\State=2-A\HF=-730.5337416\MP2=-732.9617871\RMSD=3.499e-09\PG=C
01 [X(C19H19)]\\@

Radical X = Br (60c)

1\1\GINC-NODE08\SP\ROMP2-FC\6-31G(d)\C17H13Br2(2)\CHS60A\02-Sep-2005\0
\\#P ROMP2/6-31G* SP GUESS=CHECK GEOM=CHECK\\dibromo anthracene radica
l B3LYP/6-31G* optimised single point RMP2\\0,2\H,0,-2.0289527306,-2.6
455149793,-0.5343377265\C,0,-2.0960816941,-1.5666554274,-0.6528172602\
C,0,-2.2839571551,1.2200953246,-0.9587651388\C,0,-0.9523309591,-0.8106
319891,-0.8909706035\C,0,-3.34246524,-0.9374688051,-0.5578138709\C,0,-
3.4194783533,0.4442640292,-0.7118780286\C,0,-1.0502552479,0.583385607,
-1.0453434587\C,0,0.4615482719,-1.331922444,-1.0507028054\H,0,-4.24010
5408,-1.5145340454,-0.3648967949\C,0,0.285810862,1.2467678429,-1.32730
03341\H,0,-2.3713356968,2.2955459353,-1.0764578506\C,0,0.9085821019,-0
.9356559738,-2.5370640193\H,0,0.5273008291,-2.4142462167,-0.9108314179
\C,0,1.3531477458,-0.566740659,-0.0939831546\C,0,2.2232562514,-1.12161
84276,0.8395005736\C,0,1.2499873568,0.8282998252,-0.2326179126\C,0,2.0
174908981,1.6672881393,0.5690401172\H,0,0.2002469321,2.3342229886,-1.4
117649483\C,0,0.8355185582,0.6220132319,-2.6536975192\C,0,2.9807101729
,-0.2625806014,1.6392860528\H,0,2.3142573331,-2.1971866376,0.952279094
3\C,0,2.8893654245,1.1216791544,1.5179860279\H,0,3.4877907377,1.764691
7505,2.1540089463\H,0,1.9432739456,2.7472928989,0.466148487\H,0,0.1490
944981,-1.3815444396,-3.1901001797\C,0,2.2395671543,-1.4938408527,-2.8
994129011\H,0,1.830390393,1.0349196494,-2.8506818302\H,0,0.1911951228,
0.909695398,-3.4907075632\H,0,3.1542364043,-0.9902518686,-2.601236509\
H,0,2.3270967634,-2.4972808838,-3.3051014586\Br,0,4.173493505,-1.01170
37656,2.9369812433\Br,0,-5.1245502482,1.3063929828,-0.58146681\\Versio
n=x86-Linux-G03RevB.04\State=2-A\HF=-5791.0752116\MP2=-5793.4670203\RM
SD=6.116e-09\PG=C01 [X(C17H13Br2)]\\@

Radical X = NO_2 (60d)

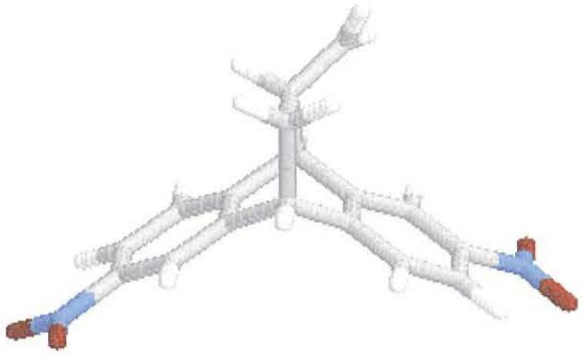

1\1\GINC-NODE06\SP\ROMP2-FC\6-31G(d)\C17H13N2O4(2)\CHS60A\02-Sep-2005\
0\\#P ROMP2/6-31G* SP GUESS=CHECK GEOM=CHECK\\dinitro anthracene radic
al B3LYP/6-31G* optimised single point RMP2\\0,2\H,0,-2.0926611876,-0.
6494132608,-2.5729811518\C,0,-1.1919821442,-1.1009469046,-2.1658028009
\C,0,1.1409875405,-2.2702257788,-1.1049448612\C,0,-0.8327146731,-0.883
3934916,-0.8366361666\C,0,-0.3855975342,-1.8978875469,-2.9799194212\C,
0,0.7636123594,-2.467753567,-2.4362654045\C,0,0.3333100627,-1.47081949
23,-0.30857814\C,0,-1.6071323847,-0.0756024872,0.1826158728\H,0,-0.629
8441413,-2.0819084757,-4.0186962789\C,0,0.5514958699,-1.1509338106,1.1
589603968\H,0,2.0435028386,-2.7380232387,-0.7292429507\C,0,-2.01419439
64,-1.1077452437,1.3402118825\H,0,-2.4993615793,0.3907150964,-0.242277
3578\C,0,-0.6585011366,0.9351464482,0.7929124586\C,0,-0.8681008206,2.3
043468695,0.8866255043\C,0,0.5168277515,0.3573135473,1.3102846633\C,0,
1.4860618933,1.1524433073,1.918901675\H,0,1.4773310296,-1.5860598772,1
.5454002891\C,0,-0.694726025,-1.6937267406,1.9381347802\C,0,0.12040664
39,3.0814106991,1.4962344708\H,0,-1.7630444738,2.7798391616,0.50297477
32\C,0,1.292201293,2.5315848463,2.0117459021\H,0,2.0267343229,3.180981
108,2.4714756717\H,0,2.3925605022,0.7056157581,2.3182293507\H,0,-2.564
7899814,-1.9057512999,0.8284365775\C,0,-2.9048468616,-0.4897227911,2.3
592760303\H,0,-0.5984157702,-1.4166060333,2.9928787581\H,0,-0.70681972
79,-2.7868689505,1.8885104677\H,0,-2.4947565116,0.0827162088,3.1856979
875\H,0,-3.9792651212,-0.4573870411,2.2077426135\N,0,-0.0850382908,4.5
34773685,1.5951657589\N,0,1.6118828742,-3.3098934242,-3.2933149318\O,0
,0.7950958196,5.203152784,2.1369793587\O,0,-1.1273983922,4.9973330449,
1.1306722166\O,0,2.6202824163,-3.8051495382,-2.788969886\O,0,1.2643042
928,-3.4719535607,-4.4628873885\\Version=x86-Linux-G03RevB.04\State=2-
A\HF=-1059.3962436\MP2=-1062.6423135\RMSD=9.736e-09\PG=C01 [X(C17H13N2
O4)]\\@